Charles University, Faculty of Science

Univerzita Karlova, Přírodovědecká fakulta

Ph.D. study program: Parasitology

Doktorský studijní program: Parazitologie

Maria Grechnikova

Iron and copper transporters in amphizoic amoebae *Naegleria fowleri* and *Acanthamoeba castellanii*

Přenašeče železa a mědi u amfizoických améb *Naegleria fowleri* a *Acanthamoeba castellanii*

Ph.D. thesis / Dizertační práce

Supervisor / Školitel: Robert Sutak, Ph.D.

Prague, 2022

Declaration of the author

I declare that the data presented in this Ph.D. thesis results from my work and collaboration with my colleagues. I also proclaim that all literary sources were appropriately cited. Neither this work nor the data presented in this thesis were used to reach any other academic degree.

Maria Grechnikova

Declaration of the thesis supervisor

I declare that the data presented in this thesis result from a team collaboration of the group of Uptake and Intracellular Metabolism of Metals and the cooperation with our collaborators. I declare that the involvement of Maria Grechnikova in this work was substantial and that she contributed significantly to obtain the results.

RNDr. Robert Sutak, Ph.D.

Acknowledgments

I want to thank my supervisor Robert Sutak for the opportunity to work on the presented project in his laboratory. I am thankful to all my colleagues for the help, fruitful debates about work, not-so-fruitful discussions of life, and a friendly and warm atmosphere. I am grateful to my parents, who led me down the path of science. I am also grateful to my best friend Nikita Bolotov, who patiently helped me prepare pictures for the publications, and, most of all, to my husband Roman Likane, who steadily supported me through all these years.

Contents

Abstract

Amphizoic amoebae *Naegleria fowleri* and *Acanthamoeba castellanii* are distributed worldwide in diverse natural and anthropogenic environments. *N*. *fowleri* can infect healthy individuals, causing a rare but deadly brain disease called primary amoebic meningoencephalitis with a mortality rate of over 95%. Infection develops if amebae from contaminated water get into the nose. *A. castellanii* can infect the central nervous system of immunocompromised patients, causing granulomatous amoebic encephalitis with a survival rate of 2-3%, and the eyes of healthy people, leading to a severe sight-threatening infection called *Acanthamoeba* keratitis.

N. *fowleri* and *A*. *castellanii* are aerobic organisms and require iron and copper cofactors. Both metals are crucial for almost all known organisms and toxic in excess, so the pathogens tightly control the homeostasis of iron and copper, which is critical for their virulence. However, the information about metal homeostasis in amphizoic amoeba is scarce. This work aimed to characterize some of the mechanisms employed by *N*. *fowleri* and *A*. *castellanii* for iron and copper acquisition and detoxification.

Despite the similar morphology and lifestyle of studied amoebae, their mechanisms of iron homeostasis under iron-limiting conditions are entirely different. Both amoebae employ a two-step reductive mechanism of iron acquisition; however, *N*. *fowleri* does not induce iron uptake, instead, it relocates available iron in favor of vital mitochondrial processes, while *A*. *castellanii* enhances iron import, upregulating an iron uptake system, which consists of a ferric reductase from the STEAP family and a divalent transporter from the NRAMP family, and downregulating an iron exporter from the VIT family. *A*. *castellanii* ferric reductase, iron importer NRAMP, and iron exporter VIT are localized to the membranes of digestive vacuoles with endocytosed bacteria and liquid medium.

N. *fowleri* employs a high-affinity copper importer homologous to yeast and human CTRs for copper uptake. The defense strategies against copper toxicity include copper efflux mediated by a Cu^{+}-translocating ATPase and upregulation of the expression of various antioxidant proteins. Efficient coping with limited copper concentrations and high copper can be advantageous for *N*. *fowleri* both in the natural environment and in the host.

Abstrakt

Amfizoické améby *Naegleria fowleri* a *Acanthamoeba castellanii* jsou rozšířeny po celém světě a vyskytují se v různých přírodních i antropogenních prostředích. *N. fowleri* může u zdravých jedinců způsobit vzácné, ale smrtelné onemocnění mozku zvané primární amébová meningoencefalitida, jejíž úmrtnost přesahuje 95 %. Infekce vzniká, pokud se améby z kontaminované vody dostanou do nosu. *A. castellanii* může infikovat centrální nervový systém pacientů se sníženou imunitou a způsobit u nich granulomatózní amébovou encefalitidu s mírou přežití 2-3 %, dale může infikovat oči zdravých lidí, což vede k závažné infekci ohrožující zrak zvané akantamébová keratitida.

N. fowleri a *A. castellanii* jsou aerobní organismy a vyžadují kofaktory železo a měď. Oba kovy jsou klíčové pro téměř všechny známé organismy a v nadbytku jsou toxické, takže patogeny přísně kontrolují homeostázu železa a mědi, což je rozhodující pro jejich virulenci. Dostupných informací o homeostáze kovů u amfizoických améb je však málo. Cílem této práce bylo charakterizovat některé mechanismy, které *N. fowleri* a *A. castellanii* využívají k získávání a detoxikaci železa a mědi.

Navzdory podobné morfologii a způsobu života studovaných améb jsou jejich mechanismy homeostázy železa v podmínkách s limitujícím obsahem železa zcela odlišné. Obě améby využívají dvoustupňový redukční mechanismus získávání železa, avšak *N. fowleri* neindukuje příjem železa, ale naopak relokalizuje dostupné železo ve prospěch životně důležitých mitochondriálních procesů, zatímco *A. castellanii* zvyšuje import železa, upreguluje systém příjmu železa, který se skládá ze železité reduktázy z rodiny STEAP a transportéru dvojmocného železa z rodiny NRAMP, a také downreguluje exportér železa z rodiny VIT. Železitá reduktáza *A. castellanii*, importér železa NRAMP a exportér železa VIT jsou lokalizovány na membránách trávicích vakuol společně s endocytovanými bakteriemi a tekutým médiem.

N. fowleri využívá pro příjem mědi vysokoafinitní importér mědi homologní s kvasinkovým a lidským CTR. Obranné strategie proti toxicitě mědi zahrnují eflux mědi zprostředkovaný Cu^{+}-translokující ATPázou a upregulaci exprese různých antioxidačních proteinů. Účinné vyrovnávání se s omezenými koncentracemi mědi a vysokým obsahem mědi může být pro *N. fowleri* výhodné jak v přirozeném prostředí, tak v hostiteli.

1. Introduction

1.1 Amphizoic amoebae cause deadly diseases

Amphizoic amoebae are generally free-living organisms that can occasionally infect humans, causing life-threatening diseases. Among them are phylogenetically distant species *Naegleria fowleri* and *Acanthamoeba castellanii*.

N. fowleri is a thermophilic amoeba living in diverse freshwater environments, both natural and anthropogenic, such as lakes, ponds, water distribution systems, power plant cooling systems, and in soils (Maclean et al., 2004; Mull et al., 2013; Sykora et al., 1983; Wagner et al., 2017). *N. fowleri* is distributed worldwide and found on all continents except Antarctica (De Jonckheere, 2011). The phenotype of *N. fowleri* depends on the environmental conditions. Under favorable conditions, it exists in amoeboid form, trophozoite; it is the only feeding and reproducing form and the only form infective to humans. In water without nutrients, trophozoites can become flagellates with two apical flagella that allow traveling long distances. Under hostile conditions, trophozoites switch to a dormant resistant cyst form (Maciver et al., 2020).

N. fowleri can cause a rare but deadly brain disease called primary amoebic meningoencephalitis (PAM). The infection usually occurs when trophozoites from contaminated water get into the nose, although "dry infections" were also reported when *N. fowleri* cysts enter the nose with dust (Maciver et al., 2020). The amoebae penetrate the nasal mucosa, cross the cribriform plate, migrate along the olfactory nerve and enter the brain (Siddiqui et al., 2014). The trophozoites feed on brain cells, causing an acute inflammatory reaction. The symptoms include severe headaches, stiff neck, fever, nausea, vomiting, seizures, brain dysfunction, and coma (Bellini et al., 2018; Siddiqui et al., 2014). The disease usually has a short incubation period (it may range from 1 to 16 days) and a high mortality rate of about 98% (Siddiqui et al., 2014).

The first stage of the infection is similar to bacterial or viral meningitis, so proper and fast diagnosis is critical for efficient medical intervention. However, the clinical diagnosis of PAM is time-consuming and technically challenging. It includes morphological analysis of cerebrospinal fluid samples, physiological tests of the found organisms such as exflagellation, encystment, and

thermotolerance, and PCR identification (Bellini et al., 2018). Thus, in many cases, PAM is only diagnosed *post-mortem*. Currently, drug combinations are used to treat PAM, including amphotericin B as the first choice and rifampin, azoles, miltefosine, chlorpromazine, azithromycin, dexamethasone (Bellini et al., 2018; Mungroo et al., 2022).

Historically, the cases of PAM have mostly been reported from developed countries; however, this might be due to the poor healthcare system in the developing regions where many PAM cases are probably not diagnosed. *N*. *fowleri* thrives in warm water basins of equatorial and tropical countries, and people's recreational activities and religious traditions combined with low education levels and poor hygiene create the perfect conditions for *N*. *fowleri* infections (Maciver et al., 2020; Siddiqui et al., 2014). The global climate changes may eventually increase the number of PAM cases by expanding *N*. *fowleri* "comfort zone" and increasing people's recreational activity (Maciver et al., 2020, 2021; Siddiqui et al., 2014), thus making the study of the parasite metabolism even more important.

Acanthamoeba spp. are among the most prevalent protozoa in the environment. They are found worldwide in soil, dust, air, water, including swimming pools and sewage, tap and bottled water, sediments, air-conditioning units, hospitals, contact lenses and lens cases, and as contaminants in laboratory cell cultures. *Acanthamoeba* spp. have also been isolated from animals, including fish, amphibia, reptiles, and mammals (Marciano-Cabral et al., 2003). In favorable conditions, *Acanthamoeba* exists as actively moving and dividing trophozoite feeding on bacteria; under poor conditions, it turns into a dormant resistant cyst (Siddiqui et al., 2012).

The genus *Acanthamoeba* has been divided into different species based on morphology; several of them can cause infections in humans, namely *A*. *castellanii*, *A*. *culbertsoni*, *A*. *hatchetti*, *A*. *healyi*, *A*. *astroonyxix*, *A*. *divionensis* and *A*. *polyphaga*. Later, about 20 genotypes (named T1, T2, etc.) of *Acanthamoeba* were established based on rRNA genes sequencing, with the *A*. *castellanii* T4 strain being the most commonly associated with human diseases (Duggal et al., 2017; Lorenzo-Morales et al., 2015; Mungroo et al., 2022).

Acanthamoeba spp. can infect the central nervous system of immunocompromised patients, causing granulomatous amoebic encephalitis (GAE), and the eyes of healthy people, leading to a severe sight-threatening infection called *Acanthamoeba* keratitis (AK) (Duggal et al.,

2017; Lorenzo-Morales et al., 2015). Also, in immunocompromised individuals, *Acanthamoeba* may disseminate to internal organs like the liver, kidneys, trachea, pancreas, lymph nodes, and bone marrow; moreover, it can cause secondary infections, especially in the disrupted skin (Mungroo et al., 2022).

GAE is a rare disease with unspecific symptoms such as low-grade fever, headaches, stiff neck, and nausea; neurological symptoms depend on the involved brain area and may include altered mental state, seizures, hemiparesis, confusion, personality changes, decreased level of consciousness and coma (Duggal et al., 2017; Mungroo et al., 2022). The incubation period of the disease is supposed to be weeks or months. Amoebae may enter the body through the respiratory tract or breaks in the skin, invading the blood vessels with the following hematogenous dissemination to the brain through the blood-brain barrier and to other organs. Also, they may enter the central nervous system through the olfactory neuroepithelium (Duggal et al., 2017; Mungroo et al., 2022). Due to the rarity of the disease and the similarity of the symptoms to fungal, viral, or bacterial encephalitis, GAE diagnostic is problematic. It includes brain imaging using computed tomography or magnetic resonance imaging, analysis of glucose and protein concentration in cerebrospinal fluid, microscopy and culturing of cerebrospinal fluid samples, detection of anti-*Acanthamoeba* antibodies in serum, and PCR detection of amoebal DNA (Duggal et al., 2017; Mungroo et al., 2022). GAE is challenging to treat because of complicated diagnostic, which postpones the start of proper medical intervention, and because most available antimicrobial agents are amoebostatic rather than amoebicidal and are toxic to the patient or do not penetrate the blood-brain barrier (Duggal et al., 2017). Moreover, the effectiveness of the treatment may depend on the exact *Acanthamoeba* strain. Thus, there is no optimal approach for GAE treatment. Drug combinations that have been tried include the compounds interacting with ergosterol and its synthesis (amphotericin B, fluconazole, voriconazole, and ketoconazole), the drugs disturbing nucleic acids metabolism (rifampin, 5-fluorocytosine, pentamidine, and amikacin) as well as other antimicrobials such as miltefosine, trimethoprim-sulfamethoxazole, meropenem, linezolid, moxifloxacin (Duggal et al., 2017; Mungroo et al., 2022). However, the survival rate of the disease does not exceed 2-3%.

AK is a severe infection of the cornea. It mainly affects contact lens wearers but is not limited to those. The symptoms include pain, tearing, photophobia, ring-like stromal infiltrate, epithelial defect, and lid edema. If AK is not treated correctly, it can lead to sight loss (Lorenzo-Morales et al., 2015). The infection occurs when corneal trauma is followed by exposure to contaminated lens solution, water, or soil (Khan, 2006). Similar to GAE, AK is difficult to diagnose due to unspecific symptoms, so it is commonly misdiagnosed as a viral infection. The diagnostic includes *in vivo* confocal microscopy, corneal scrap microscopy and culturing, and PCR-based technics. AK treatment is problematic as acanthamoebae can form cysts within the tissue. While trophozoites are readily eliminated, cysts are resistant to many chemotherapeutics, and a single cyst surviving in the cornea can induce reinfection. Thus, even after the recovery, health checks are required for about half a year (Lorenzo-Morales et al., 2015). So far, there is no single effective drug against AK, so a combination of topical antimicrobials is generally used, such as polyhexanide, chlorhexidine, propamidine isethionate, dibromopropamidine, hexamidine, and neomycin. Polyhexanide is very efficient against *Acanthamoeba* but toxic to corneal cells (Lorenzo-Morales et al., 2015). The number of AK cases is increasing every year since more and more people start using contact lenses; thus, increased awareness about the disease is required to prevent new cases, and early diagnosis and new treatments are needed for better outcomes (Lorenzo-Morales et al., 2015).

1.2 Model protozoan and fungal pathogens

1.2.1 Metal homeostasis in amphizoic amoebae is understudied

N. *fowleri* and *A*. *castellanii* are aerobic organisms using oxygen respiration to generate ATP, although both probably have hydrogenase, an enzyme generally associated with an anaerobic lifestyle (Leger et al., 2013; Tsaousis et al., 2014). Like other aerobes, *N*. *fowleri* and *A*. *castellanii* require metal cofactors for the proper function of the respiratory chain and other cellular processes, but the information about metal homeostasis in amphizoic amoeba is scarce. More data are available about other pathogenic protists, although their metal metabolism is not extensively studied either, and about pathogenic fungi. In the following chapters, I summarize

the information about iron and copper metabolism in important pathogenic protozoans, such as trypanosomatids, apicomplexans, *Entamoeba histolytica*, as well as pathogenic fungi *Candida albicans*, *Cryptococcus neoformans*, *Aspergillus fumigatus* and the non-pathogenic model yeast *Saccharomyces cerevisiae*.

1.2.2 Digenetic trypanosomatids are important human parasites

Trypanosomatids include multiple species of parasitic protists infecting various organisms, from insects to humans. The most important for human health are *Leishmania* spp. causing leishmaniases, *Trypanosoma cruzi* causing Chagas disease, and *Trypanosoma brucei* causing sleeping sickness. All these species are digenetic and circulate between intermediate mammal and definitive insect hosts. Proliferative forms in the vector's midgut are called "procyclic", and non-dividing infective forms are called "metacyclic". There are several species- and stage-specific morphotypes based on the position and length of the flagellum: "promastigotes" that have elongated form with a long flagellum anterior to the nucleus, "trypomastigotes" that are also elongated and have a long flagellum that starts from the posterior part of the cell and goes through the side of the whole cell forming so-called undulating membrane (making wavelike movements), "amastigotes" that have a circular form with non-protruding flagellum, and others (Lopes et al., 2010).

Leishmania spp. are transmitted by phlebotomine sandflies and found in most tropical and temperate regions worldwide. Leishmaniases are divided into several forms: cutaneous with ulcers on the skin, mucocutaneous with mucosa and cartilage destruction, mainly on the face, and visceral form affecting inner organs, which is lethal if untreated. *Leishmania* life cycle includes three developmental stages: procyclic promastigotes, metacyclic promastigotes and intracellular amastigotes in the phagolysosomes of the host macrophages. The amastigotes multiply in phagolysosome and eventually kill the host macrophage. The released amastigotes are phagocytosed by other macrophages (Lopes et al., 2010).

Chagas disease is transmitted by hematophagous triatomine insects and is spread in South, Central, and partly North America. Chagas disease is chronic and untreatable; the manifestation may differ depending on infected organs and usually includes cardiomyopathy and

digestive megasyndromes. At the site of entry, *T. cruzi* infects macrophages and fibroblasts. Later, the parasite may disseminate through the organism and infect different types of human cells, although stable infection usually occurs in muscles, including cardiac, and enteric nerves. In contrast to *Leishmania*, *T. cruzi* eventually escapes from the lysosomal compartment and lives and multiplies in the cytosol. Still, it has to survive at least for some time in the harsh acidic lysosomal environment (Lopes et al., 2010).

T. brucei are transmitted by tsetse flies and cause sleeping sickness in humans. Its symptoms start with fever, headaches, lymph node enlargement, hepatomegaly and splenomegaly, later, the parasites cross the blood-brain barrier and invade the central nervous system provoking insomnia, progressive mental deterioration, and psychiatric manifestations. If untreated, the disease eventually leads to death. In contrast to *Leishmania* and *T. cruzi*, *T. brucei* is exclusively extracellular and lives in the blood and lymphatic system, hence the parasites in the human host are called “bloodstream forms” or “bloodstream trypomastigotes” (Lopes et al., 2010). Bloodstream forms use glycolysis as the primary energy source and have underdeveloped mitochondria, while vector forms use respiration and have normal mitochondria with the full electron transport chain (Zíková et al., 2016).

1.2.3 Apicomplexans are among the most well-known protozoan parasites

Among the most prevalent pathogens worldwide are the parasites from Apicomplexa phylum: *Plasmodium* spp., *Toxoplasma gondii,* and *Cryptosporidium* spp. *Plasmodium falciparum*, which causes malaria in humans, is probably the most notorious parasite in the world. Its relative *P. berghei* causes malaria in rodents and is used to study animal model of the disease (Janse et al., 1995). *Plasmodium* parasites have complicated life cycles including several stages in the intermediate vertebrate host and definitive mosquito host (Fujioka et al., 2002). The infective sporozoites travel from the mosquito bite site through lymph and blood to the liver and infect hepatocytes, where each of them multiplies into thousands of new cells through a process termed schizogony, differentiate into merozoites and eventually rupture the host cells. This stage is called “pre-“ or “extraerythrocytic”. Extraerythrocytic merozoites enter the bloodstream and infect red blood cells. The merozoite multiplies within the red blood cell by erythrocytic

schizogony, which includes ring, trophozoite, and schizont stages, producing the new merozoites that invade new erythrocytes and may go through the same process or differentiate into sexual forms, female macrogametocyte and male microgametocyte. The sexual process takes place in the mosquito midgut. *Plasmodium* erythrocytic stages use host hemoglobin as a source of amino acids; however, they cannot degrade potentially toxic heme. Therefore, most heme is polymerized into specific malaria pigment hemozoin, which is stored in the food vacuoles (Fujioka et al., 2002).

T. gondii is an obligate intracellular parasite that infects more than 200 species of birds and mammals, including humans. Human toxoplasmosis is generally asymptomatic; however, it can be dangerous for the fetus if the mother is infected during pregnancy (Arisue et al., 2015). Definitive hosts of *T. gondii* are felids, all other species it infects are intermediate hosts. The primary infective stage is resistant oocysts with four sporozoites in felids' feces. If oocyst is swallowed, sporozoites are released in the digestive tract of the intermediate host and infect any nucleated cell where they live in a special parasitophorous vacuole that does not fuse with lysosomes. Sporozoites differentiate into so-called tachyzoites, rapidly multiplying cells. After several division cycles, they finally rupture and leave the host cell to infect the new one. Within a few days of infection, tachyzoites gradually slow down the metabolism and division rate, developing into bradyzoites which form cysts in tissues, especially in muscle cells and neurons. Both tachyzoites and bradyzoites are infectious if swallowed, for example, in uncooked meat (Attias et al., 2020).

Cryptosporidium species cause intestinal diarrheal infections in animals, including humans, which can be life-threatening for immunocompromised patients. The parasites exhibit unique intracellular but extracytoplasmic localization within the host cells. The life cycle of *Cryptosporidium* is complicated and involves both sexual and asexual stages developing in the same organism. The infectious stage is oocyst with four sporozoites; some oocysts stay in the intestine and reinfect the same host (Thompson et al., 2005).

1.2.4 *Entamoeba histolytica* is an anaerobic enteric amoeba

Entamoeba histolytica is an enteric parasite infecting hundreds of millions of people annually. Most cases of infection are asymptomatic; however, approximately 50 million people get invasive, potentially life-threatening diseases: amoebic colitis or amoebic liver abscess (Stauffer et al., 2003). *E*. *histolytica* has a simple two-stage life cycle. In the human intestine, it exists as amoeboid trophozoite or forms a dormant cyst to survive the external environment and infect the next host. The parasite obtains energy by anaerobic fermentation and does not have classical mitochondria (Muller et al., 2012).

1.2.5 Fungi are important opportunistic pathogens

Fungal pathogens are relatively easy to study because they don't require complicated growth conditions and are easily subjected to genetic manipulations. The most studied pathogenic fungi are *Candida albicans*, *Cryptococcus neoformans,* and *Aspergillus fumigatus*. These species are opportunistic and occupy different environmental niches within the host during infection. *C*. *albicans* usually exists on the mucosal surfaces and the skin of healthy people. Under immune deficiency, malnutrition or antibiotic treatment, it can cause superficial mycoses or even life-threatening systemic infections (López-Martínez, 2010; Martínez-Pastor et al., 2020). *C*. *neoformans* is found in nature worldwide, primarily in bird excrements and soil. It may cause pulmonary infections and meningoencephalitis in immunocompromised patients (Levitz, 1991). *A. fumigatus* normally inhabits soils and decaying vegetation. It is easily dispersed in the air as spores and causes severe pulmonary and invasive diseases in immunodeficient people (Martínez-Pastor et al., 2020).

1.3 Transition metals are crucial for biological processes

Transition metals are the elements with partially filled *d* atomic shell. Most transition metals have more than one oxidation state. Also, they can form coordination complexes, which are compounds consisting of several groups arranged around a central metal atom, the most well-known being heme. These characteristics determine the importance of transition metals in

biological systems. Biologically essential transition elements include iron, manganese, copper, cobalt, and zinc, to less extent nickel, chromium, and vanadium (Thomson, 1975). Transition metals are involved in numerous crucial biological processes such as oxygen carriage and utilization, electron transfer, reactive oxygen species detoxification, nitrogen fixation, methyl transfer, and others (Brill, 1977).

The roles performed by metals in enzymatic processes may be divided into two broad groups: redox and non-redox reactions catalysis. Transition metals usually participate in redox processes, which is based on their ability to be in different oxidation states, except for zinc, which is only present in cells as Zn^{2+} and participates in non-redox reactions (Andreini et al., 2008). The most abundant metal in redox processes is iron, followed by copper. Both are crucial for almost all known organisms and are toxic in excess. The strategies employed by the pathogens to tightly control the homeostasis of these metals, which is critical for their virulence, are further discussed.

1.4 Iron is the predominant redox metal

1.4.1 Iron and immunity

Iron is used in various cofactors such as heme, iron-sulfur (Fe-S) clusters, diiron, and mononuclear iron centers in countless proteins; it is the predominant redox metal in biological systems (Andreini et al., 2008). Such a predominance is the result of the early evolution of life, as soluble Fe(II) was highly available before the oxygenation of the atmosphere and its redox properties were suitable for early life chemistry (Crichton et al., 2001). Primordial iron-sulfur clusters, the ancestors of modern Fe-S clusters, which are widespread and broadly employed in different enzymes, were probably able to assemble spontaneously on protein templates (Imlay, 2006). The rise of oxygen levels in the atmosphere and ocean waters induced by the emergence of photosynthesis and intensified during the Neoproterozoic Oxygenation Event resulted in iron oxidation and precipitation as ferric hydroxide and insoluble salts, reducing its bioavailability (Canfield et al., 2007; Och et al., 2012; Shields-Zhou et al., 2011). Nevertheless, iron remains crucial for many biochemical processes in living cells, and iron availability is often a limiting growth factor, for example, in oceanic primary production (Boyd et al., 2007).

Limiting the amount of available transition metals, including iron, is one of the mammalian defensive strategies against invading pathogens called nutritional immunity. Initially, the term “nutritional immunity” was referred to strategies for iron withholding, although now it is known that mammals also restrict access to other transition metals such as manganese and zinc (Hennigar et al., 2016; Kehl-Fie et al., 2011). There are various approaches that mammals, including humans, use to limit the amount of iron available for pathogens. Generally, these mechanisms regulate iron homeostasis and prevent iron toxicity: free iron is a potent catalyst for the formation of hydroxyl radicals in the cells, which can cause peroxidation of lipids in membranes, oxidation of side chains of amino acids with following protein degradation, protein cross-linking, nucleic acids damage (Hershko, 2007). Therefore, “free” iron concentration in cells is profoundly low, and organisms tightly regulate iron homeostasis. During infection, some of these mechanisms are intensified and used against pathogens.

A large proportion of human iron is complexed to heme in hemoglobin of erythrocytes or myoglobin of muscle cells. If free hemoglobin is released from the cells, it gets bound by haptoglobin; heme is bound by hemopexin, albumin, and high- or low-density lipoproteins. The resulting protein complexes are cleared from the plasma by the liver or macrophages (Ascenzi et al., 2005). Intracellular non-heme iron is sequestered by the storage protein ferritin (Harrison et al., 1996). The synthesis of both haptoglobin and ferritin is increased during inflammation (Ascenzi et al., 2005; Harrison et al., 1996).

Extracellular iron is tightly bound to a glycoprotein called transferrin in plasma (Weinberg, 1975). Transferrin is the primary source of iron for most cells in the organism. Cells express transferrin receptor on their surface that binds transferrin from the bloodstream, and the transferrin-receptor complex is internalized. In the endosome, pH eventually decreases, and Fe^{3+} dissociates from transferrin. Metalloreductases reduce iron which is transported into the cytosol by divalent metal transporter 1 (DMT1), while the receptor returns to the plasma membrane and apo-transferrin is released back to the bloodstream (Kawabata, 2019). Similar glycoprotein lactoferrin is found in milk, saliva, tears, mucosal secretions, and other liquids (Weinberg, 1975). Both transferrin and lactoferrin have antimicrobial activity against a broad spectrum of pathogens, including bacteria, fungi, and protists (Bruhn et al., 2015; Jenssen et al., 2009).

Neutrophils release lactoferrin in infected tissues and blood (Legrand et al., 2005). Another protein known for antimicrobial function due to depriving pathogens of manganese, iron, and zinc is human calprotectin. It is produced by various immune cells, especially neutrophils, and epithelial cells, and is released during infection (Zygiel et al., 2019). Fecal calprotectin level detection is used as a marker of gastrointestinal inflammation (Ayling et al., 2018).

During infection, the concentration of the serum iron is notably decreased, which is mediated by the peptide hormone hepcidin. Hepcidin regulates the iron transporter ferroportin. Ferroportin exports iron from duodenal enterocytes, macrophages recycling senescent erythrocytes, and iron storing hepatocytes. Hepcidin synthesis is upregulated at the transcriptional level by inflammatory stimuli, and when hepcidin binds to ferroportin, the latter is degraded, and the export of iron to plasma is diminished, resulting in decreased iron concentration in circulation (Ganz, 2009; Kawabata, 2019).

Furthermore, there is a mechanism to limit the amount of iron for intracellular pathogens of macrophages, such as *Mycobacterium*, *Salmonella,* and *Leishmania* spp. Iron is removed from phagolysosomes by natural resistance-associated macrophage protein NRAMP1 (homolog of DMT1), whose expression is upregulated in response to infection, and the loss-of-function mutations in this protein make the host more susceptible to diseases caused by these species (Cellier et al., 2007; Searle et al., 1998).

Another known mechanism of iron withdrawal by the host is the synthesis of siderocalin, also called lipocalin 2, which is employed to scavenge secreted microbial iron chelators siderophores (Ganz, 2009). Siderocalin is highly upregulated in mucosa during infection (Nelson et al., 2005).

To sum up, while nutritional immunity does not kill the pathogen, it efficiently slows its propagation, giving the organism time to raise other immune responses and eliminate the invader.

1.4.2 Iron acquisition in parasitic protists

Despite the variety of the ways used by the host for iron withholding, pathogens employ many strategies allowing them to successfully overcome this defensive mechanism, which

include reductive iron uptake, acquisition of iron from host iron-binding proteins using specific receptors or non-specific proteases, heme uptake, iron acquisition from siderophores, and phagocytosis or trogocytosis of whole host cells or their parts. Some organisms use a combination of several different approaches (Mach et al., 2020).

Two-step reductive iron uptake is well-known since it is used by the model yeast *S. cerevisiae*. The first step, Fe^{3+} reduction by a ferric reductase, increases iron solubility and results in iron release from various complexes or host proteins since they have a lower affinity to Fe^{2+}; in the second step, iron is imported to the cytoplasm by an iron transporter. This mechanism is employed by human cells in the transferrin cycle described above, and by many fungal pathogens, including *C. albicans*, *C. neoformans,* and *A. fumigatus* (Martínez-Pastor et al., 2020). The proteins participating in the reductive iron acquisition are highly conserved in fungi. They include plasma membrane metalloreductases (Fre1 and Fre2 in *S. cerevisiae* for ferric reductase) and the complex of ferroxidase, which re-oxidizes iron to ferric form, and permease, which imports iron to the cytoplasm (Fet3 for ferrous transport and Ftr1 Fe transporter, respectively). Ferroxidase is a copper-dependent enzyme, so high-affinity iron uptake in fungi requires copper, which will be discussed later. Copper-dependent ferroxidase-permease complex is a fungal characteristic feature; plants also use reductive iron uptake; however, they employ divalent iron transporter IRT1 (iron-regulated transporter) and do not require iron re-oxidation for high-affinity iron uptake (Walker et al., 2008).

Among parasitic protists, reductive iron acquisition is employed, for instance, by *L. amazonensis. Leishmania* does not require specific receptors for the host iron-binding proteins since it is an intracellular parasite residing in the macrophage phagolysosomes, where it can take up iron released from the host-endocytosed transferrin due to acidic pH. Huynh and colleagues (2006) found that *Leishmania* has an iron transporter homologous to *Arabidopsis thaliana* IRT1, which is localized to the parasite's plasma membrane and a lysosome-like compartment and is upregulated under iron deprivation. This protein called LIT1, for *Leishmania* iron transporter, can functionally complement high sensitivity to iron deprivation of the yeast mutant defective in both high and low-affinity iron uptake systems (*fet3Δfet4Δ*). The transporter is not necessary for the axenic growth of promastigotes and their differentiation to infective metacyclic promastigotes,

nor is it required for their differentiation to amastigotes in axenic culture. However, it is crucial for replication in macrophages, both cultured and *in vivo*. Null mutant *lit1Δ*/*lit1Δ* cannot cause cutaneous lesions in mice, although the amastigotes can survive within mice macrophages for weeks. LIT1 is predicted to have the same membrane topology as IRT1 and shares five conserved amino acid residues that were demonstrated to be essential for iron transport in both *Arabidopsis* and *Leishmania* transporter (Jacques et al., 2010). Another protein of *L. amazonensis* iron acquisition pathway was characterized later in the same laboratory by Flannery and colleagues (2011). *Leishmania* ferric reductase *LFR1* was identified as a homolog of *Arabidopsis* ferric reduction oxidase gene *FRO1*; the protein is upregulated under iron-depleted conditions and displays Fe^{3+} reductase activity, which was confirmed by its overexpression. *Lfr1Δ*/*lfr1Δ* knockouts show a decreased level of differentiation into infective promastigotes or amastigotes in axenic culture and reduced viability, do not replicate within macrophages, and display impaired virulence in mice.

Another kinetoplastid, the extracellular parasite *T. brucei*, employs a different iron acquisition mechanism. In the mammalian host, *T. brucei* invades the bloodstream; accordingly, its primary iron source is transferrin. *T. brucei* expresses a heterodimeric transferrin receptor at the surface of its flagellar pocket, the only area where endocytosis occurs, and transferrin is endocytosed upon binding to the receptor. After the endosome acidification, iron is released, the apoprotein is degraded, and the receptor is recycled back to the flagellar pocket surface. The transferrin receptor expression is upregulated under iron-depleted conditions (Taylor et al., 2010). Taylor and colleagues (2013) investigated how the released iron is exported from the endocytic compartment. They discovered a *T. brucei* homolog of mucolipin 1, a human Fe^{2+} channel, which they named TbMLP (mucolipin-like protein). Interestingly, this protein is from a different protein family than *Leishmania* LIT1. TbMLP is localized to the lysosome and, in contrast to the transferrin receptor, is not regulated by iron concentration. The authors could not generate a null mutant of *TbMLP* unless an ectopic copy of the gene was introduced, which suggests that the protein is essential. *TbMLP* knockdown trypanosomes have increased sensitivity to iron chelators and superoxide; the latter can be explained by the fact that *T. brucei* only expresses iron-dependent superoxide dismutase. TbMLP is proposed to mediate the

transport of divalent iron, since the human mucolipin 1 functions as a channel for Fe^{2+} (Taylor et al., 2010) and the trypanosome homolog shares the critical conserved amino acid residues (Taylor et al., 2013). A respective ferric reductase in *T. brucei* is not known, although its genome contains two putative ferric reductases (Taylor et al., 2010). My colleagues Mach et al. (2013) demonstrated that procyclic trypanosomes, which, in contrast to bloodstream forms, are not able to take up transferrin, acquire iron by reductive mechanism. However, the exact proteins involved in the process were not questioned. Possibly, *T. brucei* employs the same ferric reductase and iron channel in procyclic and bloodstream forms; at least T*bMLP* is constitutively expressed in both stages (Taylor et al., 2013); however, this hypothesis is yet to be elucidated.

A transporter from the ZIP family (ZRT, IRT-like proteins) was demonstrated to be involved in iron uptake in *P. berghei* (Sahu et al., 2014). The protein named ZIPCO (ZIP-containing protein) is localized to the plasma membrane of the liver stage parasite. It is not essential for the parasite replication in red blood cells and the development of the mosquito stages; however, the gene disruption reduces the infectivity of pre-erythrocytic stage parasites 1000 times. *ZipcoΔ* knockout extraerythrocytic forms show reduced cell size and impaired growth and viability *in vitro*, which results in delayed and decreased release of merozoites. The impaired size and growth can be reversed by adding iron to the growth medium and partly by zinc supplementation. Sahu and colleagues conclude that ZIPCO is an essential iron transporter for the liver stage development and suggest the existence of another transporter that can import iron to the parasite cells in the absence of ZIPCO and might also be used by the erythrocytic stages of *Plasmodium*. Despite the exceptionally high concentrations of heme in *Plasmodium* environment, there is still controversial evidence on whether the parasite uses only heme-derived iron or exploits other iron sources to satisfy its metabolic needs (Scholl et al., 2005). Interestingly, homologs of *NRAMP* (the previously mentioned family of proteins involved, for instance, in iron metabolism and nutritional immunity in mammals) are identified in the genomes of several *Plasmodium* species, although not yet studied (Mach et al., 2020).

Enteric amoeba *E. histolytica* can use “free” iron, both ferric and ferrous, for growth, which indicates that it has an iron importer(s) and possibly a ferric reductase, however, the proteins involved in iron transport remain unknown (López-Soto et al., 2009). *E. histolytica* has

a specific receptor for lactoferrin, which is endocytosed and trafficked to the acidic lysosomes where iron is probably released, and the protein is degraded by proteases. Interestingly, apo-lactoferrin (lactoferrin without iron) shows a concentration-dependent microbicidal effect on *E. histolytica* trophozoites. Also, *Entamoeba* may use hemoglobin, transferrin, and ferritin as iron sources. Investigations of *Entamoeba* receptors for host iron-binding proteins, endocytosis, and multiple lysosomal and secreted proteases are reviewed by López-Soto et al. (2009); however, it is not studied how the iron enters the cytoplasm after its release from the degraded proteins in the lysosomes.

Some protozoan parasites are capable of acquiring host heme. *Leishmania*, for instance, is unable to synthesize heme *de novo,* so it must acquire it from the environment. For heme acquisition, *L. amazonensis* employs the transporter LHR1 (*Leishmania* heme response), which was discovered based on its similarity with plasma membrane heme importer HRG4 (heme responsive gene) from *Caenorhabditis elegans* (Huynh et al., 2012). LHR1 is localized to the plasma membrane and lysosomes. *Leishmania* promastigotes grown under heme depleted conditions have significantly upregulated expression of *LHR1* at the transcriptional level and substantially increased heme uptake. Also, *LHR1* can support the growth of *S. cerevisiae hem1*Δ mutant (lacking the first enzyme of the heme biosynthesis pathway) on the hemin-supplemented medium. *LHR1* seems essential for L. amazonensis since the authors could not create a double knockout of the gene. In the single knockout (*LHR1/Δlhr1*) strain, heme uptake is reduced approximately twice. The genes highly similar in sequence to *LHR1* are present in the genomes of *T. cruzi* and *T. brucei*, suggesting that trypanosomes may use them for the host heme uptake (Huynh et al., 2012). *T. brucei* is known to express a receptor for the host haptoglobin-hemoglobin complex, which it uses to acquire heme (Vanhollebeke et al., 2008). *LHR1* ortholog may be required to import heme from the endocytic compartment.

E. histolytica can use heme as a sole iron source (Cruz-Castañeda et al., 2011). Iron-starved trophozoites prefer heme over hemoglobin and can acquire the cofactor from hemoglobin in the medium. *Entamoeba* secretes two heme-scavenging proteins, namely EHHMBP26 and EHHMBP45 (26 kDa and 45 kDa *E. histolytica* hemoglobin-binding proteins), which probably act as hemophores, facilitating heme acquisition. These proteins also bind

hemoglobin, although with lower affinity. The mechanisms of uptake and the subsequent utilization of the complex of these proteins with heme are not described yet. In the more recent research, Hernandes-Cuevas and colleagues (2014) found that iron modulates transcription of several putative *Entamoeba* transporter genes, sharing homology with genes involved in siderophore transport in bacteria and heme export in humans. Some of them may be used for uptake of EHHMBP-heme complexes, or, alternatively, they may be involved in the uptake of bacterial siderophores by *Entamoeba* or transport of yet unknown *Entamoeba* own siderophores.

Interestingly, *P*. *berghei* was demonstrated to incorporate both host-derived and *de novo* synthesized heme into mitochondrial cytochromes into hemozoin (Nagaraj et al., 2013). The double knockout of the first and last genes of the heme biosynthetic pathway showed no influence on intraerythrocytic stages of parasite growth in mice, although *de novo* heme synthesis is essential for parasite development in the mosquito and liver stages. This result indicates that intraerythrocytic stage cells can acquire host heme and that host-derived heme is sufficient to satisfy the parasite's need for this cofactor. The exact mechanism of heme delivery to *Plasmodium* cytoplasm and mitochondria remains unknown, as well as how heme synthesized by the parasite ends up in hemozoin (Nagaraj et al., 2013).

The mechanisms of iron acquisition by amphizoic amoebae *A*. *castellanii* and *N*. *fowleri* are understudied. Ramírez-Rico et al. (2015) demonstrated that crude extracts of *Acanthamoeba* and the conditioned culture medium contain proteases that can cleave lactoferrin, transferrin, and ferritin; however, it remains unknown how the released iron enters the cells.

1.4.3 Iron transport to mitochondria

Acquired iron must be effectively distributed between the cell compartments, and mitochondria play an essential role in cellular iron utilization. In addition to being the main energy-generating organelles of aerobic cells, mitochondria are the central sites for synthesizing iron-containing cofactors, namely iron-sulfur clusters and heme (Mühlenhoff et al., 2015; Zíková et al., 2016). Fe-S cluster assembly function remains in altered mitochondrion-related organelles such as *Trichomonas vaginalis* anaerobic hydrogenosomes (Tachezy et al., 2001, 2022), and even

in *Giardia intestinalis* mitosomes, extremely reduced mitochondria remnants (Jedelsky et al., 2011; Tovar et al., 2003). *E*. *histolytica* employs Fe-S cluster synthesis machinery of non-mitochondrial origin, which the parasite acquired by lateral gene transfer from bacteria, however, these proteins probably also function within the mitosomes (Maralikova et al., 2010). Despite the importance of iron utilization pathways in mitochondria for the whole cell metabolism, the mechanism of iron delivery to the organelle in protists is not fully understood, although it is studied in *S. cerevisiae*.

While the transport of small hydrophilic compounds through the outer mitochondrial membrane is probably non-specific and occurs via the number of outer membrane channels (Becker et al., 2018), the transfer across the inner membrane requires specific transporters (Palmieri et al., 2010). Lange and colleagues (1999) studied the mechanism of iron transport to ferrochelatase, the terminal enzyme of the heme synthesis pathway inserting iron into the protoporphyrin ring. They demonstrated that iron import to mitochondria is a membrane potential-dependent process and requires iron in reduced (ferrous) form. Surprisingly, they showed that ferrochelatase does not utilize the iron pool in the mitochondrial matrix and gets iron directly from the inner membrane; therefore, the enzyme is probably prevented from interaction with zinc, which is known as a strong competitive ferrochelatase inhibitor, and incorporation of zinc into the porphyrin ring instead of iron is avoided. Several years later, the exact transporters responsible for iron import to mitochondria were demonstrated. Interestingly, these proteins, Mrs3 and Mrs4, were already known by that time as suppressors of mitochondrial RNA splicing defects (hence the name *MRS* for mitochondrial RNA splicing) when expressed from high copy number plasmid (Wiesenberger et al., 1991), but their role in iron metabolism was only shown in 2002 by Foury and Roganti. They studied the function and regulation of Mrs3 and Mrs4 and demonstrated that the deletion of *MRS3* together with *MRS4* severely limited iron accumulation in mitochondria, while increasing the overall amount of iron in cells, and, conversely, overexpression of *MRS4* increased the mitochondrial iron content. Soon after that Muhlenhoff and colleagues (2003) showed a strong correlation between *MRS3/4* expression and the efficiency of heme synthesis and iron-sulfur cluster assembly both *in vitro* and *in vivo*, proving the direct involvement of Mrs3 and Mrs4 in mitochondrial iron import. Mrs3 and Mrs4 are

members of mitochondrial carrier family (MCF) and both display a characteristic tripartite structure, each part comprised of two transmembrane helices and a conserved motif; Mrs3/4 specificity for iron is provided by three conserved histidine residues in helices 1, 2 and 5 (Brazzolotto et al., 2014; Long et al., 2016). In the absence of both Mrs3 and Mrs4, a mitochondrial pyrimidine nucleotide transporter Rim2 (replication in mitochondria) can overcome the low iron-related phenotype co-transporting iron with pyrimidine nucleotides to the mitochondrial matrix. However, Rim2 does not seem to play an important role in the mitochondrial iron acquisition under normal physiological conditions and probably represents a low-affinity iron transport system (Froschauer et al., 2013).

Human cells employ mitochondrial iron transporters homologous to Mrs3/4 called mitoferrin 1 and 2 (Paradkar et al., 2009); moreover, the involvement of mitoferrins in iron homeostasis has been shown in other eukaryotes such as zebrafish, *Drosophila*, *Caenorhabditis* and mice (Brazzolotto et al., 2014).

MRS3/*4* and mitoferrin homologs are required for the normal growth of some pathogenic organisms. For instance, *C*. *albicans mrs4Δ*/*mrs4Δ* double knockout mutant has fragmented and aggregated mitochondria, grows poorly on media containing non-fermentable carbon sources, and demonstrates a decrease in filamentous growth rate under hyphae-inducing conditions (Xu et al., 2012). In addition, it exhibits hypersensitivity to oxidants and most metal ions. Similarly, *A*. *fumigatus mrsAΔ* null mutant shows severe growth defects under iron depletion and increased sensitivity to oxidative stress and antifungal drug itraconazole (Long et al., 2016). Moreover, *MRSA* deletion causes significantly decreased virulence in the immunocompromised murine lung infection model: the mortality rate of the mice infected with the *mrsAΔ* mutant was 60% lower than in the case of infection with the wild-type strain, and histopathological examination of lungs of the infected mice revealed that no fungal colonies were evident in *mrsAΔ* infection, suggesting that the host immune system was able to eliminate the pathogen. The disruption of *MRS3*/*4* gene of *C*. *neoformans* leads to slow growth under low iron conditions and increased sensitivity to hydrogen peroxide (Nyhus et al., 2002).

Homologs of *MRS3*/*4* and mitoferrins are highly conserved among trypanosomatids. In *L*. *amazonensis*, expression of mitoferrin homolog LMIT1 (*Leishmania* mitochondrial iron

transporter) is presumed essential for promastigote viability since *LMIT1* null mutants could not be generated (Mittra et al., 2016). *LMIT1*/*lmit1Δ* promastigotes (lacking one *LMIT1* allele), although demonstrating a normal log phase of growth, reach a stationary phase at a lower cell density and with significantly higher iron content in the cells; they are more susceptible to ROS toxicity than the wild-type cells. *LMIT1*/*lmit1Δ* promastigotes can undergo metacyclogenesis normally; however, metacyclic promastigotes cannot cause cutaneous lesions in mice since they cannot replicate as intracellular amastigotes after infecting macrophages. 48 hours after induction of differentiation into amastigotes axenically, *LMIT1*/*Δlmit1* mutant strain demonstrated a significant drop in mitochondrial membrane potential and reduced mitochondrial aconitase activity. Moreover, the mutant failed to upregulate Fe superoxide dismutase, an iron-dependent ROS detoxifying enzyme (Mittra et al., 2016).

Furthermore, TbMCP17, mitoferrin/*LMIT1* homolog of *T. brucei*, is essential for the survival of procyclic forms, which require proper mitochondrial function, but not bloodstream forms, which lack a functional respiratory chain (Mittra et al., 2016).

Homologs of *MRS3*/*4* and mitoferrins are found in the genomes of apicomplexan parasites *Plasmodium*, *Toxoplasma* (Sloan et al., 2021), and *Cryptosporidium* (Fung, 2019), although they have not been characterized yet. Also, mitoferrin homologs are present in the genomes of both *A*. *castellanii* and *N*. *fowleri* (Mach et al., 2020). No homologs of *MRS3*/*4* were found in the genomes of *Entamoeba*, *Trichomonas,* or *Giardia* (Mach et al., 2020), although all of them have Fe-S cluster synthesis machinery present in their mitochondria-related organelles, as it was mentioned previously. They might use iron transporters from other protein families or highly divergent mitoferrin homologs that are difficult to be identified by bioinformatic tools.

Interestingly, *E*. *histolytica*, which does not have a distinguishable homolog of *MRS3*/*4*, has a homolog of yeast mitochondrial metal transporters *MMT1*/*MMT2* (Mach et al., 2020). *MMT1* and *MMT2* were discovered by Li and Kaplan (1997) as genes that, when expressed from a multicopy plasmid, were able to restore the impaired growth of *erg25Δ* mutant with defective iron-dependent methyl sterol oxidase in low iron media. The corresponding proteins were later demonstrated to be mitochondrial iron exporters (Li et al., 2014). The phenotype of *mmt1Δmmt2Δ* resembles that of the strain with overexpressed *MRS3* and *MRS4* and, *vice versa*,

the overexpression of *MMT1* and *MMT2* mimics the phenotype of *mrs3Δmrs4* knockout. The authors propose that Mmt1 and Mmt2 reduce the level of mitochondrial free iron and thus protect mitochondria from oxidative damage (Li et al., 2020). *MMT1/2* homologs were found in higher plants (but not algae) where they probably have the same function as in yeast (Li et al., 2020; Vigani et al., 2019). No homologs were identified in vertebrates, however, murine protein *ABCB8* (ATP-binding cassette subfamily B member 8) from another protein family has mitochondrial iron exporting function and is required for mitochondrial iron homeostasis and maturation of cytosolic Fe-S proteins; reduced *ABCB8* level is associated with elevated susceptibility to oxidative stress (Ichikawa et al., 2012). The role of *MMT1/2* homolog in *E*. *histolytica* is not known. *MMT* homologs are also present in trypanosomatids, *A*. *castellanii*, *N*. *fowleri* (Mach et al., 2020), however, their function is not studied.

1.4.4 Role of transporters in iron storage and detoxification

As it was mentioned previously, iron is toxic in excess, so its distribution and storage must be carefully balanced. The mechanisms of iron storage and detoxification are generally less studied than the mechanisms of iron acquisition. The best-studied iron storage protein used by most organisms, including vertebrates, mollusks, worms, insects, plants, and bacteria, is ferritin (Harrison et al., 1996). It is a multi-subunit protein capable of binding thousands of Fe^{3+} ions, which serves for iron detoxification and as a reserve at the same time. However, few if any parasitic protists have functional ferritin, relying more on iron compartmentalization or extrusion from the cell.

In fungi, including *S*. *cerevisiae*, *C*. *albicans,* and *A*. *fumigatus*, excessive iron is stored in vacuole, where it is transported by the protein called Ccc1 (Ca^{2+}-sensitivity cross complementer), (Sorribes-Dauden et al., 2020). *S*. *cerevisiae ccc1Δ* mutant is highly sensitive to elevated iron concentrations and shows signs of oxidative damage. Ccc1 is a member of CCC1/VIT (vacuolar iron transporter) family, which also includes VIT1 from *A. thaliana*, a protein with the same function, namely iron sequestration to the vacuole (Ram et al., 2021). *VIT* homologs and VIT-like proteins are widely distributed among plants.

Besides the well-known detoxification mechanism based on the accumulation of heme in the form of hemozoin crystals, *Plasmodium* has been shown to use a VIT1 homolog for iron detoxification (Slavic et al., 2016). Codon-optimized truncated *PfVIT* from *P*. *falciparum* can restore the growth of *S*. *cerevisiae ccc1Δ* mutant on media with elevated iron concentrations. PfVIT mediates iron influx to vacuolar vesicles purified from *PfVIT*-expressing *ccc1Δ* yeast cells. *P. berghei* ortholog *PbVIT* is expressed in all stages of the parasite life cycle, and the GFP- or myc-tagged protein localizes to the endoplasmic reticulum. Successful knockout of the gene demonstrates a non-essential role for the transporter during asexual blood stages of *P*. *berghei*; however, knockout-infected mice have significantly lower parasitemia and longer survival time. Knockout of *PbVIT* has no adverse effects on transmission to mosquitoes and development in the vector; thus, the gene seems significant only for the blood and liver stages of infection.

VIT orthologs are present in other alveolates, including *Cryptosporidium* and *Toxoplasma* (Mach et al., 2020; Slavic et al., 2016). In *T*. *gondii*, VIT probably also mediates iron detoxification (Aghabi et al., 2021). *T. gondii* VIT is not essential, but it does reduce intracellular growth of the parasite, although it has no effect on extracellular survival in culture. *Toxoplasma vitΔ* knockout cells are hypersensitive to iron and accumulate ROS under elevated iron concentrations; knockout parasites cause milder disease as the survival of mice after the infection was significantly increased. The authors propose that *T*. *gondii* VIT changes its localization throughout the life cycle and at least partly localizes to the vacuolar-associated compartment, which might be used for iron storage. The role of VIT in *Cryptosporidium* is not yet studied.

A putative transporter sharing homology with the so-called VIT-like group of plant iron transporters (Ram et al., 2021) from *L. amazonensis* was studied by Laranjeira-Silva et al. (2018). The protein named LIR1 (*Leishmania* iron regulator) is localized to the plasma membrane in both promastigotes and amastigotes. Experiments with heterologous LIR1 expression in *A*. *thaliana* demonstrated that in the plant cells, the protein was also targeted to the plasma membrane; moreover, it significantly reduced the amount of intracellular iron. Next, the authors preincubated iron-depleted wild-type and double knockout (*lir1Δ*/*lir1Δ*) *Leishmania* cells for 90 minutes with radioactive iron isotope ^{55}Fe and analyzed the amount of retained isotope after 18 hours. The results showed that the double knockout retained significantly more iron than wild-

type cells. Thus, the authors proposed that LIR1 is an iron exporter. Interestingly, *lir1* null mutant cells cannot replicate in macrophages, and even the single (*lir1Δ*/*LIR1*) knockout impairs the intracellular *Leishmania* replication. The knockout of both *LIR1* copies dramatically ablates and postpones the development of cutaneous lesions in infected mice lowering the parasite load 10^6-fold compared to the wild type; the single gene knockout also decreases the severity of infection, reducing the parasite load 10^3-fold. These observations are surprising since the *Leishmania* environment seems to be depleted of iron, however, the authors do not suggest any explanation to this curious contradiction. Potential orthologs of *LIR1* are also present in other trypanosomatids, including, *T*. *cruzi* and *T*. *brucei*.

A *VIT1* homolog (different from *LIR1*) *TbVIT1* was identified in the proteome of *T*. *brucei* acidocalcisomes, acidic organelles rich in polyphosphates (Huang et al., 2014). The role of the TbVIT1 and its relation to iron metabolism has not been determined, although iron is detected in acidocalcisomes in many species. Knockdown of *TbVIT1* reduces the growth of both bloodstream and procyclic forms of *T*. *brucei* to about 60% of normal.

In yeast, iron mobilization from the vacuole in response to iron depletion occurs analogously to the reductive iron uptake: Fre6 metalloreductase reduces vacuolar Fe^{3+} to Fe^{2+}, and then high-affinity Fet5-Fth1 complex (paralogs of Fet3/Ftr1, Fth1 meaning Ftr homolog) transports it across the membrane. Low-affinity iron Smf3 transporter (suppressor of mitochondria import function) also participates in iron mobilization exporting iron to the cytoplasm (Sorribes-Dauden et al., 2020). However, it is unknown whether an iron mobilization system exists in parasitic protozoa and which transporters may be used in it.

A *VIT* homolog is present in the genome of *A*. *castellanii*. Interestingly, in the genome of *N*. *fowleri* a homolog of iron exporter ferroportin was found (Mach et al., 2020). Ferroportin mediates iron export in mammalian cells and some bacteria (Bonaccorsi di Patti et al., 2015; Coffey et al., 2017). The role of both proteins in iron detoxification is yet to be elucidated. *N*. *fowleri* non-pathogenic relative *Naegleria gruberi* is one of few protozoans with a ferritin homolog; surprisingly, it has a unique mitochondrial localization (Mach et al., 2018). *N*. *fowleri* also has a ferritin homolog in the genome, but the protein localization is not yet known (Mach et al., 2020).

Interestingly, there are several, although not many, investigations on iron transporters in the secretory compartment, which are found in animals and plants. For example, BCD1 (Bush and chlorotic dwarf) from *A. thaliana* is downregulated in iron deficiency and induced by excessive iron as well as abiotic stress and dark. The protein localizes to the Golgi complex and is supposed to modulate iron redistribution in plants, possibly by excreting excess iron from damaged plant cells under stress conditions (Seo et al., 2012). ZIP-family protein OsZIP11 from rice (*Oryza sativa*), also localized to the Golgi network, is upregulated at the transcriptional level under iron deficiency; mutations in the transporter cause reduced growth and lower fertility, and the authors propose its role in iron allocation and distribution (Zhao et al., 2022). Another ZIP-family transporter, ZIP13 from *Drosophila melanogaster*, transports iron to the endoplasmic reticulum and is crucial for dietary iron absorption in the fly's gut (Xiao et al., 2014). Whether parasitic protists also require iron loading into the secretory compartment and what transporters may be involved is a topic for future studies.

1.5 Copper is crucial for aerobic organisms

1.5.1 Copper and immunity

While the oxygenation of the atmosphere resulted in the oxidation of Fe(II) into insoluble hydroxide and salts, at the same time, it led to the emergence of soluble Cu(II) compounds from insoluble Cu(I). The presence of dioxygen created the requirement for a metal acting in the higher redox potential spectrum than the previously used iron cofactors, and copper started to be used by living organisms (Crichton et al., 2001). Although there are far fewer copper-requiring proteins than iron-dependent proteins in biological processes, copper is the second most used transition metal in redox reactions (Andreini et al., 2008). Copper is crucial for aerobic respiration, the key energy-deriving process of most aerobic species (Llases et al., 2019). Copper-dependent enzymes include, for instance, superoxide dismutase, multicopper oxidases, phenol oxidases, tyrosinase, galactose oxidase, and amine oxidase; most known copper-dependent enzymes are comprehensively reviewed in (Solomon et al., 2015).

Copper, as well as iron, is toxic when present in excess. Previously, it was presumed that the mechanism of copper toxicity is similar to that of iron and consists in the generation of ROS, mainly the hydroxyl radical in reaction with peroxide (Halliwell et al., 1984; Rainsford et al., 1998). Indeed, excess copper induces oxidative stress and upregulates antioxidant enzymes in different organisms (e. g. Thounaojam et al., 2012; Ozcelik et al., 2003). However, Macomber et al. (2007) demonstrated that copper rather protects *E*. *coli* from H_2O_2-mediated killing and does not catalyze significant oxidative DNA damage *in vivo*. Pham et al. (2013) studied the kinetics of reactions of nanomolar copper concentrations with H_2O_2 at pH 8. They demonstrated that interaction between Cu(I) and H_2O_2 results in the formation of a higher oxidation state of copper, Cu(III), while the rate of hydroxide radical production as a result of Cu(III) dissociation is relatively slow at pH 8.0 and is not an important oxidant in this system. Cu(III) reacts with the used substrates at much slower rates than $^{\bullet}OH$ (Pham et al., 2013).

Macomber and Imlay (2009) suggested an alternative mechanism of copper toxicity in *E. coli* based on damaging iron-sulfur clusters. Copper can displace ferrous iron from Fe-S clusters, impairing enzymes functions; high copper concentrations disintegrate Fe-S clusters completely. This mechanism is independent of oxygen; in fact, *E. coli* is more sensitive to growth inhibition by copper in anaerobic conditions. The primary targets of copper toxicity are the enzymes with Fe-S clusters exposed to solvents such as hydratases, while the enzymes with buried clusters are resistant to copper. Copper can damage Fe-S cluster-containing enzyme fumarase A even in the presence of ROS-detoxifying enzymes, indicating that ROS are not involved in copper-mediated damage. However, it is possible that the iron released from Fe-S clusters produces ROS via the Fenton reaction and is responsible for the oxidative damage to cells (Macomber et al., 2009). Later, copper was shown to destabilize Fe-S cluster formation in *Bacillus subtilis* and upregulate the expression of genes coding for Fe-S cluster assembly (Chillappagari et al., 2010). Copper can also impair Fe-S cluster assembly in human mitochondria by occupying the cluster binding site on Fe-S cluster assembly proteins or removing the Fe-S cluster bound to the proteins (Brancaccio et al., 2017). Garcia-Santamarina et al. (2017) demonstrated that iron-sulfur clusters are critical targets of copper toxicity in *S*. *cerevisiae* and *C*. *neoformans*. These findings confirm that this is indeed the primary mechanism of copper toxicity.

The mammalian immune system exploits the toxicity of copper in antimicrobial defense. Pathogen engulfed by a macrophage gets into a phagolysosome where it meets extremely harsh conditions with low pH, reactive oxygen and nitrogen species, proteases, and high copper levels – all to kill the invader (Besold et al., 2016). An increase in the copper amount in phagolysosomes was first demonstrated during *in vitro* infection of interferon-activated macrophages by *Mycobacterium* spp. (D. Wagner et al., 2005). It was later shown that *E*. *coli*, *M*. *tuberculosis,* and *Salmonella typhimurium* mutants lacking Cu^+-exporting ATPases required for copper detoxification were more susceptible to elimination by macrophages and less virulent (García-Santamarina et al., 2015). The acidic environment of the phagolysosome in combination with reactive oxygen and nitrogen species may exaggerate copper toxicity. Copper detoxification machinery is also crucial for the virulence of *C*. *neoformans* and *A*. *fumigatus* in lung colonization and *C*. *albicans* in the early stage of kidney infection (Ding et al., 2013; Mackie et al., 2016; Wiemann et al., 2017).

Microbicidal levels of copper in the phagolysosomes are supposed to be reached due to consecutive action of two copper transporters, CTR1, which is increased during infection and imports copper into the cell, and Cu^+-transporting ATPase ATP7A, which is also induced and relocalizes from the Golgi complex to the phagolysosome (Hodgkinson et al., 2012). Microbial homologs of both CTR1 and ATP7B will be discussed later.

Copper may be exploited in infection therapy. Copper complexes are efficient against *Leishmania* promastigotes and showed antimalarial activity (Duncan et al., 2012). Copper ionophores 8-hydroxyquinoline, thiomaltol, and disulfiram demonstrated fungicidal activity against *C*. *neoformans* in the presence of copper (Helsel et al., 2017). Thus, copper compounds may potentially be used as efficient antimicrobials, although more research is required in this field.

Parasites occupy different niches within their hosts; in some of those, copper may be not dangerously high but, quite contrary, limiting. It was shown that *C*. *neoformans* and *C*. *albicans* meet copper deprivation and induce copper import in the brain and late kidney infection, respectively, and copper uptake systems are necessary for full virulence (Mackie et al., 2016; Sun et al., 2014). Copper also might be limiting in the insect hosts of the parasites. The addition of

extracellular copper chelator bathocuproine disulfonate to mosquitoes' food source reduced the average number of oocysts per midgut of *Anopheles albimanus* mosquitoes susceptible to *P. berghei* by 40% (Maya-Maldonado et al., 2021). Thus, a tight balance between copper acquisition and detoxification is required for the parasites to reproduce within their hosts efficiently.

1.5.2 Transporters for copper acquisition

In 1994, Dancis and colleagues working with *S. cerevisiae* described and characterized the first high-affinity copper uptake protein, which they named simply copper transporter, or *CTR* (Dancis, Haile, et al., 1994; Dancis, Yuan, et al., 1994). Interestingly, they found this gene while searching for mutants with impaired ferrous iron uptake, thus demonstrating the connection between copper and iron metabolism. They proposed that copper is required for the proper function of Fet3 protein, which was subsequently characterized as a membrane multicopper ferroxidase involved in high-affinity iron uptake (Dancis, Haile, et al., 1994; Stearman et al., 1996). Later, *CTR3*, a functionally redundant homolog of *CTR1*, was discovered in yeast; its expression is blocked in mostly used laboratory strains due to the transposable element in its promoter (Knight et al., 1996). A double knockout mutant *ctr1Δctr3Δ* is used for complementation studies of copper transporters from other organisms. This mutant exhibits defective growth on media with non-fermentable carbon sources as it has impaired respiratory chain function due to the lack of copper (e. g. Sancen et al., 2003; Zhang et al., 2016).

CTR proteins transport Cu(I) and therefore require Cu(II) reduction, which is mainly carried out by ferric reductases as they can reduce both iron and copper (Hassett et al., 1995; Ohgami et al., 2006). *CTRs* are usually comprised of three transmembrane domains and act as homotrimers (Dumay et al., 2006; Logeman et al., 2017; Nose et al., 2006).

The expression levels of high-affinity copper transporters have been shown to change in response to environmental copper concentration fluctuations. *S. cerevisiae* Ctr1 and Ctr3 proteins are highly upregulated by copper depletion (Dancis, Haile, et al., 1994; Knight et al., 1996). In *C. neoformans*, the levels of *CTR1* and *CTR4* transcripts are increased after adding a copper chelator to the growth medium and decreased or almost absent in copper-repleted conditions (Ding et al., 2011). Similarly, the transcript levels of *C. albicans CTR1* decrease in

response to elevated copper concentration in the medium (Mackie et al., 2016). In addition, *CTR1* is induced by iron limitation, consistent with the previously mentioned connection between iron and copper metabolism. Both *C. albicans* and *C. neoformans* mutants impaired in high-affinity copper uptake show reduced virulence in infection models (Ding et al., 2011; Mackie et al., 2016).

CTR homologs are found in the genomes of organisms belonging to all eukaryotic kingdoms, including fungi, animals, plants, and protozoa (Dumay et al., 2006). The function and regulation of copper transporters in fungi, including pathogenic, have been investigated and thoroughly reviewed in Smith et al. (2017); copper uptake in parasitic protists is much less studied.

Choveaux et al. (2012) identified two presumable *CTR* homologs in the *P. falciparum* genome and studied one of them, *CTR1* (PF14_0369). They demonstrated that the protein is expressed in the asexual stages of the parasite and is localized to the erythrocyte and parasite plasma membrane. Furthermore, it binds copper *in vitro* and *in vivo* when expressed in *E. coli*. However, the copper transporting function was not demonstrated, and the function of the protein remains disputable. The second presumable *P*. *falciparum* copper transporter paralog, *CTR2* (PF14_0211), was not studied. Orthologs of both *P*. *falciparum CTR1* and *CTR2* are present in the genome of *P*. *berghei*. In their extensive study of *P. berghei* transporters, Kenthirapalan et al. (2016) demonstrated that the deletion of *CTR1* results in normal mosquito midgut colonization but markedly reduces colonization of salivary glands by sporozoites. Natural transmission from mosquitoes to mice is also impaired. The *ctr2Δ* null mutant shows normal sporozoite production but impaired natural transmission, which could be alleviated by intravenous, but not subcutaneous, syringe delivery of sporozoites. The liver-stage development of the *ctr2Δ* parasites, as well as their gliding motility, are normal. Thus, *CTR* paralogs in *Plasmodium* species seem to have at least partly different roles during the parasite life cycle and seem critical for the transmission from mosquito to mammal host, but not for liver or intraerythrocytic stages.

Although *CTRs* were not found in *T. brucei*, trypanosomes express several copper-containing proteins, including cytochrome c oxidase, indicating another way of copper acquisition (Isah et al., 2020). There is no available information about copper transporters in *Acanthamoeba* or *Naegleria* species.

1.5.3 Intracellular copper trafficking

1.5.3.1 Copper trafficking to mitochondria

Respiration, the key energy metabolism process in aerobic cells, requires copper for its function. Three copper ions are used as cofactors for the terminal enzyme of the respiratory electron transport chain, cytochrome *c* oxidase (COX), a large multi-subunit membrane complex (Steffens et al., 1987). Cox1 subunit incorporates one copper in the so-called Cu_B site, while Cox2 contains a binuclear Cu_A site requiring two copper ions (Horn et al., 2008). Despite the central role of respiration in the metabolism of aerobic organisms, the process of COX metalation with copper is not fully understood even in *S. cerevisiae*. Several different copper chaperones are employed to load COX with copper properly. In yeast, copper chaperone Cox11, anchored to the inner mitochondrial membrane, delivers copper to Cox1, and, similarly, membrane chaperone Sco1 (suppressor of cytochrome *c* oxidase deficiency) supplies copper to Cox2. Sco1 was first identified as a multicopy suppressor of the *cox17Δ* null mutant. Cox17 is a soluble chaperone required for the proper functioning of Cox11 and Sco1; it is localized predominantly to the intermembrane space and partly in the cytosol (Horn et al., 2008). Due to this dual localization, Cox17 was previously thought to shuttle copper between the cytosol and the intermembrane space; it was later demonstrated that Cox17 is functional even when tethered to the inner mitochondrial membrane, indicating that its role is confined to the mitochondrial intermembrane space (Maxfield et al., 2004). Two Cox17 homologs, small soluble proteins Cox19 and Cox23, have a similar cellular localization to Cox17 (mainly in the intermembrane space and partly in the cytosol) and are necessary for proper COX function (Barros et al., 2004; Nobrega et al., 2002). Cox19 has been described as an interaction partner of Cox11 that is required for maintaining the cysteine residues in Cox11 in a functional fully reduced state (Bode et al., 2015). The role of Cox23 has not been characterized yet.

The mechanism of copper delivery to these chaperones is not clear. Paul Cobine et al. (2004) showed that only a small fraction of the mitochondrial copper pool is associated with known copper-containing mitochondrial proteins, while the rest is bound to an unknown low molecular weight anionic ligand. Most mitochondrial copper is localized to the mitochondrial

matrix, which is surprising since there are no known copper-dependent proteins in the matrix (Cobine et al., 2004). In yeast, copper import into the matrix is mediated by the Pic2 transporter (Vest et al., 2013). Pic2 was previously characterized as a phosphate transporter, hence the name $\underline{P_i}$ carrier isoform 2 (Hamel et al., 2004). Interestingly, *SLC25A3*, the closest Pic2 homolog in mammalian cells, has a dual function and can transport both copper and phosphate into the mitochondrial matrix (Boulet et al., 2018), whereas the yeast Pic2 paralog Mir1 transports phosphate but not copper (Zhu et al., 2021). Yeast iron transporter Mrs3 has also been shown to mediate copper import into mitochondria (Vest et al., 2016). *Pic2Δ* null mutant has a growth defect on copper-limited media with a non-fermentable carbon source, and double knockout of both *PIC2* and *MRS3* (but not MRS4) exaggerates this phenotype (Hamel et al., 2004; Vest et al., 2016). Moreover, *pic2Δmrs3Δ* accumulates less copper in mitochondria than the single knockouts (Vest et al., 2016).

The Cu-ligand pool in the mitochondrial matrix is dynamic and depends on the copper concentration in the growth medium. Presumably, it is the source of copper for COX; however, how it is mobilized to the intermembrane space, where the COX metalation occurs, remains unknown. (Cobine et al., 2004, 2006).

The information about copper trafficking to mitochondria in protozoa is even scarcer. Homologs of both copper-containing cytochrome *c* oxidase subunits *COX1* and *COX2,* as well as the above-mentioned chaperones *SCO1*, *COX11*, *COX17*, and *COX19,* were found in the genome of *P*. *falciparum* (Choveaux et al., 2015). Recombinant PfCox17 with GST tag and PfCox11 with MBP tag can bind Cu(I) *in vitro* and in *E*. *coli* (Choveaux et al., 2015; Salman et al., 2022). The expression of native PfCox17 was demonstrated in the ring, trophozoite, and schizont stages *in vitro* (Choveaux et al., 2015).

Homologs of *COX1* and *COX2*, *SCO1*, *COX11*, *COX17*, and *COX19* are present in the genomes of several *Trypanosoma* species, including *T. brucei* (Isah et al., 2020). A homolog of *PIC2* is also identified. However, considering that the mentioned above Mir1 (a paralog of Pic2) from yeast is a phosphate carrier that does not transport copper, the role of *Trypanosoma* Pic2 homolog needs to be carefully elucidated before conclusions can be drawn about its role in copper trafficking.

1.5.3.2 Copper transport to the secretory compartment

Copper delivery to the secretory compartment is comprehensively studied in *S. cerevisiae* since it is required for high-affinity iron uptake. In yeast, it is mediated by Cu^{+}-translocating ATPase called CCC2. It was identified by Fu, Beeler, and Dunn (1995) when they searched for the genes that could overcome calcium sensitive growth of *csg1Δ* mutant, hence the name *CCC2* meaning cross-complementer of Ca^{2+}-sensitivity. Fu and colleagues discovered that the gene shared considerable homology with P-type ATPases that transport copper, namely human *ATP7A* and *ATP7B* and *copA* of *Enterococcus hirae*. Mutations in *ATP7A* and *ATP7B* genes can cause Menkes and Wilson diseases, respectively. Moreover, Fu and colleagues demonstrated that *ccc2Δ* mutant required increased concentrations of copper for growth. Yuan et al. in the same year (1995) showed that the *CCC2* gene function was compulsory for high-affinity iron uptake, similarly to the previously described CTR function, and the *ccc2Δ* mutant's defect in growth on media containing non-fermentable carbon sources could be restored by adding either copper or iron to the growth medium. As the next step, Fu and colleagues determined that Ctr1 and Ccc2, acting consecutively, transported copper first across the plasma membrane and then out of the cytosol across one or more other cell membranes, finally delivering it to the multicopper oxidase Fet3. Based on the observations that mutations in several post-Golgi sorting proteins caused the same phenotype due to impaired loading of Fet3 with copper, they presumed post-Golgi localization of Ccc2. Yuan, Dancis, and Klausner (1997) confirmed the localization of Ccc2 to late or post-Golgi compartment by analyzing the Fet3 function and copper load in yeast strains with mutations of various Golgi proteins and imaging the distribution of fluorescently labeled Ccc2.

C. albicans has two Ccc2 paralogs. One of them, CaCrp1, is employed for copper detoxification and will be discussed later in the text, while the other, CaCcc2, has a similar function to *S. cerevisiae* Ccc2 and can complement the *ccc2Δ* yeast mutant growth defect in iron-depleted medium (Weissman et al., 2002). CaCcc2 is strongly upregulated at mRNA level after iron starvation induction by ferrozine; deletion of one allele does not affect the growth of the cells under iron-depleted conditions, whereas homozygous mutant fails to grow on iron-depleted medium due to impaired high-affinity iron uptake. However, the pathogenicity of the null mutant is not altered, probably since *C. albicans* can use other iron sources such as hemin or hemoglobin

independently of the ferroxidase-permease complex, which requires Ccc2 function. GFP-tagged CaCcc2 is functional and has a punctate distribution pattern similar to Ccc2 in *S. cerevisiae*, indicating probable trans-Golgi localization.

Similar to *S. cerevisiae* and *C. albicans*, the *ccc2Δ* mutant of *C. neoformans* shows impaired growth in the iron-depleted medium, indicating a similar copper-dependent iron uptake system (Walton et al., 2005). Disruption of *Cryptococcus CCC2* gene also diminishes its ability to produce melanin, which is a virulence factor of the pathogen, since laccase, the key enzyme of melanin biosynthesis, is a multicopper oxidase and, similarly to Fet3, acquires copper cofactor in Golgi apparatus (Walton et al., 2005).

Cu^+-transporting ATPases are present in phylogenetically different clades, including fungi such as *S. cerevisiae* and *C. albicans*, apicomplexans *P. falciparum,* and *Cryptosporidium*, kinetoplastids *Trypanosoma* and *Leishmania*, *N. fowleri*, *A. castellanii*. However, they appear to have various functions in the cells, including detoxifying functions, which will be discussed later.

Cu^+-transporting ATPase has also been described in *P. falciparum*. Rasoloson et al. (2004) suggested that the parasite employs ATPase to avoid copper toxicity by extruding it from the cell. According to this study, PfCuP-ATPase is localized not only to the parasite plasma membrane but also to the plasma membrane of the infected erythrocyte. They also showed that the copper content in the red blood cells infected with plasmodia is lower than in uninfected erythrocytes, which, however, contradicts the data received by Marvin et al. (2012), who showed that infected erythrocytes contain twice more copper than uninfected ones. However, the two groups used different methods and *Plasmodium* stages for copper content determination: Rasoloson et al. studied rings and trophozoites, while Marvin and colleagues used late trophozoite and schizont stage parasites, making the results difficult to compare. Further research is required, especially considering that although PfCuP-ATPase has been demonstrated to bind copper, the copper-transporting function has not been proved. In a later study, Kenthirapalan et al. (2014) demonstrated that *P. berghei* Cu^+-transporting ATPase (CuTP) is required for parasite fertility and thus for transmission to the mammal host. The number of oocysts in *cutpΔ* null mutant was dramatically reduced, and the transfer of the parasite to a mouse host was severely impaired due to reduced exflagellation of male gametes (10-15% activity compared to wild type). Female

gametes also have a fertility defect. CuTP with a red fluorescent protein tag was localized to vesicle-like structures inside the cell cytoplasm throughout the parasite life cycle, which, according to the authors' suggestion, may be an unknown storage vacuole, an acidocalcisome, or part of the Golgi complex. They propose that the primary role of the protein is copper storage or redistribution, although it cannot be ruled out that in intracellular life stages the protein has a detoxifying function.

P-type ATPase expression has also been demonstrated in the bloodstream forms of *T. brucei brucei* and *T. congolense*. In *T. b. brucei*, the ATPase was localized to subcellular vesicles, which may represent the secretory compartment, and probably in the cell membrane. The N-terminal domain of the protein has been demonstrated to bind copper, but the function of the protein has not been confirmed (Isah et al., 2020).

1.5.4 Copper detoxification

Since copper is toxic in excess, there are various strategies for keeping the concentration of free copper in the cells close to zero. Probably the best-known way of detoxifying metals, including copper, is the use of metallothioneins. Metallothioneins are small heterogeneous cysteine-rich proteins binding metals such as cadmium, zinc, or copper with high stoichiometry. The first described metallothionein was a cadmium-binding protein purified from intoxicated horse liver, and later on, metallothioneins were described in many evolutionally distinct organisms, including worms, mollusks, insects, fungi, plants, bacteria, and others. Interestingly, proteins from different groups do not share sequence homology (Capdevila et al., 2011). The role of copper metallothioneins of *S. cerevisiae* (Cup1, Crs5) and *C. neoformans* (Cmt1, Cmt2) in copper detoxification is quite well characterized. Cup1 (derived from *cuprum*), the main protein conferring copper tolerance in *S. cerevisiae*, binds seven copper ions (Narula et al., 1993). Another non-homologous metallothionein, Crs5 (copper-resistant suppressor), binds more copper per protein, 11 or 12 copper ions; however, it plays only a minor role in copper detoxification. Cup1 shows a higher copper-binding affinity compared to Crs5. The yeast genome usually contains several copies of the *CUP1* gene; also, *CUP1* promoter responsiveness is higher than that of *CRS5*, so *CUP1* is much more upregulated by increased copper concentrations than

CRS5 (Jensen et al., 1996). It was later demonstrated that in addition to its copper-binding ability, Crs5 can coordinate 6-7 zinc ions and is, in fact, required for zinc detoxification (Pagani et al., 2007). Copper metallothioneins of *C. neoformans* Cmt1 and Cmt2 exhibit remarkably high copper-binding capacity, coordinating 16 and 24 copper ions, respectively, and although these two proteins have redundant functions, the presence of at least one of them is essential for the pathogen's virulence (Ding et al., 2013).

Another mechanism of copper detoxification used by various organisms is the metal expulsion from the cell using Cu^+-translocating P-type ATPase. In 2000, two groups independently demonstrated that a Cu^+-transporting ATPase (CRP1, for copper resistance-associated P-type ATPase) is the major determinant of resistance to elevated copper concentrations in *C. albicans* (Riggle et al., 2000; Weissman et al., 2000). *CRP1* is a homolog of the above-described *CCC2*; however, it has a different function and is localized to the plasma membrane. The sensitivity of *crp1Δ*/*crp1Δ* knockout mutant to copper is 40-fold higher compared to the wild type, and increased copper highly upregulates CRP1 at the transcriptional level (Weissman et al., 2000). Although *C. albicans* also has a metallothionein (named Cup1 analogously to *S. cerevisiae*), it plays a minor role in the detoxification of copper, binding residual metal in the cytoplasm (Riggle et al., 2000; Weissman et al., 2000).

The first heavy metal ATPase identified in protists is a Cu^+-transporting ATPase in apicomplexan parasite *Cryptosporidium parvum* (LaGier et al., 2001). The protein, named CpATPase2, is expressed in sporozoites and asexual intracellular stages of the parasite, and its N-terminal part, containing a presumed heavy metal binding domain, can bind Cu^+ with the proposed stoichiometry of 1:1. The diffuse and patchy localization of CpATPase2 in *Cryptosporidium* sporozoites led the authors to suggest that the transporter may be present in the plasma membrane and also associated with membranes of some cytoplasmatic organelles, similarly to human copper ATPases, and propose the copper extrusion function of the protein. Since *Cryptosporidium* is an enteric pathogen, the mechanism of copper detoxification by expulsion agrees with the proposed concept of Weissman et al. (2000): in their work describing the formerly mentioned *Candida* CRP1, they noted that many bacteria with known copper expulsion ATPases are commensal or pathogenic enteric organisms, and found that under the

acidic anaerobic conditions, which characterize a part of the digestive system, copper becomes much more toxic. The latter fact complies with the observations of Beswick et al. (1976), who demonstrated that copper is more toxic to *E*. *coli* grown in anoxic conditions. Weissman proposes that copper extruding ATPase may confer higher resistance to copper than metallothioneins because it acts catalytically rather than stoichiometrically.

Recently, the same mechanism of copper detoxification was demonstrated in *Leishmania major*, an intracellular parasite residing in phagolysosomes of macrophages. Overexpression of LmATP7, the Cu^+-translocating ATPase of *L. major*, provides the parasite with elevated tolerance to toxic copper concentrations, higher survival level in macrophages, and increased virulence compared to the wild type, whereas all these parameters are significantly decreased in heterozygous knockout (Paul et al., 2021). The ATPase localizes primarily to the plasma membrane, although it is also present in intracellular membrane structures, where it might perform other functions apart from detoxification. Paul and colleagues proposed that LmATP7 could also deliver copper to the secretory compartment providing it to essential enzymes, in parallel with mammalian copper ATPases ATP7A and ATP7B, which transport copper to the secretory pathway and participate in copper detoxification. This hypothesis is based not only on the localization of LmATP7 but also on the repeated failures to generate a complete knockout, which suggests an essential function for LmATP7.

In *T. cruzi*, a homolog of Cu^+-transporting ATPase is upregulated at the transcriptional level in the intracellular stage in mammalian host cells compared to the extracellular stage in the insect vector (Meade, 2019). The intracellular stage must survive for some time in the phagosomal compartment with excessive copper levels, and the upregulation of Cu^+-translocating ATPase may indicate its role in detoxification.

2. Aims and objectives

1) To study the iron uptake system employed by *N. fowleri*

2) To elucidate the iron acquisition and detoxification mechanisms in *A. castellanii*

3) To characterize the *N. fowleri* transporters involved in the copper acquisition and detoxification

3. Contribution to publications

The thesis is based on the following articles (listed according to the author's logic):

1) Arbon, D., Ženíšková, K., Mach, J., Grechnikova, M., Malych, R., Talacko, P., & Sutak, R. (2020). Adaptive iron utilization compensates for the lack of an inducible uptake system in *Naegleria fowleri* and represents a potential target for therapeutic intervention. *PLoS Neglected Tropical Diseases*, *14*(6), 1–25. doi: 10.1371/journal.pntd.0007759

Preparation of transcriptomic libraries, data analysis.

2) Grechnikova, M., Arbon, D., Ženíšková, K., Malych, R., Mach, J., Krejbichová, L., Šimáčková, A., & Sutak, R. (2022). Elucidation of iron homeostasis in *Acanthamoeba castellanii*. *International Journal for Parasitology*, *52*(8), 497–508. doi: 10.1016/j.ijpara.2022.03.007

Proteomic data analysis, *Acanthamoeba* transfection, confocal microscopy, ^{55}Fe radioisotope uptake experiments, expression in yeast, qPCR, manuscript preparation.

3) Ženíšková, K., Grechnikova, M., & Sutak, R. (2022). Copper metabolism in *Naegleria gruberi* and its deadly relative *Naegleria fowleri*. *Frontiers in Cell and Developmental Biology*, *10*, 1–17. doi: 10.3389/fcell.2022.853463

Bioinformatic analysis of CTRs, experimental work with yeast, confocal microscopy, qPCR.

4) Grechnikova, M., Ženíšková, K., Malych, R., Mach, J., & Sutak, R. (2020). Copper detoxification machinery of the brain-eating amoeba *Naegleria fowleri* involves copper-translocating ATPase and the antioxidant system. *International Journal for Parasitology: Drugs and Drug Resistance*, *14*, 126–135. doi: 10.1016/j.ijpddr.2020.10.001

ICP-MS sample preparation, qPCR, proteomic data analysis, expression in yeast, manuscript preparation.

4. Results, conclusions, and future prospective

For successful propagation in the human body, parasites have to overcome the iron deprivation caused by nutritional immunity, and iron uptake machinery is crucial for the virulence of many pathogens. Also, some niches in the human organism, including the brain, are supposed to be depleted of copper, another crucial metal. At the same time, both iron and copper are toxic when present in excess, and the parasites must have efficient mechanisms to avoid this toxicity. The means of metal transport in amphizoic amoebae are generally unknown. It was shown that *A. castellanii* can cleave the host iron-containing proteins (Ramírez-Rico et al., 2015); however, the proteins responsible for iron import to the cytoplasm are not studied. Thus, this work aimed to investigate the transporters participating in iron and copper acquisition, distribution across the cell compartments, and detoxification in *N. fowleri* and *A. castellanii*.

First, we studied the iron uptake system in *N. fowleri.* To determine whether *Naegleria* employs a reductive mechanism of iron uptake, we compared the uptake of ^{55}Fe radioisotope in the oxidized and reduced form. Our results suggest that *N. fowleri* has a preference for divalent iron, indicating the presence of a reductive step. Surprisingly, we could not observe any increase in iron uptake, neither ferric nor ferrous, by iron-starved cells compared to the control. The activity of ferric reductase was not changed either. We also examined whether iron starvation can stimulate phagocytosis of bacteria, which might be the primary source of iron for amoebae in nature. However, the phagocytic activity of iron-depleted cells was even lower than in control.

To get a hint about proteins participating in iron acquisition, we performed the proteomic analysis of the whole-cell lysates and the total membrane fraction of the amoebae grown under iron-limited and iron-supplemented conditions. We observed the changes in expression of multiple iron-dependent proteins; however, we did not detect any transporters or metalloreductases that could serve for iron uptake. Considering that membrane proteins may be under-represented in proteomic analyses due to losses during sample preparation (Tan et al., 2008), we additionally performed the whole-cell transcriptomic analysis.

In general, the transcriptomic data did not correlate with the results of proteomic analysis, indicating that most changes in protein expression in iron-starved *N*. *fowleri* cells are likely to happen at the post-translational level. Post-transcriptional regulation of important developmental processes has also been demonstrated in *Leishmania donovani* (Arvan et al., 2002). We observed the transcripts of two ZIP-family transporters (NF0080770 and NF0002900) that share homology with *L*. *amazonensis* iron importer *LIT1* and *Arabidopsis IRT1* (Huynh et al., 2006; Jacques et al., 2010). Interestingly, the five amino acid residues essential for LIT1 and IRT1 iron transport are conserved in both NF0080770 and NF0002900. However, none of these genes were regulated by iron availability. Furthermore, we observed the transcripts of ferroportin, an iron exporter of bacteria and mammals that we propose might participate in iron detoxification; however, it was not regulated by iron either. Since there are no established methods for genetic manipulations of *Naegleria* species, we cannot knock out these genes to observe the corresponding phenotype. Heterologous ferroportin expression in yeast mutant did not show functional complementation (unpublished data). The absence of regulation by iron does not allow us to make any conclusions about the functions of these genes.

Our findings suggest that *N. fowleri* fails to stimulate iron acquisition in response to iron starvation. Instead, *Naegleria* rebalances the iron homeostasis in favor of more crucial mitochondrial processes, downregulating the iron-demanding non-essential proteins in the cytoplasm. Importantly, this conclusion is consistent with the fact that the only presumable iron transporter significantly upregulated in iron-depleted cells was the mitochondrial Fe^{2+} importer homologous to yeast Mrs3/4 and human mitoferrin. It was the only iron transporter we observed in the proteomic data; the proteins participating in *N*. *fowleri* iron uptake remain enigmatic.

A. *castellanii* has an entirely different response to iron depletion. The whole-cell proteomic analysis demonstrated the upregulation of a ferric reductase from the STEAP family and a divalent metal transporter from the NRAMP family in iron-depleted cells, proteins homologous to human STEAP3 and DMT1 (NRAMP2), which supply most body cells with iron through the transferrin cycle. We overexpressed these proteins in acanthamoebae with the GFP tag and determined that they localize to the membranes of multiple acidified digestive vacuoles with endocytosed bacteria and liquid medium. In contrast to *N*. *fowleri*, iron-starved *A*. *castellanii*

cells acquired ^{55}Fe radioisotope at a significantly higher rate than iron-supplemented cells, although the total pinocytosis rate was reduced. Interestingly, we identified a novel protein in the proteomic data with no homologs in other organisms. The protein, which we named IDIP, was significantly upregulated in iron-depleted cells and increased the rate of iron uptake when overexpressed. Our assumption that it is a transcription regulator of iron uptake-responsible genes proved wrong, as the transcript levels of both ferric reductase and NRAMP remained unchanged in cells overexpressing GFP-tagged IDIP, while the iron uptake was increased. Our later yet unpublished data suggest that this protein may regulate endocytosis.

The most downregulated protein in iron-depleted cells was a divalent transporter from Ccc1/VIT family. The proteins from this family participate in iron detoxification in different organisms removing excess iron from the cytosol. VIT from *Acanthamoeba* restored the growth of iron-sensitive yeast mutant on the medium containing the inhibitory iron concentration. We expressed this protein with the GFP tag, and surprisingly, according to our observations, it was localized to the same digestive vacuoles as the ferric reductase and NRAMP. Later, we demonstrated the colocalization of coexpressed VIT and NRAMP with GFP and RFP tags, respectively (unpublished data). We propose that the amoebae balance the abundance of iron importer NRAMP and exporter VIT in dependence on iron availability.

Thus, despite the similar morphology and lifestyle of studied amoebae, their mechanisms of iron homeostasis under iron-limiting conditions are entirely different. While both employ a two-step reductive mechanism of iron acquisition, *N*. *fowleri* does not induce the iron uptake but balances available iron in favor of vital mitochondrial processes, and *A*. *castellanii* upregulates the iron uptake system and downregulates the iron exporter, thereby enhancing iron import.

Our study of copper metabolism in *N*. *fowleri* began with a search for *CTR* homologs in the genome. We identified two potential copper transporters, NF0078940 and NF0118930, and expressed them in yeast *ctr1Δctr3Δ* mutant. One of the genes, NF0078940, rescued the growth of the mutant on the medium with a non-fermentable carbon source, indicating a copper import function. To determine their localization, we expressed both proteins in yeast with a GFP tag. While NF0078940 was localized to the plasma membrane, consistent with its role as a copper importer, the second presumed CTR, NF0118930, was stuck in the endoplasmic reticulum.

Retention of membrane proteins in ER occurs when they do not pass the quality control mechanisms, which might often happen with heterologously expressed proteins, even when they are fully functional (Arvan et al., 2002; Villalba et al., 1992). Thus, we propose that NF0078940 is a high-affinity copper importer, while the function of NF0118930 is unclear. It may be another high-affinity importer, like in *S*. *cerevisiae*, which has redundant Ctr1 and Ctr3, or represents a low-affinity copper import system, or it may mobilize copper from some storage compartment within the cell like yeast Ctr2.

Next, we analyzed the proteomic response of *N*. *fowleri* to copper deprivation and toxic copper concentration. *N*. *fowleri* seems to have very efficient copper uptake and/or homeostasis mechanisms as its growth was hardly affected by extracellular copper chelator, in contrast to its non-pathogenic relative *N*. *gruberi*. We did not observe the presumed CTRs in the whole-cell proteomic data, either in low copper concentration or in control or toxic conditions; however, as mentioned above, it is not surprising as membrane proteins may not be detected. We assessed the transcript levels of the CTRs by RT-qPCR, expecting the upregulation of one or both genes in response to copper deprivation and downregulation in response to high copper, as in *C. neoformans* or *C. albicans* (García-Santamarina et al., 2015; Mackie et al., 2016). However, neither was regulated by copper availability at the transcriptional level. If the expression of transporters is changed, it happens post-translationally, similar to the response to iron deprivation.

N. *fowleri* can survive copper concentrations around 1 mM without changing growth rate or cell density, indicating an effective copper detoxification mechanism. We demonstrated that the defense strategies include copper efflux mediated by a Cu^{+}-translocating ATPase (NfCuATPase) and upregulation of the expression of various antioxidant proteins. Expulsion of excessive copper is employed by *C*. *albicans*, *L*. *amazonensis*, and presumably *T*. *cruzi*. *N*. *fowleri* copper ATPase restored the copper-sensitive *cup2Δ* yeast mutant growth on the medium with elevated copper concentration. Moreover, it reduced the amount of copper in the yeast cells, indicating copper export rather than compartmentalization within the cell. Interestingly, NfCuATPase was upregulated at both protein and transcript levels.

Efficient coping with limited copper concentrations and the high copper tolerance provided by the copper-exporting ATPase in combination with the antioxidant system can be advantageous for *N*. *fowleri* both in the natural environment and in the host. However, it is implausible that any of these strategies appeared as the result of evolutionary benefits for the pathogenicity since human brain infection is infrequent and a dead end for *N*. *fowleri*.

The investigation of *A*. *castellanii* response to copper deprivation and toxicity is now in progress. Our preliminary data suggest that acanthamoebae cope less well with elevated copper concentration than *N*. *fowleri* and start to encyst, although they also upregulate a presumable copper-exporting ATPase. We want to compare the strategies that both amoebae employ to overcome copper deprivation and toxicity. It will be interesting to investigate whether these strategies differ as much as their responses to iron deficiency.

5. References

Aghabi, D., Sloan, M., Dou, Z., Guerra, A. J., & Harding, C. R. (2021). The vacuolar iron transporter mediates iron detoxification in *Toxoplasma gondii*. *BioRxiv*. doi: https://doi.org/10.1101/2021.09.08.458725

Andreini, C., Bertini, I., Cavallaro, G., Holliday, G. L., & Thornton, J. M. (2008). Metal ions in biological catalysis: from enzyme databases to general principles. *Journal of Biological Inorganic Chemistry*, *13*(8), 1205–1218. doi: 10.1007/s00775-008-0404-5

Arisue, N., & Hashimoto, T. (2015). Phylogeny and evolution of apicoplasts and apicomplexan parasites. *Parasitology International*, *64*(3), 254–259. doi: 10.1016/j.parint.2014.10.005

Arvan, P., Zhao, X., Ramos-Castaneda, J., & Chang, A. (2002). Secretory pathway quality control operating in Golgi, plasmalemmal, and endosomal systems. *Traffic*, *3*(11), 771–780. doi: 10.1034/j.1600-0854.2002.31102.x

Ascenzi, P., Bocedi, A., Visca, P., Altruda, F., Tolosano, E., Beringhelli, T., & Fasano, M. (2005). Hemoglobin and heme scavenging. *IUBMB Life*, *57*(11), 749–759. doi: 10.1080/15216540500380871

Attias, M., Teixeira, D. E., Benchimol, M., Vommaro, R. C., Crepaldi, P. H., & De Souza, W. (2020). The life-cycle of *Toxoplasma gondii* reviewed using animations. *Parasites and Vectors*, *13*(1), 1–13. doi: 10.1186/s13071-020-04445-z

Ayling, R. M., & Kok, K. (2018). Fecal calprotectin. In Advances in clinical chemistry (Vol. 87, pp. 161–190). Elsevier Ltd. doi: 10.1016/bs.acc.2018.07.005

Barros, M. H., Johnson, A., & Tzagoloff, A. (2004). COX23, a homologue of COX17, is required for cytochrome oxidase Assembly. *Journal of Biological Chemistry*, *279*(30), 31943–31947. doi: 10.1074/jbc.M405014200

Becker, T., & Wagner, R. (2018). Mitochondrial outer membrane channels: emerging diversity in transport processes. *BioEssays*, 1800013. doi: 10.1002/bies.201800013

Bellini, N. K., Santos, T. M., Alves da Silva, M. T., & Thiemann, O. H. (2018). The therapeutic strategies against *Naegleria fowleri*. *Experimental Parasitology*, *187*, 1–11. doi: 10.1016/j.exppara.2018.02.010

Besold, A. N., Culbertson, E. M., & Culotta, V. C. (2016). The Yin and Yang of copper during infection. *Journal of Biological Inorganic Chemistry*, *21*(2), 137–144. doi: 10.1007/s00775-016-1335-1

Beswick, P. H., Hall, G. H., Hook, A. J., Little, K., McBrien, D. C. H., & Lott, K. A. K. (1976). Copper toxicity: Evidence for the conversion of cupric to cuprous copper in vivo under anaerobic conditions. *Chemico-Biological Interactions*, *14*(3–4), 347–356. doi: 10.1016/0009-2797(76)90113-7

Bode, M., Woellhaf, M. W., Bohnert, M., Laan, M. Van Der, Sommer, F., Jung, M., Zimmermann, R., Schroda, M., & Herrmann, J. M. (2015). Redox-regulated dynamic interplay between Cox19 and the

copper-binding protein Cox11 in the intermembrane space of mitochondria facilitates biogenesis of cytochrome c oxidase. *Molecular Biology of the Cell*, *26*, 2385–2401. doi: 10.1091/mbc.E14-11-1526

Bonaccorsi di Patti, M. C., Polticelli, F., Tortosa, V., Furbetta, P. A., & Musci, G. (2015). A bacterial homologue of the human iron exporter ferroportin. *FEBS Letters*, *589*(24), 3829–3835. doi: 10.1016/j.febslet.2015.11.025

Boulet, A., Vest, K. E., Maynard, M. K., Gammon, M. G., Russell, A. C., Mathews, A. T., Cole, S. E., Zhu, X., Phillips, C. B., Kwong, J. Q., Dodani, S. C., Leary, S. C., & Cobine, P. A. (2018). The mammalian phosphate carrier SLC25A3 is a mitochondrial copper transporter required for cytochrome c oxidase biogenesis. *Journal of Biological Chemistry*, *293*(6), 1887–1896. doi: 10.1074/jbc.RA117.000265

Boyd, P. W., Jickells, T., Law, C. S., Blain, S., Boyle, E. A., Buesseler, K. O., Coale, K. H., Cullen, J. J., De Baar, H. J. W., Follows, M., Harvey, M., Lancelot, C., Levasseur, M., Owens, N. P. J., Pollard, R., Rivkin, R. B., Sarmiento, J., Schoemann, V., Smetacek, V., … Watson, A. J. (2007). Mesoscale iron enrichment experiments 1993-2005: synthesis and future directions. *Science*, *315*(5812), 612–617. doi: 10.1126/science.1131669

Brancaccio, D., Gallo, A., Piccioli, M., Novellino, E., Ciofi-Baffoni, S., & Banci, L. (2017). [4Fe-4S] cluster assembly in mitochondria and its impairment by copper. *Journal of the American Chemical Society*, *139*(2), 719–730. doi: 10.1021/jacs.6b09567

Brazzolotto, X., Pierrel, F., & Pelosi, L. (2014). Three conserved histidine residues contribute to mitochondrial iron transport through mitoferrins. *Biochemical Journal*, *460*(1), 79–89. doi: 10.1042/BJ20140107

Brill, A. S. (1977). *Transition metals in biochemistry* (1st ed.). Springer Berlin, Heidelberg.

Bruhn, K. W., & Spellberg, B. (2015). Transferrin-mediated iron sequestration as a novel therapy for bacterial and fungal infections. *Current Opinion in Microbiology*, *27*, 57–61. doi: 10.1016/j.mib.2015.07.005.

Canfield, D. E., Poulton, S. W., & Narbonne, G. M. (2007). Late-Neoproterozoic deep-ocean oxygenation and the rise of animal life. *Science*, *315*, 92–94. doi: 10.1126/science.1135013

Capdevila, M., & Atrian, S. (2011). Metallothionein protein evolution: a miniassay. *Journal of Biological Inorganic Chemistry*, *16*(7), 977–989. doi: 10.1007/s00775-011-0798-3

Cellier, M. F., Courville, P., & Campion, C. (2007). Nramp1 phagocyte intracellular metal withdrawal defense. *Microbes and Infection*, *9*, 1662–1670. doi: 10.1016/j.micinf.2007.09.006

Chillappagari, S., Seubert, A., Trip, H., Kuipers, O. P., Marahiel, M. A., & Miethke, M. (2010). Copper stress affects iron homeostasis by destabilizing iron-sulfur cluster formation in *Bacillus subtilis*. *Journal of Bacteriology*, *192*(10), 2512–2524. doi: 10.1128/JB.00058-10

Choveaux, D. L., Krause, R. G. E., Przyborski, J. M., & Goldring, J. P. D. (2015). Identification and initial characterisation of a *Plasmodium falciparum* Cox17 copper metallochaperone. *Experimental*

Parasitology, *148*, 30–39. doi: 10.1016/j.exppara.2014.11.001

Choveaux, D. L., Przyborski, J. M., & Goldring, J. (2012). A *Plasmodium falciparum* copper-binding membrane protein with copper transport motifs. *Malaria Journal*, *11*(1), 397. doi: 10.1186/1475-2875-11-397

Cobine, P. A., Ojeda, L. D., Rigby, K. M., & Winge, D. R. (2004). Yeast contain a non-proteinaceous pool of copper in the mitochondrial matrix. *Journal of Biological Chemistry*, *279*(14), 14447–14455. doi: 10.1074/jbc.M312693200

Cobine, P. A., Pierrel, F., Bestwick, M. L., & Winge, D. R. (2006). Mitochondrial matrix copper complex used in metallation of cytochrome oxidase and superoxide dismutase. *Journal of Biological Chemistry*, *281*(48), 36552–36559. doi: 10.1074/jbc.M606839200

Coffey, R., & Ganz, T. (2017). Iron homeostasis: An anthropocentric perspective. *Journal of Biological Chemistry*, *292*(31), 12727–12734. doi: 10.1074/jbc.R117.781823

Crichton, R. R., & Pierre, J.-L. (2001). Old iron, young copper: from Mars to Venus. *Biometals*, *14*(2), 99–112.

Cruz-Castañeda, A., López-Casamichana, M., & Olivares-Trejo, J. J. (2011). Entamoeba histolytica secretes two haem-binding proteins to scavenge haem. *Biochemical Journal*, *434*(1), 105–111. doi: 10.1042/BJ20100897

Dancis, A., Haile, D., Yuan, D. S., & Klausner, R. D. (1994). The Saccharomyces cerevisiae copper transport protein (Ctr1p). Biochemical characterization, regulation by copper, and physiologic role in copper uptake. *Journal of Biological Chemistry*, *269*(41), 25660–25667. doi: 10.1016/s0021-9258(18)47300-0

Dancis, A., Yuan, D. S., Haile, D., Askwith, C., Eide, D., Moehle, C., Kaplan, J., & Klausner, R. D. (1994). Molecular characterization of a copper transport protein in *S. cerevisiae*: an unexpected role for copper in iron transport. *Cell*, *76*(2), 393–402. doi: 10.1016/0092-8674(94)90345-X

De Jonckheere, J. F. (2011). Origin and evolution of the worldwide distributed pathogenic amoeboflagellate *Naegleria fowleri*. *Infection, Genetics and Evolution*, *11*(7), 1520–1528. doi: 10.1016/j.meegid.2011.07.023

Ding, C., Festa, R. A., Chen, Y. L., Espart, A., Palacios, Ò., Espín, J., Capdevila, M., Atrian, S., Heitman, J., & Thiele, D. J. (2013). *Cryptococcus neoformans* copper detoxification machinery is critical for fungal virulence. *Cell Host and Microbe*, *13*(3), 265–276. doi: 10.1016/j.chom.2013.02.002

Ding, C., Yin, J., Tovar, E. M. M., Fitzpatrick, D. A., Higgins, D. G., & Thiele, D. J. (2011). The copper regulon of the human fungal pathogen *Cryptococcus neoformans* H99. *Molecular Microbiology*, *81*(6), 1560–1576. doi: 10.1111/j.1365-2958.2011.07794.x

Duggal, S. D., Rongpharpi, S. R., Duggal, A. K., Kumar, A., & Biswal, I. (2017). Role of *Acanthamoeba* in granulomatous encephalitis: a review. *Journal of Infectious Diseases & Immune Therapies*, *1*(1).

Dumay, Q. C., Debut, A. J., Mansour, N. M., & Saier, M. H. (2006). The copper transporter (Ctr) family of Cu^{+} uptake systems. *Journal of Molecular Microbiology and Biotechnology*, *11*(1–2), 10–19. doi: 10.1159/000092815

Duncan, C., & White, A. R. (2012). Copper complexes as therapeutic agents. *Metallomics*, *4*(2), 127–138. doi: 10.1039/c2mt00174h

Flannery, A. R., Huynh, C., Mittra, B., Mortara, R. A., & Andrews, N. W. (2011). LFR1 ferric iron reductase of *Leishmania amazonensis* is essential for the generation of infective parasite forms. *Journal of Biological Chemistry*, *286*(26), 23266–23279. doi: 10.1074/jbc.M111.229674

Foury, F., & Roganti, T. (2002). Deletion of the mitochondrial carrier genes MRS3 and MRS4 suppresses mitochondrial iron accumulation in a yeast frataxin-deficient strain. *The Journal of Biological Chemistry*, *277*(27), 24475–24483. doi: 10.1074/jbc.M111789200

Froschauer, E. M., Rietzschel, N., Hassler, M. R., Binder, M., Schweyen, R. J., Lill, R., Uhlenhoff, U. M., & Wiesenberger, G. (2013). The mitochondrial carrier Rim2 co-imports pyrimidine nucleotides and iron. *Biochemical Journal*, *455*(1), 57–65. doi: 10.1042/BJ20130144

Fu, D., Beeler, T. J., & Dunn, T. M. (1995). Sequence, mapping and disruption of CCC2, a gene that cross-complements the Ca^{2+}-sensitive phenotype of *csg1* mutants and encodes a P-type ATPase belonging to the Cu^{2+}-ATPase subfamily. *Yeast*, *11*(3), 283–292. doi: 10.1002/yea.320110310

Fujioka, H., & Aikawa, M. (2002). Structure and life cycle. In Malaria Parasites and Disease. In P. Perlmann & M. Troye-Blomberg (Eds.), Malaria Immunology. Chem Immunol. Basel, Karger (Vol. 80, pp. 1–26). doi: 10.1159/000058837

Fung, S. A. (2019). Exploring the diversity of mitochondrion related organelles in *Cryptosporidium* species. University of Kent.

Ganz, T. (2009). Iron in innate immunity: starve the invaders. *Current Opinion in Immunology*, *21*(1), 63–67. doi: doi.org/10.1016/j.coi.2009.01.011

García-Santamarina, S., & Thiele, D. J. (2015). Copper at the fungal pathogen-host axis. *Journal of Biological Chemistry*, *290*(31), 18945–18953. doi: 10.1074/jbc.R115.649129

Garcia-Santamarina, S., Uzarska, M. A., Festa, R. A., Lill, R., & Thiele, D. J. (2017). *Cryptococcus neoformans* iron-sulfur protein biogenesis machinery is a novel layer of protection against Cu stress. *MBio*, *8*(5), 1–18. doi: 10.1128/mBio.01742-17

Halliwell, B., & Gutteridget, J. M. C. (1984). Oxygen toxicity, oxygen radicals, transition metals and disease. *Biochemical Journal*, *219*, 1–14. doi: 10.1042/bj2190001

Hamel, P., Saint-georges, Y., Pinto, B. De, Lachacinski, N., Altamura, N., & Dujardin, G. (2004). Redundancy in the function of mitochondrial phosphate transport in *Saccharomyces cerevisiae* and *Arabidopsis thaliana*. *Molecular Microbiology*, *51*(2), 307–317. doi: 10.1046/j.1365-2958.2003.03810.x

Harrison, P. M., & Arosio, P. (1996). The ferritins: molecular properties, iron storage function and cellular regulation. *Biochimica et Biophysica Acta*, *1275*(3), 161–203. doi: 10.1016/0005-2728(96)00022-9

Hassett, R., & Kosman, D. J. (1995). Evidence for Cu(II) reduction as a component of copper uptake by *Saccharomyces cerevisiae*. *Journal of Biological Chemistry*, *270*(1), 128–134. doi: 10.1074/jbc.270.1.128

Helsel, M. E., White, E. J., Razvi, S. Z. A., Alies, B., & Franz, K. J. (2017). Chemical and functional properties of metal chelators that mobilize copper to elicit fungal killing of *Cryptococcus neoformans*. *Metallomics*, *9*(1), 69–81. doi: 10.1039/c6mt00172f

Hennigar, S. R., & McClung, J. P. (2016). Nutritional immunity: starving pathogens of trace minerals. *American Journal of Lifestyle Medicine*, *10*(3), 170–173. doi: 10.1177/1559827616629117.

Hernandes-Cuevas, N. A., Weber, C., Hon, C., & Guillen, N. (2014). Gene expression profiling in *Entamoeba histolytica* identifies key components in iron uptake and metabolism. *PLoS ONE*, *9*(9), e107102. doi: 10.1371/journal.pone.0107102

Hershko, C. (2007). Mechanism of iron toxicity. *Food and Nutrition Bulletin*, *28*(4 SUPPL.), 500–509. doi: 10.1177/15648265070284s403

Hodgkinson, V., & Petris, M. J. (2012). Copper homeostasis at the host-pathogen interface. *Journal of Biological Chemistry*, *287*(17), 13549–13555. doi: 10.1074/jbc.R111.316406

Horn, D., & Barrientos, A. (2008). Mitochondrial copper metabolism and delivery to cytochrome c oxidase. *Life*, *60*(7), 421–429. doi: 10.1002/iub.50

Huang, G., Ulrich, P. N., Storey, M., Johnson, D., Tischer, J., Tovar, J. A., Moreno, S. N. J., Orlando, R., & Docampo, R. (2014). Proteomic analysis of the acidocalcisome, an organelle conserved from bacteria to human cells. *PLoS Pathogens*, *10*(12), e1004555. doi: 10.1371/journal.ppat.1004555

Huynh, C., Sacks, D. L., & Andrews, N. W. (2006). A *Leishmania amazonensis* ZIP family iron transporter is essential for parasite replication within macrophage phagolysosomes. *Journal of Experimental Medicine*, *203*(10), 2363–2375. doi: 10.1084/jem.20060559

Huynh, C., Yuan, X., Miguel, D. C., Renberg, R. L., Protchenko, O., Philpott, C. C., Hamza, I., & Andrews, N. W. (2012). Heme uptake by *Leishmania amazonensis* is mediated by the transmembrane protein LHR1. *PLoS Pathogens*, *8*(7), 36. doi: 10.1371/journal.ppat.1002795

Ichikawa, Y., Bayeva, M., Ghanefar, M., Potini, V., Sun, L., Mutharasan, R. K., Wu, R., Khechaduri, A., Naik, T. J., & Ardehali, H. (2012). Disruption of ATP-binding cassette B8 in mice leads to cardiomyopathy through a decrease in mitochondrial iron export. *Proceedings of the National Academy of Sciences of the United States of America*, *109*(11), 4152–4157. doi: 10.1073/pnas.1119338109

Imlay, J. A. (2006). Iron-sulphur clusters and the problem with oxygen. *Molecular Microbiology*, *59*(4), 1073–1082. doi: 10.1111/j.1365-2958.2005.05028.x

Isah, M. B., Goldring, J. P. D., & Coetzer, T. H. T. (2020). Expression and copper binding properties of the N-terminal domain of copper P-type ATPases of African trypanosomes. *Molecular and Biochemical Parasitology*, *235*, 111245. doi: 10.1016/j.molbiopara.2019.111245

Jacques, I., Andrews, N. W., & Huynh, C. (2010). Functional characterization of LIT1, the *Leishmania amazonensis* ferrous iron transporter. *Molecular and Biochemical Parasitology*, *170*(1), 28–36. doi: 10.1016/j.molbiopara.2009.12.003

Janse, C. J., & Waters, A. P. (1995). *Plasmodium berghei*: the application of cultivation and purification techniques to molecular studies of malaria parasites. *Parasitology Today*, *11*(4), 138–143. doi: 10.1016/0169-4758(95)80133-2

Jedelsky, P. L., Dolezal, P., Rada, P., Pyrih, J., Smıd, O., Hrdy, I., Miroslava, S., Marcincikova, M., Perry, A. J., Beltran, N. C., Lithgow, T., & Tachezy, J. (2011). The minimal proteome in the reduced mitochondrion of the parasitic protist *Giardia intestinalis*. *PloS ONE*, *6*(2), e17285. doi: 10.1371/journal.pone.0017285

Jensen, L. T., Howard, W. R., Strain, J. J., Winge, D. R., & Culotta, V. C. (1996). Enhanced effectiveness of copper ion buffering by CUP1 metallothionein compared with CRS5 metallothionein in *Saccharomyces cerevisiae*. *Journal of Biological Chemistry*, *271*(31), 18514–18519. doi: 10.1074/jbc.271.31.18514

Jenssen, H., & Hancock, R. E. W. (2009). Antimicrobial properties of lactoferrin. *Biochimie*, *91*, 19–29. doi: 10.1016/j.biochi.2008.05.015

Kawabata, H. (2019). Transferrin and transferrin receptors update. *Free Radical Biology and Medicine*, *133*, 46–54. doi: 10.1016/j.freeradbiomed.2018.06.037

Kehl-Fie, T. E., & Skaar, E. P. (2011). Nutritional immunity beyond iron: a role for manganese and zinc. *Current Opinion in Chemical Biology*, *14*(2), 218–224. doi: 10.1016/j.cbpa.2009.11.008

Kenthirapalan, S., Waters, A. P., Matuschewski, K., & Kooij, T. W. A. (2014). Copper-transporting ATPase is important for malaria parasite fertility. *Molecular Microbiology*, *91*(2), 315–325. doi: 10.1111/mmi.12461

Kenthirapalan, S., Waters, A. P., Matuschewski, K., & Kooij, T. W. A. (2016). Functional profiles of orphan membrane transporters in the life cycle of the malaria parasite. *Nature Communications*, *7*, 10519. doi: 10.1038/ncomms10519

Khan, N. A. (2006). *Acanthamoeba*: biology and increasing importance in human health. *FEMS Microbiology Reviews*, *30*(4), 564–595. doi: 10.1111/j.1574-6976.2006.00023.x

Knight, S. A. B., Labbé, S., Kwon, L. F., Kosman, D. J., & Thiele, D. J. (1996). A widespread transposable element masks expression of a yeast copper transport gene. *Genes and Development*, *10*(15), 1917–1929. doi: 10.1101/gad.10.15.1917

LaGier, M. J., Zhu, G., & Keithly, J. S. (2001). Characterization of a heavy metal ATPase from the

apicomplexan *Cryptosporidium parvum*. *Gene*, *266*(1–2), 25–34. doi: 10.1016/S0378-1119(01)00382-1

Lange, H., Kispal, G., & Lill, R. (1999). Mechanism of iron transport to the site of heme synthesis inside yeast mitochondria. *Journal of Biological Chemistry*, *274*(27), 18989–18996. doi: 10.1074/jbc.274.27.18989

Laranjeira-Silva, M. F., Wang, W., Samuel, T. K., Maeda, F. Y., Michailowsky, V., Hamza, I., Liu, Z., & Andrews, N. W. (2018). A MFS-like plasma membrane transporter required for *Leishmania* virulence protects the parasites from iron toxicity. *PLoS Pathogens*, *14*(6), 1–24. doi: 10.1371/journal.ppat.1007140

Leger, M. M., Gawryluk, R. M. R., Gray, M. W., & Roger, A. J. (2013). Evidence for a hydrogenosomal-type anaerobic ATP generation pathway in *Acanthamoeba castellanii*. *PLoS ONE*, *8*(9). doi: 10.1371/journal.pone.0069532

Legrand, D., Elass, E., Carpentier, M., & Mazurier, J. (2005). Lactoferrin: a modulator of immune and inflammatory responses. *Cellular and Molecular Life Sciences*, *62*, 2549–2559. doi: 10.1007/s00018-005-5370-2

Levitz, S. M. (1991). The ecology of *Cryptococcus neoformans* and the epidemiology of cryptococcosis. *Reviews of Infectious Diseases*, *13*(6), 1163–1169. doi: 10.1093/clinids/13.6.1163

Li, L., Bertram, S., Kaplan, J., Jia, X., & Ward, D. M. (2020). The mitochondrial iron exporter genes MMT1 and MMT2 in yeast are transcriptionally regulated by Aft1 and Yap1. *Journal of Biological Chemistry*, *295*(6), 1716–1726. doi: 10.1074/jbc.RA119.011154

Li, L., & Kaplan, J. (1997). Characterization of two homologous yeast genes that encode mitochondrial iron transporters. *Journal of Biological Chemistry*, *272*(45), 28485–28493. doi: 10.1074/jbc.272.45.28485

Li, L., Miao, R., Jia, X., Ward, D. M., & Kaplan, J. (2014). Expression of the yeast cation diffusion facilitators Mmt1 and Mmt2 affects mitochondrial and cellular iron homeostasis: evidence for mitochondrial iron export. *Journal of Biological Chemistry*, *289*(24), 17132–17141. doi: 10.1074/jbc.M114.574723

Llases, M.-E., Morgada, M. N., & Vila, A. J. (2019). Biochemistry of copper site assembly in heme-copper oxidases: a theme with variations. *International Journal of Molecular Sciences*, *20*(15), 3830. doi: 10.3390/ijms20153830

Logeman, B. L., Wood, L. K., Lee, J., & Thiele, D. J. (2017). Gene duplication and neo-functionalization in the evolutionary and functional divergence of the metazoan copper transporters Ctr1 and Ctr2. *Journal of Biological Chemistry*, *292*(27), 11531–11546. doi: 10.1074/jbc.M117.793356

Long, N., Xu, X., Qian, H., Zhang, S., & Lu, L. (2016). A putative mitochondrial iron transporter MrsA in *Aspergillus fumigatus* plays important roles in azole-, oxidative stress responses and virulence. *Frontiers in Microbiology*, *7*(MAY), 1–15. doi: 10.3389/fmicb.2016.00716

Lopes, A. H., Souto-Padrón, T., Dias, F. A., Gomes, M. T., Rodrigues, G. C., Zimmermann, L. T., Alves e Silva, T. L., & Vermelho, A. B. (2010). Trypanosomatids: odd organisms, devastating diseases. *The Open Parasitology Journal*, *4*, 30–59. doi: 10.2174/1874421401004010030

López-Martínez, R. (2010). Candidosis, a new challenge. *Clinics in Dermatology*, *28*(2), 178–184. doi: 10.1016/j.clindermatol.2009.12.014

López-Soto, F., León-Sicairos, N., Reyes-López, M., Serrano-Luna, J., Ordaz-Pichardo, C., Piña-Vázquez, C., Ortiz-Estrada, G., & de la Garza, M. (2009). Use and endocytosis of iron-containing proteins by *Entamoeba histolytica* trophozoites. *Infection, Genetics and Evolution*, *9*(6), 1038–1050. doi: 10.1016/j.meegid.2009.05.018

Lorenzo-Morales, J., Khan, N. A., & Walochnik, J. (2015). An update on *Acanthamoeba* keratitis: diagnosis, pathogenesis and treatment. *Parasite*, *22*(10). doi: 10.1051/parasite/2015010

Mach, J., Bíla, J., Ženíšková, K., Arbon, D., Malych, R., Glavanakovová, M., Nývltová, E., & Sutak, R. (2018). Iron economy in Naegleria gruberi reflects its metabolic flexibility. *International Journal for Parasitology*, *48*(9–10), 719–727. doi: 10.1016/j.ijpara.2018.03.005

Mach, J., & Sutak, R. (2020). Iron in parasitic protists-from uptake to storage and where we can interfere. *Metallomics*, *12*(9), 1335–1347. doi: 10.1039/d0mt00125b

Mach, J., Tachezy, J., & Sutak, R. (2013). Efficient iron uptake via a reductive mechanism in procyclic *Trypanosoma brucei*. *Journal of Parasitology*, *99*(2), 363–364. doi: 10.1645/GE-3237.1

Maciver, S. K., McLaughlin, P. J., Apps, D. K., Piñero, J. E., & Lorenzo-Morales, J. (2021). Opinion: iron, climate change and the 'brain eating amoeba' *Naegleria fowleri*. *Protist*, *172*, 125791. doi: 10.1016/j.protis.2020.125791

Maciver, S. K., Piñero, J. E., & Lorenzo-Morales, J. (2020). Is *Naegleria fowleri* an emerging parasite? *Trends in Parasitology*, *36*(1), 19–28. doi: 10.1016/j.pt.2019.10.008

Mackie, J., Szabo, E. K., Urgast, D. S., Ballou, E. R., Childers, D. S., MacCallum, D. M., Feldmann, J., & Brown, A. J. P. (2016). Host-imposed copper poisoning impacts fungal micronutrient acquisition during systemic *Candida albicans* infections. *PLoS ONE*, *11*(6), 1–18. doi: 10.1371/journal.pone.0158683

Maclean, R. C., Richardson, D. J., LePardo, R., & Marciano-Cabral, F. (2004). The identification of *Naegleria fowleri* from water and soil samples by nested PCR. *Parasitology Research*, *93*(3), 211–217. doi: 10.1007/s00436-004-1104-x

Macomber, L., & Imlay, J. A. (2009). The iron-sulfur clusters of dehydratases are primary intracellular targets of copper toxicity. *Proceedings of the National Academy of Sciences of the United States of America*, *106*(20), 8344–8349. doi: 10.1073/pnas.0812808106

Macomber, L., Rensing, C., & Imlay, J. A. (2007). Intracellular copper does not catalyze the formation of oxidative DNA damage in *Escherichia coli*. *Journal of Bacteriology*, *189*(5), 1616–1626.

doi: 10.1128/JB.01357-06

Maralikova, B., Ali, V., Nakada-Tsukui, K., Nozaki, T., van der Giezen, M., Henze, K., & Tovar, J. (2010). Bacterial-type oxygen detoxification and iron-sulfur cluster assembly in amoebal relict mitochondria. *Cellular Microbiology*, *12*(3), 331–342. doi: 10.1111/j.1462-5822.2009.01397.x

Marciano-Cabral, F., & Cabral, G. (2003). *Acanthamoeba* spp. as agents of disease in humans. *Clinical Microbiology Reviews*, *16*(2), 273–307. doi: 10.1128/CMR.16.2.273-307.2003

Martínez-Pastor, M. T., & Puig, S. (2020). Adaptation to iron deficiency in human pathogenic fungi. *BBA - Molecular Cell Research*, *1867*, 118797. doi: 10.1016/j.bbamcr.2020.118797

Marvin, R. G., Wolford, J. L., Kidd, M. J., Murphy, S., Ward, J., Que, E. L., Mayer, M. L., Penner-hahn, J. E., Haldar, K., & O'Halloran, T. V. (2012). Fluxes in "free" and total zinc are essential for progression of intraerythrocytic stages of *Plasmodium falciparum*. *Chemistry & Biology*, *19*(6), 731–741. doi: 10.1016/j.chembiol.2012.04.013

Maxfield, A. B., Heaton, D. N., & Winge, D. R. (2004). Cox17 is functional when tethered to the mitochondrial inner membrane. *Journal of Biological Chemistry*, *279*(7), 5072–5080. doi: 10.1074/jbc.M311772200

Maya-Maldonado, K., Cardoso-Jaime, V., González-Olvera, G., Osorio, B., Recio-Tótoro, B., Manrique-Saide, P., Rodríguez-Sánchez, I. P., Lanz-Mendoza, H., Missirlis, F., & de la Cruz Hernández-Hernández, F. (2021). Mosquito metallomics reveal copper and iron as critical factors for *Plasmodium* infection. *PLoS Neglected Tropical Diseases*, *15*(6), 1–20. doi: 10.1371/journal.pntd.0009509

Meade, J. C. (2019). P-type transport ATPases in *Leishmania* and *Trypanosoma*. *Parasite*, *26*(69). doi: 10.1051/parasite/2019069

Mittra, B., Laranjeira-Silva, M. F., Perrone Bezerra de Menezes, J., Jensen, J., Michailowsky, V., & Andrews, N. W. (2016). A trypanosomatid iron transporter that regulates mitochondrial function is required for *Leishmania amazonensis* virulence. *PLoS Pathogens*, *12*(1), e1005340. doi: 10.1371/journal.ppat.1005340

Mühlenhoff, U., Hoffmann, B., Richter, N., Rietzschel, N., Spantgar, F., Stehling, O., Uzarska, M. A., & Lill, R. (2015). Compartmentalization of iron between mitochondria and the cytosol and its regulation. *European Journal of Cell Biology*, *94*(7–9), 292–308. doi: 10.1016/j.ejcb.2015.05.003

Muhlenhoff, U., Stadler, J. A., Richhardt, N., Seubert, A., Eickhorst, T., Schweyen, R. J., Lill, R., & Wiesenberger, G. (2003). A specific role of the yeast mitochondrial carriers Mrs3/4p in mitochondrial iron acquisition under iron-limiting conditions. *The Journal of Biological Chemistry*, *278*(42), 40612–40620. doi: 10.1074/jbc.M307847200

Mull, B. J., Narayanan, J., & Hill, V. R. (2013). Improved method for the detection and quantification of *Naegleria fowleri* in water and sediment using immunomagnetic separation and real-time PCR. *Journal of Parasitology Research*, *2013*. doi: 10.1155/2013/608367

Muller, M., Mentel, M., van Hellemond, J. J., Henze, K., Woehle, C., Gould, S. B., Yu, R.-Y., van der Giezen, M., Tielens, A. G. M., & Martin, W. F. (2012). Biochemistry and evolution of anaerobic energy metabolism in eukaryotes. *Microbiology and Molecular Biology Reviews*, *76*(2), 444–495. doi: 10.1128/MMBR.05024-11

Mungroo, M. R., Khan, N. A., Maciver, S., & Siddiqui, R. (2022). Opportunistic free-living amoebal pathogens. *Pathogens and Global Health*, *116*(2), 70–84. doi: 10.1080/20477724.2021.1985892

Nagaraj, V. A., Sundaram, B., & Varadarajan, N. M. (2013). Malaria parasite-synthesized heme is essential in the mosquito and liver stages and complements host heme in the blood stages of infection. *PLoS Pathogens*, *9*(8), e1003522. doi: 10.1371/journal.ppat.1003522

Narula, S. S., Armitage, I. M., & Winge, D. R. (1993). Copper- and silver-substituted yeast metallothioneins: sequential 1H NMR assignments reflecting conformational heterogeneity at the C terminus. *Biochemistry*, *32*(26), 6773–6787. doi: 10.1021/bi00077a032

Nelson, A. L., Barasch, J. M., Bunte, R. M., & Weiser, J. N. (2005). Bacterial colonization of nasal mucosa induces expression of siderocalin, an iron-sequestering component of innate immunity. *Cellular Microbiology*, *7*(10), 1404–1417. doi: 10.1111/j.1462-5822.2005.00566.x

Nobrega, M. P., Bandeira, S. C. B., Beers, J., & Tzagoloff, A. (2002). Characterization of COX19, a widely distributed gene required for expression of mitochondrial cytochrome oxidase. *Journal of Biological Chemistry*, *277*(43), 40206–40211. doi: 10.1074/jbc.M207348200

Nose, Y., Rees, E. M., & Thiele, D. J. (2006). Structure of the Ctr1 copper trans'PORE'ter reveals novel architecture. *Trends in Biochemical Sciences*, *31*(11), 604–607. doi: 10.1016/j.tibs.2006.09.003

Nyhus, K. J., Ozaki, L. S., & Jacobson, E. S. (2002). Role of mitochondrial carrier protein Mrs3/4 in iron acquisition and oxidative stress resistance of *Cryptococcus neoformans*. *Medical Mycology*, *40*(6), 581–591. doi: 10.1080/mmy.40.6.581.591

Och, L. M., & Shields-Zhou, G. A. (2012). The Neoproterozoic oxygenation event: environmental perturbations and biogeochemical cycling. *Earth Science Reviews*, *110*, 26–57. doi: 10.1016/j.earscirev.2011.09.004

Ohgami, R. S., Campagna, D. R., McDonald, A., & Fleming, M. D. (2006). The Steap proteins are metalloreductases. *Blood*, *108*(4), 1388–1394. doi: 10.1182/blood-2006-02-003681

Ozcelik, D., Ozaras, R., Gurel, Z., Uzun, H., & Aydin, S. (2003). Copper-mediated oxidative stress in rat liver. *Biological Trace Element Research*, *96*(1), 209–215. doi: 10.1385/BTER:96:1-3:209

Pagani, A., Villarreal, L., Capdevila, M., & Atrian, S. (2007). The *Saccharomyces cerevisiae* Crs5 metallothionein metal-binding abilities and its role in the response to zinc overload. *Molecular Microbiology*, *63*(1), 256–269. doi: 10.1111/j.1365-2958.2006.05510.x

Palmieri, F., & Pierri, C. L. (2010). Mitochondrial metabolite transport. *Essays in Biochemistry*, *47*, 37–52. doi: 10.1042/BSE0470037

Paradkar, P. N., Zumbrennen, K. B., Paw, B. H., Ward, D. M., & Kaplan, J. (2009). Regulation of mitochondrial iron import through differential turnover of mitoferrin 1 and mitoferrin 2. *Molecular and Cellular Biology*, *29*(4), 1007–1016. doi: 10.1128/mcb.01685-08

Paul, R., Banerjee, S., Sen, S., Dubey, P., Maji, S., Bachhawat, A. K., Datta, R., & Gupta, A. (2021). A novel leishmanial copper P-type ATPase plays a vital role in parasite infection and intracellular survival. *Journal of Biological Chemistry*, *298*(2). doi: 10.1016/j.jbc.2021.101539

Pham, A. N., Xing, G., Miller, C. J., & Waite, T. D. (2013). Fenton-like copper redox chemistry revisited: Hydrogen peroxide and superoxide mediation of copper-catalyzed oxidant production. *Journal of Catalysis*, *301*, 54–64. doi: 10.1016/j.jcat.2013.01.025

Rainsford, K. D., Milanino, R., Sorenson, J. R. J., & Velo, G. P. (Eds.). (1998). *Copper and zinc in inflammatory and degenerative diseases*. Springer Science+Business Media Dordrecht. doi: 10.1007/978-94-011-3963-2

Ram, H., Sardar, S., & Gandass, N. (2021). Vacuolar Iron Transporter (like) proteins: regulators of cellular iron accumulation in plants. *Physiologia Plantarum*, *171*(4), 823–832. doi: 10.1111/ppl.13363

Ramírez-Rico, G., Martínez-Castillo, M., De La Garza, M., Shibayama, M., & Serrano-Luna, J. (2015). *Acanthamoeba castellanii* proteases are capable of degrading iron-binding proteins as a possible mechanism of pathogenicity. *Journal of Eukaryotic Microbiology*, *62*(5), 614–622. doi: 10.1111/jeu.12215

Rasoloson, D., Shi, L., Chong, C. R., Kafsack, B. F., & Sullivan, D. J. (2004). Copper pathways in *Plasmodium falciparum* infected erythrocytes indicate an efflux role for the copper P-ATPase. *The Biochemical Journal*, *381*(Pt 3), 803–811. doi: 10.1042/BJ20040335

Riggle, P. J., & Kumamoto, C. A. (2000). Role of a *Candida albicans* P1-type ATPase in resistance to copper and silver ion toxicity. *Journal of Bacteriology*, *182*(17), 4899–4905. doi: 10.1128/JB.182.17.4899-4905.2000

Sahu, T., Boisson, B., Lacroix, C., Bischoff, E., Richier, Q., Formaglio, P., Thiberge, S., Dobrescu, I., Ménard, R., & Baldacci, P. (2014). ZIPCO, a putative metal ion transporter, is crucial for *Plasmodium* liver-stage development. *EMBO Molecular Medicine*, *6*(11), 1387–1397. doi: 10.15252/emmm.201403868

Salman, A. A., & Goldring, J. P. D. (2022). Expression and copper binding characteristics of *Plasmodium falciparum* cytochrome c oxidase assembly factor 11, Cox11. *Malaria Journal*, *21*(173), 1–15. doi: 10.1186/s12936-022-04188-5

Sancen, V., Puig, S., Mira, H., Thiele, D. J., & Peñarrubia, L. (2003). Identification of a copper transporter family in *Arabidopsis thaliana*. *Plant Molecular Biology*, *51*(4), 577–587. doi: 10.1023/A:1022345507112

Scholl, P. F., Tripathi, A. K., & Sullivan, D. J. (2005). Bioavailable iron and heme metabolism in *Plasmodium falciparum*. *Current Topics in Microbiology and Immunology*, *295*, 293–324. doi: 10.1007/3-540-

29088-5_12

Searle, S., Bright, N. A., Roach, T. I. A., Atkinson, P. G. P., Barton, C. H., Meloen, R. H., & Blackwell, J. M. (1998). Localisation of Nramp1 in macrophages: modulation with activation and infection. *Journal of Cell Science*, *111*(19), 2855–2866. doi: 10.1242/jcs.111.19.2855

Seo, P. J., Park, J., Park, M., Kim, Y., Kim, S., Jung, J., & Park, C. (2012). A Golgi-localized MATE transporter mediates iron homoeostasis under osmotic stress in *Arabidopsis*. *Biochemical Journal*, *442*, 551–561. doi: 10.1042/BJ20111311

Shields-Zhou, G., & Och, L. (2011). The case for a Neoproterozoic Oxygenation Event: geochemical evidence and biological consequences. *GSA Today*, *21*(3), 4–11. doi: 10.1130/GSATG102A.1

Siddiqui, R., & Khan, N. A. (2012). Biology and pathogenesis of *Acanthamoeba*. *Parasites and Vectors*, *5*(1), 1–13. doi: 10.1186/1756-3305-5-6

Siddiqui, R., & Khan, N. A. (2014). Primary amoebic meningoencephalitis caused by *Naegleria fowleri*: an old enemy presenting new challenges. *PLoS Neglected Tropical Diseases*, *8*(8), e3017. doi: 10.1371/journal.pntd.0003017

Slavic, K., Krishna, S., Lahree, A., Bouyer, G., Hanson, K. K., Vera, I., Pittman, J. K., Staines, H. M., & Mota, M. M. (2016). A vacuolar iron-transporter homologue acts as a detoxifier in *Plasmodium*. *Nature Communications*, *7*(1), 1–10. doi: 10.1038/ncomms10403

Sloan, M. A., Aghabi, D., & Harding, C. R. (2021). Orchestrating a heist: uptake and storage of metals by apicomplexan parasites. *Microbiology (Reading)*, *167*(12). doi: 10.1099/mic.0.001114

Smith, A. D., Logeman, B. L., & Thiele, D. J. (2017). Copper acquisition and utilization in fungi. *Annual Review of Microbiology*, *71*, 597–623. doi: http://www.annualreviews.org/doi/10

Solomon, E. I., Heppner, D. E., Johnston, E. M., Ginsbach, J. W., Qayyum, M., Kieber-emmons, M. T., Kjaergaard, C. H., Hadt, R. G., & Tian, L. (2015). Copper active sites in biology. *Chemical Reviews*, *114*(7), 3659–3853. doi: 10.1021/cr400327t.

Sorribes-Dauden, R., Peris, D., Martínez-Pastor, M. T., & Puig, S. (2020). Structure and function of the vacuolar Ccc1/VIT1 family of iron transporters and its regulation in fungi. *Computational and Structural Biotechnology Journal*, *18*, 3712–3722. doi: 10.1016/j.csbj.2020.10.044

Stauffer, W., & Ravdin, J. I. (2003). *Entamoeba histolytica*: an update. *Current Opinion in Infectious Diseases*, *16*(5), 479–485. doi: 10.1097/00001432-200310000-00016

Stearman, R., Yuan, D. S., Yamaguchi-Iwai, Y., Klausner, R. D., & Dancis, A. (1996). A permease-oxidase complex involved in high-affinity iron uptake in yeast. *Science*, *271*(5255), 1552–1557. doi: 10.1126/science.271.5255.1552

Steffens, G. C. M., Biewald, R., & Buse, G. (1987). Cytochrome c oxidase is a three-copper, two-heme-A protein. *European Journal of Biochemistry*, *164*(2), 295–300. doi: 10.1111/j.1432-

1033.1987.tb11057.x

Sun, T. S., Ju, X., Gao, H. L., Wang, T., Thiele, D. J., Li, J. Y., Wang, Z. Y., & Ding, C. (2014). Reciprocal functions of *Cryptococcus neoformans* copper homeostasis machinery during pulmonary infection and meningoencephalitis. *Nature Communications*, *5*(1), 1–13. doi: 10.1038/ncomms6550

Sykora, J. L., Keleti, G., & Martinez, A. J. (1983). Occurrence and pathogenicity of *Naegleria fowleri* in artificially heated waters. *Applied and Environmental Microbiology*, *45*(3), 974–979. doi: 10.1128/aem.45.3.974-979.1983

Tachezy, J., Makki, A., & Hrdý, I. (2022). The hydrogenosome of *Trichomonas vaginalis*. *Journal of Eukaryotic Microbiology*, e12922. doi: 10.1111/jeu.12922

Tachezy, J., Sanchez, L. B., & Muller, M. (2001). Mitochondrial type iron-sulfur cluster assembly in the amitochondriate eukaryotes *Trichomonas vaginalis* and *Giardia intestinalis*, as indicated by the phylogeny of IscS. *Molecular Biology and Evolution*, *18*(10), 1919–1928. doi: 10.1093/oxfordjournals.molbev.a003732

Tan, S., Hwee, T. T., & Chung, M. C. M. (2008). Membrane proteins and membrane proteomics. *Proteomics*, *8*, 3924–3932. doi: 10.1002/pmic.200800597

Taylor, M. C., & Kelly, J. M. (2010). Iron metabolism in trypanosomatids, and its crucial role in infection. *Parasitology*, *137*(6), 899–917. doi: 10.1017/S0031182009991880

Taylor, M. C., Mclatchie, A. P., & Kelly, J. M. (2013). Evidence that transport of iron from the lysosome to the cytosol in African trypanosomes is mediated by a mucolipin orthologue. *Molecular Microbiology*, *89*(3), 420–432. doi: 10.1111/mmi.12285

Thompson, R. C. A., Olson, M. E., Zhu, G., Enomoto, S., Abrahamsen, M. S., & Hijjawi, N. S. (2005). *Cryptosporidium* and cryptosporidiosis. *Advances in Parasitology*, *59*, 77–158. doi: 10.1016/S0065-308X(05)59002-X

Thomson, A. J. (1975). Biochemistry of transition metals. *Nature*, *257*, 536–537.

Thounaojam, T. C., Panda, P., Mazumdar, P., Kumar, D., Sharma, G. D., Sahoo, L., & Panda, S. K. (2012). Excess copper induced oxidative stress and response of antioxidants in rice. *Plant Physiology and Biochemistry*, *53*, 33–39. doi: 10.1016/j.plaphy.2012.01.006

Tovar, J., Leon-Avila, G., Sanchez, L. B., Sutak, R., Tachezy, J., Giezen, M. van der, Hernandez, M., Muller, M., & Lucocq, J. M. (2003). Mitochondrial remnant organelles of *Giardia* function in iron-sulphur protein maturation. *Nature*, *426*, 172–176.

Tsaousis, A. D., Nývltová, E., Šuták, R., Hrdý, I., & Tachezy, J. (2014). A nonmitochondrial hydrogen production in *Naegleria gruberi*. *Genome Biology and Evolution*, *6*(4), 792–799. doi: 10.1093/gbe/evu065

Vanhollebeke, B., de Muylder, G., Nielsen, M. J., Pays, A., Tebabi, P., Dieu, M., Raes, M., Moestrup, S. K.,

& Pays, E. (2008). A haptoglobin-hemoglobin receptor conveys innate immunity to *Trypanosoma brucei* in humans. *Science*, *320*, 677–681. doi: 10.1126/science.1156296

Vest, K. E., Leary, S. C., Winge, D. R., & Cobine, P. A. (2013). Copper import into the mitochondrial matrix in *Saccharomyces cerevisiae* is mediated by Pic2, a mitochondrial carrier family protein. *Journal of Biological Chemistry*, *288*(33), 23884–23892. doi: 10.1074/jbc.M113.470674

Vest, K. E., Wang, J., Gammon, M. G., Maynard, M. K., White, O. L., Cobine, J. A., Mahone, W. K., & Cobine, P. A. (2016). Overlap of copper and iron uptake systems in mitochondria in *Saccharomyces cerevisiae*. *Open Biology*, *6*(1), 150223. doi: 10.1098/rsob.150223

Vigani, G., Solti, Á., Thomine, S., & Philippar, K. (2019). Essential and detrimental – an update on intracellular iron trafficking and homeostasis. *Plant and Cell Physiology*, *60*(7), 1420–1439. doi: 10.1093/pcp/pcz091

Villalba, J. M., Palmgren, M. G., Berberian, G. E., Ferguson, C., & Serrano, R. (1992). Functional expression of plant plasma membrane H^+-ATPase in yeast endoplasmic reticulum. *Journal of Biological Chemistry*, *267*(17), 12341–12349. doi: 10.1016/s0021-9258(19)49845-1

Wagner, C., Vethencourt Ysea, M. A., Galindo, M. V., Guzmán De Rondón, C., Nessi Paduani, A. J., Reyes-Batlle, M., López-Arencibia, A., Sifaoui, I., Pérez De Galindo, M. V., Martínez-Carretero, E., Valladares, B., Maciver, S. K., Piñero, J. E., & Lorenzo-Morales, J. (2017). Isolation of *Naegleria fowleri* from a domestic water tank associated with a fatal encephalitis in a 4 month-old Venezuelan child. *Tropical Biomedicine*, *34*(2), 332–337.

Wagner, D., Maser, J., Lai, B., Cai, Z., Barry III, C. E., Höner zu Bentrup, K., Russell, D. G., & Bermudez, L. E. (2005). Elemental analysis of *Mycobacterium avium*-, *Mycobacterium tuberculosis*-, and *Mycobacterium smegmatis*-containing phagosomes indicates pathogen-induced microenvironments within the host cell's endosomal system. *The Journal of Immunology*, *174*(3), 1491–1500. doi: 10.4049/jimmunol.174.3.1491

Walker, E. L., & Connolly, E. L. (2008). Time to pump iron: iron-deficiency-signaling mechanisms of higher plants. *Current Opinion in Plant Biology*, *11*(5), 530–535. doi: 10.1016/j.pbi.2008.06.013

Walton, F. J., Idnurm, A., & Heitman, J. (2005). Novel gene functions required for melanization of the human pathogen *Cryptococcus neoformans*. *Molecular Microbiology*, *57*(5), 1381–1396. doi: 10.1111/j.1365-2958.2005.04779.x

Weinberg, E. D. (1975). Nutritional immunity: host's attempt to withhold iron from microbial invaders. *JAMA: The Journal of the American Medical Association*, *231*(1), 39–41. doi: 10.1001/jama.1975.03240130021018

Weissman, Z., Berdicevsky, I., Cavari, B. Z., & Kornitzer, D. (2000). The high copper tolerance of *Candida albicans* is mediated by a P-type ATPase. *Proceedings of the National Academy of Sciences of the United States of America*, *97*(7), 3520–3525. doi: 10.1073/pnas.97.7.3520

Weissman, Z., Shemer, R., & Kornitzer, D. (2002). Deletion of the copper transporter CaCCC2 reveals two

distinct pathways for iron acquisition in *Candida albicans*. *Molecular Microbiology*, *44*(6), 1551–1560. doi: 10.1046/j.1365-2958.2002.02976.x

Wiemann, P., Perevitsky, A., Lim, F. Y., Shadkchan, Y., Knox, B. P., Landero Figueora, J. A., Choera, T., Niu, M., Steinberger, A. J., Wüthrich, M., Idol, R. A., Klein, B. S., Dinauer, M. C., Huttenlocher, A., Osherov, N., & Keller, N. P. (2017). *Aspergillus fumigatus* copper export machinery and reactive oxygen intermediate defense counter host copper-mediated oxidative antimicrobial offense. *Cell Reports*, *19*(5), 1008–1021. doi: 10.1016/j.celrep.2017.04.019

Wiesenberger, G., Link, T. A., Von Ahsen, U., Waldherr, M., & Schweyen, R. J. (1991). MRS3 and MRS4, two suppressors of mtRNA splicing defects in yeast, are new members of the mitochondrial carrier family. *Journal of Molecular Biology*, *217*(1), 23–37. doi: 10.1016/0022-2836(91)90608-9

Xiao, G., Wan, Z., Fan, Q., Tang, X., & Zhou, B. (2014). The metal transporter ZIP13 supplies iron into the secretory pathway in *Drosophila melanogaster*. *ELife*, *3*, e03191. doi: 10.7554/eLife.03191

Xu, N., Cheng, X., Yu, Q., Zhang, B., Ding, X., Xing, L., & Li, M. (2012). Identification and functional characterization of mitochondrial carrier Mrs4 in *Candida albicans*. *FEMS Yeast Research*, *12*(7), 844–858. doi: 10.1111/j.1567-1364.2012.00835.x

Yuan, D. S., Dancis, A., & Klausner, R. D. (1997). Restriction of copper export in *Saccharomyces cerevisiae* to a late Golgi or post-Golgi compartment in the secretory pathway. *Journal of Biological Chemistry*, *272*(41), 25787–25793. doi: 10.1074/jbc.272.41.25787

Yuan, D. S., Stearman, R., Dancis, A., Dunn, T., Beeler, T., & Klausner, R. D. (1995). The Menkes/Wilson disease gene homologue in yeast provides copper to a ceruloplasmin-like oxidase required for iron uptake. *Proceedings of the National Academy of Sciences of the United States of America*, *92*(7), 2632–2636. doi: 10.1073/pnas.92.7.2632

Zhang, P., Zhang, D., Zhao, X., Wei, D., & Wang, Y. (2016). Effects of CTR4 deletion on virulence and stress response in *Cryptococcus neoformans*. *Antonie van Leeuwenhoek*, *August*. doi: 10.1007/s10482-016-0709-2

Zhao, Y. N., Lii, C., Li, H., Liu, X. S., & Yang, Z. M. (2022). OsZIP11 is a trans-Golgi-residing transporter required for rice iron accumulation and development. *Gene*, *836*, 146678. doi: 10.1016/j.gene.2022.146678

Zhu, X., Boulet, A., Buckley, K. M., Phillips, C. B., Gammon, M. G., Oldfather, L. E., Moore, S. A., Leary, S. C., & Cobine, P. A. (2021). Mitochondrial copper and phosphate transporter specificity was defined early in the evolution of eukaryotes. *ELife*, *10*, 1–65. doi: 10.7554/eLife.64690

Zíková, A., Hampl, V., Paris, Z., Týč, J., & Lukeš, J. (2016). Aerobic mitochondria of parasitic protists: diverse genomes and complex functions. *Molecular and Biochemical Parasitology*, *209*, 46–57. doi: 10.1016/j.molbiopara.2016.02.007

Zygiel, E. M., & Nolan, E. M. (2019). Exploring iron withholding by the innate immune protein human calprotectin. *Accounts of Chemical Research*, *52*, 2301–2308. doi: 10.1021/acs.accounts.9b00250

6. Publications

PLOS NEGLECTED TROPICAL DISEASES

RESEARCH ARTICLE

Adaptive iron utilization compensates for the lack of an inducible uptake system in *Naegleria fowleri* and represents a potential target for therapeutic intervention

Dominik Arbon[1], Kateřina Ženíšková[1], Jan Mach[1], Maria Grechnikova[1], Ronald Malych[1], Pavel Talacko[2], Robert Sutak[1]*

1 Department of Parasitology, Faculty of Science, BIOCEV, Charles University, Vestec, Czech Republic, **2** BIOCEV proteomics core facility, Faculty of Science, BIOCEV, Charles University, Vestec, Czech Republic

* robert.sutak@natur.cuni.cz

Citation: Arbon D, Ženíšková K, Mach J, Grechnikova M, Malych R, Talacko P, et al. (2020) Adaptive iron utilization compensates for the lack of an inducible uptake system in *Naegleria fowleri* and represents a potential target for therapeutic intervention. PLoS Negl Trop Dis 14(6): e0007759. https://doi.org/10.1371/journal.pntd.0007759

Editor: Steven M. Singer, Georgetown University, UNITED STATES

Received: September 4, 2019

Accepted: April 20, 2020

Published: June 18, 2020

Data Availability Statement: All relevant data are within the manuscript and its Supporting Information files.

Funding: This work was supported by "The equipment for metabolomic and cell analyses" (CZ.1.05/2.1.00/19.0400, Research and Development for Innovations Operational Programme); Czech-BioImaging large RI projects (LM2015062 and CZ.02.1.01/0.0/0.0/16_013/0001775) and LQ1604 NPU II funded by Ministry

Abstract

Naegleria fowleri is a single-cell organism living in warm freshwater that can become a deadly human pathogen known as a brain-eating amoeba. The condition caused by *N. fowleri*, primary amoebic meningoencephalitis, is usually a fatal infection of the brain with rapid and severe onset. Iron is a common element on earth and a crucial cofactor for all living organisms. However, its bioavailable form can be scarce in certain niches, where it becomes a factor that limits growth. To obtain iron, many pathogens use different machineries to exploit an iron-withholding strategy that has evolved in mammals and is important to host-parasite interactions. The present study demonstrates the importance of iron in the biology of *N. fowleri* and explores the plausibility of exploiting iron as a potential target for therapeutic intervention. We used different biochemical and analytical methods to explore the effect of decreased iron availability on the cellular processes of the amoeba. We show that, under iron starvation, nonessential, iron-dependent, mostly cytosolic pathways in *N. fowleri* are downregulated, while the metal is utilized in the mitochondria to maintain vital respiratory processes. Surprisingly, *N. fowleri* fails to respond to acute shortages of iron by inducing the reductive iron uptake system that seems to be the main iron-obtaining strategy of the parasite. Our findings suggest that iron restriction may be used to slow the progression of infection, which may make the difference between life and death for patients.

Author summary

Naegleria fowleri is a unicellular amoeba living in warm freshwater that is able to infect humans and cause a serious and mostly fatal disease with rapid progression. When water with the amoeba enters the nose, *Naegleria* penetrates the mucosa and invades the human brain, where it destroys cells and causes massive inflammation. It is a rare infection with unspecific symptoms, which slows the critical process of identifying the cause of the disease. Iron is a necessary element for all living organisms used in many biological

of Education, Youth and Sports of the Czech Republic; Czech Science Foundation (18-07822S; 20-28072S); MiCoBion project funded from EU Horizon 2020 (No 810224) and CePaViP provided by The European Regional Development Fund and Ministry of Education, Youth and Sports of the Czech Republic (CZ.02.1.01/0.0/0.0/16_019/0000759). The funders had no role in study design, data collection and analysis, decision to publish, or preparation of the manuscript.

Competing interests: The authors have declared that no competing interests exist.

pathways; therefore, iron acquisition and iron metabolism have the potential to be exploited against this parasite to clear or slow the infection. It was discovered that *N. fowleri* is unable to efficiently regulate iron uptake in an environment with a low iron concentration and merely changes its energy metabolism to handle the lack of this element. Because of this limited response, *N. fowleri* is more sensitive to low iron conditions than are human cells, and treatment by iron chelators has the potential to kill the pathogen or slow the infection in the host.

Introduction

There are several free-living protists that, under certain conditions, are able to parasitize suitable hosts. The genus *Naegleria* consists of several species, the most studied of which are *Naegleria gruberi* and *Naegleria fowleri*, the latter being widely known as the "brain-eating amoeba". Its rather vivid nickname is attributed to the condition known as primary amoebic meningoencephalitis (PAM). The amoeba is found in warm freshwaters across most continents and can transition between three distinguishable forms: a durable cyst, trophozoite amoeba and mobile flagellate [1]. Its presence in water is a health risk for people participating in recreational activities involving bodies of water [2]. The disease is acquired when *N. fowleri* trophozoites forcefully enter through the nasal cavity, invade the olfactory neuroepithelium and follow the olfactory nerve to the brain, which is their final destination [3]. The disease has a rapid onset, and the nonspecific symptoms resemble those of more common bacterial or viral meningoencephalitis–headache, fever, vomiting–with rapid progress, causing seizures, coma, and death [4,5]. Since PAM occurs commonly in healthy individuals, *N. fowleri* is regarded not as an opportunistic parasite but as a pathogen [3]. The fatality rate for PAM is reported to be above 97% [6]. Treating PAM is difficult because the symptoms are typical of other maladies and have rapid onset and because no specific or efficient medication is available for ameliorating the disease. For successful treatment, it is crucial that a correct diagnosis is made quickly and that therapy is immediately delivered. The currently accepted treatment includes administering several medications simultaneously, such as amphotericin B, fluconazole, rifampin, azithromycin and/or miltefosine, in combination with methods that decrease brain swelling [4,7]. Thus, the need for an efficient cure or at least novel compounds that will slow the progression of the infection persists. Among other free-living amoebae, that can cause life-threatening diseases are species of *Acanthamoeba*, *Balamuthia* and *Sappinia*. These amoebae cause rare granulomatous amoebic encephalitis, a deadly disease with symptoms similar to PAM but that progress more slowly and with additional manifestations [8,9]. Nevertheless, the issues with battling these diseases, such as difficulty making a diagnosis, are the same.

There is very limited knowledge about the biochemistry and physiology of *N. fowleri*, and practically nothing is known about its metabolism of iron, even though this metal may represent the parasite's Achilles heel. Iron is an essential constituent of many biochemical processes, including redox reactions, the detoxification of oxygen, and cell respiration, and is a cofactor of various enzymes [10]. The ubiquitous role of iron is mainly due to its ability to transition between different oxidation states, enabling to participate in redox reactions, often in the form of iron-sulfur clusters [11]. Iron is essential for virtually all known forms of life, and its availability is shown to be the factor that limits organism growth in certain locations [12]. Its acquisition becomes especially challenging for pathogens that inhabit another living organism, as demonstrated by *Plasmodium*, in which iron-deficient human and mouse models manifest unfavorable conditions for parasite development; therefore, iron is a limiting factor for parasite

propagation [13,14]. As a defense mechanism, mammals minimize the presence of free iron in their body using several proteins, such as lactoferrin, ferritin or transferrin, which bind the metal, decreasing its bioavailability [15]. Parasitic organisms are known to have adopted various means of acquiring iron from their environments, ranging from engaging in opportunistic xenosiderophore uptake to expressing specific receptors for mammalian iron-containing proteins [16]. This two-sided competition between pathogens and their hosts indicates the importance of iron metabolism in disease and underlines the importance of further research on this topic in the search for new methods of therapeutic intervention.

In this study, we demonstrate how *N. fowleri* acquires iron from its environment and how it adapts to iron-deficient conditions and we propose that the amoeba iron metabolism can be exploited to the advantage of PAM patients. We tested several potential iron uptake mechanisms and observed that the iron uptake system was not induced under iron starvation conditions and that the parasite used no alternative metabolic pathway to adjust for the resulting iron deficiency. Proteomic and metabolomic investigations showed that *N. fowleri* responded to low iron levels by maintaining iron-containing proteins in mitochondria, while the activity of nonvital, mostly cytosolic, iron-requiring pathways declined. These findings revealed a possible exploitable weakness in the survival strategy of the amoeba within the host. Although the host brain is relatively rich in iron content [17], not all of the iron is readily available for the parasite to use, as we have shown that it is not able to utilize iron bound to transferrin, the main source of iron in the human brain [18]. Thus, by using artificial chelators to decrease the availability of iron in this organ, we show a possible complementary antiparasite strategy, which is already utilized for different purposes, against this deadly pathogen [19].

Results

N. fowleri uses an uninducible reductive mechanism to acquire iron, while transferrin is not utilized

Iron is generally available in the environment in two distinct oxidation states. Due to the different solubilities of the two forms, many organisms use ferric reductase to reduce ferric iron to ferrous iron, which is more soluble and therefore easier to assimilate. To explore the mechanism by which *N. fowleri* acquires iron from its surroundings, cell cultures were supplemented with different sources of iron: ^{55}Fe-transferrin, ^{55}Fe(III)-citrate and ^{55}Fe(II)-ascorbate. For all the experiments conducted in this study, unless stated otherwise, iron deprivation was achieved using 25 μM of the common extracellular chelator bathophenanthroline disulfonic acid (BPS) to create a condition in which cell growth was significantly affected but microscopy showed no encystation or flagellated forms, and the cells did not lose their ability to multiply or attach to the surface. This condition was an important prerequisite, particularly for the proteomic and transcriptomic analysis, where very complex changes are accompanied by unfavorable cell processes that could bias the data. To achieve iron-rich conditions in this study, the cultivation medium was supplemented with 25 μM ferric nitrilotriacetate (Fe-NTA). The results presented in Fig 1A show that ferrous iron is taken up and incorporated into intracellular protein complexes more rapidly than was its trivalent counterpart. Densitometry of the radioactive signal in dried native electrophoresis gels was used to calculate the difference in iron utilization between the two forms: The utilization of ferric iron in comparison to ferrous iron was decreased in iron-rich cells to 65% (±8%; p-value <0.05) and in iron-deficient cells to 61% (±3%; p-value <0.01), suggesting the involvement of ferric reductase in the effective assimilation. Surprisingly, there was no significant difference in iron uptake between cells preincubated in the iron-rich and iron-deficient conditions, showing that the organism failed to stimulate its iron uptake machinery. The insignificant uptake of transferrin, shown in S1(B)

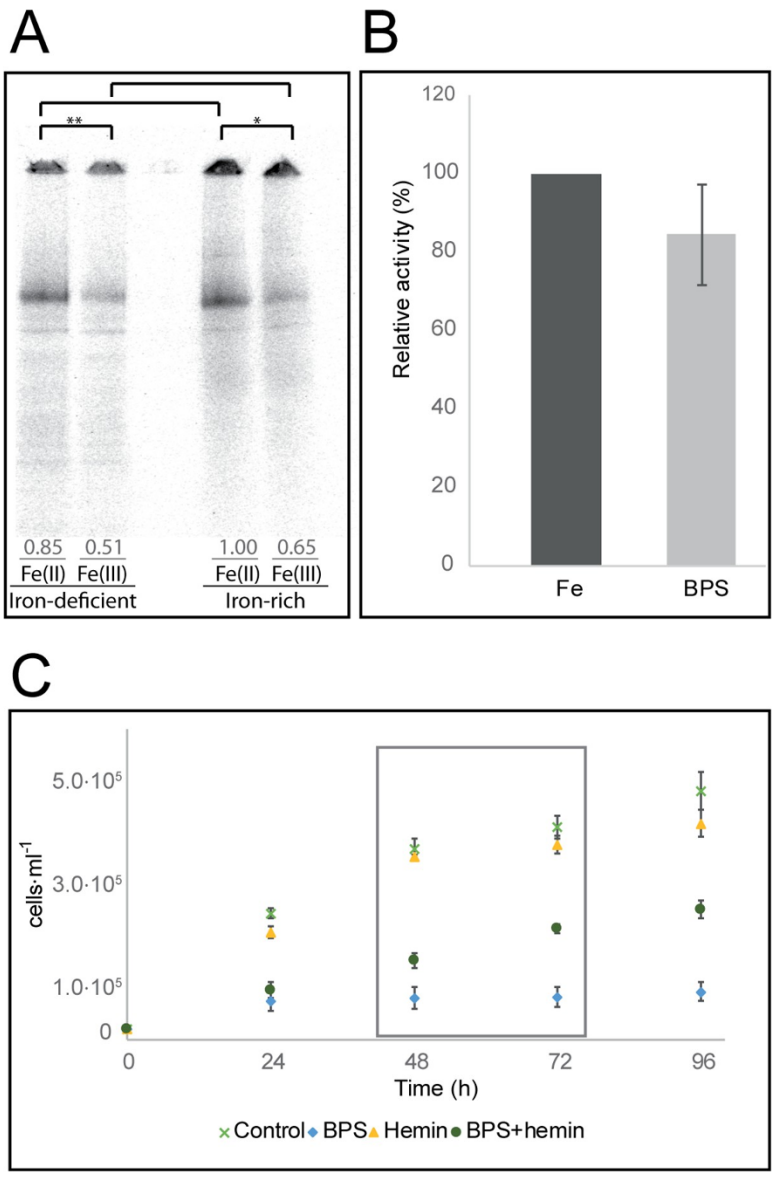

Fig 1. Iron uptake in *N. fowleri*. (A) Ferrous and ferric iron uptake by *N. fowleri* precultivated under iron-rich and iron-deficient conditions. Autoradiography of blue native electrophoresis gels of whole cell extracts from *N. fowleri* previously cultivated for 72 hours under iron-deficient conditions (25 μM BPS) or iron-rich conditions (25 μM Fe-NTA) and further incubated with ^{55}Fe(II) (ferrous ascorbate) or ^{55}Fe(III) (ferric citrate). Equal protein concentrations were loaded, and the loading control is shown in S1(A) Fig. The gel is representative of three independent replicates. Numbers indicate average relative densitometry values for the appropriate lines. Significant differences between band densitometry values are denoted by asterisk (*, $p<0.05$; **, $p<0.01$). (B) Ferric reductase activity under iron-rich and iron-deficient conditions. Relative values of *N. fowleri* ferric reductase activities in the iron-rich (Fe) and iron-deficient (BPS). The difference between the two conditions was not significant, p-value >0.05. Data are presented as the relative percentage ± SD from three independent replicates. (C) Growth restoration of *N. fowleri* in culture by hemin under iron-deficient conditions. Cells in regular growth medium (control) and with 50 μM hemin (hemin) exhibited similar levels of propagation, while the cells under iron-deficient conditions, achieved with 50 μM chelator bathophenanthroline disulfonic acid (BPS), showed stagnated growth in the first 24 hours. The addition of 50 μM hemin to the iron-deficient medium (BPS+hemin) partially restored culture growth. The boxed area indicates the time from which growth restoration was calculated. Data are presented as the means ± SD from four independent replicates.

https://doi.org/10.1371/journal.pntd.0007759.g001

Fig, means that this protein is not a viable source of iron for *N. fowleri*, corresponding to the fact that it is not found in the usual water habitat of this organism.

To confirm that *N. fowleri* uses a reductive iron uptake mechanism, the cell cultures were treated with a ferric iron radionuclide in the presence and absence of the ferrous iron chelator BPS. The results shown in S1(C) Fig demonstrate that, while *N. fowleri* readily incorporates ferric iron into its protein complexes, BPS chelates the initially reduced ferrous iron and prevents it from being further utilized, confirming that ferric iron uptake requires a reduction step.

We have shown that neither ferrous nor ferric iron uptake is induced by iron starvation (Fig 1A). Considering the involvement of the reduction step needed for *N. fowleri* iron acquisition, the activity of a ferric reductase was assessed in cells preincubated under iron-rich and iron-deficient conditions. As shown in Fig 1B, measurements of ferric reductase activity revealed that the level of ferric iron converted to ferrous iron was not significantly changed in the iron-deprived cells (p-value >0.05). This finding confirms that *N. fowleri* cannot efficiently adjust the rate of iron acquisition from its surroundings to overcome its dependence on iron availability.

Heme-containing proteins are potential source of iron or heme for several parasitic protists [20,21]. Although we did not identify a homolog of heme oxygenase in the *N. fowleri* genome, which is necessary for the breakdown of heme and the release of iron, we tested the effect of the presence of hemin in the cultivation medium on the growth of the amoebae. As shown in Fig 1C, cells cultivated in regular growth medium had a propagation pattern similar to that of the cells grown in medium supplemented with 50 μM hemin; therefore, at the given concentration, hemin was not toxic to *N. fowleri*, nor did it significantly support its growth under standard cultivation conditions. The profound iron-deficient conditions achieved with 50 μM BPS arrested culture growth to 31% (±12%) during the first 24 hours, and the propagation at later time points remained below this value. The addition of 50 μM hemin partially restored culture growth to 42% (±10%; p-value <0.01) after 48 hours, and by 72 hours, the growth reached 52% (±7%; p-value <0.01). Therefore, it appears that the hemin compound is used as a partial source of iron for the pathogen, although it cannot fully support its growth when other sources of iron are limited.

Proteomic analysis findings illuminate the iron-starvation response of *N. fowleri*, while the transcriptomic analysis does not reflect the proteomic changes

Since iron has an irrefutable role as a cofactor for various enzymes and its metabolism is dependent on a great number of proteins, we aimed to examine the overall effect of iron availability on the *N. fowleri* proteome. Therefore, we compared the whole-cell proteomes of cells grown under iron-rich and iron-deficient conditions, and we have additionally analyzed membrane-enriched fractions of cells to obtain a higher coverage of the membrane proteins. The aim was to reveal the metabolic remodeling accompanying iron starvation and to identify proteins responsible for iron homeostasis, such as membrane transporters, signaling and storage proteins or proteins involved in iron metabolism, for example, the formation of iron-sulfur clusters.

S1 Table lists the proteins that were significantly upregulated or downregulated under iron-deficient conditions based on the analysis of the *N. fowleri* whole-cell proteome, and S2 Table contains the regulated proteins in the membrane-enriched fraction. No major changes in encystation or flagellation markers or apoptotic pathway proteins between the two conditions were detected in the proteomic analysis. The proteins most relevant for this study are

Table 1. Effect of iron deprivation on the abundance of selected *N. fowleri* proteins.

Gene ID	Protein	Whole cell (membrane fraction) proteomics fold-change in iron deficiency	*p*-value
NF0117840	Protoglobin	ND in iron-deficient	NA
NF0127030	Hemerythrin	-7045.1	<0.05
NF0119700	Hemerythrin	-11.4	NA
NF0106930	Phenylalanine hydroxylase	-5.7	<0.05
NF0008540	Hydrogenase	-3.7	<0.05
NF0081220	HydE	-2.8	<0.05
NF0081230	HydG	-2.4	<0.05
NF0036800	Iron-containing cholesterol desaturase daf-36-like	-2.0 (-3.4)	NA (<0.05)
NF0001470	Tyrosine aminotransferase	-2.0	<0.05
NF0073220	Homogentisate 1,2-dioxygenase	-1.8	<0.05
NF0084900	4-Hydroxyphenylpyruvate dioxygenase	-1.5	<0.05
NF0121200	Catalase	-1.3	<0.05
NF0044680	Iron III Superoxide Dismutase	1.1	0.47
NF0004720	Alternative oxidase	1.5	<0.05
NF0014630	Mitochondrial carnitine/acylcarnitine transferase *	ND (1.5)	NA (0.39)
NF0015750	Manganese superoxide dismutase	1.6	<0.05
NF0079420	Mitoferrin *	1.8 (1.7)	<0.05 (0.08)
NF0020800	Fe superoxide dismutase	1.8	<0.05
NF0048730	Glutathione peroxidase	2.0	<0.05
NF0071710	Deferrochelatase	2.3	<0.05
NF0060430	IscU *	3.0	<0.05
NF0001440	Cysteine desulfurase	3.7	<0.05
NF0030360	Cu-Zn superoxide dismutase	5.8	<0.05
NF0001420	Mitochondrial phosphate carrier protein *	8.0 (8.4)	NA (<0.05)

Proteins were manually annotated using HHPRED or by sequence alignment with homologous proteins from other organisms (denoted with a star). The fold change based on proteomic analysis of whole cells and membrane fractions (for selected proteins; in brackets) is given for cells cultivated under iron-deficient conditions. Significantly regulated proteins (with a fold change above 2.3 and *p*-value not higher than 0.05) are highlighted in green. ND, not detected; NA, not applicable.

https://doi.org/10.1371/journal.pntd.0007759.t001

summarized in Table 1. The list of downregulated proteins based on whole-cell proteomics under iron-deficient conditions contained 20% of predicted iron-containing proteins, most of which were nonheme enzymes such as desaturases and oxygenases, or hydrogenase (NF0008540) and its maturases HydE (NF0081220) and HydG (NF0081230). Importantly, most of the downregulated iron-containing proteins were typically located outside mitochondria. The dramatic downregulation of the hemerythrin homolog (NF0127030) was confirmed by Western blotting using an antibody generated in-house against *N. gruberi* hemerythrin (Fig 2A).

In the phenylalanine catabolism pathway, all three iron-dependent enzymes, phenylalanine hydroxylase (NF0106930), p-hydroxyphenylpyruvate dioxygenase (NF0084900) and homogentisate 1,2-dioxygenase (NF0073220), were downregulated in iron-deprived cells, even though the decrease in the expression of the last two enzymes was below our set threshold.

The proteins upregulated under iron-deficient conditions included two essential mitochondrial components of iron-sulfur cluster assembly machinery, namely, cysteine desulfurase (NF0001440) and iron-sulfur cluster assembly enzyme IscU (NF0060430); two mitochondrial transporters, phosphate carrier (NF0001420) and iron-transporting mitoferrin (NF0079420); and a potential homologue of deferrochelatase (NF0071710). The increase in the expression of mitoferrin was below our set threshold, but the results from the comparative analysis of the

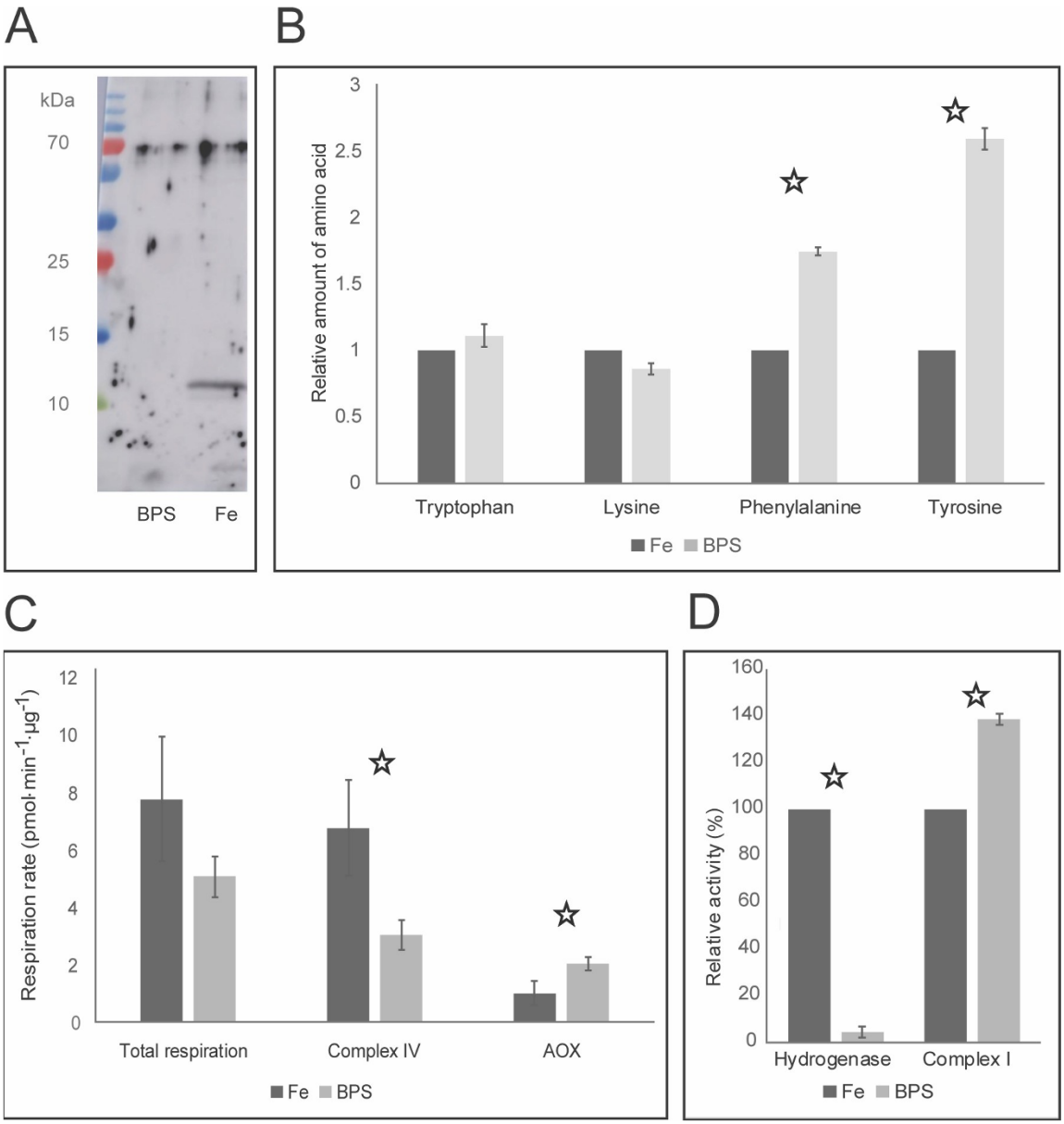

Fig 2. Effect of iron deficiency on *N. fowleri*. (A) Downregulation of *N. fowleri* hemerythrin under iron-deficient conditions. Results from the Western blot analysis of cells cultivated under iron-rich (Fe) and iron-deficient (BPS) conditions using an antibody against *Naegleria gruberi* hemerythrin. Equal protein concentrations were loaded, and the loading control is shown in S1(D) Fig. The gel represents one of three independent replicates. (B) Cellular content of selected amino acids in *N. fowleri* cells cultivated under iron-rich and iron-deficient conditions. Relative amounts of phenylalanine and tyrosine were significantly increased under the iron-deficient condition, while those of tryptophan and lysine remained unchanged. t-test p-values <0.01 are marked with a star. The total protein concentration was equal in all the samples, and the values shown are relative to those under the iron-rich conditions for each amino acid. Fe, cells cultivated under iron-rich conditions; BPS, cells cultivated under iron-deficient conditions. Data are presented as the means ± SD from three independent replicates. (C) Respiration of *N. fowleri* grown under iron-rich and iron-deficient conditions. Using selective inhibitors of complex IV (potassium cyanide) and of alternative oxidase (salicyl-hydroxamic acid), the contribution of alternative oxidase and complex IV activity was assessed with respect to total respiration levels. AOX, alternative oxidase; Fe, cells cultivated under iron-rich conditions; and BPS, cells cultivated under iron-deficient conditions. The t-test p-values <0.01 are marked with a star. Data are presented as the means ± SD from five independent replicates. (D) Activity of hydrogenase and NADH: ubiquinone dehydrogenase (complex I) under iron-rich and iron-deficient conditions. While hydrogenase was significantly downregulated, complex I was significantly upregulated as a result of the iron-deficient conditions. Relative values are shown. Fe, cells cultivated under iron-rich conditions; and BPS, cells cultivated under iron-deficient conditions. The t-test p-values <0.01 are marked with a star. Data are presented as the means ± SD from four independent replicates.

https://doi.org/10.1371/journal.pntd.0007759.g002

membrane-enriched fraction of *N. fowleri* grown under different iron conditions (S2 Table and Table 1) confirmed the upregulation of this transporter as it did for the mitochondrial phosphate carrier. Additionally, in the membrane-enriched proteomic analysis, a carnitine/acylcarnitine transferase (NF0014630) was identified and found to be slightly, although not significantly, upregulated.

Iron metabolism is interconnected with the production and detoxification of reactive oxygen species. Among the antioxidant defense proteins, one family of superoxide dismutases contains iron as a cofactor. Our proteomic analysis showed that while iron-dependent SODs (NF0020800 and NF0044680) were not significantly changed, Cu-Zn-dependent SOD (NF0030360) was upregulated under iron-deficient conditions, suggesting a compensatory mechanism for the mismetallated iron-dependent enzyme. Other radical oxygen species detoxification enzymes, such as catalase (NF0121200), manganese SOD (NF0015750), or glutathione peroxidase (NF0048730), were not significantly regulated under iron-deficient conditions.

To uncover a broader spectrum of the affected proteins that we were unable to detect in the proteomic analysis, we performed a transcriptomic analysis of *N. fowleri* grown under the same conditions of iron availability as used in the proteomic analysis (S3 Table). To our surprise, the data did not correspond to the proteomics results. Overall, the number of genes that were significantly changed in the transcriptomic analysis results was 287 (182 upregulated and 105 downregulated genes), which is more than those regulated in whole cell proteomic analysis; however, the only genes regulated in the same way as the proteins observed in the proteomic analysis were hemerythrins, protoglobin (NF0117840) and the iron-containing cholesterol desaturase daf-36-like (NF0036800). The response of *N. fowleri* to iron starvation is thus most likely posttranslational. The large proportion of nonheme iron-containing enzymes among the downregulated proteins indicates that the degradation of mismetallated/misfolded/nonfunctional proteins plays an important role in iron-induced proteome changes. To confirm the physiological relevance of the changes observed at the proteome level, we further investigated selected biochemical pathways that were indicated by the proteomic results.

N. fowleri responds to iron deficiency by metabolic rearrangement that favors mitochondria

Considering the iron-dependent changes in the abundance of proteins participating in the phenylalanine degradation pathway, the next aim of this study was to analyze this effect by directly detecting metabolites, namely quantifying the cellular levels of corresponding amino acids by metabolomics. Cells grown under iron-rich and iron-deficient conditions were lysed, the protein concentrations were equalized, and the resulting material was analyzed for amino acid content by liquid chromatography coupled with mass spectrometry. Since the phenylalanine degradation pathway was predicted to be downregulated by the proteomic analysis results, we assessed the intracellular amounts of phenylalanine and tyrosine, amino acids likely affected by a decrease in iron-dependent enzymes. As expected, under iron-deficient conditions, the amount of phenylalanine was significantly increased, by 75% (±3%; p-value <0.01), and tyrosine was increased by 160% (±8%; p-value <0.01) (data are shown in Fig 2B). As controls, relative amounts of tryptophan and lysine, the levels of which were not expected to change according to iron levels, were determined in the same samples.

N. fowleri cells possess lactate dehydrogenase and are therefore potentially able to produce lactate from pyruvate while replenishing the level of NAD^+ cofactor, thereby utilizing cytosolic pathways for energy metabolism. To analyze the effect of iron starvation on this metabolic pathway, lactate production was analyzed by gas chromatography coupled with mass

spectrometry detection. The level of intracellular lactate in the iron-deficient cells was decreased by 32% (±13%; p-value <0.05), showing that this metabolic pathway was not used in a compensatory strategy during iron deficiency.

Alternative oxidase (AOX), present in *N. fowleri*, is a part of the mitochondrial respiratory chain. It accepts electrons from ubiquinol to reduce the final electron acceptor, oxygen. Therefore, the function of AOX is similar to that of complex IV; however, the branching electron flow towards AOX bypasses some of the proton pumping complexes, decreasing the effect of the respiration chain. Using selective inhibitors of respiration complex IV and AOX enables the study of their participation in respiration. Here, the effect of decreased iron availability on the respiratory chain was determined. The results are shown in Fig 2C and demonstrate that the total respiration of the cells grown under iron-deficient conditions was decreased by 35%, although this change was not statistically significant (p-value >0.01), and that this decrease was based on the diminished activity of complex IV (55% decrease; p-value <0.01). In contrast, in the iron-deficient cells, the activity of AOX increased by 104% (p-value <0.01). This finding shows that AOX, despite being an iron-containing enzyme, is able to rescue respiration when iron deficiency causes a decrease in complex IV activity.

To further support the hypothesis that iron-starved *N. fowleri* maintains essential mitochondrial iron-dependent proteins at the expense of nonessential cytosolic proteins, we assessed iron-induced changes in the activity levels of mitochondrial NADH:ubiquinone dehydrogenase (complex I) and hydrogenase, which was shown to be cytosolic in *Naegleria* [22]. As shown in Fig 2D, the activity of hydrogenase was dramatically decreased, by 95%, under iron-deficient conditions (p-value <0.01), indicating that it is a dispensable component of the pathway when iron is scarce. In contrast, the activity level of mitochondrial complex I was increased by 39% under iron-deficient conditions (p-value <0.01), thus it was maintained as part of a vital pathway. Hence, the increased activity levels of the mitochondrial iron-containing enzymes AOX and complex I were able to rescue total mitochondrial respiration despite the decrease in the activity of complex IV. This finding demonstrates that the mitochondrial respiration chain is essential and maintained under iron-deficient conditions even if it is strongly iron demanding.

Iron chelators significantly hinder *N. fowleri* growth

Iron plays a vital role in many biochemical processes; therefore, it is rational to expect that decreasing the bioavailability of iron in the surrounding environment would hinder cell growth. To determine the effect of iron on the propagation of *N. fowleri* in culture, three different iron chelators were added to the growth medium: bathophenanthroline disulfonic acid (BPS), 2,2′-dipyridyl (DIP) and deferoxamine (DFO). The compounds inhibited the growth of the cultures to different extents compared to the growth under iron-rich conditions (Table 2 and S2(A) Fig). The most potent effect in hindering culture growth was observed with the siderophore DFO. Both BPS and DIP had notably higher IC_{50} values.

Trophozoites of the amoebae feed on bacteria in their natural environment, making the bacteria potential sources of iron. Moreover, we presume that phagocytosis of human cells can represent one of *N. fowleri* virulence factors [23]. To investigate overall cell viability and to test whether *N. fowleri* cells induce phagocytosis as a potential way to acquire iron, the ability of iron-deficient cells to phagocytose bacteria was investigated. Quantification of phagocytosis was determined by flow cytometry using *Escherichia coli* that present increased fluorescence within acidic endocytic compartments. The values were calculated as percentages of amoebae in the total population with phagocytosed bacteria. Under iron-rich conditions, the percentage of phagocytosing amoebae was 70% (±6%), while under iron-deficient conditions, it was 53%

Table 2. Iron chelator IC_{50} values for *N. fowleri* cultures after 48 hours.

Compound	IC_{50} (μM)
DIP	30.39 (±3.49)
BPS	17.01 (±2.42)
DFO	6.32 (±0.85)

DIP, 2,2′-dipyridyl; BPS, bathophenanthroline disulfonic acid; and DFO, deferoxamine. The data used for the IC_{50} extrapolation are depicted in S2(B) Fig.

https://doi.org/10.1371/journal.pntd.0007759.t002

(±4%). This significant decrease (p-value <0.01) shows that iron availability plays a role in this process. A representative dot plot from the flow cytometry data is shown in S3 Fig, including the controls of *N. fowleri* cells with no bacteria and a bacterial culture. A typical cell phagocytizing fluorescent bacteria is shown in the S1 video.

To show the extent to which iron-deficient *N. fowleri* is able to restore its own growth by phagocytosing bacteria, we presented attenuated *Enterobacter aerogenes* to amoebae cultivated under different iron conditions. As shown in S4 Fig, while the iron-deficient cells proliferated significantly more slowly than the iron-rich cells did, the addition of bacteria did not increase the proliferation of the cells cultivated under iron-deficient or iron-rich conditions. In contrast, the addition of iron to previously iron-deficient cultures fully reestabilished the original cell proliferation rate. In summary, iron is a vital element for *N. fowleri* cell propagation and chelators have a cytostatic effect on amoebae. Phagocytosis of bacteria is not a sufficient strategy of iron acquisition and is even suppressed during iron deficiency.

Discussion

To maintain an optimal level of cellular iron in a hostile environment, such as host tissues, pathogens possess selective and effective mechanisms for iron uptake. These strategies of obtaining iron include the utilization of various sources from the host, including transferrin, lactoferrin or heme, and some parasites even exploit bacterial siderophores as sources of iron [16]. Transferrin, an abundant human blood protein that transports iron to various tissues, including the brain [18], serves as a viable source of iron for different parasites [16]. It was demonstrated that *N. fowleri* possesses proteases able to degrade human holotransferrin, although the study did not identify the intracellular fate of the iron [24]. Our study shows that *N. fowleri* does not appear to have the means of efficiently utilizing iron from this host protein (S1B Fig), perhaps because it is a facultative pathogen with no advantage of such an iron uptake mechanism in its natural environment. We further demonstrated the preference of *N. fowleri* for ferrous iron compared to ferric iron (Fig 1A), the inhibitory effect of ferrous iron chelator on ferric iron uptake (S1C Fig) and the presence of extracellular ferric reductase activity (Fig 1B). Based on these observations, we argue that the main strategy of iron acquisition by this parasite could be the reductive two-step iron uptake mechanism, as described for *Saccharomyces cerevisiae* [16].

S. cerevisiae possesses the ability to upregulate the expression of ferric reductase, which is responsible for the first step of the reductive iron uptake mechanism, up to 55 times under iron-deficient conditions [25], therefore increasing the rate of iron uptake. Our study shows that in *N. fowleri*, the activity of ferric reductase is not induced by iron starvation nor is the ferric and ferrous iron uptake and further incorporation of iron into cellular proteins (Fig 1A and 1B). The lack of an inducible iron uptake system has also been described in the parasite *Tritrichomonas foetus* [26]. However, contrary to *N. fowleri*, the obligatory parasite *T. foetus* appears to be able to utilize a wide range of iron sources, including host transferrin or bacterial

siderophores. Another potential source of iron for *N. fowleri* can be heme from heme-containing proteins. The ability to utilize exogenous metal-containing porphyrins may be advantageous for protists feeding on bacteria. Moreover, *Naegleria* species phagocyte erythrocytes [27,28], and their ability to degrade hemoglobin using proteases was also described [24]. However, it appears that heme oxygenase is not present in the genome of *N. fowleri*; therefore, it is unlikely to be able to employ this enzyme to obtain iron from hemoglobin, as is the case of *T. foetus* [26]. A potential homologue of bacterial deferrochelatase, a protein able to directly acquire iron from heme [29], was identified as significantly upregulated under iron-deficient conditions by proteomic analysis (Table 1); however, further investigation is required to clarify the function of this protein. Nevertheless, hemin was shown to partially restore *N. fowleri* growth in very strong iron-deficient conditions (Fig 1C). Since *N. fowleri* requires exogenous porphyrins for growth [30], the fact that the addition of hemin partly suppresses the conditions of iron starvation can be attributed to a metabolic rearrangement towards heme-dependent pathways. Although phagocytosis could be an alternative strategy for obtaining iron in natural and host environments, according to our data, it does not appear to be utilized under iron-deficient conditions. We showed that the actual rate of phagocytosis was decreased in this case and that the extent of iron-deficient culture propagation could be restored by the addition of iron but not by attenuated bacteria (S4 Fig). Considering these findings, it is important to note that the relationship between decreased phagocytosis and decreased hemerythrin expression was previously described [31]. While *N. fowleri* is unable to utilize iron from transferrin, it is possible that phagocytosis is one of the strategies for obtaining iron from the host and thus may represent a virulence factor that can be diminished by iron starvation. This presents an opportunity to use chelation-based therapy to decrease the ability of the pathogen to gain access to the available iron from host tissues and thereby further increases the iron deficiency of the parasite.

Proteomic analysis proved to be a valuable resource in determining the cellular changes in *N. fowleri* induced by iron starvation and provided a foundation for further discoveries that are shown in this study (Table 1). The most fundamental finding of comparative proteomic analysis is that mainly cytosolic iron-containing proteins were downregulated when iron was limited. These proteins are likely components of nonessential pathways, such as the phenylalanine degradation, hydrogenase maturation and hydrogen production pathways. The accumulation of phenylalanine was observed in *S. cerevisiae*, where iron-deficient cells contained about 50% more of the amino acid than iron-rich cells [32]. On the other hand, mitochondrial iron-dependent proteins were generally unchanged, while some components of the iron-sulfur cluster synthesis machinery were upregulated under iron-deficient conditions, emphasizing the essential role of iron-dependent respiration process. This mitochondrial sequestration of iron to ensure respiration was confirmed by increased complex I activity with a concomitant decrease in the activity level of hydrogenase (Fig 2D) as well as a reduction in the iron-dependent catabolism of amino acids (Fig 2B). Consistent with this observation, the mitochondrial iron transporter was upregulated under iron-deficient conditions. Moreover, the carnitine/acylcarnitine carrier was identified in the membrane-enriched proteomic analysis, and its expression was slightly increased in iron-starved cells. This mitochondrial membrane-bound protein is involved in lipid metabolism, which was recently shown to be vital for *N. gruberi* [33]. Another mitochondrial transport protein, a phosphate carrier, was strongly upregulated under iron-deficient conditions, likely to compensate for impaired respiration and decreased ATP production in the mitochondria of iron-deficient cells.

N. fowleri, as well as *N. gruberi*, possesses an AOX in the mitochondria, and our study indicates one of the possible advantages of this respiratory chain element for these organisms. Under iron-deficient conditions, the activity of AOX was significantly increased (Fig 2C), even

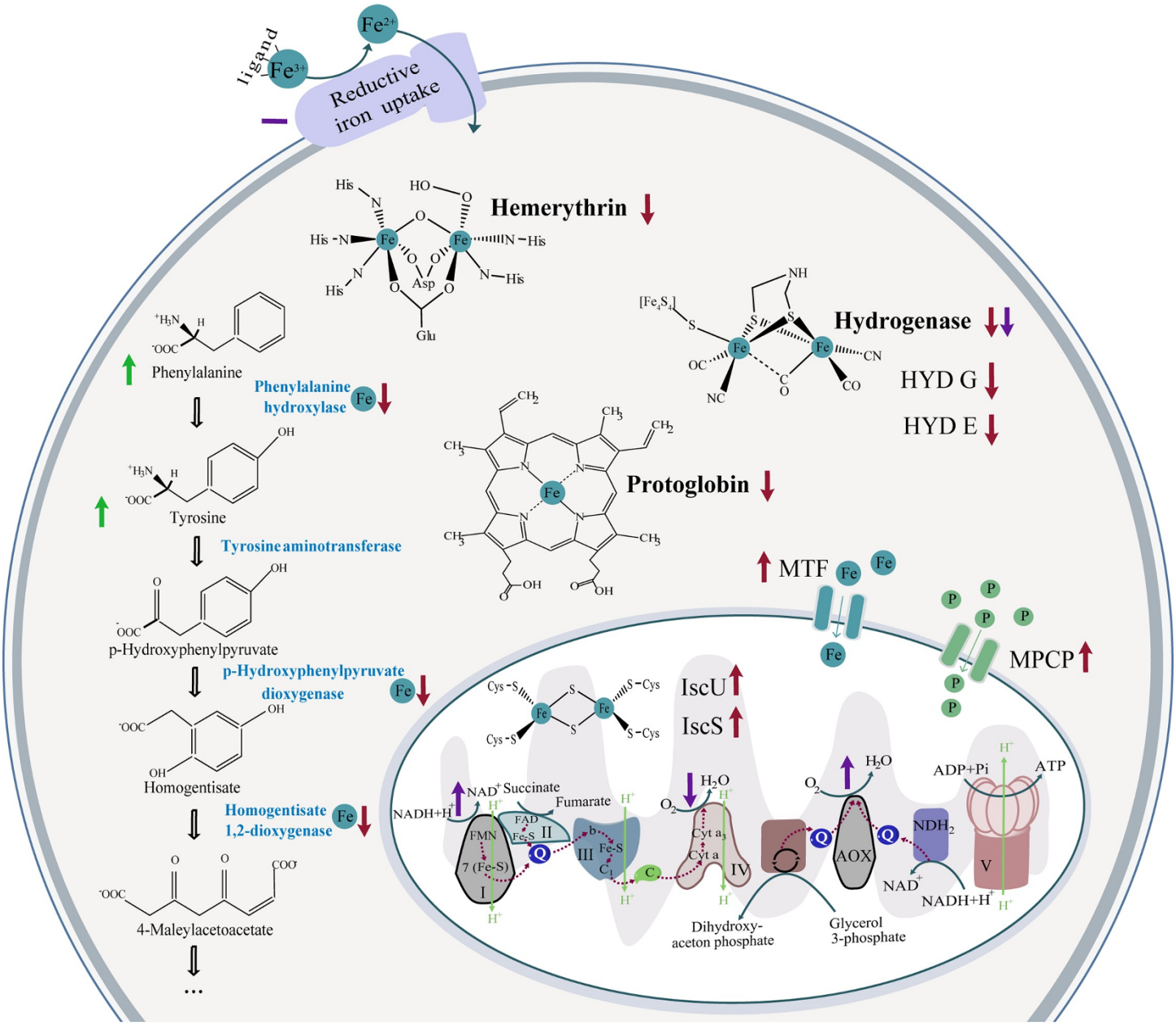

Fig 3. Illustration of the main effects of iron-deficient conditions on the selected cellular processes of *N. fowleri*. The results of proteomic analysis for selected proteins are depicted in red, the results from measured metabolite levels are in green and the assessed enzyme activities are in purple. Upwards pointing arrows stand for increased in the iron-deficient condition, downwards pointing arrows represent decreased in the iron-deficient conditions and dashes mean no significant change in the different iron conditions. Respiration chain complexes are represented by appropriate numbers, Fe represents iron-containing/involving protein/process. C, cytochrome C; MTF, mitoferrin; MPCP, mitochondrial phosphate carrier protein; P, phosphate; Q, ubiquinol/ubiquinone.

https://doi.org/10.1371/journal.pntd.0007759.g003

though it requires iron, suggesting that this unusual branch of the respiratory chain may take over a portion of the activity in the iron-demanding conventional pathway of respiratory complexes III, IV and cytochrome c, an observation noted in the nonpathogenic amoeba *N. gruberi* previously [34]. This could represent a favorable compensation pathway, even though the overall generation of the proton gradient and therefore ATP synthesis is hindered. In addition, we observed an increase in the activity of complex I (Fig 2D), supporting the claim that the respiration is shifted towards the less-efficient but also less iron-dependent AOX pathway.

Considering the reduced efficiency of respiration by iron-starved cells and the presence of lactate dehydrogenase in the genome of *N. fowleri*, it would be reasonable to expect the employment of the lactate dehydrogenase pathway in the regeneration of the cofactor NAD^+. Such an effect was observed in *Trichomonas vaginalis*, where the cells modulate this pathway as a way of compensating for the metronidazole-induced loss of hydrogenosomal metabolism [35]. However, our metabolomic analysis showed the opposite change; the production of lactate was decreased upon iron starvation, suggesting another, most likely nonessential, function of this pathway that is attenuated due to the hindered rate of overall energy metabolism. Another possible compensatory pathway, ethanol production, is improbable because of the absence of pyruvate decarboxylase or bifunctional aldehyde/alcohol dehydrogenase in the *N. fowleri* genome. The function of cytosolic hydrogenase, which was significantly downregulated in the iron-limited conditions together with its maturation factors, is unknown in *Naegleria*.

Consistent with our previous study of iron metabolism in *N. gruberi* [34], hemerythrin was dramatically downregulated under iron-deficient conditions (Fig 2A), while it appears to be an abundant protein under standard conditions, based on the intensities obtained in proteomic analysis from iron-rich cells. The involvement of hemerythrin in the iron metabolism of *Naegleria* is suggestive but unclear. The presence of unbound metals in the cell must be strictly regulated since the imbalance in iron homeostasis can lead to the formation of ROS, mismetallation or other anomalies leading to the incorrect function of proteins. The relationship between hemerythrin and defense against oxidative stress was previously suggested in bacteria [36,37] and so was the role of hemerythrin-related proteins in iron homeostasis [38] or oxygen sensing [39]. One of the basic mechanisms of maintaining the proper intracellular level of metals is the regulation of their acquisition. Since our study shows the lack of such regulation for iron, it is possible that the sequestration of toxic free iron, as well as its storage for use under iron-deficient conditions, is ensured by hemerythrin functioning as a cytosolic iron pool. This hypothesis is supported by the fact that hemerythrin is a nonheme, noniron-sulfur metalloenzyme and is among the most strongly regulated proteins by iron availability, and unlike other proteins, its regulation was detected even at the mRNA level. Another oxygen-binding protein with unclear function, protoglobin, was detected only under iron-sufficient conditions. The role of protoglobin in the metabolism of *N. fowleri* remains to be elucidated.

Due to the irreplaceable role of iron in cellular processes, it is unsurprising that iron chelators have the ability to hinder the proliferation of *N. fowleri* [40]. The different chelators used in this study have distinct properties that influence their impact on cells. DIP is a membrane-permeable compound with affinity to ferrous iron [41] and a ratio of three chelator molecules binding one molecule of metal [42]. BPS is a membrane-impermeable chelator that binds ferrous iron with a ratio of three chelator molecules to one metal ion [43]. Finally, DFO is a membrane-impermeable, ferric iron-binding siderophore [44] with a binding ratio of one iron per molecule [45]. Quite surprisingly, the only tested membrane-permeable iron chelator, DIP, had the highest IC_{50} value (30.39 μM; SD = 3.49). In comparison with BPS, with which it shares an affinity to ferrous iron and the same denticity, DIP was almost half as effective in inhibiting culture growth. BPS and DFO differed not only by the oxidation state of bound iron but also by the ratio of molecules bound to the chelated iron. Their IC_{50} values were 17.01 μM (SD = 2.42) and 6.32 μM (SD = 0.85), respectively, showing an apparent tendency of the approximately three-fold amount of BPS required to have the same effect as DFO, probably because of the binding ratio. Therefore, surprisingly, it appears that from the selected chelators, the membrane-impermeable chelators are more effective against *N. fowleri*. It is important to consider that the growth medium used in this study was adjusted to the amoeba requirements, while in its host, the parasite is expected to meet much harsher conditions. The inhibiting concentrations of chelators shown in this study were of a magnitude that can be

achieved in the human body, such as has been shown for DFO [46], demonstrating that chelation therapy could be considered in the case of PAM. It must be emphasized, that experiments in this study were performed in axenic cultures under optimal growth conditions. Thus, the anticipated *in vivo* antiparasitic effect of suitable chelators may be more pronounced. This laboratory setting undoubtably differs from the natural habitat of the pathogen or the host, where the conditions are harsher, and many interactions take place; therefore, further *in vivo* experiments are required to extend these results towards practical utilization. Our study could not conclusively assess the viability of chelators as suitable therapeutics. However, based on our data, we believe that iron chelation therapy is a promising approach to hinder and attenuate the progress of the disease while not being hazardous to the host, since even long-term intensive exposure of iron chelators can be safely applied to humans [47]. Considering the severity of the disease, we do not assume that chelators may fully cure PAM in patients, but we are aiming to safely hinder the rapid progression of the infection, thus securing more time for correct diagnosis determination and to deploy effective combination therapy.

In conclusion, our study suggests that *N. fowleri* possesses only limited capabilities of adaptation to an iron-deficient environment and is surprisingly not able to utilize transferrin as an alternative source of the metal; neither can it effectively induce the rate of iron acquisition under iron starvation, reflecting the lifestyle of a facultative parasite with limited ability of survival in a host. The main strategy of acquiring iron appears to be reductive iron uptake. Proteomic analysis of the response to iron starvation demonstrated that a large amount of proteins downregulated under the iron-deficient conditions were nonmitochondrial and nonheme enzymes. The exception is the heme-containing protein protoglobin, whose expression is regulated at the transcriptional level, unlike the expression of most other affected proteins. Therefore, it can be hypothesized that the fundamental effect of iron deprivation is the degradation of mismetallated cytosolic proteins with a simultaneous increase in iron delivery to mitochondria and induction of iron-sulfur cluster synthesis machinery to ensure essential cell processes. The overall changes in cellular processes in the iron-deficient conditions discussed in this paper are illustrated in Fig 3. These findings are in agreement with our previous study focused on iron metabolism in the nonpathogenic model organism *N. gruberi* [34], where the mitochondrion was shown to be the center of the iron economy. Together, these results show that iron-deficiency is a highly unfavorable condition for *N. fowleri*, and targeted interference with its uptake could be an effective method of controlling the propagation or viability of this organism in the host.

Materials and methods

Statistical analysis

Unless stated otherwise, two-tailed Student's *t*-test with two-sample equal variance was used to determine the *p*-values. For comparative proteomic analysis, the data was analyzed using the Perseus [48] package Maxquant [49] with two-tailed T-test of equal variance, S0 = 0.5, FDR = 0.01, quantification and normalization procedure MaxLFQ [50] was used.

Unless stated otherwise, all experiments were performed in three or more independent replicates, meaning parallel experiments on independently cultivated cultures.

Organisms

Naegleria fowleri, strain HB-1, kindly provided by Dr. Hana Pecková (Institute of Parasitology, Biology Center CAS) was maintained in 2% Bacto-Casitone (Difco, USA) supplemented with 10% heat-inactivated fetal bovine serum (Thermo Fisher Scientific, USA), penicillin (100 U/ml) and streptomycin (100 μg/ml) in 25 cm^2 aerobic cultivation flasks at 37˚C. When required,

the cells were cultivated for 72 hours with the addition of 25 μM BPS (Sigma-Aldrich, USA), simulating the iron-deficient environment, or with 25 μM Fe-NTA (Sigma-Aldrich, USA) to ensure iron-rich conditions.

Iron uptake

N. fowleri cells grown for 72 hours under iron-rich and iron-deficient conditions were washed with phosphate buffered saline (PBS) (1000 g for 15 min) and transferred to measuring buffer (50 mM glucose; 20 mM HEPES; pH 7.2). Cells were counted using a Guava easyCyte 8HT flow cytometer (Merck, Germany), and 2.5×10^5 cells were equally split onto a 24-well plate. To assess iron uptake, cells were supplemented with 2 μM ^{55}Fe-citrate, 2 μM ^{55}Fe-citrate with 1 mM ascorbate, or 6.3 μM ^{55}Fe-transferrin. Samples were incubated at 37˚C for 1 hour, and then EDTA was added to a final concentration of 1 mM to chelate extracellular iron. Cells were washed three times by measuring buffer, and the protein concentration was assessed using a BCA kit (Sigma-Aldrich, USA). Samples were diluted to equal concentrations and separated using the Novex Native PAGE Bis–Tris Gel system (4–16%; Invitrogen, USA). The gel was vacuum-dried for 2 hours and autoradiographed using a tritium storage phosphor screen. The experiment was performed in three independent replicates. If applicable, densitometry was used to compare signal strength, using Fiji distribution of ImageJ [51].

Ferric reductase activity

To assess the activity of *N. fowleri* ferric reductase under different iron conditions, a ferrozine assay was used to compare the formation of ferrous iron, as described previously [52]. Cells were grown under iron-rich and iron-deficient environments for 72 hours. Samples containing no cells and samples without Fe-EDTA were used as controls. The cells were washed twice and resuspended in glucose buffer (50 mM glucose, 0.5 mM $MgCl_2$, 0.3 mM $CaCl_2$, 5.1 μM KH_2PO_4, 3 μM Na_2HPO_4, pH 7.4). The total amount of proteins was assessed using a BCA kit, and samples were diluted to equal concentrations. All further work was performed with minimum light exposure. Ferrozine was added to a total concentration of 1.3 mM and Fe-EDTA to a concentration of 0.5 mM. Samples were incubated at 37˚C for three hours, pelleted (1000 g for 10 min) and the supernatant was used to determine the formation of the colored Fe(II)-ferrozine complex, accompanied by a change in absorbance at 562 nm using 1 cm cuvettes and a UV-2600 UV-VIS spectrophotometer (Shimadzu, Japan). The experiment was performed in three independent replicates.

Hemin utilization

To assess the ability of *N. fowleri* to utilize hemin, 2×10^4 cells were cultivated in each well of a 24-well plate in fresh growth medium. Cultures were supplemented with 50 μM BPS, 50 μM hemin, or 50 μM hemin and 50 μM BPS. Cells without chelator or hemin were used as a control. The cell concentration was measured every 24 hours for four days using a Guava easyCyte 8HT flow cytometer. The experiment was performed in four independent replicates.

Comparative proteomic analysis

N. fowleri cells were cultivated in 75 cm^2 aerobic cultivation flasks under iron-rich and iron-deficient environments for 72 h. For whole-cell proteomic analysis, cells were washed three times in PBS (1000 g, 15 min, 4˚C) and pelleted. The experiment was performed in three independent replicates.

In addition, a membrane-enriched fraction was prepared. Approximately 1.5×10^7 cells were harvested (1000 g, 15 min, 4˚C), washed in 15 ml of sucrose-MOPS buffer (250 mM sucrose, 20

mM 3-morpholinopropanesulfonic acid, pH 7.4, supplemented with complete EDTA-free protease inhibitors, Roche, Switzerland) and resuspended in 4 ml of sucrose-MOPS buffer. The suspension was sonicated using a Q125 sonicator (Qsonica, USA) (45% amplitude, total time of 4 min using 1 s pulse and 1 s pause). The resulting suspension was centrifuged (5000 g, 5 min) to spin down the unlysed cells. The obtained supernatant was further centrifuged (200 000 g, 20 min). The supernatant was discarded, and the membrane-enriched pellet was washed with distilled water. The experiment was performed in three independent replicates.

Label-free proteomic analysis of the samples was assessed using the method described in *Mach et al. 2018* [34], utilizing liquid chromatography coupled with mass spectrometry. The resulting MS/MS spectra were compared with the *Naegleria fowleri* database, downloaded from amoebaDB [53] on 25/7/2017. The set thresholds to filter proteins were Q-value = 0, unique peptides detected >2, and the protein had to be identified at least twice in one condition from the six runs. For proteins identified only in one of the conditions, intensity of 23 was selected as a lowest value to be included, on basis of previous imputation experience. To distinguish significantly downregulated or upregulated proteins in the iron-deficient conditions in S1 and S2 Tables, the threshold of fold change >2.3 and <-2.3 was chosen, based on previous experience and published results on comparative proteomics in *N. gruberi* and *Ostreococcus tauri* [34,54].

The annotations and identifications of the selected proteins discussed in this study were confirmed using the tool HHPRED [55]. In addition, alignments were constructed using the chosen proteins and their homologues from different organisms: NF0014630 identified as mitochondrial carnitine/acylcarnitine transferase [56], NF0001420 identified as mitochondrial phosphate carrier [57], NF0060430 identified as IscU [58,59] and NF0079420 identified as mitoferrin [60,61]. Alignments with the indicated conserved sequences are shown in S5 Fig and were constructed using Geneious version 11.1.5 software with the muscle alignment tool.

Western blot

To analyze the expression of *N. fowleri* hemerythrin in different iron conditions, cells cultivated in iron-rich and iron-deficient conditions for 72 hours were pelleted, washed by PBS and protein concentration was assessed using BCA kit. Equal amounts were boiled in SDS sample buffer (Merck Millipore, USA) for 5 min and samples were separated using sodium dodecyl sulphate–polyacrylamide gel electrophoresis as first described in [62]. Proteins were transferred to nitrocellulose membrane by western blotting using semi-dry method, for 75 minutes under 1.5 current of mA/cm^2. The proteins were visualized by Ponceau S stain (0.5% Ponceau S, Merck Millipore, USA, 1% acetic acid), confirming a unified loading of the two samples.

The membrane was blocked for one hour, using 5% dried fat-free milk and 0.05% Tween 20 (Sigma-Aldrich, USA) in PBS. Afterwards, the blot was transferred to fresh blocking solution with primary antibody in ratio 500:1 for one hour. The polyclonal antibody was made in-house, against the whole protein (13.5 kDa) in rat with no adjuvants and was previously used in [34]. After washing with fresh blocking solution, secondary anti-rat antibody conjugated with horse-radish peroxidase (Sigma-Aldrich, USA) was added in 1:2000 ratio for one hour. After washing with fresh blocking buffer and PBS, the antibody was visualized using Chemiluminescent Peroxidase Substrate-1 (Sigma-Aldrich, USA) according to manufacturer protocol, on Amersham Imager 600 (GE Life Sciences, USA).

Comparative transcriptomic analysis

To obtain the transcriptome data of *N. fowleri*, five independent replicates of approximately 1×10^6 cells each were grown under iron-rich and iron-deficient conditions for 72 hours. A

High Pure RNA Isolation Kit (Roche, Switzerland) was used to isolate cell RNA, and an Illumina-compatible library was prepared using QuantSeq 3′ mRNA-Seq Library Prep Kit FWD for Illumina (Lexogen, Austria). The RNA concentration was determined using a Quantus fluorometer (Promega, USA), and the quality of RNA was measured on a 2100 Bioanalyzer Instrument (Agilent technologies, USA). Equimolar samples were pooled to 10 pM and sequenced with MiSeq Reagent Kit v3 (Illumina, USA) using 150-cycles on the MiSeq platform. The obtained results were filtered using the p-value of >0.05 followed by analysis on the BlueBee platform with the method DESeq [63].

Amino acid quantification assay

Approximately 3×10^6 cells cultivated under iron-rich and iron-deficient environments were harvested by centrifugation (1000 g, 15 min, 4˚C), washed with PBS supplemented with cOmplete EDTA-free protease inhibitor, and the total concentration of proteins was measured. Cells were transferred to 1 ml of buffer solution (20 mM Tris, 1 mM $MgCl_2$, pH 8, cOmplete EDTA-free protease inhibitor) and sonicated with Sonopuls mini20 (Bandelin, Germany) (90% amplitude, 4˚C, total time 120 s, 1 s pulse and 1 s pause). The resulting suspension was mixed at a ratio of 1:4 with ice-cold acetonitrile and maintained overnight at -20˚C. Samples were centrifuged (16000 g, 20 min, 4˚C) and filtered using Ultrafree Centrifugal Filter Units (Merck Millipore, USA). The experiment was performed in three independent replicates.

Samples were analyzed using liquid chromatography on a Dionex Ultimate 3000 HPLC system with on-line mass spectrometry detection (Thermo Scientific, USA). The separation was achieved using a HILIC column iHILIC-Fusion (150 x 2.1 mm, 1.8 μm particles, 100 Å pore size, HILICON, Sweden). The entire analysis flow rate was 0.3 ml/min, and the column was equilibrated with 100% of solution A (80% acetonitrile in water, 25 mM ammonium formate, pH 4.8) for 3 min. Amino acids were eluted by increasing the gradient of solution B (5% acetonitrile in water, 25 mM ammonium formate, pH 4.8), where 50% of solution B was reached in 7 min. After separation, the column was washed with 80% solution B for 3 min and then equilibrated with 100% solution A for 5 min.

Amino acids were detected by mass spectrometry using the triple quadrupole instrument TSQ Quantiva (Thermo Scientific, USA) in Selected Reaction Monitoring mode. Analytes were ionized using electrospray ionization on an H-ESI ion source and analyzed with positive charge mode with a spray voltage of 3500 V, ion transfer tube temperature of 325˚C, and vaporizer temperature of 350˚C. All transitions, collision energies, and RF voltages were optimized prior to analysis using appropriate amino acid standards. Each analyte was detected using at least two transitions. Cycle time was set to 1.8 s and both Q1 and Q3 resolutions were set to 0.7 s. To analyze the ion chromatograms and calculate peak areas, Skyline daily version 4.2.1.19004 [64] was used.

Lactate production

To assess the difference in the intracellular production of lactate, 3×10^6 cells cultivated under iron-rich or iron-deficient conditions were prepared for analysis in the same way as for quantifying the amino acid content. The experiment was performed in three independent replicates. After incubation with acetonitrile and filtration, the cell sample was dried and resuspended in 100 μl of anhydrous pyridine (Sigma-Aldrich, USA), and 25 μl of a silylation agent (N-tert-butyldimethylsilyl-N-methyl-trifluoroacetamide, Sigma-Aldrich, USA) was added. The sample was incubated at 70˚C for 30 min. After incubation, 300 μl of hexane (Sigma-Aldrich, USA) and 10 μl of an internal standard (102 μg/ml 1-bromononane solution in hexane) were added. Selected compounds were analyzed as tert-butyl silyl derivatives.

Samples were analyzed using two-dimensional gas chromatography coupled with mass detection (GCxGC-MS; Pegasus 4D, Leco Corporation, USA) with ChromaTOF 4.5 software. Mass detection was equipped with an EI ion source and TOF analyzer with unite resolution. A combination of Rxi-5Sil (30 m x 0.25 mm, Restek, Australia) and BPX-50 (0.96 m x 0.1 mm, SGE, Australia) columns were used. The input temperature was set to 300˚C, the injection volume was 1 μl in spitless mode, and constant helium flow of 1 ml/min, modulation time 3 s (hot pulse 1 s) and modulation temperature offset with respect to the secondary oven 15˚C were used. The temperature program applied on the primary oven was 50˚C (hold 1 min), which was increased by the rate of 10˚C/min to a final temperature of 320˚C (hold 3 min). The temperature offset applied on the secondary column was +5˚C.

Cell respiration

Five independent replicates of 3×10^6 *N. fowleri* cells grown for 72 hours under iron-rich and iron-deficient conditions were washed twice and resuspended in 1 ml of glucose buffer, and the protein concentration was assessed using a BCA kit. Total cell respiration was measured as the decrease in oxygen concentration using an Oxygen meter model 782 (Strathkelvin instruments, UK) with Mitocell Mt 200 cuvette of total volume of 700 μl at 37˚C. Measurements were carried out with 5×10^5 cells for 5 min, after which potassium cyanide was added to a final concentration of 4 mM to block complex IV, and after 5 min, salicyl hydroxamic acid was added to a final concentration of 0.2 mM to completely block AOX. Values gained after the addition of potassium cyanide and salicyl hydroxamic acid were subtracted to acquire canonical respiratory chain and AOX activity, respectively.

Hydrogenase and complex I activity levels

Approximately 1×10^6 cells cultivated under iron-rich or iron-deficient conditions were washed and resuspended in 0.2 ml of saccharose-MOPS buffer (250 mM saccharose, 10 mM 3-morpholinopropanesulfonic acid, pH 7.2). To assess the hydrogenase activity, we used a protocol previously described [65]. Briefly, the reaction was initiated by the addition of cells lysed with 0.02% Triton X-100 to 2 ml of measuring buffer (0.1 M Tris; 50 mM KCl buffer, pH 7.4; 1 μM methylviologen and 0.5% β-mercaptoethanol, saturated with hydrogen gas). Activity level was assessed on the basis of the change in 600 nm absorbance using 1-cm quartz cuvettes on a Shimadzu UV-2600 UV-VIS spectrophotometer with UVProbe software (Shimadzu, Japan). To assess the complex I activity level, we used a protocol previously described [66]. Briefly, 1% digitonin-treated cells were added to 2 ml of measuring buffer (0.1 M KPi buffer, pH 7.5, and 0.2 mM NADH), and the reaction was initiated by the addition of 50 μM oxidized coenzyme Q2 (Sigma-Aldrich, USA) suspended in ethanol. Activity level was assessed on the basis of the change in 340 nm absorbance using 1-cm quartz cuvettes on the same spectrophotometer as used to assess hydrogenase activity. As a control, 0.2 mM rotenone was added after the measurement as a specific inhibitor of complex I to confirm that the background activity was negligible. Both experiments were performed in four independent replicates.

Chelators

The growth dependence of *N. fowleri* on iron availability was defined using the iron chelators BPS (Sigma-Aldrich, USA), DIP (Sigma-Aldrich, USA) and DFO (Sigma-Aldrich, USA). 5000 *N. fowleri* cells per ml were cultivated in 24-well plates in a total volume of 1 ml in a humid chamber. Each chelator and control were tested in four independent replicates (final concentrations of 100, 50, 25, 12.5, 6.3, 3.1, 1.6 and 0.8 μM). Cells were cultivated for 48 hours, the plates were placed on ice for 10 min, and the medium was gently pipetted to detach the cells. The number of cells in

each sample was counted using a Guava easyCyte 8HT flow cytometer. The value of half-maximal inhibitory concentration (IC_{50}) was calculated using the online calculator on the AAT Bioquest webpage [67]. Graphs were created using GraphPad Prism 6 (GraphPad software, USA).

Growth curves of the organism under the influence of different iron chelators were constructed by inoculating 5000 cells/ml *N. fowleri* trophozoites into 10 ml of cultivation medium with the appropriate compound (25 μM Fe-NTA; 45 μM DIP; 25 μM BPS or 10 μM DFO) in four independent replicates. Counting the number of the cells in culture at 24, 48 and 72 hours was performed by flow cytometry using a Guava easyCyte 8HT flow cytometer.

N. fowleri bacterial phagocytosis

Approximately 3×10^6 cells cultivated under iron-rich and iron-deficient conditions were washed in cultivation flasks by replacing the growth medium with 10 ml of PBS warmed to 37˚C and resuspending in 7 ml of 37˚C PBS. To assess the ability of the cells to phagocytose, 150 μl of pHrodo Green *E. coli* BioParticles Conjugate for Phagocytosis (Thermo Fisher Scientific, USA) was added, and the cells were incubated for 3 hours at 37˚C. Following incubation, the cells were washed with PBS, detached on ice for 15 min, and the fluorescence caused by the phagocytosed particles was consecutively analyzed using a Guava easyCyte 8HT flow cytometer using a 488 nm laser and a Green-B 525/30 nm detector. A negative control (without the addition of BioParticles) was used to determine an appropriate threshold for *N. fowleri* cells. BioParticles resuspended in PBS were measured in the same way to determine the background noise and gave a negligible signal. The effect of different iron availability on the efficiency of phagocytosis of *N. fowleri* was established as the percentage of cells in culture that had increased fluorescence. The experiment was performed with nine independent replicates.

To visualize the ability of *N. fowleri* to phagocytize, live amoebae incubated with fluorescent *E. coli* were imaged with a Leica TCS SP8 WLL SMD-FLIM microscope (Leica, Germany) equipped with an HC PL APO CS2 63x/1.20 water objective with 509 nm excitation, 526 nm-655 nm excitation was detected with a HyD SMD detector, and a PMT detector was used for brightfield imaging. Images were processed using LAS X 3.5.1.18803 (Leica, Germany).

To test the effect of attenuated strain of bacteria on the propagation of iron-starved *N. fowleri* in culture, we preincubated amoebae under iron-rich and iron-deficient conditions for 72 hours and inoculated approximately 1000 cells into 96-well plates to a total volume of 200 μl under select conditions with or without the equivalent of 1×10^6 *Enterobacter aerogenes* that had been attenuated. Preincubated iron-rich cells were inoculated into iron-rich medium as a control, and simultaneously, preincubated iron-deficient cells were inoculated into either iron-deficient or iron-rich medium. The cells were cultivated in a humid chamber at 37˚C for 48 hours and then counted using a Guava easyCyte 8HT flow cytometer. The experiment was performed with six independent replicates.

Supporting information

S1 Fig. (A) Loading control corresponding to Fig 1A, ferrous and ferric iron uptake by *N. fowleri* precultivated under iron-rich and iron-deficient conditions. Coomassie brilliant blue loading stain showed that equal protein concentrations in the samples were subjected to native electrophoresis gels. The proteins were determined from whole cell extracts of *N. fowleri* previously cultivated for 72 hours under iron-deficient conditions (25 μM BPS) or iron-rich conditions (25 μM Fe-NTA) and further incubated with ^{55}Fe(II) (ferrous ascorbate) and ^{55}Fe (III) (ferric citrate). **(B) Lack of ^{55}Fe-transferrin uptake in *N. fowleri*, cultivated under iron-rich and iron-deficient conditions.** The uptake of transferrin-bound iron was assessed by incubation of *N. fowleri* with ^{55}Fe-transferrin. Tf, pure ^{55}Fe-transferrin; Fe, *N. fowleri*

cultivated under iron-rich conditions for 72 hours, consecutively incubated with ^{55}Fe-transferrin for 1 hour; BPS, *N. fowleri* cultivated under iron-deficient conditions for 72 hours, consecutively incubated with ^{55}Fe-transferrin for 1 hour; Ctr, iron uptake control of *N. fowleri* culture cultivated in iron deficiency incubated with ^{55}Fe(III)-citrate for 1 hour. The utilization of iron was analyzed by blue native electrophoresis as described in the Methods section. Equal protein concentrations were loaded, as shown on the Coomassie brilliant blue loading stain. Gel is a representative from three independent replicates. **(C) Mechanism of ferric iron uptake involves the reductive step.** *N. fowleri* culture was incubated for 1 hour with ^{55}Fe(III)-citrate with and without the addition of 0.2 mM BPS. Incorporation of ^{55}Fe(III)-citrate to cellular proteins was higher in the sample without the presence of BPS, indicating that a reductive iron uptake mechanism takes place. Several distinct signals on the lower part of +BPS probably correspond to residues of BPS complexed with ferrous iron radionuclides. The utilization of iron was analyzed by blue native electrophoresis as described in the Methods section. -BPS, cell sample without addition of BPS chelator; +BPS, cell sample with the addition of BPS chelator. Equal protein concentrations were loaded, as shown on the Coomassie brilliant blue loading stain. Gel is a representative from three independent replicates. **(D) Loading control corresponding to Fig 2A, *N. fowleri* cell lysate for Western blot analysis of hemerythrin expression.** Ponceau S loading stain shows equal protein concentrations of loaded samples of *N. fowleri* cultivated under iron-deficient (BPS) and iron-rich (Fe) conditions.
(TIF)

S2 Fig. (A) A representative growth curve of *N. fowleri* treated with different chelators. The chelators hindered the propagation of the cells in culture. The graphs show the cytostatic effect of chosen concentrations of the iron chelators compared with the effect of iron-rich cultivation conditions. Fe, cells cultivated under iron-rich conditions (25 μM Fe-NTA); DIP, cells cultivated in 45 μM DIP; BPS, cells cultivated in 25 μM BPS; and DFO, cells cultivated in 10 μM DFO. Data are presented as the means ± SD from four independent replicates. **(B) *N. fowleri* growth in different concentrations of chelators after 48 hours.** The shown graphs were used to calculate the IC_{50} values for different chelators. The graph was created using GraphPad Prism 6 (GraphPad software, USA). Data are presented as the means ± SD from four independent replicates.
(TIF)

S3 Fig. *N. fowleri* cell phagocytosis. Representative dot plots of flow cytometry results of *N. fowleri* phagocyting bacteria using a pHrodo green *E. coli* BioParticles conjugate to measure phagocytosis (Thermo Fisher Scientific, USA) in nine independent replicates. *N. fowleri*, control culture with no added bacteria; Bacteria, control for the bacteria cells; *N. fowleri* Fe, *N. fowleri* under iron-rich conditions with added bacteria; *N. fowleri* BPS, *N. fowleri* under iron-deficient conditions with added bacteria.
(TIF)

S4 Fig. Phagocytosis of bacteria is not an iron acquisition strategy of *N. fowleri*. Effect of adding the attenuated bacteria *Enterobacter aerogenes* on the propagation of *N. fowleri* under different iron conditions. After 48 hours, amoebae growth was not changed when bacteria were added under any condition (iron-rich cells, iron-deficient cells or cells preincubated under iron-deficient conditions and subsequently transferred into an iron-rich environment all had p-values >0.05). The propagation of the amoebae in the iron-deficient culture was significantly lower than that in the iron-rich culture (23% with bacteria and 26% without bacteria, p-values <0.01 for both), confirming the effect of iron deficiency on amoeba culture propagation. Furthermore, cultures preincubated under iron-deficient conditions and subsequently

transferred into iron-rich environments had the same propagation as those under the iron-rich culture conditions (p-values >0.05 with and without bacteria). Data are presented as the means ± SD from six independent replicates.
(TIF)

S5 Fig. Alignments of *N. fowleri* proteins with homologues from other organisms. (A) Alignment of *N. fowleri* NF0060430 with the IscU proteins from *Homo sapiens*, *Saccharomyces cerevisiae* and *T. brucei*. Red arrows point to the conserved cysteine required for iron-sulfur cluster assembly, based on a previous study [58]. The red rectangle denotes the conserved LPPVK motif of the IscU proteins [59]. (B) Alignment of *N. fowleri* NF0079420 with the mitoferrin proteins of *Trypanosoma brucei*, *Leishmania mexicana*, *Saccharomyces cerevisiae* and *Homo sapiens*. Red arrows point to the sequence motif Px(D/E)xx(K/R)x(K/R), and yellow circles mark residues in contact with substrate, according to a previous study [60]. Conserved histidine residues responsible for iron transport are marked with blue stars [61]. (C) Alignment of *N. fowleri* NF0001420 with the mitochondrial phosphate carriers of *Saccharomyces cerevisiae*, *Homo sapiens* and *Arabidopsis thaliana*. Red arrows point to residues important for the phosphate transport activity, according to a previous study [57]. (D) Alignment of *N. fowleri* NF0014630 with mitochondrial carnitine/acylcarnitine transferases of *Saccharomyces cerevisiae*, *Arabidopsis thaliana*, *Homo sapiens* and *Caenorhabditis elegans*. The red rectangle denotes the signature motifs Px(D/E)xx(R/K)x(R/K), and the arrows point to conserved residues, according to a previous study [56].
(TIF)

S1 Table. Comparison of whole-cell proteomes of *N. fowleri* in iron-rich and iron-deficient environments. List of whole-cell proteomes of *N. fowleri* compared in iron-rich and iron-deficient conditions sorted into four sheets: raw data, all detected proteins, significantly upregulated proteins and significantly downregulated proteins under iron-deficient conditions. With the exception of raw data, the tables are simplified to show only fold change values. Proteins with > 2.3 (denoting upregulated under iron-deficient conditions) or < -2.3-fold change (denoting downregulated under iron-deficient conditions) are regarded as significantly regulated. Proteins were annotated from amoebaDB [53] on 25/7/2017, and manual annotation was performed for selected proteins, as described in the Methods section. Probable iron-containing proteins of the significantly downregulated and upregulated proteins are highlighted in yellow. Experiment was performed with three independent replicates.
(XLSX)

S2 Table. Comparison of membrane-enriched proteomes of *N. fowleri* in iron-rich and iron-deficient environments. List of membrane-enriched proteomes of *N. fowleri* compared in iron-rich and iron-deficient conditions sorted into four sheets: raw data, all detected proteins, significantly upregulated proteins and significantly downregulated proteins under iron-deficient conditions. With the exception of raw data, the tables are simplified to show only fold change values. Proteins with >2.3 (denoting upregulated under iron-deficient conditions) or < -2.3-fold change (denoting downregulated under iron-deficient conditions) are regarded as significantly regulated. Proteins were annotated from amoebaDB [53] on 25/7/2017, and manual annotation was performed for selected proteins, as described in the Methods section. Experiment was performed with three independent replicates.
(XLSX)

S3 Table. Comparison of transcriptomes of *N. fowleri* in iron-rich and iron-deficient environments. List of genes significantly downregulated and upregulated under iron-deficient conditions. Raw data are included, and manual annotation was performed for selected proteins, as described

in the Methods section. Experiment was performed with five independent replicates.
(XLSX)

S4 Table. Raw data.
(XLSX)

S1 Video. The video shows a demonstration of *N. fowleri* phagocytizing bacteria. In the video, a single *N. fowleri* amoeba phagocytoses several fluorescently modified pHrodo green *E. coli* BioParticles (bright blue). In the lysosomes, they fluoresced due to the decreased pH value. In the background, several non-fluorescing bacteria were observed (dim blue). Images were acquired with a Leica TCS SP8 WLL SMD-FLIM microscope (Leica, Germany) equipped with an HC PL APO CS2 63×/1.20 water objective with 509 nm excitation, 526 nm-655 nm excitation was detected with a HyD SMD detector, and a PMT detector was used for brightfield imaging. Images were processed using LAS X 3.5.1.18803 (Leica, Germany). Video was created and edited using the Fiji distribution package of ImageJ software [51].
(MP4)

Acknowledgments

Special thanks to Ivánek for fruitful biochemical discussions.

Author Contributions

Conceptualization: Robert Sutak.

Data curation: Dominik Arbon, Kateřina Ženíšková.

Funding acquisition: Robert Sutak.

Investigation: Dominik Arbon, Kateřina Ženíšková, Maria Grechnikova, Ronald Malych, Pavel Talacko.

Methodology: Jan Mach, Ronald Malych, Pavel Talacko.

Project administration: Robert Sutak.

Supervision: Jan Mach, Robert Sutak.

Validation: Jan Mach, Robert Sutak.

Visualization: Dominik Arbon, Kateřina Ženíšková.

Writing – original draft: Dominik Arbon.

Writing – review & editing: Jan Mach, Maria Grechnikova, Robert Sutak.

References

1. De Jonckheere JF. What do we know by now about the genus *Naegleria*? Exp Parasitol. 2014 Nov; 145 (S):S2–9.
2. Kelly RB, Francine M-C, Charles PG. Occurrence of *Naegleria fowleri* in Arizona drinking water supply wells. J Am Water Works Assoc. 2009 Nov; 101(11):43–50.
3. Visvesvara GS, Moura H, Schuster FL. Pathogenic and opportunistic free-living amoebae: *Acanthamoeba spp.*, *Balamuthia mandrillaris*, *Naegleria fowleri*, and *Sappinia diploidea*. FEMS Immunol Med Microbiol. 2007 Jun; 50(1):1–26. https://doi.org/10.1111/j.1574-695X.2007.00232.x PMID: 17428307
4. Grace E, Asbill S, Virga K. *Naegleria fowleri*: Pathogenesis, diagnosis, and treatment options. Antimicrob Agents Chemother. 2015 Nov 1; 59(11):6677–81. https://doi.org/10.1128/AAC.01293-15 PMID: 26259797

5. Ma P, Visvesvara GS, Martinez AJ, Theodore FH, Daggett PM, Sawyer TK. *Naegleria* and *acanthamoeba* infections: Review. Clin Infect Dis. 1990 May 1; 12(3):490–513.
6. Centers for Disease Control and Prevention, *Naegleria fowleri* general information. Available at: https://www.cdc.gov/parasites/naegleria/general.html, last modified July 17/7/2018, accessed 15/3/2019 [Internet].
7. Linam WM, Ahmed M, Cope JR, Chu C, Visvesvara GS, Da Silva AJ, et al. Successful treatment of an adolescent with *Naegleria fowleri* primary amebic meningoencephalitis. Pediatrics. 2015 Mar 1; 135(3): e744–8. https://doi.org/10.1542/peds.2014-2292 PMID: 25667249
8. Pana A, Vijayan V, Anilkumar AC. Amebic meningoencephalitis [Internet]. StatPearls. 2019.
9. Cabello-Vílchez AM, Chura-Araujo MA, Anicama Lima WE, Vela C, Asencio AY, García H, et al. Fatal granulomatous amoebic encephalitis due to free-living amoebae in two boys in two different hospitals in Lima, Perú. Neuropathology. 2019 Nov 22;neup.12617.
10. Crichton R. Iron metabolism: From molecular mechanisms to clinical consequences: Fourth edition. Chichester, UK: John Wiley & Sons, Ltd; 2016. 1–556 p.
11. Lill R, Broderick JB, Dean DR. Special issue on iron-sulfur proteins: Structure, function, biogenesis and diseases. Biochim Biophys Acta—Mol Cell Res. 2015 Jun 1; 1853(6):1251–2.
12. Boyd PW, Jickells T, Law CS, Blain S, Boyle EA, Buesseler KO, et al. Mesoscale iron enrichment experiments 1993–2005: Synthesis and future directions. Science (80-). 2007 Feb 2; 315(5812):612–7.
13. Koka S, Föller M, Lamprecht G, Boini KM, Lang C, Huber SM, et al. Iron deficiency influences the course of malaria in *Plasmodium berghei* infected mice. Biochem Biophys Res Commun. 2007 Jun; 357(3):608–14. https://doi.org/10.1016/j.bbrc.2007.03.175 PMID: 17445762
14. Kabyemela ER, Fried M, Kurtis JD, Mutabingwa TK, Duffy PE. Decreased susceptibility to *Plasmodium falciparum* infection in pregnant women with iron deficiency. J Infect Dis. 2008 Jul 15; 198(2):163–6. https://doi.org/10.1086/589512 PMID: 18500927
15. Ganz T. Iron in innate immunity: Starve the invaders. Curr Opin Immunol. 2009; 21(1):63–7. https://doi.org/10.1016/j.coi.2009.01.011 PMID: 19231148
16. Sutak R, Lesuisse E, Tachezy J, Richardson DR. Crusade for iron: Iron uptake in unicellular eukaryotes and its significance for virulence. Trends Microbiol. 2008 Jun 1; 16(6):261–8. https://doi.org/10.1016/j.tim.2008.03.005 PMID: 18467097
17. Singh N, Haldar S, Tripathi AK, Horback K, Wong J, Sharma D, et al. Brain iron homeostasis: From molecular mechanisms to clinical significance and therapeutic opportunities. Antioxidants Redox Signal. 2014 Mar 10; 20(8):1324–63.
18. Leitner DF, Connor JR. Functional roles of transferrin in the brain. Vol. 1820, Biochimica et Biophysica Acta—General Subjects. 2012. p. 393–402.
19. Mobarra N, Shanaki M, Ehteram H, Nasiri H, Sahmani M, Saeidi M, et al. A review on iron chelators in treatment of iron overload syndromes. Vol. 10, International Journal of Hematology-Oncology and Stem Cell Research. Tehran University of Medical Sciences (TUMS); 2016. p. 239–47.
20. Cruz-Castañeda A, López-Casamichana M, Olivares-Trejo JJ. *Entamoeba histolytica* secretes two haem-binding proteins to scavenge haem. Biochem J. 2011 Feb 15; 434(1):105–11. https://doi.org/10.1042/BJ20100897 PMID: 21126234
21. Basu S, Horáková E, Lukeš J. Iron-associated biology of *Trypanosoma brucei*. Vol. 1860, Biochimica et Biophysica Acta—General Subjects. Elsevier; 2016. p. 363–70.
22. Tsaousis AD, Nývltová E, Šuták R, Hrdý I, Tachezy J. A Nonmitochondrial hydrogen production in *Naegleria gruberi*. Genome Biol Evol. 2014 Apr; 6(4):792–9. https://doi.org/10.1093/gbe/evu065 PMID: 24682152
23. Marciano-Cabral FM, Patterson M, John DT, Bradley SG. Cytopathogenicity of *Naegleria fowleri* and *Naegleria gruberi* for established mammalian cell cultures. J Parasitol. 1982 Dec; 68(6):1110–6. PMID: 6816913
24. Martínez-Castillo M, Ramírez-Rico G, Serrano-Luna J, Shibayama M. Iron-binding protein degradation by cysteine proteases of *Naegleria fowleri*. Biomed Res Int. 2015 May 18; 2015:1–8.
25. Dancis A, Roman DG, Anderson GJ, Hinnebusch AG, Klausner RD. Ferric reductase of *Saccharomyces cerevisiae*: Molecular characterization, role in iron uptake, and transcriptional control by iron. Proc Natl Acad Sci U S A. 1992 May 1; 89(9):3869–73. https://doi.org/10.1073/pnas.89.9.3869 PMID: 1570306
26. Sutak R, Chamot C, Tachezy J, Camadro JM, Lesuisse E. Siderophore and haem iron use by *Tritrichomonas foetus*. Microbiology. 2004 Dec 1; 150(12):3979–87.

27. Alonso P, Zubiaur E. Phagocytic activity of three *Naegleria* strains in the presence of erythrocytes of various types. J Protozool. 1985 Nov; 32(4):661–4. https://doi.org/10.1111/j.1550-7408.1985.tb03097.x PMID: 4067878

28. Scaglia M, Gatti S, Brustia R, Chichino G, Rondanelli EG. Phagocytosis of human erythrocytes by *Naegleria* is not related to species pathogenicity. A phase-contrast cinemicrographic study. Microbiologica. 1991 Jan; 14(1):45–53. PMID: 2067415

29. Létoffé S, Heuck G, Delepelaire P, Lange N, Wandersman C. Bacteria capture iron from heme by keeping tetrapyrrol skeleton intact. Proc Natl Acad Sci U S A. 2009 Jul 14; 106(28):11719–24. https://doi.org/10.1073/pnas.0903842106 PMID: 19564607

30. Bradley SG, Toney DM, Zhang Y, Marciano-Cabral F. Dependence of growth, metabolic expression, and pathogenicity of *Naegleria fowleri* on exogenous porphyrins. J Parasitol. 1996 Oct; 82(5):763–8. PMID: 8885886

31. Jung SY, Kim JH, Song KJ, Lee YJ, Kwon MH, Kim K, et al. Gene silencing of nfa1 affects the *in vitro* cytotoxicity of *Naegleria fowleri* in murine macrophages. Mol Biochem Parasitol. 2009 May 1; 165 (1):87–93. https://doi.org/10.1016/j.molbiopara.2009.01.007 PMID: 19393165

32. Shakoury-Elizeh M, Protchenko O, Berger A, Cox J, Gable K, Dunn TM, et al. Metabolic response to iron deficiency in *Saccharomyces cerevisiae*. J Biol Chem. 2010; 285(19):14823–33. https://doi.org/10.1074/jbc.M109.091710 PMID: 20231268

33. Bexkens ML, Zimorski V, Sarink MJ, Wienk H, Brouwers JF, De Jonckheere JF, et al. Lipids Are the Preferred Substrate of the Protist *Naegleria gruberi*, Relative of a Human Brain Pathogen. Cell Rep. 2018 Oct 16; 25(3):537–543.e3. https://doi.org/10.1016/j.celrep.2018.09.055 PMID: 30332635

34. Mach J, Bíla J, Ženíšková K, Arbon D, Malych R, Glavanakovová M, et al. Iron economy in *Naegleria gruberi* reflects its metabolic flexibility. Int J Parasitol. 2018 May 5; 48(9–10):719–27. https://doi.org/10.1016/j.ijpara.2018.03.005 PMID: 29738737

35. Kulda J, Tachezy J, Čerkasovová A. *In vitro* induced anaerobic resistance to metronidazole In *Trichomonas vaginalis*. J Eukaryot Microbiol. 1993 May; 40(3):262–9. https://doi.org/10.1111/j.1550-7408.1993.tb04915.x PMID: 8508165

36. Li X, Li J, Hu X, Huang L, Xiao J, Chan J, et al. Differential roles of the hemerythrin-like proteins of *Mycobacterium smegmatis* in hydrogen peroxide and erythromycin susceptibility. Sci Rep. 2015 Nov 26; 5:16130. https://doi.org/10.1038/srep16130 PMID: 26607739

37. Ma Z, Strickland KT, Cherne MD, Sehanobish E, Rohde KH, Self WT, et al. The Rv2633c protein of *Mycobacterium tuberculosis* is a non-heme di-iron catalase with a possible role in defenses against oxidative stress. J Biol Chem. 2018; 293(5):1590–5. https://doi.org/10.1074/jbc.RA117.000421 PMID: 29242190

38. Selote D, Samira R, Matthiadis A, Gillikin JW, Long TA. Iron-binding e3 ligase mediates iron response in plants by targeting basic helix-loop-helix transcription factors1[open]. Plant Physiol. 2015 Jan; 167 (1):273–86. https://doi.org/10.1104/pp.114.250837 PMID: 25452667

39. Zeng WB, Chen WB, Yan QP, Lin GF, Qin YX. Hemerythrin is required for *Aeromonas hydraphlia* to survive in the macrophages of *Anguilla japonica*. Genet Mol Res. 2016; 15(2).

40. Newsome AL, Wilhelm WE. Inhibition of *Naegleria fowleri* by microbial iron-chelating agents: Ecological implications. Applied and Environmental Microbiology. 1983;45.

41. Romeo AM, Christen L, Niles EG, Kosman DJ. Intracellular chelation of iron by bipyridyl inhibits DNA virus replication: Ribonucleotide reductase maturation as a probe of intracellular iron pools. J Biol Chem. 2001 Jun 29; 276(26):24301–8. https://doi.org/10.1074/jbc.M010806200 PMID: 11301321

42. Megger N, Welte L, Zamora F, Müller J. Metal-mediated aggregation of DNA comprising 2,2′-bipyridine nucleoside, an asymmetrically substituted chiral bidentate ligand. Dalt Trans. 2011 Feb 8; 40(8):1802–7.

43. Nyayapati S, Afshan G, Lornitzo F, Byrnes RW, Petering DH. Depletion of cellular iron by BPS and ascorbate: Effect on toxicity of adriamycin. Free Radic Biol Med. 1996 Jan 1; 20(3):319–29. https://doi.org/10.1016/0891-5849(96)02054-0 PMID: 8720902

44. Ihnat PM, Vennerstrom JL, Robinson DH. Synthesis and solution properties of deferoxamine amides. J Pharm Sci. 2000 Dec; 89(12):1525–36. https://doi.org/10.1002/1520-6017(200012)89:12<1525::aid-jps3>3.0.co;2-t PMID: 11042600

45. Kontoghiorghe CN, Kontoghiorghes GJ. Efficacy and safety of iron-chelation therapy with deferoxamine, deferiprone, and deferasirox for the treatment of iron-loaded patients with non-transfusion-dependent thalassemia syndromes. Drug Des Devel Ther. 2016; 10:465–81. https://doi.org/10.2147/DDDT.S79458 PMID: 26893541

46. Porter JB. Deferoxamine pharmacokinetics. Semin Hematol. 2001 Jan; 38(1 Suppl 1):63–8. https://doi.org/10.1016/s0037-1963(01)90061-7 PMID: 11206963

47. Crichton RR, Ward RJ, Hider RC. The efficacy of iron chelators for removing iron from specific brain regions and the pituitary—Ironing out the brain. Vol. 12, Pharmaceuticals. MDPI AG; 2019.

48. Tyanova S, Temu T, Sinitcyn P, Carlson A, Hein MY, Geiger T, et al. The Perseus computational platform for comprehensive analysis of (prote)omics data. Nature Methods. Nature Publishing Group; 2016; 13. p. 731–40. https://doi.org/10.1038/nmeth.3901 PMID: 27348712

49. Tyanova S, Temu T, Cox J. The MaxQuant computational platform for mass spectrometry-based shotgun proteomics. Nat Protoc. 2016 Dec 1; 11(12):2301–19. https://doi.org/10.1038/nprot.2016.136 PMID: 27809316

50. Cox J, Hein MY, Luber CA, Paron I, Nagaraj N, Mann M. Accurate proteome-wide label-free quantification by delayed normalization and maximal peptide ratio extraction, termed MaxLFQ. Mol Cell Proteomics. 2014 Sep 1; 13(9):2513–26. https://doi.org/10.1074/mcp.M113.031591 PMID: 24942700

51. Schindelin J, Arganda-Carreras I, Frise E, Kaynig V, Longair M, Pietzsch T, et al. Fiji: An open-source platform for biological-image analysis. Vol. 9, Nature Methods. 2012. p. 676–82. https://doi.org/10.1038/nmeth.2019 PMID: 22743772

52. Stookey LL. Ferrozine-a new spectrophotometric reagent for iron. Anal Chem. 1970 Jun; 42(7):779–81.

53. Aurrecoechea C, Barreto A, Brestelli J, Brunk BP, Caler E V., Fischer S, et al. AmoebaDB and MicrosporidiaDB: Functional genomic resources for *Amoebozoa* and *Microsporidia* species. Nucleic Acids Res. 2011 Jan 1; 39(SUPPL. 1):D612–9.

54. Scheiber IF, Pilátová J, Malych R, Kotabova E, Krijt M, Vyoral D, et al. Copper and iron metabolism in: *Ostreococcus tauri* -the role of phytotransferrin, plastocyanin and a chloroplast copper-transporting ATPase. Metallomics. 2019 Oct 1; 11(10):1657–66. https://doi.org/10.1039/c9mt00078j PMID: 31380866

55. Zimmermann L, Stephens A, Nam SZ, Rau D, Kübler J, Lozajic M, et al. A Completely Reimplemented MPI Bioinformatics Toolkit with a New HHpred Server at its Core. J Mol Biol. 2018 Jul 20; 430(15):2237–43. https://doi.org/10.1016/j.jmb.2017.12.007 PMID: 29258817

56. Indiveri C, Iacobazzi V, Tonazzi A, Giangregorio N, Infantino V, Convertini P, et al. The mitochondrial carnitine/acylcarnitine carrier: Function, structure and physiopathology. Mol Aspects Med. 2011 Aug 1; 32(4–6):223–33. https://doi.org/10.1016/j.mam.2011.10.008 PMID: 22020112

57. Hamel P, Saint-Georges Y, De Pinto B, Lachacinski N, Altamura N, Dujardin G. Redundancy in the function of mitochondrial phosphate transport in *Saccharomyces cerevisiae* and *Arabidopsis thaliana*. Mol Microbiol. 2004 Feb 23; 51(2):307–17. https://doi.org/10.1046/j.1365-2958.2003.03810.x PMID: 14756774

58. Šmíd O, Horáková E, Vilimova V, Hrdý I, Cammack R, Horvath A, et al. Knock-downs of iron-sulfur cluster assembly proteins IscS and IscU down-regulate the active mitochondrion of procyclic *Trypanosoma brucei*. J Biol Chem. 2006 Sep 29; 281(39):28679–86. https://doi.org/10.1074/jbc.M513781200 PMID: 16882667

59. Hoff KG, Cupp-Vickery JR, Vickery LE. Contributions of the LPPVK motif of the iron-sulfur template protein IscU to interactions with the Hsc66-Hsc20 chaperone system. J Biol Chem. 2003 Sep 26; 278(39):37582–9. https://doi.org/10.1074/jbc.M305292200 PMID: 12871959

60. Mittra B, Laranjeira-Silva MF, Perrone Bezerra de Menezes J, Jensen J, Michailowsky V, Andrews NW. A trypanosomatid iron transporter that regulates mitochondrial function is required for *Leishmania amazonensis* virulence. Horn D, editor. PLoS Pathog. 2016 Jan 7; 12(1):e1005340. https://doi.org/10.1371/journal.ppat.1005340 PMID: 26741360

61. Brazzolotto X, Pierrel F, Pelosi L. Three conserved histidine residues contribute to mitochondrial iron transport through mitoferrins. Biochem J. 2014 May 15; 460(1):79–89. https://doi.org/10.1042/BJ20140107 PMID: 24624902

62. Laemmli UK. Cleavage of structural proteins during the assembly of the head of bacteriophage T4. Nature. 1970 Aug; 227(5259):680–5. https://doi.org/10.1038/227680a0 PMID: 5432063

63. Anders S, Huber W. Differential expression analysis for sequence count data. Genome Biol. 2010 Oct 27; 11(10):R106. https://doi.org/10.1186/gb-2010-11-10-r106 PMID: 20979621

64. MacLean B, Tomazela DM, Shulman N, Chambers M, Finney GL, Frewen B, et al. Skyline: An open source document editor for creating and analyzing targeted proteomics experiments. Bioinformatics. 2010 Apr 1; 26(7):966–8. https://doi.org/10.1093/bioinformatics/btq054 PMID: 20147306

65. Rasoloson D, Vaňáčová Š, Tomková E, Rázga J, Hrdý I, Tachezy J, et al. Mechanisms of in vitro development of resistance to metronidazole in *Trichomonas vaginalis*. Microbiology. 2002; 148(8):2467–77.

66. Verner Z, Čermáková P, Škodová I, Kriegová E, Horváth A, Lukeš J. Complex I (NADH:ubiquinone oxidoreductase) is active in but non-essential for procyclic *Trypanosoma brucei*. Mol Biochem Parasitol. 2011 Feb; 175(2):196–200. https://doi.org/10.1016/j.molbiopara.2010.11.003 PMID: 21074578

67. IC50 Calculator, available at: https://www.aatbio.com/tools/ic50-calculator, accessed 07/03/2019 [Internet].

International Journal for Parasitology 52 (2022) 497–508

Contents lists available at ScienceDirect

International Journal for Parasitology

journal homepage: www.elsevier.com/locate/ijpara

Elucidation of iron homeostasis in *Acanthamoeba castellanii*

Maria Grechnikova, Dominik Arbon, Kateřina Ženíšková, Ronald Malych, Jan Mach, Lucie Krejbichová, Aneta Šimáčková, Robert Sutak *

Department of Parasitology, Charles University, Faculty of Science, BIOCEV, Průmyslová 595, 252 50 Vestec, Czech Republic

ARTICLE INFO

Article history:
Received 3 December 2021
Received in revised form 21 March 2022
Accepted 27 March 2022
Available online 6 May 2022

In memory of Emmanuel Lesuisse, who made major contributions to our understanding of the general mechanisms of iron uptake by eukaryotic cells

Keywords:
Acanthamoeba castellanii
Iron metabolism
Iron uptake
Ferric reductase
Iron transporter
Pinocytosis

ABSTRACT

Acanthamoeba castellanii is a ubiquitously distributed amoeba that can be found in soil, dust, natural and tap water, air conditioners, hospitals, contact lenses and other environments. It is an amphizoic organism that can cause granulomatous amoebic encephalitis, an infrequent fatal disease of the central nervous system, and amoebic keratitis, a severe corneal infection that can lead to blindness. These diseases are extremely hard to treat; therefore, a more comprehensive understanding of this pathogen's metabolism is essential for revealing potential therapeutic targets. To propagate successfully in human tissues, the parasites must resist the iron depletion caused by nutritional immunity. The aim of our study is to elucidate the mechanisms underlying iron homeostasis in *A. castellanii*. Using a comparative whole-cell proteomic analysis of cells grown under different degrees of iron availability, we identified the primary proteins involved in *Acanthamoeba* iron acquisition. Our results suggest a two-step reductive mechanism of iron acquisition by a ferric reductase from the STEAP family and a divalent metal transporter from the NRAMP family. Both proteins are localized to the membranes of acidified digestive vacuoles where endocytosed medium and bacteria are trafficked. The expression levels of these proteins are significantly higher under iron-limited conditions, which allows *Acanthamoeba* to increase the efficiency of iron uptake despite the observed reduced pinocytosis rate. We propose that excessive iron gained while grown under iron-rich conditions is removed from the cytosol into the vacuoles by an iron transporter homologous to VIT/Ccc1 proteins. Additionally, we identified a novel protein that may participate in iron uptake regulation, the overexpression of which leads to increased iron acquisition.

1. Introduction

Protozoa from the genus *Acanthamoeba* are ubiquitously distributed free-living amoebae. They were first discovered as contaminants of a yeast culture (Castellani, 1930) and later isolated from different environments around the world including soil, dust, air, natural water and sediments, tap water, seawater, swimming pools, sewage, air-conditioning units, hospitals, contact lenses, and fecal material from birds, reptiles, and mammals, and human throat swabs and mucosa (Martinez, 1991; Marciano-Cabral and Cabral, 2003). *Acanthamoeba* has two stages in its life cycle: an actively moving trophozoite with typical thin protrusions on pseudopodia called acanthopodia (from the Greek "acanth" meaning "spikes") and a dormant cyst stage (Siddiqui and Khan, 2012). Acanthamoebae feed on organic particles or consume bacteria and fungi, and they can be grown on agar containing *Escherichia coli* or yeasts, or axenically in liquid medium (Byers, 1979; Rodríguez-Zaragoza, 1994).

Several species in the genus, including the best known *Acanthamoeba castellanii,* are causative agents of the deadly CNS disease called granulomatous amoebic encephalitis (GAE; Martinez, 1991) and the sight-threatening corneal infection known as *Acanthamoeba* keratitis (Lorenzo-Morales et al., 2015). GAE is a rare but severe disease, with immunocompromised patients being at the greatest risk. Amoebae are most likely spread in the organism hematogenously, entering through the lower respiratory tract or skin ulcers, or invading the brain via the olfactory epithelium. The disease usually starts with a headache, nausea and vomiting, dizziness and low-grade fever. Neurological symptoms develop gradually, depending on the area of the brain involved, and include confusion, irritability, somnolence, hallucinations, seizures, cranial nerve palsies, visual disturbances, anorexia, ataxia, and coma. GAE is lethal within 1–2 months of symptom onset and almost incurable (Martinez, 1991; Duggal et al., 2017). Acanthamoebic keratitis mostly affects contact lens wearers, although it is not limited to this population. Corneal abrasion followed by exposure to a heavily

* Corresponding author.
E-mail address: robert.sutak@natur.cuni.cz (R. Sutak).

https://doi.org/10.1016/j.ijpara.2022.03.007
0020-7519/

contaminated solution or water may lead to the disease. The symptoms include pain in the eye, tearing photophobia, ring-like stromal infiltrate, and lid edema, and without proper therapy, acanthamoebic keratitis can lead to complete vision loss. Amoeba cysts formed within the cornea are highly resistant to antimicrobials, which lowers the effectiveness of treatment, because the survival of a single cyst in the infected tissue can lead to reinfection (Lorenzo-Morales et al., 2015). Additionally, *Acanthamoeba* spp. have been associated with cutaneous lesions in immunocompromised people (Marciano-Cabral and Cabral, 2003).

As an organism that survives and propagates in human tissues, *Acanthamoeba* must resist human immunity mechanisms. One of the mammalian defensive strategies called nutritional immunity is based on restricting the amount of iron available to pathogens. Iron is essential for virtually all known forms of life: based on its ability to cycle between oxidized and reduced states, it serves as a cofactor for different enzymes necessary for various biochemical processes including respiration and nucleic acid metabolism. Iron is an essential constituent of ferredoxins, cytochromes and many others. Host iron is tightly bound to the intracellular protein ferritin or extracellular transferrin and lactoferrin (Gulec and Collins, 2014). During infection, the extracellular iron concentration is significantly reduced via the action of the peptide hormone hepcidin. Furthermore, a protein called siderocalin or lipocalin 2 is employed to bind some of the secreted microbial iron chelators, or siderophores, that are used to obtain iron (Ganz, 2009).

Nevertheless, pathogens employ several strategies, allowing them to elude this host defensive system (for a comprehensive review check Mach and Sutak, 2020). One possibility for iron acquisition is the secretion of siderophores, which have a higher affinity for iron than the host proteins and cannot be bound by siderocalin (Sutak et al., 2008). Siderophores with iron are subsequently transported into the cell by specific transporters, and iron is released intracellularly. Analogously, hemophores binding the host heme are used by some pathogens (Wandersman and Delepelaire, 2004). Another mechanism employed, for instance, by *Candida albicans*, is the high affinity, two-step reductive iron uptake mechanism. During the first step, ferric reductase reduces ferric iron (Fe^{3+}) to the ferrous state (Fe^{2+}), which lowers the affinity of iron to the host proteins (for example, transferrin). The second step is performed by a protein complex consisting of a multicopper oxidase and a ferrous permease, which oxidizes Fe^{2+} back to Fe^{3+}, and the Fe^{3+} is taken up (Knight et al., 2005) *Leishmania amazonensis* also employs a reductive iron uptake mechanism, however, the iron reduced by ferric reductase is taken up by a divalent iron transporter with no oxidation step (Flannery et al., 2011). Another way of obtaining iron occurs through the receptor-mediated internalization of the host iron-binding proteins with subsequent intracellular iron release as shown for different parasites such as *Trichomonas vaginalis,* which acquires hemoglobin, and *Trypanosoma brucei,* which uses transferrin (Ardalan et al., 2009; Kariuki et al., 2019) *Entamoeba histolytica* was shown to use several different mechanisms of iron uptake; one is to secrete proteases capable of destroying host hemoglobin and two heme-binding proteins that facilitate acquisition of the released heme (Ocádiz et al., 2005; Cruz-Castañeda et al., 2011). In some respects, a similar mechanism may also be employed by *Acanthamoeba*: Ramírez-Rico et al. (2015) identified several proteases in *Acanthamoeba* crude extracts and conditioned medium that are able to cleave different iron-binding proteins, namely, human holo-lactoferrin, holo-transferrin and hemoglobin, and horse spleen ferritin. However, despite the importance of efficient iron uptake machinery in parasitic organisms, it remains unknown how the released metal is internalized by *Acanthamoeba*.

Moreover, nothing is known about iron storage and redistribution mechanisms in *Acanthamoeba,* which are very important for every organism since iron is toxic if present in excess; it may catalyze the production of hydroxyl radicals via the Fenton and Haber-Weiss reactions, which damage DNA, RNA, proteins and lipids (Hershko, 2007) Generally, to store iron and avoid its toxicity, many organisms keep it bound to the conserved intracellular protein ferritin (Harrison and Arosio, 1996) or sequester it from the cytoplasm using iron transporters such as *Saccharomyces cerevisiae* Ccc1, which transfers iron to the vacuole (Li et al., 2001) *Acanthamoeba* does not possess ferritin according to bioinformatic data; however, a homolog of yeast *ccc1* is present in its genome.

The present study is aimed at investigating the iron homeostasis machinery of *A. castellanii*. We analyzed the whole-cell proteomic response to iron deprivation and investigated the localization of several proteins for which the expression levels were significantly affected by iron availability. Our results demonstrate that *A. castellanii* employs a ferric reductase and a divalent metal transporter that are expressed in membranes of multiple intracellular vesicles and promote iron delivery to cytosol. These proteins are significantly upregulated under iron deprivation, which probably allows iron-starved cells to increase the efficiency of iron uptake despite a decreased pinocytosis rate. When iron is abundant, its excess is removed from the cytosol by another divalent iron transporter from a different family.

2. Materials and methods

2.1. Acanthamoeba growth conditions

The *A. castellanii* Neff strain was maintained in 25 cm^2 aerobic cultivation flasks at 27 °C in PYG medium (0.75% yeast extract, 0.75% proteose peptone, and 1.5% glucose); *A. castellanii* transformants were maintained in PYG medium with the additives (PYG-A) described in dx.https://doi.org/10.17504/protocols.io.s4regv6 without added iron citrate (0.75% yeast extract, 0.75% proteose peptone, 2 mM KH2PO4, 1 mM MgSO4, 1.5% glucose, 0.05 mM CaCl2, 1 μg/mL of thiamine, 0.2 μg/mL of D-biotin, and 1 ng/mL of vitamin B12).

2.2. Growth curves

Acanthamoeba castellanii cells (5×10^4) were inoculated into 5 ml of PYG-A supplemented with iron in ferric nitrilotriacetate (Fe-NTA) form at concentrations of 25 μM or 50 μM, supplemented with the iron chelator bathophenanthrolinedisulfonic acid (BPS, Sigma-Aldrich, USA) at concentrations of 25 μM or 50 μM, or without iron or BPS supplementation as a control. Cells were grown in biological triplicate. Every 24 h, the cells were counted with a Z2 Particle Count and Size Analyzer (Beckman Coulter, USA).

2.3. Whole-cell proteomics

Acanthamoeba castellanii was grown in 75 cm^2 aerobic cultivation flasks in 20 ml of PYG medium supplemented with 25 μM Fe-NTA or 25 μM BPS for 72 h in triplicate. The cells were washed three times with PBS (1000 g, 10 min, 4 °C) and pelleted. Whole-cell proteomic analysis of the samples was performed using the method described by Mach et al. (2018), employing nanoflow liquid chromatography coupled with mass spectrometry (MS). The resulting MS data were searched with MaxQuant software (Cox et al., 2014) against the AmoebaDB (Aurrecoechea et al., 2011) *A. castellanii* database as downloaded on March 10th, 2020. The carbamidomethylation of cysteine (Unimod #: 4) was set as a fixed modification, and methionine oxidation (Unimod #: 35) was allowed as a variable modification. Further processing of the data was performed with Perseus software (Tyanova et al., 2016). We

used normalized label-free quantitation values of intensities. We filtered out reverse hits, potential contaminants and proteins identified only by site with posttranslational modification. Then, we took the binary logarithms of the intensities and filtered out the proteins with insufficient numbers of valid quantification values, leaving only those with at least two values per group. Student's t-test with Benjamini-Hochberg correction was used to evaluate significantly changed proteins at the 5% false discovery rate level. Only the proteins that changed more than 1.5–fold were considered. The selected proteins were manually annotated using HHpred (Söding et al., 2005, https://toolkit.tuebingen.mpg.de/tools/hhpred) or by sequence alignment with homologous proteins from other organisms using BLAST (Altschul et al., 1990, https://blast.ncbi.nlm.nih.gov/Blast.cgi). Transmembrane domains were predicted using TMHMM v 2.0 (Krogh et al., 2001, https://www.cbs.dtu.dk/services/TMHMM/). Protein localization was predicted with DeepLoc (Armenteros et al., 2017, https://www.cbs.dtu.dk/services/DeepLoc/). Sequence analysis was performed using Geneious Prime® 2019.2.3 (www.geneious.com).

2.4. Cloning of Acanthamoeba genes of interest

We introduced a polylinker with several restriction sites into pTPBF and pGAPDH plasmids kindly provided by Morgan Colp (PhD Candidate in John Archibald's laboratory at Dalhousie University, Canada). The sequence of the polylinker is provided in Supplementary Table S1. We cloned *A. castellanii* genes *fered*, *nramp* and *vit* into both plasmids using suitable restriction sites. The native *vit* promoter was cloned instead of the *gapdh* promoter, and the resulting plasmid was called pACVIT (Supplementary Table S1). To clone *vit* with an N-terminal GFP tag, we introduced another polylinker immediately after the GFP in the pTPBF and pGAPDH plasmids (the resulting plasmids were named pTN and pGN, respectively).

2.5. Acanthamoeba transfection

Transfection was performed according to doi.org/10.17504/protocols.io.s4regv6. In brief, the cells were grown in PYG medium supplemented with 10 mM iron citrate for 3 days, collected and resuspended in encystment medium (20 mM Tris-HCl (pH 8.8), 100 mM KCl, 8 mM $MgSO_4$, 0.4 mM $CaCl_2$, and 1 mM $NaHCO_3$). A total of 5×10^4 cells in 500 µl of medium were placed in each well of a 6-well plate. Then, 20 µl of SuperFect Transfection Reagent (Qiagen, Germany) were added to 4 µg of plasmid DNA diluted in 100 µl of encystment medium, incubated at room temperature for 10 min, mixed with 600 µl of encystment medium and added to the cells (the same mixture without DNA was used as a negative control). The cells were incubated with DNA and SuperFect reagent for 3 h at room temperature, the mixture was pipetted out, and fresh PYG-A and iron were added. The cells were allowed to recover for 24 h at 27 °C, and then 10 µg/ml of geneticin (G418 disulfate salt, Sigma-Aldrich, USA) were added to each well. Fresh PYG-A with antibiotic was added once during approximately 1.5 weeks. After sufficient growth of transformants occurred (3–5 weeks), the transformants were transferred to 25 cm^2 flasks with PYG-A and 50 µg/ml of geneticin.

2.6. Microscopy

To localize the proteins of interest, *A. castellanii* expressing GFP-tagged proteins were placed on cover slips in growth medium and left for 30 min to attach to the surface. Then, the medium was removed, and the cover slips were mounted to microscope slides and imaged with a Leica TCS SP8 WLL SMD-FLIM microscope (Leica, Germany) equipped with an HC PL APO CS2 63x/1.20 water objective. The fluorescence excitation was at 488 nm, the emission at 498–551 nm was detected with a hybrid HyD SMD detector, and a photomultiplier tube (PMT) detector was used for phase contrast imaging. To visualize the localization of phagocytosed particles and pinocytosed medium, live amoebae were incubated with the fluorescent bacteria pHrodo Red *E. coli* BioParticles Conjugate for phagocytosis or pHrodo Red Dextran 10,000 MW for endocytosis (Invitrogen, USA), and the fluorescent signal was detected using excitation and emission wavelengths set according to the manufacturer's manual. To investigate the mitochondrial localization, 25 nM MitoTracker Red CMXRos (Thermo Fisher Scientific, USA) were added to the medium for 15 min and then carefully changed to fresh medium. Fluorescent signals were detected according to the manual. Images were processed using LAS X 3.5.1.18803 (Leica, Germany). To observe the localization of phagocytosed particles with pH-independent fluorescence, approximately 5×10^5 live cells were resuspended in HEPES-glucose buffer (50 mM glucose, 20 mM HEPES, pH 7.2), transferred to 6-well plates suitable for microscopy and left to settle at 27 °C for 30 min. Fluorescent *E. coli* (*E. coli* BioParticles Alexa Fluor 594 conjugate, Invitrogen) were added to final concentration of 10 µg/ml. The cells were observed with a Nikon CSU-W1 Spinning disc confocal microscope using the dual camera setting with 488 nm and 561 nm excitation lasers, 503–548 nm and 575–625 nm detection.

2.7. Western blotting

Acanthamoeba castellanii expressing GFP-VIT and wild type cells were grown in PYG-A medium for 72 h. The whole-cell lysates were used for the protein detection in western blotting analysis using the primary monoclonal antibody against GFP (Santa Cruz Biotechnology, USA) and secondary anti-mouse peroxidase-conjugated antibodies (Merck, Germany) with Luminata Forte Western horseradish peroxidase substrate (Merck, Germany).

2.8. Iron uptake

Acanthamoeba castellanii was grown for 72 h under iron-supplemented (25 µM Fe-NTA) and iron-depleted (25 µM BPS) conditions in pentaplicate. Starting cultures were chosen so that the cells would reach similar cell densities just before forming a monolayer. The cells were washed three times with HEPES-glucose buffer (50 mM glucose, 20 mM HEPES, pH 7.2; 1200*g* for 5 min) and resuspended in the same buffer. Then, the number of cells in each sample was counted using a Guava EasyCyte8HT flow cytometer (Luminex Corporation, USA), and 5×10^5 cells were dispensed into 1.5 ml tubes. To assess their iron uptake, the cells were supplemented with 2 µM ^{55}Fe citrate as a ferric iron source or 2 µM ^{55}Fe citrate and 1 mM ascorbate as a ferrous iron source. The samples were incubated at 27 °C for 2 h, washed three times with the same buffer, and pelleted and lysed with 50 µl of 0.2% Triton X-100. Two 5 µl aliquots were taken to measure the protein concentration using a bicinchoninic acid (BCA) kit. To the rest of the lysed cells, 800 µl of liquid scintillation cocktail Ultima Gold LLT (PerkinElmer, USA) were added, and the samples were vortexed and analyzed with Triathler Multilabel Tester (Hidex, Finland). To calculate the iron contents in the cells, a calibration curve with the same radioactive iron sample was plotted. Student's t-test with Bonferroni correction for multiple comparisons was used to evaluate statistical significance. To assess the iron uptake by acanthamoebae expressing *Ac*NRAMP or *Ac*IDIP, the cells were grown in tetraplicate for 72 h under iron-supplemented conditions. The following procedures were the same as those described above, and only ferrous iron (2 µM ^{55}Fe citrate and 1 mM ascorbate) was used as an iron source. Two independent experiments were performed.

2.9. Quantitative reverse transcription PCR

Acanthamoeba castellanii was grown in triplicate for 72 h under iron-supplemented and iron-depleted conditions. Acanthamoebae expressing *Ac*IDIP and wild type cells were grown in tetraplicate for 72 h in PYG-A medium without iron or chelator supplementation. Total RNA was purified using the High Pure RNA Isolation Kit (Roche, Switzerland). Quantitative reverse transcription quantitative PCR (qRT-PCR) was conducted using the KAPA SYBR® FAST One-Step universal kit (Sigma-Aldrich, USA) according to the manufacturer's protocol in the RotorGene 3000 PCR cycler (Corbett Research, Australia) with the following thermocycling conditions: reverse transcription at 42 °C for 30 min, DNA denaturation at 95 °C for 5 min, 40 cycles of 95 °C for 10 s, 56 °C for 20 s, and 72 °C for 20 s; and melt-curve analysis from 55 °C to 95 °C with 1 °C step for 5 s per step. For normalization we used actin gene ACA1_151070 as an endogenous reference. The gene for normalization was chosen using the proteomic data; it was expressed at the same level under all conditions. The list of the primers is presented in Supplementary Table S2. The fold change was calculated using $2^{-\Delta\Delta Ct}$ method, for the statistical analysis used 2^{-Ct} values were used (Livak and Schmittgen, 2001).

2.10. Pinocytosis rate

To quantify the iron deficiency effects on pinocytosis, amoebae were cultivated under iron-supplemented and iron-deficient conditions for 72 h to similar cell densities in quadruplicate. The sizes of the cells were analyzed with Z2 Particle Count and Size Analyzer. The cells were washed and transferred into HEPES-glucose buffer and counted using the Guava flow cytometer, and 1×10^6 cells were dispensed into the wells of a 12-well plate. The amoebae were left to settle down at 27 °C for 30 min and afterwards checked under a light microscope. Fluorescent pHrodo Green Dextran 10,000 MW for endocytosis (Invitrogen, USA) was added to a final concentration of 10 μg/ml and incubated for 4 h at 27 °C. Cell aliquots were taken immediately after dextran addition, at 15 min and then every hour. The cells were released by gentle pipetting and immediately measured with the Guava flow cytometer using 488 nm excitation and 525/30 nm acquisition. Acquisition was set to 10,000 events, and the mean fluorescence intensity of each sample was recorded. Student's t-test with Bonferroni correction for multiple testing was used to evaluate statistical significance.

2.11. Yeasts procedures

The *fre1-his3* yeast strain was kindly provided by Emmanuel Lesuisse (Institut Jacques Monod, France), *vit* was cloned into a pCM189 plasmid (Garí et al., 1997). Yeast transformations were performed according to Gietz and Schiestl (2007). For phenotype assays, yeast cultures were grown overnight in liquid synthetic complete (SC) medium without uracil, with 2% glucose as the energy source. Five microliters of five serial ten-fold dilutions starting from OD_{600} 0.2 were plated on agar plates with SC medium without both uracil and histidine; the plates were supplemented with 10 μM or 15 μM BPS with or without the addition of 1 μg/ml of doxycycline. SC plates without uracil and with histidine were used as a control.

3. Results

3.1. Iron deprivation reduces Acanthamoeba growth

The growth curves of *A. castellanii* under iron-deprived and iron-rich conditions are shown in Fig. 1. Iron deprivation noticeably reduced the rate of cell growth as well as the maximum cell density; adding 25 μM BPS resulted in an approximately 50% reduction in the maximum cell count, while 50 μM BPS reduced it more than 12 times. The addition of ferrous iron at a 25 μM concentration did not significantly influence cell growth, which corresponds with the data obtained by Hryniewiecka et al. (1980), who showed that there was only a negligible difference between *Acanthamoeba* growth in 6 μM and 32 μM iron, while in the absence of iron cell growth significantly decreased. The addition of 100 μM iron reduces the rate of cell replication but allows continuous growth so that the cell density ultimately reaches almost the same number as that of the control.

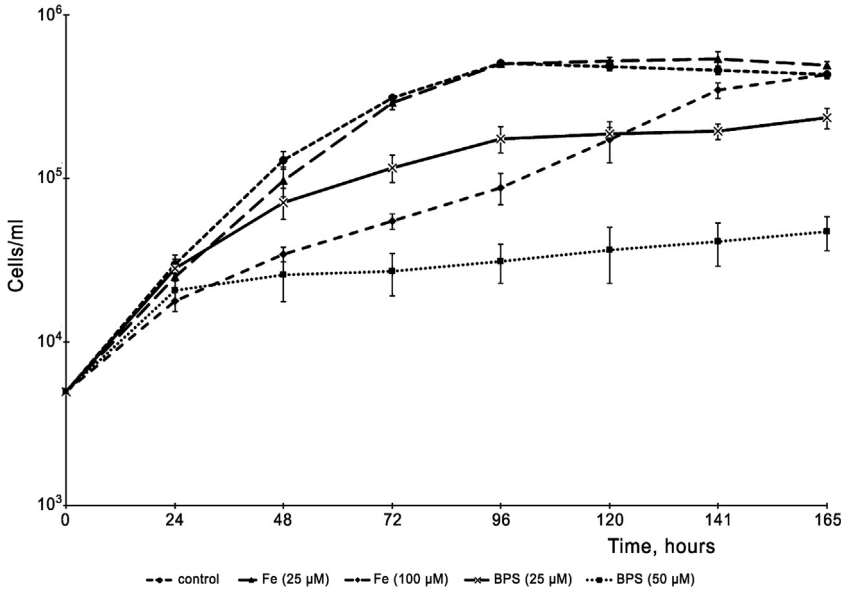

Fig. 1. Iron-dependent growth curves of *Acanthamoeba castellanii*. Amoebae were grown in PYG-A medium supplemented with 25 μM ferric nitrilotriacetate (Fe-NTA), 100 μM Fe-NTA, 25 μM bathophenanthrolinedisulfonic acid (BPS), or 50 μM BPS, or without iron and BPS supplementation as a control. Cells were counted every 24 h. Mean values with S.D.s are shown.

Based on growth curves, for future experiments we used cells grown in 25 μM iron or 25 μM BPS. The chosen chelator concentration ensures iron deficiency but allows the cells to multiply, which is a prerequisite for a successful proteomic analysis without excessive changes accompanying cell death or cyst formation. As a control, we used the medium with 25 μM iron added to guarantee iron supplementation.

3.2. Whole-cell proteomics reveals the proteins involved in iron metabolism

To identify the proteins participating in *A. castellanii* iron metabolism, we compared the whole-cell proteomes of amoebae grown for 72 h in media supplemented with 25 μM Fe-NTA (iron-sufficient conditions) and with 25 μM BPS (to induce iron deprivation). The expression of 224 proteins was changed significantly: 104 proteins were upregulated and 120 were downregulated under iron starvation (Supplementary Table S3). The proteins most relevant for our study are summarized in Table 1.

The most upregulated protein (ACA1_155690 in the AmoebaDB database, 18.6 times upregulation) under iron-deprived conditions is homologous to STEAP metalloreductases. The name STEAP is derived from the 6-transmembrane epithelial antigen of the prostate; these proteins share similarity at the C terminus to the transmembrane domains of yeast FRE metalloreductases and promote the reduction of iron (Ohgami et al., 2006). Based on protein sequence homology and dramatic regulation by iron availability, we propose that ACA1_155690 (called below *Ac*FERED) is a ferric reductase that reduces Fe^{3+} to Fe^{2+}, the latter of which is consequently taken up by divalent metal transporter(s).

The second most upregulated protein (ACA1_099250, 12.1 times) did not show significant homology to any other known proteins, and HHpred analysis did not reveal any probable function. Therefore, we called it *Ac*IDIP (iron deprivation-induced protein). Bioinformatic analysis, namely TMHMM (Krogh et al., 2001) and DeepLoc (Armenteros et al., 2017), predicted a soluble protein with presumed nuclear localization; however, our experimental determination showed cytosolic localization (see below).

The protein exhibiting the third strongest upregulation upon iron deprivation (ACA1_225890, 5.2 times) was a homolog of the metal transporter NRAMP (natural resistance-associated macrophage protein). NRAMP proteins are present in bacteria and eukaryotes, and comprise a large family of metal transporters (Nevo and Nelson, 2006). In *Dictyostelium discoideum*, a social amoeba that is a distant relative of *A. castellanii*, two NRAMP homologs were demonstrated to transport Fe^{2+}, with one of them mediating iron export from phagosomes and macropinosomes (Buracco et al., 2015). We assume that ACA1_225890 (*Ac*NRAMP) is an Fe^{2+} transporter that participates in the uptake of iron reduced by the ferric reductase *Ac*FERED.

Importantly, 10 different proteases were upregulated 1.7 – 3.2 times. Previously, Ramírez-Rico et al. (2015) reported that there were several proteases in *Acanthamoeba* cell extracts and conditioned medium capable of cleaving different iron-containing proteins. The upregulation of these proteases in natural habitats may result in increased iron consumption due to the more efficient use of proteins containing iron cofactors.

The most downregulated protein (ACA1_261050, 4.6 times downregulation) was homologous to proteins from the vacuolar iron transporter (VIT) family and yeast Ccc1 (Ca^{2+}-sensitive cross-complementer). In yeasts, the Ccc1 protein is an iron transporter that removes excessive iron from the cytosol, transferring it into the vacuole (Li et al., 2001). Its homolog participates in iron detoxification in *Plasmodium falciparum* (Slavic et al., 2016). It is thus reasonable to propose that, analogously, *Acanthamoeba* uses the VIT homolog (*Ac*VIT) to eliminate iron from the cytosol when it is present in excess; thus, a significant reduction in its expression would be beneficial during iron starvation.

Table 1
Selected *Acanthamoeba castellanii* proteins that were significantly changed in cells grown in 25 μM bathophenanthrolinedisulfonic acid compared with 25 μM ferric nitrilotriacetate. Arrows indicate upregulation or downregulation.

Gene number in AmoebaDB database	Manual annotation with BLAST and HHpred	Fold change
ACA1_155690	Ferric reductase STEAP	↑18.6
ACA1_099250	Unknown protein	↑12.1
ACA1_225890	Iron transporter NRAMP	↑5.2
ACA1_264610	Leucine aminopeptidase	↑3.2
ACA1_236350	Leucine aminopeptidase	↑2.7
ACA1_223330	Serine proteinase	↑2.6
ACA1_033570	Methionine aminopeptidase	↑2.6
ACA1_144920	Metallo-endopeptidase	↑2.6
ACA1_222700	Serine proteinase	↑2.5
ACA1_399750	Carboxypeptidase	↑2.2
ACA1_092600	Dipeptidyl-peptidase	↑2.0
ACA1_087870	Tripeptidyl-peptidase	↑1.8
ACA1_286170	Oligopeptidase	↑1.7
ACA1_261050	Vacuolar iron transporter (VIT)	↓4.6

3.3. Localization of proteins involved in iron metabolism

To determine the cellular localization of *Ac*FERED, *Ac*NRAMP, *Ac*IDIP and *Ac*VIT, we cloned the genes with a C-terminal GFP tag into two plasmids with different promoters: glyceraldehyde-3-phosphate dehydrogenase (GAPDH, pGAPDH plasmid) and TATA-box binding factor (TPBF, pTPBF plasmid). The *tpbf* promoter drives a moderate level of protein expression, whereas more protein is produced from the *gapdh* promoter (Bateman, 2010). The genes *fered* and *nrampP* appeared to be present in the genome in two allelic variants with minor sequence differences (Supplementary Table S1); thus, both variants were cloned in both plasmids. All the resulting plasmids were transfected into *A. castellanii,* and living cells expressing the investigated proteins were imaged under a fluorescence microscope. The localization pattern was the same for allelic variants and did not depend on the promoter either, so here, we only show the cells expressing the proteins under the *gapdh* promoter (Fig. 2A–D). GFP-expressing cells were used as a control (Fig. 2A).

To rule out the possibility that the expression of GFP-tagged proteins may lead to their mislocalization in acanthamoebae, we expressed the iron-sulfur cluster assembly protein IscA under the same conditions. This protein has a predicted mitochondrial localization, so we used the mitochondrial dye MitoTracker Red CMXRos to confirm that expressed IscA-GFP is directed to the mitochondria. The GFP signal indeed colocalized with mitochondrially targeted dye (Supplementary Fig. S1); therefore, we assume that our experimental design does not affect the localization of proteins.

Both *Ac*FERED and *Ac*NRAMP localize to the membranes of multiple intracellular vesicles, which probably comprise the digestive vacuolar system to which phagocytosed food particles and pinocytosed solutes are delivered for the digestion and internalization of nutrients (see below).

*Ac*IDIP appears to be localized to the cytosol, despite its predicted nuclear localization (Fig. 2B); its localization is analogous to GFP itself. Nevertheless, we cannot exclude the possibility that *Ac*IDIP requires posttranslational modification or binding to yet unknown ligands to be translocated to the nucleus under specific conditions.

Using the abovementioned plasmids, we were unable to obtain conclusive images of *Ac*VIT localization since only a weak green signal was left in the cytoplasm or vesicles, probably due to the

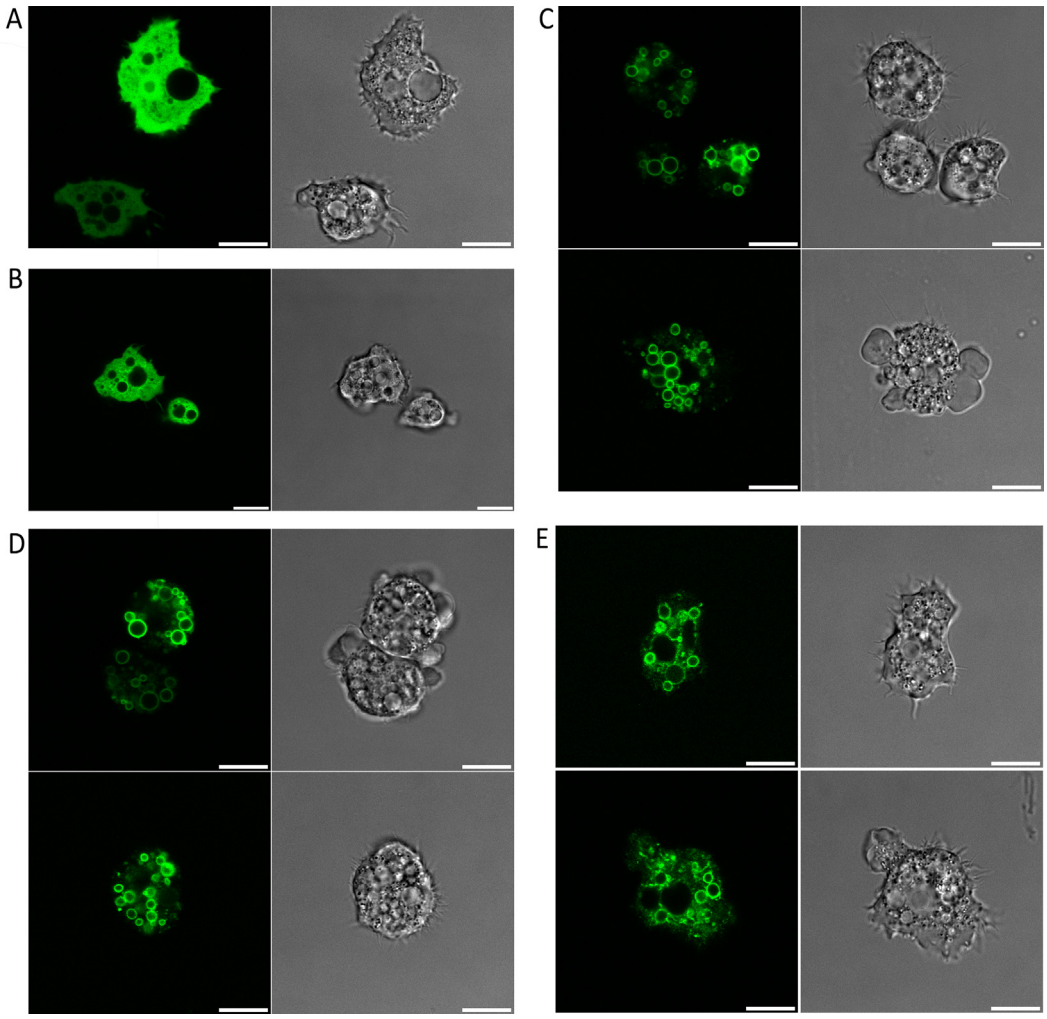

Fig. 2. Localization of GFP-tagged proteins involved in iron metabolism in *Acanthamoeba castellanii*. The proteins were expressed under the constitutive promoter of the *gapdh* gene (A-D) or *tpbf* gene (E). All scale bars are 10 µm. (A) GFP (control). (B) *Ac*IDIP-GFP. (C) *Ac*FERED-GFP. (D) *Ac*NRAMP-GFP. (E) GFP-*Ac*VIT.

degradation of the chimeric protein. The recloning of the GFP-tagged gene under its native promoter did not improve our ability to visualize the protein in the cells. We thus recloned *Ac*VIT with an N-terminal GFP tag, ultimately allowing us to assess its localization (Fig. 2E) even though the signal was still weaker than that of *Ac*FERED or *Ac*NRAMP. Expression was visible only under the moderate *tpbf* promoter. Nevertheless, this experiment revealed that, similar to *Ac*FERED and *Ac*NRAMP, *Ac*VIT is localized to membranes in the intracellular vesicular system.

To verify that we observed the localization of the full-length GFP-*Ac*VIT and not GFP-fused signal peptide cut from the protein, we performed western blotting analysis of whole-cell lysates of GFP-*Ac*VIT using anti-GFP antibodies (Supplementary Fig. S2). The major band corresponds to the size of GFP-*Ac*VIT (55.7 kDa) confirming the expression of the full-size fusion protein in the cells.

3.4. AcFERED, AcNRAMP and AcVIT are colocalized with food particles

Considering the localization of *Ac*FERED and *Ac*NRAMP as well as the fact that acanthamoebae are believed to obtain food by pino- and phagocytosis (Byers, 1979), we proposed that these two proteins participate in iron acquisition from pinocytosed medium or phagocytosed particles. Therefore, we expected endocytosed material to be trafficked into vesicles containing the expressed proteins. To check whether the vesicles with *Ac*FERED and *Ac*NRAMP represent the terminal points for endocytosis, we incubated the transformants with fluorescently labeled dextran (10,000 MW) or *E. coli*. The fluorescence of the selected pHrodo Red dye increases strongly with decreasing pH, meaning that the fluorescent signal is probably mostly gained from digestive vacuoles with acidic content. Indeed, the fluorescent label is targeted into the vesicles framed with the expressed proteins (Fig. 3A–B, D–E, Supplementary Movies S1-S3), confirming the role of *Ac*FERED and *Ac*NRAMP in nutrient acquisition. From these data, we cannot unequivocally conclude that these proteins are present in the same vesicles within the cell; nevertheless, we believe that they act consecutively in one compartment to deliver iron into the cytosol.

Furthermore, we performed the same experiment with *Ac*VIT-expressing cells (Fig. 3C, F). Similar to *Ac*FERED and *Ac*NRAMP, *Ac*VIT is targeted to the acidic vesicular compartment, which is consistent with the vacuolar localization of the yeast Ccc1 iron transporter.

Since pHrodo dyes are pH-dependent, they can only be visualised in an acidic environment developing in late endosomal stages. Taking into consideration that *Ac*NRAMP is presumably an iron importer and *Ac*VIT is an iron exporter, we would expect the former to be more abundant in early endosomes and the latter to be present mostly in later endocytosis stages. Thus, we decided to investigate phagocytosis of bacteria labelled with Alexa Fluor

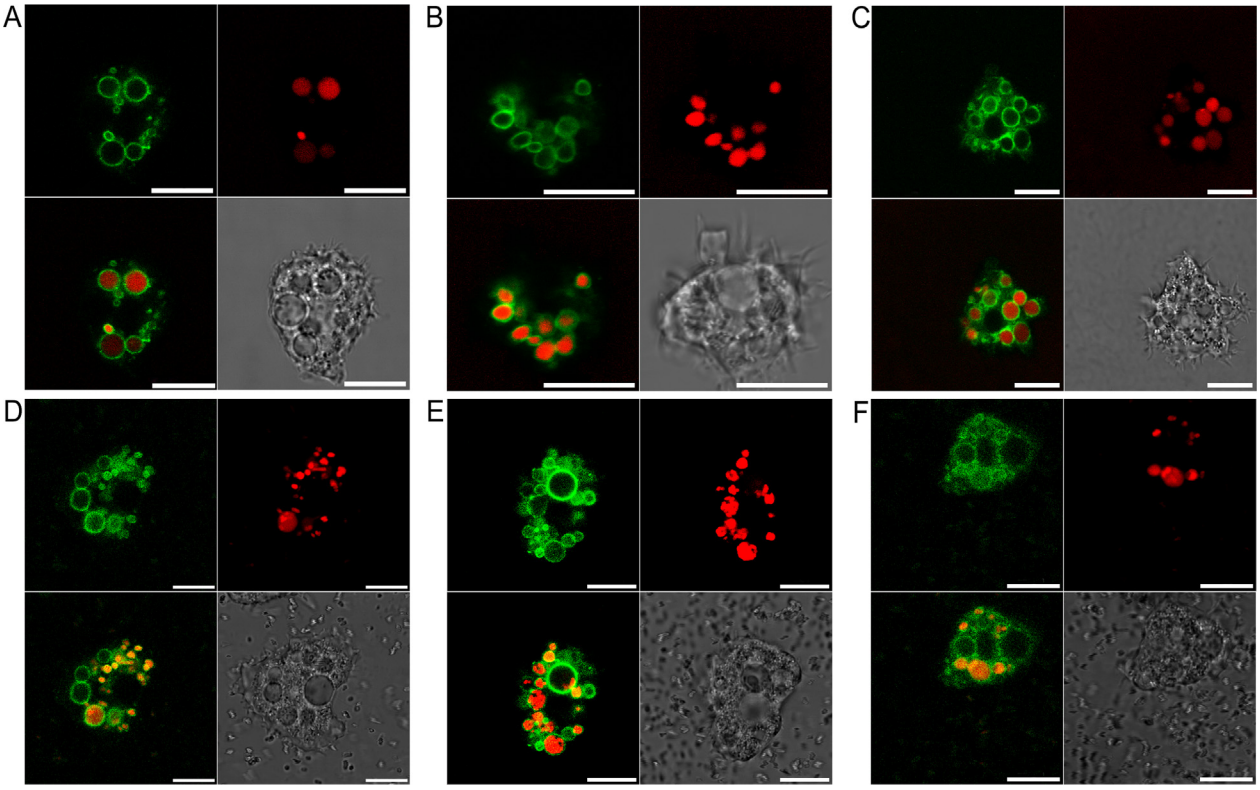

Fig. 3. Colocalization of GFP-tagged proteins involved in the iron metabolism of *Acanthamoeba castellanii* and fluorescent food particles or solutes. Live *A. castellanii* cells expressing GFP-tagged proteins were incubated with pHrodo Red Dextran 10,000 MW for endocytosis (A–C) or pHrodo Red *Escherichia coli* BioParticles Conjugate for phagocytosis (D–F). All scale bars are 10 μm. (A) *Ac*FERED-GFP+dextran. (B) *Ac*NRAMP-GFP+dextran. (C) GFP-*Ac*VIT+dextran. (D) *Ac*FERED-GFP+*E. coli*. (E) *Ac*NRAMP-GFP +*E. coli*. (F) GFP-*Ac*VIT+*E. coli*.

dye which does not depend on pH. However, we were not able to see any difference in bacteria trafficking between the cells expressing *Ac*FERED, *Ac*NRAMP and *Ac*VIT (Supplementary Fig. S3). In all three transformant lines we were able to observe both intact rod-shaped bacteria and dissolved red fluorophore, presumably derived from digested bacteria, in vacuoles framed by GFP-tagged protein. Based on our observations, *Ac*VIT was present in vacuoles with early and medium endocytic stages represented with intact bacteria, while *Ac*FERED and *Ac*NRAMP were present in vacuoles with dissolved fluorophore which we assume to represent phagocytosed material on later stages. Thus, we propose that there is at least partial colocalization of *Ac*FERED, *Ac*NRAMP and *Ac*VIT; however, further investigation is needed to prove this hypothesis.

3.5. Iron acquisition effectiveness is induced by iron starvation and expression of AcIDIP

Upregulation in the expression of the proteins participating in iron uptake is expected to increase the efficiency of iron acquisition. Since our proteomic analysis revealed that *Ac*FERED and *Ac*NRAMP are among the three most induced proteins upon iron starvation, we compared the uptake of ^{55}Fe radioisotopes by acanthamoebae grown for 72 h under iron-sufficient (25 μM Fe-NTA) and iron-depleted (25 μM BPS) conditions. The cells were washed clean of any external iron or chelator and placed in HEPES buffer with glucose to supplement the cells with an energy source and avoid low osmolarity. Then, the cells were supplemented with a source of iron radioisotope, either as Fe^{3+} (ferric citrate) or Fe^{2+} (ascorbate was added to the reaction buffer as a reducing agent). The results are shown in Fig. 4A. As expected, the acquisition of iron by cells grown under iron-depleted conditions was significantly more efficient, regardless of the provided form of iron. However, the uptake of the Fe^{2+} form occurs more effectively, indicating the requirement for the reduction step.

Peracino et al. (2006) demonstrated in their work that the *Dictyostelium* NRAMP-GFP chimera is at least partially functional in terms of iron translocation. Therefore, we decided to compare iron uptake in *Acanthamoeba* cells expressing GFP-tagged *Ac*NRAMP under the *gapdh* promoter and wild-type cells. Additionally, we assessed iron uptake in cells expressing *Ac*IDIP-GFP. Cells were grown for 72 h in 25 μM iron to decrease the levels of intrinsic *Ac*NRAMP and *Ac*IDIP. The summarized results of two independent experiments, each performed in biological tetraplicate, are shown in Fig. 4B; there was no difference in iron uptake between the cells expressing *Ac*NRAMP-GFP and the wild type cells. We believe, however, that this observation is due to the GFP tag, which impaired the protein function. Interestingly, expression of the *Ac*IDIP-GFP fusion protein induced iron acquisition approximately twice. Since bioinformatic analysis did not reveal any potential function of this protein, we can only hypothesize its role to be regulatory.

3.6. QRT-PCR demonstrates the change in expression of fered, idip, nramp and vit genes

To further investigate the regulation of iron metabolism related proteins, we conducted qRT-PCR using cells grown under iron-depleted and iron-rich conditions (Table 2). Our results demonstrated that all four proteins are changed at a transcription level. The transcript level changes reflect the changes we observed at a proteomic level: *fered*, *idip* and *nramp* are upregulated under low iron conditions while *vit* is downregulated, although the fold change of transcript amounts differ from protein amount fold

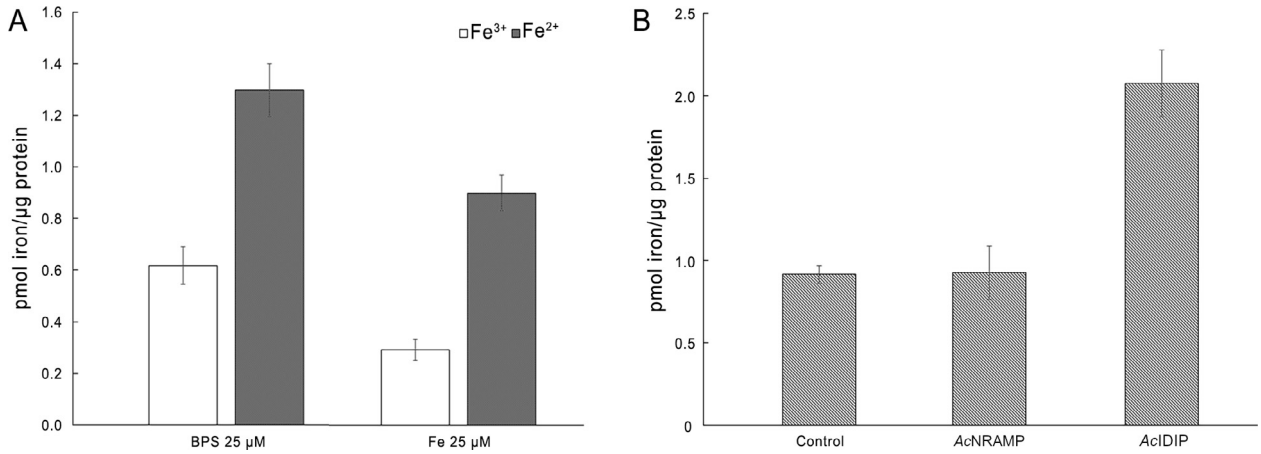

Fig. 4. ^{55}Fe radioisotope uptake in *Acanthamoeba castellanii*. (A) Wild type cells were grown under iron deprivation (bathophenanthrolinedisulfonic acid (BPS) 25 µM) or iron supplementation (ferric nitrilotriacetate (Fe-NTA) 25 µM), and the acquisition of Fe^{2+} and Fe^{3+} was determined by liquid scintillation counting. The means of five biological replicates with 95% confidence intervals are shown (adjusted for multiple testing, $\alpha = 0.0125$). Asterisks indicate statistical significance of the difference: $^{**}P < 0.005$, $^{***}P < 0.001$. (B) Iron uptake in *A. castellanii* control (wild type) cells and cells expressing GFP-tagged *Ac*NRAMP and *Ac*IDIP. The means of eight biological replicates with 95% confidence intervals are shown (adjusted for multiple testing, $\alpha = 0.0167$). Asterisks indicate statistical significance of the difference: $^{***}P < 0.001$.

Table 2
The changes in transcript abundance of selected genes in cells grown in 25 µM bathophenanthrolinedisulfonic acid compared with 25 µM ferric nitrilotriacetate, determined with quantitative reverse transcription PCR. Arrows indicate upregulation or downregulation. Asterisks indicate statistical significance of the change: $^{*}P < 0.05$, $^{**}P < 0.005$, $^{***}P < 0.001$.

	Fold change with S.D.	*P* value
idip	↑ 52.9 ± 8.3 **	0.0015
fered	↑ 2.6 ± 0.8 *	0.007
nramp	↑ 12.4 ± 1.4 ***	0.0008
vit	↓ 1.5 ± 0.2 *	0.03

changes, which might be due to different transcript stability in the cell or due to additional regulation of expression at the protein level.

Additionally, we investigated the changes in expression of iron metabolism-related proteins in cells expressing *Ac*IDIP-GFP compared with wild type cells using qPCR. As expected, the transcript level of *idip* in the cells expressing *Ac*IDIP-GFP is dramatically higher (1863 times) than in the wild type cells (Supplementary Table S4). However, we did not observe any differences in transcript abundance of *nramp*, *fered* or *vit*. Thus, expression of *Ac*IDIP-GFP does not increase the expression of presumed iron transporters or ferric reductase at a transcriptional level.

3.7. Pinocytosis is reduced in iron-depleted amoebae

Considering that *A. castellanii* axenic culture in liquid medium takes up nutrients, including iron, by pinocytosis (Bowers and Olszewski, 1972), the observed increase in iron uptake could possibly be a result of enhanced pinocytosis. Therefore, we compared the pinocytosis rate in cells grown under iron-sufficient and iron-depleted conditions. The cells were incubated for 15 min, 1, 2 or 3 h with fluorescent pHrodo Green dextran in HEPES buffer with glucose and analyzed by flow cytometry. We found that pinocytosis was, in fact, reduced ~1.7 times in the cells grown under iron deficiency (Fig. 5). Also, we estimated the average size of the cells grown under different conditions since the reduction in pinocytosis rate might have happened due to the decrease in cell size. However, it did not depend on the growth conditions: the mean size of cells grown with the addition of iron was 15.30 µm with S.D. = 2.166 µm while the size of the cells under iron-starved conditions was 15.33 µm (S.D. = 1.870 µm).

Thus, we conclude that the increase in iron acquisition occurs due to the upregulation of proteins directly involved in iron uptake (e.g., *Ac*FERED and *Ac*NRAMP) and not due to more intensive pinocytosis.

3.8. AcVIT is able to complement iron-sensitive yeast mutants functionally

To validate the iron transport function of the *Ac*VIT protein, we performed complementation assays using the *Saccharomyces cerevisiae* strain with an iron-regulated *fre1/his3* reporter construct (Shi et al., 2008) containing the imidazole glycerol-phosphate dehydratase gene (*his3*, which participates in the histidine biosynthesis pathway) under the *fre1* promoter. This construct confers histidine prototrophy to cells when the reporter is activated by Aft1 (the activator of ferrous transport), the major iron-dependent transcription factor in yeast. Aft1 is activated during cytosolic iron depletion, meaning that under iron deficiency, this strain can grow without added histidine, while an increase in the cytosolic iron concentration impairs histidine biosynthesis. *Ac*VIT expression partly restored the defective growth of the mutant on synthetic medium without uracil and histidine (Fig. 6); *Ac*VIT-expressing cells were able to grow under higher iron concentrations than the transformant with empty plasmid, although the addition of some amount of iron chelator was still needed to support growth. The effect was eliminated by adding doxycycline, which blocks the transcription of the gene from the plasmid, which confirms that the effect is indeed caused by *Ac*VIT expression. The lower efficiency of functional complementation may be due to the low expression of heterologous proteins, partial misfolding or mislocalization, or the absence of interaction partners in the yeast cell. Nevertheless, this result clearly shows that the *Ac*VIT protein functions in the transport of iron from the cytosol, which, together with its vesicular localization and reduced expression upon iron starvation, strongly indicates its role in iron detoxification/storage in *Acanthamoeba*.

4. Discussion

It was already demonstrated by Hryniewiecka et al. (1980) that *Acanthamoeba* growth is significantly affected by iron availability; in their work, excluding iron from the medium resulted in a notable reduction in the growth rate and a decrease in the steady-stage

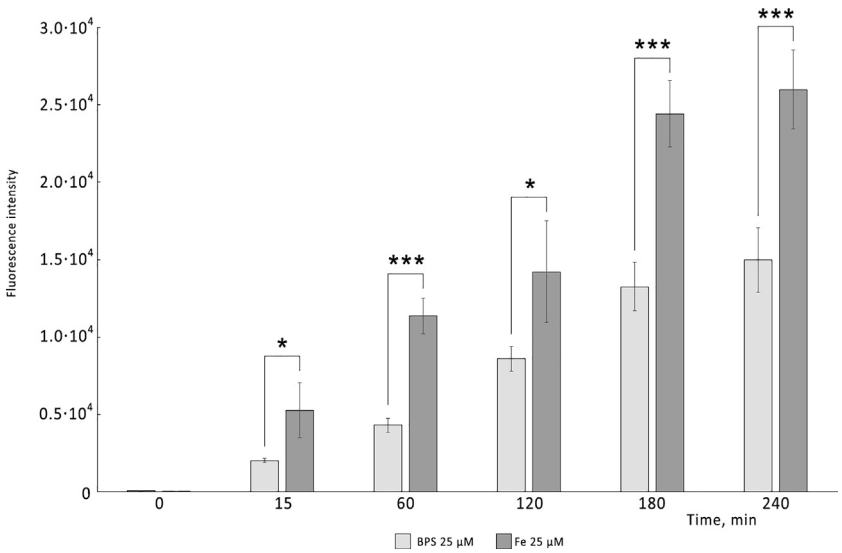

Fig. 5. Pinocytosis in *Acanthamoeba castellanii* iron-deprived and iron-supplemented cells. The cells were incubated with pHrodo Green Dextran 10,000 MW for up to 4 h. Fluorescence was measured in aliquots immediately after dextran addition and during incubation by flow cytometry. The means of four biological replicates with 95% confidence intervals are shown (adjusted for multiple testing, $\alpha = 0.01$). Asterisks indicate statistical significance of the difference: $^{*}P < 0.05$, $^{***}P < 0.001$.

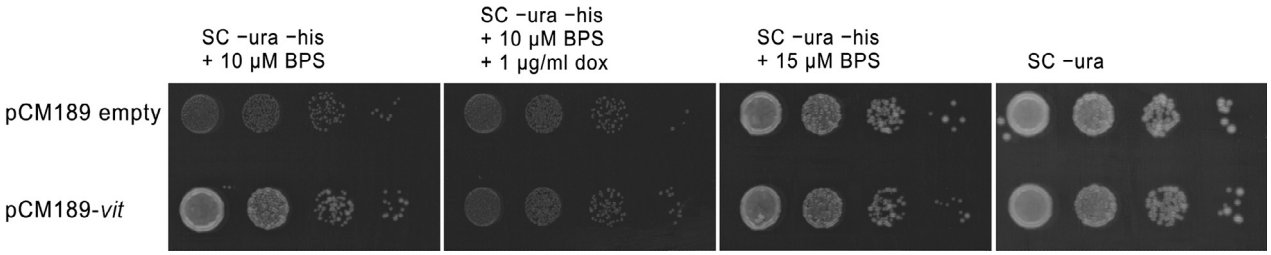

Fig. 6. Functional complementation of the iron-sensitive *fre1-his3* yeast strain by *Ac*VIT. The *fre1-his3* strain was transformed with empty tetracycline-regulatable plasmid pCM189 or pCM189 carrying *vit* gene, spotted on synthetic complete medium without uracil and histidine (SC-ura -his) or without uracil and with histidine (SC -ura) and grown for 3 days at 30 °C. *Ac*VIT-expressing cells were able to grow under higher iron concentrations than the transformant containing empty plasmid. This effect was eliminated by doxycycline (dox), which blocks transcription from the vector. BPS, bathophenanthrolinedisulfonic acid.

cell density. Using different cultivation methods (cells grown in monolayers instead of agitated cultures), we observed a similarly substantial decrease in growth under iron depletion (Fig. 1). Hryniewiecka and her colleagues (1980) showed that the overall respiratory level is lower under iron deprivation and that the ratio between cytochrome oxidase- and alternative oxidase-dependent respiration depends on the availability of iron; when there is a limited iron supply, the cells rely on a more energetically effective cytochrome oxidase pathway. Interestingly, it was demonstrated that another amphizoic amoeba, *Naegleria fowleri*, decreases its complex IV activity under iron deficiency, while the activity of (less iron-demanding) alternative oxidase is, by contrast, significantly increased (Arbon et al., 2020).

To identify the proteins participating in iron metabolism, we first studied the whole-cell proteomic response to iron deprivation, since these conditions are expected to result in the induction of the components of the iron uptake system. Based on the growth curves, we chose the iron chelator concentration that promotes iron deficiency, allowing for sufficient cell growth without cyst formation or cell death. Iron was added to the control cells at a concentration that ensured iron repletion without toxic effects. The first and third most upregulated proteins under iron deprivation were a homolog of STEAP metalloreductases, *Ac*FERED (Table 1) and a homolog of NRAMP metal transporters, *Ac*NRAMP; qPCR confirmed the upregulation of expression of the corresponding genes at a transcriptional level (Table 2). STEAP3 protein was discovered in human erythroid cells as a part of the transferrin cycle, a classical iron acquisition pathway in mammalian cells (Ohgami et al., 2005). In this cycle, the transferrin receptor mediates transferrin endocytosis by the cell, followed by endosome acidification which facilitates the release of ferric iron from transferrin. The released iron is transported to the cytosol by the NRAMP2 (or DMT1) transporter. NRAMP2 is a divalent metal transporter, so the reduction of ferric iron is essential. STEAP3 was demonstrated to implement this function in erythroid cells; later, it was shown that its homologs STEAP2 and STEAP4 also have ferric reductase activity (Ohgami et al., 2006). We assume that a similar pathway of iron trafficking is employed by *Acanthamoeba* cells: endocytosed ferric iron is reduced by *Ac*FERED and transported to the cytosol by *Ac*NRAMP. This mechanism is confirmed by the fact that *Acanthamoeba* preferably takes up divalent iron, while Fe^{3+} is acquired with less efficiency. This type of system was proposed for the distantly related social amoeba *D. discoideum* (Bozzaro et al., 2013; Buracco et al., 2015). In *Dictyostelium* cells, NRAMP1 mediates Fe^{2+} export from phagosomes and macropinosomes, and although STEAP homologs are not found in the *D. discoideum* genome, there are at least two putative ferric reductases present, one of which is recruited to phagosomes according to preliminary data (Buracco et al., 2015).

Both *Ac*FERED and *Ac*NRAMP in *A. castellanii* are localized to membranes of multiple intracellular vesicles of different sizes (Fig. 2C–D). Although a two-step reductive mechanism for iron

assimilation is employed by many organisms including bacteria and archaea, yeasts such as *Candida albicans* and *S. cerevisiae*, parasitic protists such as *Leishmania amazonensis*, plants and others, its components are typically localized to the plasma membrane (Moog and Brüggemann, 1994; Schröder et al., 2003; Flannery et al., 2011). Therefore, the localization of *Ac*FERED and *Ac*NRAMP to intracellular vesicles is quite unusual. Unfortunately, it does not allow us to assess ferric reductase activity using ferrozine or BPS assays to detect ferrous iron complex production, as is done for plasma membrane ferric reductases (for example, in Knight et al., 2005 or Arbon et al., 2020). Our results demonstrate that phagocytosed bacteria and pinocytosed medium are trafficked into this vesicular compartment (Fig. 3A–B, D–E), and at least some of these vesicles are acidified, since we were able to observe the signal of pH-sensitive fluorescent dye inside them. These data are consistent with studies demonstrating that different NRAMP proteins function as metal-proton symporters (Coutville et al., 2006), which means that the acidification of vesicles would facilitate iron transport, and with the findings of Peracino et al. (2006) showing that in *Dictyostelium* amoebae, NRAMP1 colocalizes with v-type H^+-ATPase.

Unfortunately, there are no well-established methods to knock out genes in *A. castellanii* yet. Since there are several papers describing gene knockdowns in *Acanthamoeba* (Lorenzo-Morales et al., 2005, 2010; Huang et al., 2017), we tried to use this method, however, the fitness of the cells was strongly affected by the procedure and, in our opinion, further analysis would be arguable. Therefore, we were not able to directly prove the function of the investigated proteins and had to study their function indirectly, focusing on physiological characteristics of the cells grown under iron-rich and iron-limited conditions.

Considering the higher expression levels of the proteins importing iron to cytosol under iron starvation, we expected that the efficiency of iron uptake would be increased. Indeed, cell growth in iron-depleted medium results in more efficient iron uptake (Fig. 4A), demonstrating the ability of amoebae to respond to nutrient deprivation.

Bowers and Olszewski (1972) demonstrated that acanthamoebae obtain different compounds such as albumin, inulin, leucine and glucose at similar rates, and linearly, over time without any evident saturation, and therefore proposed pinocytosis to be the feeding mechanism of *Acanthamoeba* in liquid media. Thus, the increase in iron uptake that we observed in cells grown under iron deficiency could possibly be caused by a higher pinocytosis rate rather than the upregulation of the expression of proteins participating in iron efflux from vacuoles to cytosol. However, according to our findings, pinocytosis is in fact notably reduced in iron-starved cells (Fig. 5). It was shown that both pino- and phagocytosis are energy-dependent processes that require oxidative phosphorylation (Bowers, 1977), and their high energy demand is not surprising since membrane turnover due to pino- and phagocytosis was estimated to be strikingly high in *Acanthamoeba* (2–10 times per h), especially compared with other amoebae and macrophages (Bowers and Olszewski, 1972). As mentioned above, the total respiration level in iron-starved *Acanthamoeba* was decreased, probably indicating a lower energy production level, which might not be sufficient to maintain the same level of endocytosis as in iron-supplemented cells. Hence, pinocytosis in iron-depleted amoebae is reduced, and the increased iron acquisition level in these cells appears to occur due to the upregulation of proteins participating in iron import to cytosol, presumably *Ac*FERED and *Ac*NRAMP.

Ramírez-Rico et al. (2015) studied the ability of *Acanthamoeba* crude cell extracts and conditioned medium to cleave different iron-containing proteins. They found that there were several proteases that can break down human holo-lactoferrin, holo-transferrin and hemoglobin, and horse spleen ferritin. They searched the MEROPS database and found several proteases with molecular weights similar to those discovered in their study. Based on our proteomic data, two of the suggested proteases (https://www.uniprot.org/uniprot/L8H8J9 or ACA1_184420 in AmoebaDB database and https://www.uniprot.org/uniprot/L8GXX7 or ACA1_066290) are indeed expressed in *Acanthamoeba* cells, although there was no change in expression depending on iron availability. Nevertheless, we discovered that several proteases and peptidases were upregulated under iron-deprived conditions. Higher protease levels may be beneficial for acanthamoebae both in soil where bacteria are believed to be their food source (Rodríguez-Zaragoza, 1994) and in host tissues, because they would result in increased iron assimilation due to the more efficient use of host iron-containing proteins. Interestingly, one of the upregulated proteases, aminopeptidase M20/M25/M40 family protein (ACA1_264610), has recently been studied by Huang et al. (2017), who demonstrated its ability to induce cell cytopathic effects on rat glial cells, mediating contact-independent host cell injury. This protein might be upregulated upon *Acanthamoeba* colonization of the host tissues due to iron depletion caused by nutritional immunity.

Interestingly, our proteomic analysis revealed a protein that is highly upregulated by iron starvation and does not share any pronounced homology to other known proteins (*Ac*IDIP). Although we were not able to predict its function, based on bioinformatic tool prediction, we expected a soluble protein with nuclear localization. It was thus temping to speculate that the protein is involved in the regulation of gene expression, however our further experiment revealed its cytosolic localization. Interestingly, expression of the *Ac*IDIP-GFP fusion protein induced iron acquisition by acanthamoebae more than twice (Fig. 4B), indeed suggesting its role in iron acquisition. We proposed that *Ac*IDIP might function as a transcriptional regulator, despite its cytosolic localization, since many transcription factors reside in the cytosol and require specific conditions to be translocated to the nucleus, such as phosphorylation by specific kinases, ligand binding or interaction with other proteins (Whiteside and Goodbourn, 1993; Cyert, 2001). However, our further analysis revealed that there is no upregulation of transcription of ferric reductase or iron transporters in the transfected cells expressing *Ac*IDIP-GFP fusion protein (Supplementary Table S4). The mechanism of its participation of *Ac*IDIP in iron uptake remains unknown; it might regulate one or several proteins of the iron trafficking machinery by direct interaction. We believe that it is of great interest to focus further investigation on the elucidation of the function of this novel unique protein.

Since iron is toxic when present in excess, all organisms must tightly balance iron acquisition with its storage and/or removal. The major iron storage/detoxification protein ferritin is ubiquitously distributed among living species (Harrison and Arosio, 1996); however *Saccharomyces*, *Plasmodium* and some other organisms, including *Acanthamoeba*, lack its homologs. We assume that *Ac*VIT, which was the most downregulated protein under iron-depleted conditions, performs the iron detoxification function in *A. castellanii*. *Ac*VIT is a homolog of *Arabidopsis thaliana* VIT1 and yeast Ccc1. Ccc1/VIT family proteins are widely distributed in nature and found in plants, fungi, and protists (Ram et al., 2021). In yeasts, Ccc1 promotes iron accumulation in the vacuole, and its disruption affects cytosolic iron levels and causes increased sensitivity to external iron (Li et al., 2001). Similarly, VIT-deficient *Plasmodium* parasites are more sensitive to increased iron concentrations and have higher levels of labile iron in cells. Curiously, the VIT in *Plasmodium* localizes to the endoplasmic reticulum rather than the vacuolar compartment (Slavic et al., 2016). In *A. thaliana,* VIT1 also mediates iron sequestration into vacuoles, although this protein serves in iron storage; VIT1-deficient seedlings grow poorly when iron availability is low, even though plant cells possess ferritin (Kim et al., 2006).

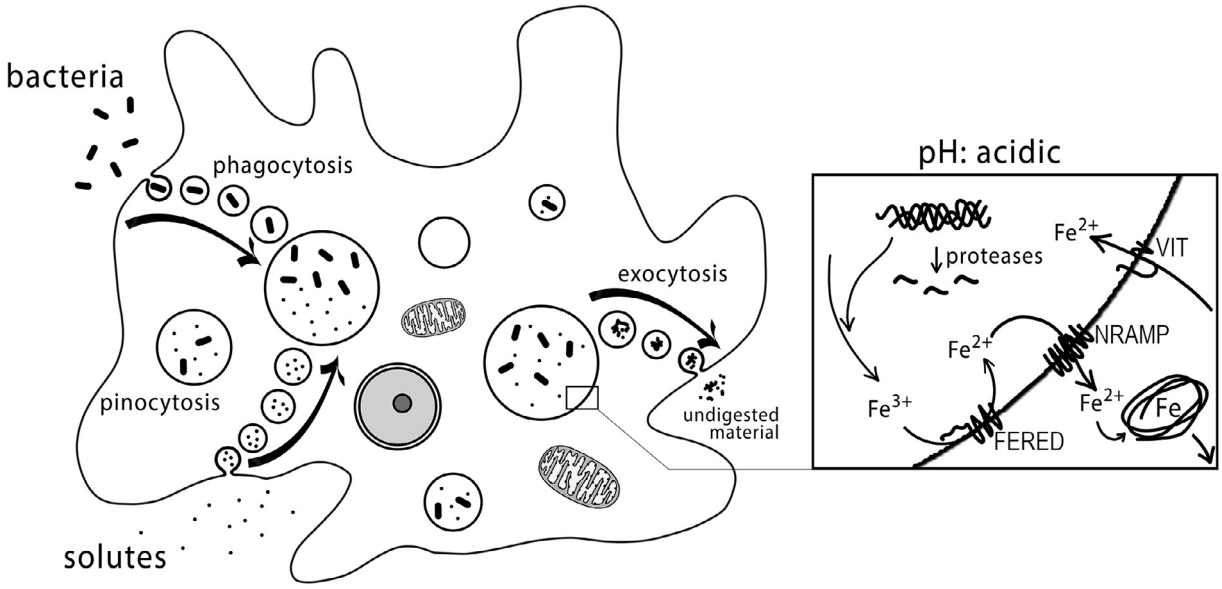

Fig. 7. Schematic representation of iron uptake and detoxification in *Acanthamoeba castellanii*. Amoebae phagocytose bacteria or pinocytose solutes that are trafficked into acidified digestive vacuoles. Acidic pH and protease activity destroy bacterial cells and break down proteins containing iron. The released ferric iron is reduced by the ferric reductase *Ac*FERED, and ferrous iron is taken up by the iron transporter *Ac*NRAMP and introduced into the cell proteins. When iron is abundant, its excess amount is removed from the cytosol by the *Ac*VIT iron transporter into the same digestive vacuoles and stored or exocytosed with undigested material.

According to our data, *Ac*VIT localizes, at least partly, to the same compartment as *Ac*FERED and *Ac*NRAMP, namely, to the membranes of multiple vesicles (Figs. 2E, 3C, F, Supplementary Fig. S3), and it is able to complement iron-sensitive yeast mutants functionally (Fig. 6). Unlike *D. discoideum*, in which the contractile vacuole network seems to be used for iron storage (Peracino et al., 2013), *A. castellanii* probably extrudes excessive iron into digestive vacuoles, where it might be transiently stored or discarded together with undigested food remnants by exocytosis.

In conclusion, our study elucidates the primary mechanisms of iron acquisition and detoxification in *A. castellanii* cells (Fig. 7). Amoebae pinocytose liquid with solutes or phagocytose bacteria/other food particles, which are trafficked into acidified digestive vacuoles. These vacuoles somehow resemble the digestive system of higher organisms: the nutrients are internalized but are not necessarily available for utilization in cell metabolism, and amoebae employ different proteins to efficiently assimilate them. The drop in pH and protease activity destroys the internalized bacteria and breaks down the proteins containing iron. The released ferric iron is reduced by the ferric reductase *Ac*FERED, and ferrous iron is delivered to cytoplasm by the divalent iron transporter *Ac*NRAMP. When iron availability is limited, the rate of pinocytosis is reduced, while the expression of *Ac*FERED and *Ac*NRAMP, as well as multiple proteases, is increased, allowing more efficient iron assimilation. When iron is abundant, its excess is removed from the cytosol by the *Ac*VIT iron transporter into the same digestive vacuoles and stored or exocytosed together with the remaining undigested material. Elucidating the iron acquisition and assimilation machinery in pathogens is especially important for our understanding of virulence mechanisms, since nutritional immunity causes iron deprivation within the host tissue and iron plays an important role in the host-pathogen battle. Consequently, iron homeostasis-related proteins represent potential targets in future research regarding the treatment of diseases caused by pathogens such as *Acanthamoeba*.

Acknowledgements

This project was supported by the Czech Science Foundation (20-28072S), Charles University Grant Agency (1218120), CePaViP provided by The European Regional Development Fund and Ministry of Education, Youth and Sports of the Czech Republic (CZ.02.1.01/0.0/0.0/16_019/0000759), MiCoBion project funded from European Union Horizon 2020 (810224). We acknowledge Imaging Methods Core Facility at BIOCEV, institution supported by the MEYS CR (Large RI Project LM2018129 Czech-BioImaging) and ERDF (project No. CZ.02.1.01/0.0/0.0/18_046/0016045) for their support with obtaining imaging data presented in this paper. We thank Karel Harant and Pavel Talacko from the laboratory of mass spectrometry, BIOCEV, Charles University, the Faculty of Science, where proteomic and mass spectrometric analyses were done. We thank Roman Likane for help with iron uptake experiments.

Appendix A. Supplementary data

Supplementary data to this article can be found online at https://doi.org/10.1016/j.ijpara.2022.03.007.

References

Altschul, S.F., Gish, W., Miller, W., Myers, E.W., Lipman, D.J., 1990. Basic local alignment search tool. J. Mol. Biol. 215, 403–410. https://doi.org/10.1016/S0022-2836(05)80360-2.

Arbon, D., Ženíšková, K., Mach, J., Grechnikova, M., Malych, R., Talacko, P., Sutak, R., 2020. Adaptive iron utilization compensates for the lack of an inducible uptake system in *Naegleria fowleri* and represents a potential target for therapeutic intervention. PLoS Negl. Trop. Dis. 14, 1–25. https://doi.org/10.1371/journal.pntd.0007759.

Ardalan, S., Craig Lee, B., Garber, G.E., 2009. *Trichomonas vaginalis*: the adhesins AP51 and AP65 bind heme and hemoglobin. Exp. Parasitol. 121, 300–306. https://doi.org/10.1016/j.exppara.2008.11.012.

Armenteros, J.J.A., Sønderby, C.K., Sønderby, S.K., Nielsen, H., Winther, O., Hancock, J., 2017. DeepLoc: prediction of protein subcellular localization using deep learning. Bioinformatics 33 (21), 3387–3395.

Aurrecoechea, C., Barreto, A., Brestelli, J., Brunk, B.P., Caler, E.V., Fischer, S., Gajria, B., Gao, X., Gingle, A., Grant, G., Harb, O.S., Heiges, M., Iodice, J., Kissinger, J.C., Kraemer, E.T., Li, W., Nayak, V., Pennington, C., Pinney, D.F., Pitts, B., Roos, D.S., Srinivasamoorthy, G., Stoeckert, C.J., Treatman, C., Wang, H., 2011. AmoebaDB and MicrosporidiaDB: functional genomic resources for Amoebozoa and Microsporidia species. Nucleic Acids Res. 39, 612–619. https://doi.org/10.1093/nar/gkq1006.

Bateman, E., 2010. Expression plasmids and production of EGFP in stably transfected *Acanthamoeba*. Protein Expr. Purif. 70, 95–100. https://doi.org/10.1016/j.pep.2009.10.008.Expression.

Bowers, B., 1977. Comparison of pinocytosis and phagocytosis in *Acanthamoeba castellanii*. Exp. Cell Res. 110, 409–417. https://doi.org/10.1016/0014-4827(77)90307-X.

Bowers, B., Olszewski, T.E., 1972. Pinocytosis in *Acanthamoeba castellanii*. J. Cell Biol. 53, 681–694. https://doi.org/10.1083/jcb.53.3.681.

Bozzaro, S., Buracco, S., Peracino, B., 2013. Iron metabolism and resistance to infection by invasive bacteria in the social amoeba *Dictyostelium discoideum*. Front. Cell. Infect. Microbiol. 4, 1–9. https://doi.org/10.3389/fcimb.2013.00050.

Buracco, S., Peracino, B., Cinquetti, R., Signoretto, E., Vollero, A., Imperiali, F., Castagna, M., Bossi, E., Bozzaro, S., 2015. *Dictyostelium* Nramp1, which is structurally and functionally similar to mammalian DMT1 transporter, mediates phagosomal iron efflux. J. Cell Sci. 128, 3304–3316. https://doi.org/10.1242/jcs.173153.

Byers, T.J., 1979. Growth, reproduction, and differentiation in *Acanthamoeba*. Int. Rev. Cytol. 61, 283–338. https://doi.org/10.1016/S0074-7696(08)62000-8.

Castellani, A., 1930. An amoeba found in culture of a yeast: preliminary note. J. Trop. Med. Hyg. 33, 160.

Coutville, P., Chaloupka, R., Cellier, M.F.M., 2006. Recent progress in structure-function analyses of Nramp proton-dependent metal-ion transporters. Biochem. Cell Biol. 84, 960–978. https://doi.org/10.1139/O06-193.

Cox, J., Hein, M.Y., Luber, C.A., Paron, I., Nagaraj, N., Mann, M., 2014. Accurate proteome-wide label-free quantification by delayed normalization and maximal peptide ratio extraction, termed MaxLFQ. Mol. Cell. Proteomics 13, 2513–2526. https://doi.org/10.1074/mcp.M113.031591.

Cruz-Castañeda, A., López-Casamichana, M., Olivares-Trejo, J.J., 2011. *Entamoeba histolytica* secretes two haem-binding proteins to scavenge haem. Biochem. J. 434, 105–111. https://doi.org/10.1042/BJ20100897.

Cyert, M.S., 2001. Regulation of nuclear localization during signaling. J. Biol. Chem. 276, 20805–20808. https://doi.org/10.1074/jbc.R100012200.

Duggal, S.D., Rongpharpi, S.R., Duggal, A.K., Kumar, A., Biswal, I., 2017. Role of *Acanthamoeba* in granulomatous encephalitis: a review. J. Infect. Dis. Immune Ther. 1, 2.

Flannery, A.R., Huynh, C., Mittra, B., Mortara, R.A., Andrews, N.W., 2011. LFR1 ferric iron reductase of *Leishmania* amazonensis is essential for the generation of infective parasite forms. J. Biol. Chem. 286, 23266–23279. https://doi.org/10.1074/jbc.M111.229674.

Ganz, T., 2009. Iron in innate immunity: starve the invaders. Curr. Opin. Immunol. 21, 63–67. https://doi.org/10.3816/CLM.2009.n.003.Novel.

Garí, E., Piedrafita, L., Aldea, M., Herrero, E., 1997. A set of vectors with a tetracycline-regulatable promoter system for modulated gene expression in *Saccharomyces cerevisiae*. Yeast 13, 837–848. https://doi.org/10.1002/(SICI)1097-0061(199707)13:9<837::AID-YEA145>3.0.CO;2-T.

Gietz, R.D., Schiestl, R.H., 2007. High-efficiency yeast transformation using the LiAc/SS carrier DNA/PEG method. Nat. Protoc. 2, 38–41. https://doi.org/10.1038/nprot.2007.15.

Gulec, S., Collins, J.F., 2014. Molecular mediators governing iron-copper interactions. Annu. Rev. Nutr. 34, 95–116. https://doi.org/10.1146/annurev-nutr-071812-161215.

Harrison, P.M., Arosio, P., 1996. The ferritins: molecular properties, iron storage function and cellular regulation. Biochim. Biophys. Acta 1275, 161–203. https://doi.org/10.1016/0005-2728(96)00022-9.

Hershko, C., 2007. Mechanism of iron toxicity. Food Nutr. Bull. 28, 500–509. https://doi.org/10.1177/156482650702284s403.

Hryniewiecka, L., Jenek, J., Michejda, J.W., 1980. Necessity of iron for the alternative respiratory pathway in *Acanthamoeba castellanii*. Biochem. Biophys. Res. Commun. 93, 141–148. https://doi.org/10.1016/S0006-291X(80)80257-9.

Huang, J.M., Liao, C.C., Kuo, C.C., Chen, L.R., Huang, L.L.H., Shin, J.W., Lin, W.C., 2017. Pathogenic *Acanthamoeba castellanii* secretes the extracellular aminopeptidase m20/m25/m40 family protein to target cells for phagocytosis by disruption. Molecules 22, 2263. https://doi.org/10.3390/molecules22122263.

Kariuki, C.K., Stijlemans, B., Magez, S., 2019. The trypanosomal transferrin receptor of *Trypanosoma brucei* – a review. Trop. Med. Infect. Dis. 4, 126. https://doi.org/10.3390/tropicalmed4040126.

Kim, S.A., Punshon, T., Lanzirotti, A., Li, A., Alonso, J.M., Ecker, J.R., Kaplan, J., Guerinot, M.L., 2006. Localization of iron in *Arabidopsis* seed requires the vacuolar membrane transporter VIT1. Science (80) 314, 1295–1298. https://doi.org/10.1126/science.1132563.

Knight, S.A.B., Vilaire, G., Lesuisse, E., Dancis, A., 2005. Iron acquisition from transferrin by *Candida albicans* depends on the reductive pathway. Infect. Immun. 73, 5482–5492. https://doi.org/10.1128/IAI.73.9.5482-5492.2005.

Krogh, A., Larsson, B., Von Heijne, G., Sonnhammer, E.L.L., 2001. Predicting transmembrane protein topology with a hidden Markov model: application to complete genomes. J. Mol. Biol. 305, 567–580. https://doi.org/10.1006/jmbi.2000.4315.

Li, L., Chen, O.S., Ward, D.M.V., Kaplan, J., 2001. CCC1 is a transporter that mediates vacuolar iron storage in yeast. J. Biol. Chem. 276, 29515–29519. https://doi.org/10.1074/jbc.M103944200.

Livak, K.J., Schmittgen, T.D., 2001. Analysis of relative gene expression data using real-time quantitative PCR and the $2^{-\Delta\Delta CT}$ method. Methods 25 (4), 402–408.

Lorenzo-Morales, J., Khan, N.A., Walochnik, J., 2015. An update on *Acanthamoeba* keratitis: diagnosis, pathogenesis and treatment. Parasite 22, 10. https://doi.org/10.1051/parasite/2015010.

Lorenzo-Morales, J., Martín-Navarro, C.M., López-Arencibia, A., Santana-Morales, M. A., Afonso-Lehmann, R.N., Maciver, S.K., Valladares, B., Martínez-Carretero, E., 2010. Therapeutic potential of a combination of two gene-specific small interfering RNAs against clinical strains of *Acanthamoeba*. Antimicrob. Agents Chemother. 54, 5151–5155. https://doi.org/10.1128/AAC.00329-10.

Lorenzo-Morales, J., Ortega-Rivas, A., Foronda, P., Abreu-Acosta, N., Ballart, D., Martínez, E., Valladares, B., 2005. RNA interference (RNAi) for the silencing of extracellular serine proteases genes in *Acanthamoeba*: molecular analysis and effect on pathogenecity. Mol. Biochem. Parasitol. 144, 10–15. https://doi.org/10.1016/j.molbiopara.2005.07.001.

Mach, J., Bíla, J., Ženíšková, K., Arbon, D., Malych, R., Glavanakovová, M., Nývltová, E., Sutak, R., 2018. Iron economy in *Naegleria gruberi* reflects its metabolic flexibility. Int. J. Parasitol. 48, 719–727. https://doi.org/10.1016/j.ijpara.2018.03.005.

Mach, J., Sutak, R., 2020. Iron in parasitic protists-from uptake to storage and where we can interfere. Metallomics 12, 1335–1347. https://doi.org/10.1039/d0mt00125b.

Marciano-Cabral, F., Cabral, G., 2003. *Acanthamoeba* spp. as agents of disease in humans. Clin. Microbiol. Rev. 16, 273–307. https://doi.org/10.1128/CMR.16.2.273-307.2003.

Martinez, A.J., 1991. Infection of the central nervous system due to *Acanthamoeba*. Rev. Infect. Dis. 13, S399–S402. https://doi.org/10.1093/clind/13.Supplement_5.S399.

Moog, P.R., Brüggemann, W., 1994. Iron reductase systems on the plant plasma membrane – a review. Plant Soil 165, 241–260. https://doi.org/10.1007/BF00008068.

Nevo, Y., Nelson, N., 2006. The NRAMP family of metal-ion transporters. Biochim. Biophys. Acta - Mol. Cell Res. 1763, 609–620. https://doi.org/10.1016/j.bbamcr.2006.05.007.

Ocádiz, R., Orozco, E., Carrillo, E., Quintas, L.I., Ortega-López, J., García-Pérez, R.M., Sánchez, T., Castillo-Juárez, B.A., García-Rivera, G., Rodríguez, M.A., 2005. EhCP112 is an *Entamoeba histolytica* secreted cysteine protease that may be involved in the parasite-virulence. Cell. Microbiol. 7, 221–232. https://doi.org/10.1111/j.1462-5822.2004.00453.x.

Ohgami, R.S., Campagna, D.R., Greer, E.L., Antiochos, B., McDonald, A., Chen, J., Sharp, J.J., Fujiwara, Y., Barker, J.E., Fleming, M.D., 2005. Identification of a ferrireductase required for efficient transferrin-dependent iron uptake in erythroid cells. Nat. Genet. 37, 1264–1269. https://doi.org/10.1038/ng1658.

Ohgami, R.S., Campagna, D.R., McDonald, A., Fleming, M.D., 2006. The Steap proteins are metalloreductases. Blood 108, 1388–1394. https://doi.org/10.1182/blood-2006-02-003681.

Peracino, B., Buracco, S., Bozzaro, S., 2013. The Nramp (Slc11) proteins regulate development, resistance to pathogenic bacteria and iron homeostasis in *Dictyostelium discoideum*. J. Cell Sci. 126, 301–311. https://doi.org/10.1242/jcs.116210.

Peracino, B., Wagner, C., Balest, A., Balbo, A., Pergolizzi, B., Noegel, A.A., Steinert, M., Bozzaro, S., 2006. Function and mechanism of action of *Dictyostelium* Nramp1 (Slc11a1) in bacterial infection. Traffic 7, 22–38. https://doi.org/10.1111/j.1600-0854.2005.00356.x.

Ram, H., Sardar, S., Gandass, N., 2021. Vacuolar iron transporter (like) proteins: regulators of cellular iron accumulation in plants. Physiol. Plant. 171, 823–832. https://doi.org/10.1111/ppl.13363.

Ramírez-Rico, G., Martínez-Castillo, M., De La Garza, M., Shibayama, M., Serrano-Luna, J., 2015. Acanthamoeba castellanii proteases are capable of degrading iron-binding proteins as a possible mechanism of pathogenicity. J. Eukaryot. Microbiol. 62, 614–622. https://doi.org/10.1111/jeu.12215.

Rodríguez-Zaragoza, S., 1994. Ecology of free-living amoebae. Crit. Rev. Microbiol. 20, 225–241. https://doi.org/10.3109/10408419409114556.

Schröder, I., Johnson, E., De Vries, S., 2003. Microbial ferric iron reductases. FEMS Microbiol. Rev. 27, 427–447. https://doi.org/10.1016/S0168-6445(03)00043-3.

Shi, H., Bencze, K.Z., Stemmler, T.L., Philpott, C.C., 2008. A cytosolic iron chaperone that delivers iron to ferritin. Science 80 (320), 1207–1210. https://doi.org/10.1126/science.1157643.

Siddiqui, R., Khan, N.A., 2012. Biology and pathogenesis of Acanthamoeba. Parasites Vectors 5, 1–13. https://doi.org/10.1186/1756-3305-5-6.

Slavic, K., Krishna, S., Lahree, A., Bouyer, G., Hanson, K.K., Vera, I., Pittman, J.K., Staines, H.M., Mota, M.M., 2016. A vacuolar iron-transporter homologue acts as a detoxifier in *Plasmodium*. Nat. Commun. 7, 10403. https://doi.org/10.1038/ncomms10403.

Söding, J., Biegert, A., Lupas, A.N., 2005. The HHpred interactive server for protein homology detection and structure prediction. Nucleic Acids Res. 33, 244–248. https://doi.org/10.1093/nar/gki408.

Sutak, R., Lesuisse, E., Tachezy, J., Richardson, D.R., 2008. Crusade for iron: iron uptake in unicellular eukaryotes and its significance for virulence. Trends Microbiol. 16, 261–268. https://doi.org/10.1016/j.tim.2008.03.005.

Tyanova, S., Temu, T., Sinitcyn, P., Carlson, A., Hein, M.Y., Geiger, T., Mann, M., Cox, J., 2016. The Perseus computational platform for comprehensive analysis of (prote)omics data. Nat. Methods 13, 731–740. https://doi.org/10.1038/nmeth.3901.

Wandersman, C., Delepelaire, P., 2004. Bacterial iron sources: from siderophores to hemophores. Annu. Rev. Microbiol. 58, 611–647. https://doi.org/10.1146/annurev.micro.58.030603.123811.

Whiteside, S.T., Goodbourn, S., 1993. Signal transduction and nuclear targeting: regulation of transcription factor activity by subcellular localisation. J. Cell Sci. 104, 949–955. https://doi.org/10.1242/jcs.104.4.949.

frontiers | Frontiers in Cell and Developmental Biology

ORIGINAL RESEARCH
published: 11 April 2022
doi: 10.3389/fcell.2022.853463

Copper Metabolism in *Naegleria gruberi* and Its Deadly Relative *Naegleria fowleri*

*Kateřina Ženíšková, Maria Grechnikova and Robert Sutak**

Department of Parasitology, Faculty of Science, Charles University, BIOCEV, Vestec, Prague, Czechia

Although copper is an essential nutrient crucial for many biological processes, an excessive concentration can be toxic and lead to cell death. The metabolism of this two-faced metal must be strictly regulated at the cell level. In this study, we investigated copper homeostasis in two related unicellular organisms: nonpathogenic *Naegleria gruberi* and the "brain-eating amoeba" *Naegleria fowleri*. We identified and confirmed the function of their specific copper transporters securing the main pathway of copper acquisition. Adjusting to different environments with varying copper levels during the life cycle of these organisms requires various metabolic adaptations. Using comparative proteomic analyses, measuring oxygen consumption, and enzymatic determination of NADH dehydrogenase, we showed that both amoebas respond to copper deprivation by upregulating the components of the branched electron transport chain: the alternative oxidase and alternative NADH dehydrogenase. Interestingly, analysis of iron acquisition indicated that this system is copper-dependent in *N. gruberi* but not in its pathogenic relative. Importantly, we identified a potential key protein of copper metabolism of *N. gruberi*, the homolog of human DJ-1 protein, which is known to be linked to Parkinson's disease. Altogether, our study reveals the mechanisms underlying copper metabolism in the model amoeba *N. gruberi* and the fatal pathogen *N. fowleri* and highlights the differences between the two amoebas.

Keywords: copper, alternative oxidase, alternative NADH dehydrogenase, *Naegleria gruberi*, *Naegleria fowleri*, DJ-1, CTR copper transporters, electron transport chain

OPEN ACCESS

Edited by:
Kourosh Honarmand Ebrahimi, King's College London, United Kingdom

Reviewed by:
Anastasios D. Tsaousis, University of Kent, United Kingdom
Svetlana Lutsenko, Johns Hopkins Medicine, United States

****Correspondence:***
Robert Sutak
sutak@natur.cuni.cz

Specialty section:
This article was submitted to Cellular Biochemistry, a section of the journal Frontiers in Cell and Developmental Biology

Received: *12 January 2022*
Accepted: *18 March 2022*
Published: *11 April 2022*

Citation:
Ženíšková K, Grechnikova M and Sutak R (2022) Copper Metabolism in Naegleria gruberi and Its Deadly Relative Naegleria fowleri. Front. Cell Dev. Biol. 10:853463. doi: 10.3389/fcell.2022.853463

INTRODUCTION

Transition metals are required in many crucial biological processes of all living organisms. The most abundant redox-active metal in cells is iron, which is followed by other metals such as copper, manganese, cobalt, molybdenum, and nickel (Andreini et al., 2008). Both iron and copper are crucial for the survival of organisms; however, excess concentrations of these metals can be toxic: iron can catalyze the generation of free radicals through the Fenton reaction, causing cellular damage, while copper probably binds to proteins and replaces iron from iron-sulfur cluster-containing proteins, impairing their function and causing iron-induced toxicity (Macomber and Imlay, 2009; Festa and Thiele, 2012; García-Santamarina and Thiele, 2015). On the other hand, copper is a cofactor of at least 30 cuproenzymes with a wide variety of roles, such as electron transport in respiration (cytochrome c oxidase CCOX) or free radical detoxification (superoxide dismutase SOD) (Solomon et al., 2014), and its necessity for biological systems arises from its ability to cycle between two redox states, Cu^{1+} and Cu^{2+}, all of which contribute to

organisms needing to evolve mechanisms to strictly regulate intracellular levels of these potentially harmful metals. Homeostatic mechanisms consist of their uptake, transport, storage, and detoxification pathways. Interestingly, the metabolism of iron and copper are linked, which is best demonstrated by the copper dependence of iron acquisition by the cell, as was shown in yeasts with FET3 multicopper oxidase in the high-affinity iron uptake system (Askwith et al., 1994). The best-described mechanism of copper acquisition involves high-affinity copper transporters named Ctrs. Their function and structure are widely conserved from yeast to humans (Nose et al., 2006; Maryon et al., 2007).

Very little is known about copper transporters in parasitic protists. In *Plasmodium falciparum*, a copper efflux P-ATPase has been identified and partly characterized (Rasoloson et al., 2004), as was a copper-binding protein with sequence features characteristic of copper transporters, including three transmembrane domains: an extracellular copper-binding methionine motif and transmembrane Gx_3G and Mx_3M motifs (Choveaux et al., 2012). Copper transporting ATPases were also identified in trypanosomatid parasites (Isah et al., 2020; Paul et al., 2021). Significantly more research has been performed on copper metabolism in pathogenic yeasts. Ctr homologs responsible for cellular copper uptake were identified in *Candida albicans* (CTR1) (Marvin et al., 2003) and in *Cryptococcus neoformans* (CTR1 and CTR4) (Sun et al., 2014). Importantly, homologs of these proteins are present in the genomes of both amoebas used in our study, *Naegleria gruberi* and *Naegleria fowleri* (Fritz-Laylin et al., 2010; Liechti et al., 2019).

N. gruberi and *N. fowleri* are unicellular organisms living worldwide in freshwater environments (De Jonckheere, 2004; Mull et al., 2013). *N. gruberi* is considered to be the best safe system to study the pathogenic "brain-eating amoeba" *N. fowleri*, which can infect people and cause primary amoebic meningoencephalitis (PAM), a rare but almost always fatal disease (Mungroo et al., 2021). The genomes of these organisms suggest canonical aerobic metabolism, such as the employment of cytochromes and ubiquinone in the respiratory chain, as well as properties of anaerobic metabolism, such as Fe-hydrogenase (Tsaousis et al., 2014), which is typically utilized in metabolic processes of organisms adapted to anaerobic conditions (Fritz-Laylin et al., 2011; Herman et al., 2021). Both amoebas were recently shown to be able to adjust their metabolism to reflect iron availability, downregulating nonessential and predominantly cytosolic iron-dependent pathways and utilizing available iron primarily in mitochondria to maintain essential energy metabolism (Mach et al., 2018; Arbon et al., 2020). In our previous study, we described how *N. fowler*i handles copper toxicity by upregulating a specific copper-exporting ATPase, a key protein of the copper detoxification pathway (Grechnikova et al., 2020). Recent study has found that *Cryptococcus neoformans* is able to sense different Cu environment during infection: high Cu in lungs and low Cu level in brain and is able to adapt its Cu acquisition in these different niches (Sun et al., 2014). Consequently, we focused the current study on the effect of copper deficiency on the metabolism of the brain-eating amoeba as well as its related nonpathogenic model amoeba *N. gruberi*. Herein, we show the role of Ctr homologs identified in both amoebas by functional complementation of mutant yeast lacking high-affinity copper transporters and demonstrate the effect of copper availability on several important components of cell proteomes, iron acquisition, and respiration in both amoebas. We demonstrate that both amoebas can reflect copper-limited conditions by upregulating parts of the respiratory chain to maintain maximal cell respiration. *N. gruberi* adapts to copper-limited conditions by inducing alternative oxidase, similar to the mechanism described in *C. albicans* (Broxton and Culotta, 2016), while *N. fowleri* upregulates alternative NDH-2 dehydrogenase. Moreover, we identified the potential key protein of copper metabolism in *N. gruberi*, the homolog of the DJ-1 protein.

MATERIALS AND METHODS

Identification of *Naegleria* CTRs

Naegleria CTR genes were found by BLAST in the genomes of *N. fowleri* in the AmoebaDB database (Amos et al., 2021) and *N. gruberi* in the JGI PhycoCosm database (Grigoriev et al., 2021) using *Saccharomyces cerevisiae* CTR1 (YPR124 W), CTR2 (YHR175 W), and CTR3 (YHR175 W) gene sequences. Two predicted CTRs of *N. fowleri* (NF0078940, NF0118930) and three predicted CTRs of *N. gruberi* (gene IDs: NAEGRDRAFT_61759, NAEGRDRAFT_61987, and NAEGRDRAFT_62836) were identified.

Functional Complementation Spot Assay of Predicted Ctrs of *N. gruberi* and *N. fowleri*

To synthesize *N. gruberi* and *N. fowleri* cDNA, SuperScript™ III reverse transcriptase (Thermo Fisher Scientific, United States) was used according to the manufacturer's protocol. CTR genes were amplified from cDNA using a Q5 (NEB, United States) and Pfu DNA polymerase mixture (Promega, United States). The resulting products were subcloned into a pUG35 plasmid with a GFP tag (Güldener and Hegemann, http://mips.gsf.de/proj/yeast/info/tools/hegemann/gfp.html) and a pCM189 plasmid (Garí et al., 1997) with a tetracycline-regulatable promotor. The yeast mutant strain ctr1Δ/ctr3Δ (kindly provided by Dennis J. Thiele, Duke University, Durham, North Carolina) was transformed with pCM189 plasmids containing one of the predicted CTRs from *N. fowleri* (NF0078940, NF0118930) or *N. gruberi* (NAEGRDRAFT_61759, NAEGRDRAFT_61987, NAEGRDRAFT_62836). To observe the effect of complementation on phenotype, transformed yeasts were grown overnight in liquid SC-ura medium with 2% glucose (complete synthetic medium without uracil) at 30°C. Cells were diluted to an OD_{600} of 0.2, and 5-µl aliquots of four serial 10-fold dilutions were spotted onto SC-ura plates containing 2% raffinose as a carbon source.

Localization of Ctrs by Fluorescence Microscopy

For protein localization, wild-type (WT) yeast BY4741 cells were transformed with pUG35 containing either the NgCTR or NfCTR gene, and transformants were grown overnight at 30°C in liquid SC-ura medium, washed and resuspended in phosphate-buffered saline (PBS), pipetted onto a microscope slide and mixed with the same volume of 2% agarose. The microscope slide was then covered with a cover slide and sealed. A fluorescent signal was detected using a Leica TCS SP8 WLL SMD confocal microscope (Leica, Germany) with an HC PL APO CS2 63x/1.20 water objective, excited at 488 nm and detected within 498–551 nm by a HyD SMD detector. The PMT detector was used for bright-field imaging. The resulting images were processed by LAS X imaging software (Leica Microsystems, Germany) and ImageJ (Schneider et al., 2012). Yeast transformation was performed according to a previously published protocol (Gietz and Schiestl, 2007).

Amoeba Cultivation

Organisms

a) *N. gruberi* strain NEG-M, which was kindly provided by Lilian Fritz-Laylin (University of Massachusetts Amherst, United States), was grown axenically at 27°C in M7 medium (Fulton, 1974) with the addition of penicillin (100 U/ml) and streptomycin (100 μg/ml) in a 25-cm^2 aerobic cultivation flask.
b) Axenic culture of *N. fowleri* strain HB-1, which was kindly provided by Dr. Hana Peckova (Institute of Parasitology, Biology Center CAS), was maintained at 37°C in 2% Bactocasitone (Difco) medium supplemented with 10% heat-inactivated fetal bovine serum (Thermo Fisher Scientific) with the addition of penicillin (100 U/ml) and streptomycin (100 μg/ml).

Cultivation Conditions

a) For comparative proteomic analysis, oxygen consumption measurements, measurement of the enzyme activity of complex I and NDH-2, and preparation of the samples for SDS–PAGE, copper deprivation was achieved by incubation of cells for 72 h in the presence of 5 μM neocuproine or 25 μM bathocuproinedisulfonic acid disodium salt (BCS), while copper enrichment was achieved by the addition of 25 μM Cu_2SO_4.
b) To examine the effect of copper availability on NgDJ-1 expression by western blot, cells were grown in 25 μM BCS or 1 μM, 25 μM, or 750 μM Cu_2SO_4 for 72 h.
c) The localization of NgDJ-1 was determined by western blotting of crude fractions of *N. gruberi* cultivated without the addition of copper or chelators and by fluorescence microscopy of cells cultivated for 72 h with 100 μM Cu_2SO_4 or 25 μM BCS.
d) To investigate the effect of ROS on NgDJ-1 expression, *N. gruberi* cells were preincubated in 10 μM rotenone or 20 μM PEITEC for 24 h, and cells with no addition of ROS-inducing agents were used as a control.

Crude Fractionation of *N. gruberi* and *N. fowleri* Cells

The grown cells were washed twice in S-M buffer (250 mM Saccharose, 10 mM MOPS, pH 7.2) and disrupted by sonication using SONOPULS ultrasonic homogenizer mini20 (BANDELIN, Germany) with the following settings: amplitude 30%, 1/1 s pulse for 1 min on ice. Disrupted cells were evaluated under a microscope, and sonication was repeated until most of the cells were disrupted. The samples were then centrifuged for 10 min at 1,200 g and 4°C. To obtain the mitochondria-enriched fraction, the supernatant was centrifuged at 14,000 g for 20 min at 4°C. The pellet was used as a mitochondrial-enriched fraction and diluted to the same protein concentration as the supernatant (cytosol-enriched fraction).

The Effect of Different Copper Chelators on the Growth of *N. gruberi* and *N. fowleri*

To investigate the effect of copper deprivation on the growth of *N. gruberi* and *N. fowleri*, the cultures were grown in the presence of copper chelators BCS (concentrations: 25 and 100 μM) and neocuproine (concentrations: 5 and 20 μM). Copper-rich conditions (25 μM Cu_2SO_4) were used as a control. Since BCS binds copper extracellularly and consequently its effect may only be evident after a longer period, we observed the effect of this chelator in long-term growth analysis with a dilution of the cells after 2 days. Each condition was set up in three independent biological replicates with starting culture concentrations of 50 000 cell/ml (*N. gruberi*) and 5,000 cell/ml (*N. fowleri*), and the cell concentration was measured every day by a Cell Counter (Beckman Coulter, United States). The effect of the intracellular copper chelator neocuproine was observed only at one time point: 72 h. Cells were grown in three biological replicates with starting concentrations of 1×10^4 cells/ml (*N. gruberi*) and 4×10^3 cells/ml (*N. fowleri*), and the cell concentration was measured on a Guava easyCyte 8HT flow cytometer (Merck, Germany) after treatment with 2% paraformaldehyde.

ICP–MS Analysis

Cultures of *N. gruberi* and *N. fowleri* were grown in triplicate for each condition, washed three times (1,200 g, 10 min, 4°C) in 10 mM HEPES with 140 mM NaCl buffer, pH 7.2, and pelleted by centrifugation. The pellets were dried at 100°C, digested in 65% HNO_3 in Savillex vials overnight at room temperature, incubated for 2 h at 130°C in Savillex vials (Millipore, United States) and diluted to a final volume of 10 ml in deionized water. The copper concentration was determined by inductively coupled plasma–mass spectrometry (ICP–MS) using iCAP Q ICP–MS (Thermo Fisher Scientific).

LC–MS

N. gruberi and *N. fowleri* cells were grown in biological triplicates for each condition. After incubation, cells were pelleted by centrifugation (1,200 g, 10 min, 4°C) and washed three times with phosphate-buffered saline (PBS). Whole-cell label-free

proteomic analysis followed by the same method as that described in (Mach et al., 2018) was performed by applying nanoflow liquid chromatography (LC) coupled with mass spectrometry (MS). Data were evaluated with MaxQuant software (Cox et al., 2014) using the AmoebaDB *N. fowleri* database downloaded in August 2018 or the *N. gruberi* database (downloaded from UniProt August 2018). Selected proteins (lacking annotation) were manually annotated using HHpred (Zimmermann et al., 2018) or NCBI BLAST (Altschul et al., 1990). The resulting data were further processed by Perseus software (Tyanova et al., 2016). Potential contaminants and reverse hits were filtered out. To evaluate significantly changed proteins at the level of the false discovery rate, Student's t test with Benjamini–Hochberg correction was used. Proteins that were significantly changed and those found in only one condition (in at least two of three replicates) were selected. Proteins identified by only one peptide and proteins with Q-value higher than 0 were excluded from the selection.

RT–qPCR

Naegleria cells were grown in copper-rich and copper-deficient conditions, and control untreated cells were grown for 72 h in quadruplicate. Cells were washed twice with PBS and spun (1,200 g, 4°C, 10 min). Total RNA was isolated using the High Pure RNA Isolation Kit (Roche, Switzerland). The KAPA SYBR® FAST One-Step universal kit (Sigma Aldrich, United States) was used for RT–PCR according to the manufacturer's protocol. RT–PCR was performed on a RotorGene 3000 PCR cycler (Corbett Research, Australia) under the following conditions: 42°C for 30 min (reverse transcription), 95°C for 5 min, and 40 cycles of 95°C for 10 s, 55°C for 20 s, and 72°C for 20 s; for melt-curve analysis, the temperature change was set from 55 to 95°C with a 1°C step and 5 s per step. The abundance of transcripts was calculated after normalization to the endogenous reference gene β-actin.

Obtaining the NgDJ-1 Recombinant Protein for Antibody Preparation

The sequence of NgDJ-1 (XP_002680488.1) was obtained from the UniProt database (in August 2019), and bioinformatic analysis was performed by InterProScan in Geneious Prime® 2019 2.3 (www.geneious.com), including protein domain prediction software such as Phobius (Käll et al., 2004), Pfam (Mistry et al., 2021), PANTHER (Thomas et al., 2003), and SignalP 5.0 (Almagro Armenteros et al., 2019) (see **Supplementary Figure S4**). The NgDJ-1 gene was amplified from cDNA without the transmembrane domain at the N-terminal part of the NgDJ-1 gene (primers: forward 5′-CAC CATATGGTCGAGGCTCAGAATATTGATCAC-3′, reverse 5′-CACGGATCCATTTTGCTTATTCAAGAGCTTGT-3′) and subcloned into the vector pET42b (Merck) containing the C-terminal histidine tag. The protein was expressed in *E. coli* BL21 (DE3) (Merck) induced by 0.5 mM isopropyl β-D-1-thiogalactopyranoside (IPTG, Sigma Aldrich) for 4 h at 37°C. Protein was purified under denaturing conditions according to the manufacturer's protocol using Ni-NTA agarose beads (Qiagen, Germany).

NfNDH-2 and NgDJ-1 Antibody Production

NgDJ-1 and NfNDH-2 polyclonal antibodies were produced by David Biotechnology (Germany) in rabbits. NgDJ-1 antibody was prepared using purified HIS-tagged recombinant protein, while NfNDH-2 was prepared by 3 synthesized immunogenic peptides preselected by David Biotechnology (HDRQVSFAKSIHKPNEKKN, HEDYHYFEGKAIAIDTENQR, DPKSKKILVTDHLKVKGFE). To obtain a more specific signal, the produced antibodies NgDJ-1 and NfNDH-2 were purified by the SulfoLink Immobilization Kit for Proteins (Thermo Fisher Scientific) or the AminoLink Plus Immobilization Kit (Thermo Fisher Scientific), respectively. All purification procedures were performed following the manufacturer's manual.

Sample Preparation for SDS–PAGE, Native PAGE, and Western Blot

Cells were grown under specific conditions for 72 h, washed two times with PBS, pelleted at 1,000 g, 10 min, 4°C, and diluted to equal protein concentration determined by BCA Protein Assay Kit (Sigma Aldrich). Denatured samples (100°C for 5 min) were separated by SDS electrophoresis, blotted onto a nitrocellulose membrane (Amersham Protram 0.2 μm PC, GE Healthcare Life Sciences, United States), and incubated with specific polyclonal antibody at the following concentrations: anti-AOX (Agrisera, Sweden) 1:100, anti-NgDJ-1 1 1:50, and anti-NfNDH-2 1:1,000. HRP-conjugated goat anti-rabbit or anti-mouse antibodies (BioRad, United States) were used as secondary antibodies. Antibodies were detected using Immobilon Forte Western HRP substrate (Merck) on an Amersham Imager 600 (GE Health care Life Sciences, United States).

Crude fractions of *N. gruberi* (Chapter 2.5) used for localization of NgDJ-1 by western blot were prepared the same as SDS samples described above, but crude fractions of *N. fowleri* (Chapter 2.5) used for localization of NfNDH-2 were treated with 1% digitonin (Sigma Aldrich), incubated for 5 min on ice and resuspended in ×5 native sample buffer. The samples were then loaded on a native gel (containing 0.1% Triton TX-100, Sigma Aldrich) and separated by PAGE under native conditions.

Immunofluorescence Microscopy

N. gruberi cells were stained with 100 nM MitoTracker Red CMXRos (Thermo Fisher Scientific) for 30 min in M7 medium in the dark at 27°C. After incubation, the medium was exchanged, and the cells were fixed with 1% formaldehyde for another 30 min. The treated cells were then carefully centrifuged (800 g, 5 min, 24°C), resuspended in PEM (100 mM piperazine-N,N′-bis(2-ethane sulfonic acid), 1 mM ethylene glycol-bis(β-aminoethyl ether)-N,N,N′,N′-tetraacetic acid, and 0.2 mM $MgSO_4$) and transferred onto cover slides. The cell slides were then incubated for 1 h in PEMBALG blocking solution (1% BSA, 0.1% NaN_3, 100 mM L-lysin, 0.5% cold water fish skin gelatin in PEM). The NgDJ-1 protein was visualized by an anti-rat antibody coupled to Alexa Fluor 488 (Thermo Fisher Scientific) (dilution 1:1,000) bound to a custom-made rat polyclonal antibody (dilution 1:100). Slides with stained cells were mounted by Vectashield with DAPI (Vector Laboratories,

United States). The signal was detected by a TCS SP8 WLL SMD confocal microscope (Leica) equipped with an HC PL APO CS2 63x/1.20 oil objective, excited by 509 nm and detected within 526–655 nm by a HyD SMD detector. The PMT detector was used for bright-field imaging and processed as described in Chapter 2.3.

N. fowleri microscopy slides for visualization of NfNDH-2 were prepared as described above except that *N. fowleri* cells were immobilized on slides covered with poly-L-lysine and all the staining, including 10 nM MitoTracker Red CMXRos and primary and secondary antibodies, were completed on slides rather than in a cultivation flask.

Measurements of Oxygen Consumption

N. fowleri and *N. gruberi* cells were grown for 72 h in biological triplicates or tetraplicates, respectively, under copper-depleted and copper-rich conditions, pelleted (1,200 g, 10 min, 4°C), washed twice, and resuspended to the same cell concentration in glucose buffer (50 mM glucose, 0.5 mM $MgCl_2$, 0.3 mM $CaCl_2$, 5.1 μM KH_2PO_4, 3 μM Na_2HPO_4, pH 7.4). The cell concentration was measured on a Guava easyCyte 8HT flow cytometer (Merck). Cell respiration in each sample was measured by detecting oxygen decreases using the Clark-type electrode system Oxygen meter Model 782 (Strathkelvin) in a Mitocell Mt 200 cuvette in a total volume of 700 μl. The whole system was calibrated for 27°C for *N. gruberi* and 37°C for *N. fowleri*. Specific inhibitors of alternative oxidase, salicyl hydroxamic acid (SHAM) at concentrations of 0.5 mM (*N. gruberi*) or 0.2 mM (*N. fowleri*), and an inhibitor of complex IV, KCN, at concentrations of 2.4 mM (*N. gruberi*) or 2.05 mM (*N. fowleri*) were used. The protein concentration of the sample was determined using a BCA kit (Sigma Aldrich).

Complex I and NDH-2 Enzyme Activity of *Naegleria fowleri*

Total NADH dehydrogenase activity was measured by the following protocol. Three biological replicates of *N. fowleri* were cultivated for 72 h in copper-rich or copper-deficient conditions. The cells were spun down, washed with S-M buffer (250 mM saccharose, 10 mM MOPS, pH 7.2), and diluted to the same cell concentration. Next, the cells were treated with 1% digitonin (Sigma Aldrich) for 5 min on ice and added to a reaction mixture containing 100 μM KPi buffer at pH 7.5 and 300 μM NADH. The reaction was started by the addition of 50 μM nonnatural coenzyme Q2 (in 99.9% ethanol, Sigma Aldrich), an analog of Q10. The activity was measured for 5 min at 340 nM wavelength on a Shimadzu UV-2600 UV–VIS spectrophotometer (Shimadzu, Japan) with UV Probe software (Shimadzu).

The activity of alternative NADH dehydrogenase (NDH-2) was estimated as the remaining activity measured in digitonine-treated culture preincubated for 5 min with the inhibitor of Complex I, 75 μM rotenone. The activity of complex I was calculated as the remaining activity after NDH-2 activity subtraction from overall NADH dehydrogenase activity. The protein concentration was determined by a BCA kit (Sigma Aldrich).

Iron Uptake

N. fowleri and *N. gruberi* cells were grown in copper-rich and copper-deficient conditions for 72 h, pelleted (1,200 g, 10 min, 4°C), washed twice, resuspended in glucose-HEPES medium (50 mM glucose, 20 mM HEPES, pH 7.2) and diluted to the same cell concentration of 1×10^6 cells per sample. The cell concentration was estimated by a Guava easyCyte 8HT flow cytometer (Merck). Samples were incubated for 1 h with 1 μM ^{55}Fe-citrate or with 1 μM ^{55}Fe-citrate with the addition of 1 m mM ascorbate to reduce iron to the ferrous form. Uptake was stopped by the addition of 1 mM EDTA, and the cells were then washed three times with glucose-HEPES buffer, diluted to the same protein concentration [using a BCA kit (Sigma Aldrich)] and separated using the Novex Native PAGE Bis-Tris Gel system (4–16%, Invitrogen, United States). The gel was dried for 2 h in a vacuum and autoradiographed by Typhoon FLA 7000 (GE Life Sciences, United States) using a tritium storage phosphor screen (GE Life Sciences).

RESULTS

Identification of Copper Uptake Proteins (Ctrs) of *N. gruberi* and *N. fowleri*

In the genomes of both amoebas, we identified several homologs of copper transporters based on a BLAST search using *S. cerevisiae* CTR1, CTR2, and CTR3. To confirm the copper uptake function of these candidate transporters, we performed a functional complementation assay using copper transporter 1 and copper transporter 3 double knockout yeast strain (ctr1Δ/ctr3Δ). One of the selected Ctrs from each amoeba (NgCTR1, NAEGRDRAFT_61759, and NfCTR1, NF0078940) restored copper transporter function in the yeast mutant and showed typical localization to the yeast plasma membrane (**Figure 1A** and **Figure 1B**). The localization of the other homologs is shown in **Supplementary Figure S1**. To determine whether *N. fowleri* and *N. gruberi* regulate the copper acquisition pathway depending on the availability of the metal at the transcriptional level, as shown in *S. cerevisiae* (Winge et al., 1998), we analyzed the abundance of CTR transcripts by RT–PCR in cells grown under low copper and copper-rich conditions. Our data showed no significant copper-induced changes in the RNA levels of the selected CTR genes (NF0078940, NF0118930, NAEGRDRAFT_61759, NAEGRDRAFT_61987, NAEGRDRAFT_62836) (**Supplementary Figure S2**). This result is not unexpected considering our previous study, where we found that iron starvation-induced changes in *N. fowleri* were mostly posttranslational (Arbon et al., 2020).

Comparative Proteomic Analysis Revealed That ETC Components and NgDJ-1 Are the Most Affected by Copper Deprivation

Since *Naegleria* is not prone to genetic manipulations, we chose whole-cell label-free comparative proteomics to gain complex insight into the metabolic adaptation to copper limitations. To

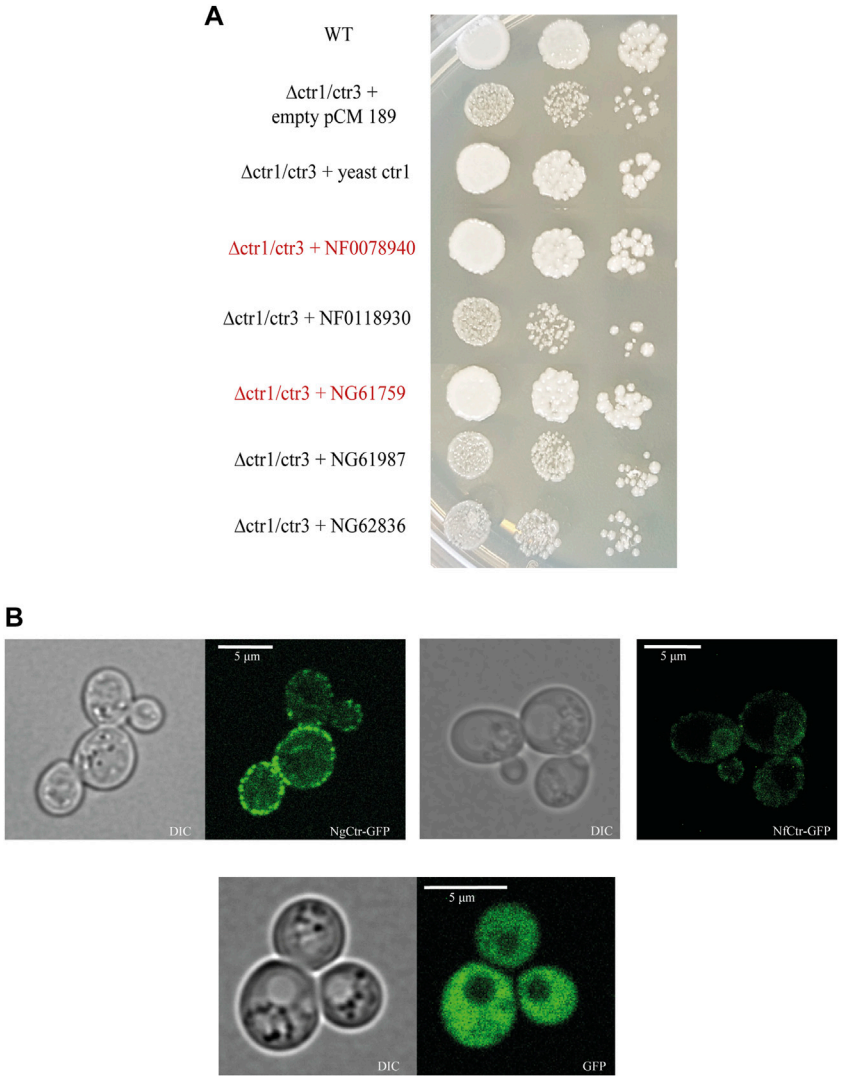

FIGURE 1 | Identification of copper uptake proteins (Ctrs) of *Naegleria gruberi* and *Naegleria fowleri*. **(A)** Functional complementation spot assay of NgCTRs and NfCTRs in Δctr1/ctr3 mutant yeast cells lacking genes for high-affinity copper transporters. Wild-type BY4741 cells transformed with the empty tetracycline-regulated expression vector pCM189 and Δctr1/ctr3 mutant cells transformed with the same plasmid carrying yeast CTR1, NfCTRs (NF0078940, NF0118930) or NgCTRs (NG61759, NG61987, NG62836) were spotted onto synthetic complete medium without uracil with 2% raffinose as the carbon source and grown for 72 h at 30°C. Mutant yeast cells with plasmids containing CTR genes from *N. fowleri* (NF0078940) and *N. gruberi* (NG61759), which functionally complement the missing yeast copper transporters CTR1 and CTR3, are marked in red. **(B)** Localization of NfCtr (NF0078940) and NgCtr (NG61759) by fluorescence microscopy. Wild-type yeast BY4147 expressing copper transporters linked with GFP from *N. gruberi* NgCTR1-GFP (NG61759 + pUG35), *N. fowleri* NfCTR1-GFP (NF0078940 + pUG35), and GFP (empty pUG35 vector).

elucidate the effect of copper deprivation on the viability of *N. gruberi* and *N. fowleri* cells, we cultivated both amoebas for 72 h in the presence of the copper chelators bathocuproinedisulphonic acid (BCS) and neocuproine (Neo). Both chelators are selective for Cu^{+}, and in contrast to the extracellular copper chelator BCS, neocuproine can chelate copper intracellularly.

To determine the amount of copper within the cells grown in the presence of BCS, we analyzed those samples using ICP–MS. **Figure 2A** shows that this extracellular copper chelator causes a significant decrease in copper accumulation compared to control (cells cultivated in presence of 25 μM Cu_2SO_4) after 72 h, while the effect is not further increased using a 10-fold higher concentration. The effect of BCS on copper accumulation was more pronounced in *N. fowleri*, which has a higher overall intracellular amount of copper under control conditions; however, the growth of *N. fowleri*, unlike *N. gruberi*, was not affected by this chelator (**Supplementary Figure S3**). This indicates that *N. fowleri* possesses more efficient copper homeostasis mechanisms than its nonpathogenic relative, and the use of an intracellular chelator is required to observe the physiological response to copper starvation. Based on these results, we decided to perform two proteomic analyses using

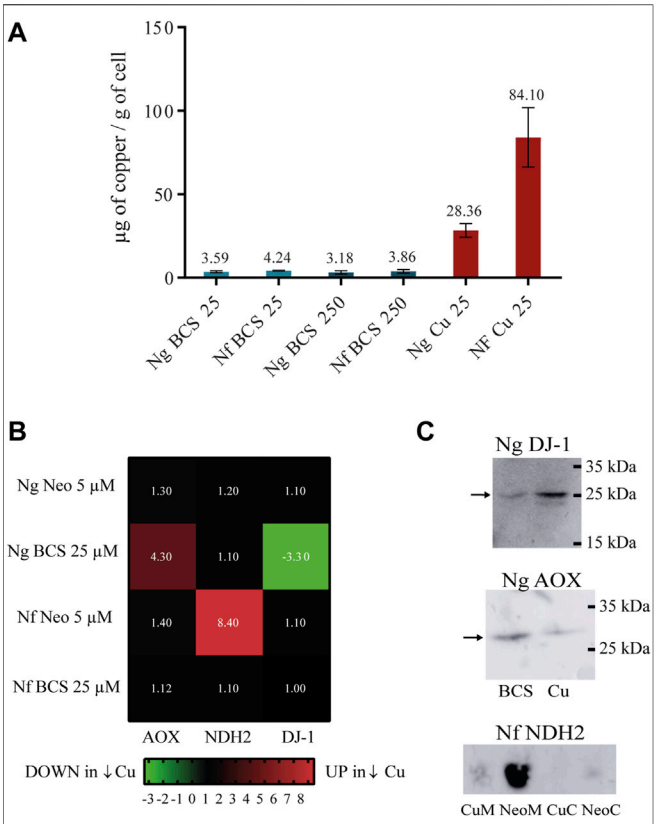

FIGURE 2 | Effect of copper availability on *Naegleria gruberi* and *Naegleria fowleri*. **(A)** Copper contents in *N. gruberi* and *N. fowleri* supplemented with 25 µM Cu_2SO_4, 25 µM BCS, or 250 µM BCS for 72 h. The values represent the mean of copper content of three individual replicates. **(B)** The fold changes of the most relevant proteins in this article are demonstrated on the heatmap; upregulation under copper-limited conditions is indicated by red color and downregulation by green color. The heatmap demonstrates that the chelators have different effects on both amoebas. **(C)** western blot analysis confirming the proteomic results using the specific antibodies antiNgDJ-1, antiNfNDH2, and antiAOX on cell lysates of *N. gruberi* incubated with 25 µM BCS (BCS) or 25 µM Cu_2SO_4 (Cu) and separated by SDS–PAGE and on cytosolic (C) and mitochondrial (M) fractions of *N. fowleri* cells incubated with 25 µM Cu_2SO_4 (Cu) or 5 µM neocuproine (Neo) separated by clear native PAGE.

the cells grown with the addition of 25 µM BCS and the cells grown in 5 µM neocuproine to achieve copper deprivation for both amoebas. To ensure sufficient copper status, the cells cultivated in presence of 25 µM Cu_2SO_4 were used as a control sample for both proteomic analyses. This concentration was used based on our previous work where we elucidated the IC50 of copper being 1 mM for *N. gruberi* and as high as 1.6 mM for *N. fowleri* (Grechnikova et al., 2020).

The list of all proteins that were significantly changed under copper deprivation is presented in **Supplementary Table S1**. In the analysis of the resulting proteomic data, we focused on proteins that are likely to bind copper or are related to copper metabolism, potentially compensating for the lack of copper or being involved in the oxidative stress response or energy metabolism. The selected proteins meeting these criteria are listed in **Table 1**. A heatmap presenting the most relevant proteins identified in this study demonstrates that selected chelators cause different effects on amoebas (**Figure 2B**).

The mitochondrial electron transport chain of *Naegleria gruberi* and *Naegleria fowleri* consists of complexes I, II, and III, two terminal oxidases: alternative oxidase (AOX) and cytochrome c oxidase (complex IV), and an alternative NADH ubiquinone oxidoreductase. Our proteomic analysis revealed that both amoebas responded to copper starvation by upregulating alternative enzymes involved in the electron transport chain. AOX (XP_002681229.1) from *N. gruberi* showed a 4.3-fold upregulation under copper-limited conditions. In contrast to *N. gruberi, N. fowleri* reacted to copper starvation through 8.4-fold upregulation of the protein NF0090420 (partial sequence) identified as nonproton pumping alternative NADH dehydrogenase (NDH-2). The complete sequence of this protein was obtained from genome of *N. fowleri* strain ATCC 30894 (AmoebaDB - FDP41_010952) (**Supplementary Figure S4**).

Additionally, the proteins involved in reactive oxygen species (ROS) detoxification pathways were significantly downregulated in copper-limited *N. gruberi* (thioredoxin reductase and two homologs of glutathione-S-transferase). Furthermore, in both amoebas, we observed significant upregulation in the expression of hemerythrin under copper limitation, a protein that probably plays a role in the defense against oxidative stress in bacteria (Li X. et al., 2015; Ma et al., 2018). Together, these results indicate that copper deprivation in naeglerias may lead to the generation of ROS.

Interestingly, one of the most downregulated proteins (fold change 3.3) of *N. gruberi* in copper-limited conditions was protein XP_002680488.1, which is a homolog of DJ-1 family proteins (**Supplementary Figure S4**). These proteins are thought to perform many functions (Bandyopadhyay and Cookson, 2004; Wei et al., 2007). Some studies on the human homolog of DJ-1 claim its ability to bind copper and serve as a copper chaperone for Cu, Zn superoxide dismutase (Girotto et al., 2014).

The copper-induced changes in protein abundance were also confirmed using western blot analysis with specific antibodies (**Figure 2C**). The localization of NfNDH-2 by fluorescence microscopy to demonstrate the antibody specificity is shown in **Supplementary Figure S5**.

RT qPCR Analysis Revealed That Changes Caused by Copper Deprivation Are Posttranslational

Selected genes encoding copper-regulated proteins (NfNDH-2, NfHemerythrin) were also analyzed by RT qPCR using copper-starved and control cells. Transcript abundance was normalized to the endogenous reference gene β-actin. Analogous to CTRs, no changes in the transcriptional level of these selected genes were observed, suggesting that the proteomic response of both amoebas to copper starvation occurs at the posttranslational level (**Supplementary Figure S2**).

TABLE 1 | Selected *N. gruberi* and *N. fowleri* proteins whose abundance was significantly changed under copper-limited conditions in at least one condition and in one amoeba. Arrows indicate significant upregulation or downregulation, and no arrow sign in proteins with a fold change lower than 1.5 indicates no significant change.

Naegleria gruberi			
Fold Change in BCS	**Fold Change in Neo**	**Accession Number in Database**	**Database Annotation/Manual Annotation**
↑4.3	1.3	XP_002681229.1	AOX
1.1	1.2	XP_002672148.1	NDH-2
↓3.3	1.1	XP_002680488.1	DJ-1
↑2.0	Not Found	XP_002680302.1	Hemerythrin
1.4	↓1.9	XP_002674924.1	Thioredoxin reductase
↓2.2	1.2	XP_002670102.1	Glutathione-S-transferase
↓1.6	1.3	XP_002670607.1	Glutathione-S-transferase III
Naegleria fowleri			
Fold change in BCS	**Fold change in Neo**	**Accession Number in Database**	**Database Annotation/Manual Annotation**
1.1	1.4	NF0004720	AOX
1.1	↑8.4	NF0090420	NDH-2
1	1.1	NF0125230	DJ-1
1.4	↑3.5	NF0127030	Hemerythrin
1.0	1.2	NF0014440	Thioredoxin reductase
1.1	1.3	NF0101120	Glutathione-S-transferase
1.1	Not Found	NF0101840	Glutathione-S-transferase
1.1	1.1	NF0039660	Glutathione-S-transferase

The Activity of NgAOX and NfNADH-2 Reflects Copper Availability

Our proteomic analysis indicated rearrangement of the mitochondrial electron transport chain in both amoebas under copper starvation. To determine the physiological effect of copper availability on respiration, we performed an oxygen consumption assay with amoebas grown in copper-limited conditions. Both organisms possess two terminal oxidases, cytochrome c oxidase (CCOX) and alternative oxidase (AOX), which couple the electron flow from ubiquinol with the reduction of O_2 to H_2O (Cantoni et al., 2020). In contrast with CCOX, AOX does not participate in ATP generation. The activity of NgAOX corresponded to the proteomic results: in copper-limited *N. gruberi,* the activity of AOX was almost twice as high as that in control cells (**Figure 3A**). In *N. fowleri*, copper starvation did not result in the upregulation of alternative oxidase at the protein level, but its activity in neocuproine-treated cells was significantly increased (**Figure 3A**). Interestingly, our results also demonstrate that *N. gruberi* respiration is predominantly mediated by alternative oxidases, whereas *N. fowleri* respires mainly through complex IV (**Figure 3A**).

In addition to the classical rotenone-sensitive NADH dehydrogenase, the electron transport chain of both amoebas additionally contains an alternative rotenone-insensitive NADH dehydrogenase (NDH-2). These enzymes share the same functions, but NDH-2 does not contribute to the generation of the transmembrane proton gradient. The comparative proteomic analysis indicated that *N. fowleri* adapts to copper-deprived conditions by upregulation of NDH-2. The resistance of NDH-2 to rotenone was used to distinguish this enzyme from classical rotenone-sensitive NADH dehydrogenase. When NADH dehydrogenase activity of lysates of control and copper-limited cells were compared, the rotenone-sensitive complex I activity was not affected by copper, while the rotenone-resistant activity was higher in the neocuproine-treated cells than in the control sample. Although we cannot exclude that other enzymes contribute to this activity, considering the proteomic data, we believe that the main enzyme responsible for the measured activity is NfNDH-2 (**Figure 3B**).

Expression of the Mitochondrially Localized Protein NgDJ-1 is Copper-dependent and is Not Induced by ROS Accumulation

One of the most downregulated proteins in copper-deprived *N. gruberi* cells (3.3-fold change downregulation in BCS) is protein XP_002680488.1 (named NgDJ-1 in this article), which shows homology to proteins belonging to the DJ-1/ThiJ/PfpI superfamily (**Supplementary Figure S4**). This superfamily contains functionally and structurally diverse proteins, many of which remain only poorly characterized at the biochemical level (Bandyopadhyay and Cookson, 2004). To confirm the connection between copper availability and NgDJ-1 expression, we performed a western blot analysis of whole-cell lysates of *N. gruberi* grown in copper-deprived conditions as well as in media supplemented with copper at different concentrations (1 μM, 25 μM, and 750 μM). The results demonstrate that the copper-induced expression of DJ-1 observed in our proteomic analysis is even more pronounced when cells are exposed to copper at levels that probably lead to toxicity, indicating a role of this protein in copper metabolism (**Figure 4A**).

The human homolog of DJ-1 has many predicted functions but is mainly annotated as a redox sensor and ROS scavenger (Zhang et al., 2020). Considering this, we analyzed the lysates of

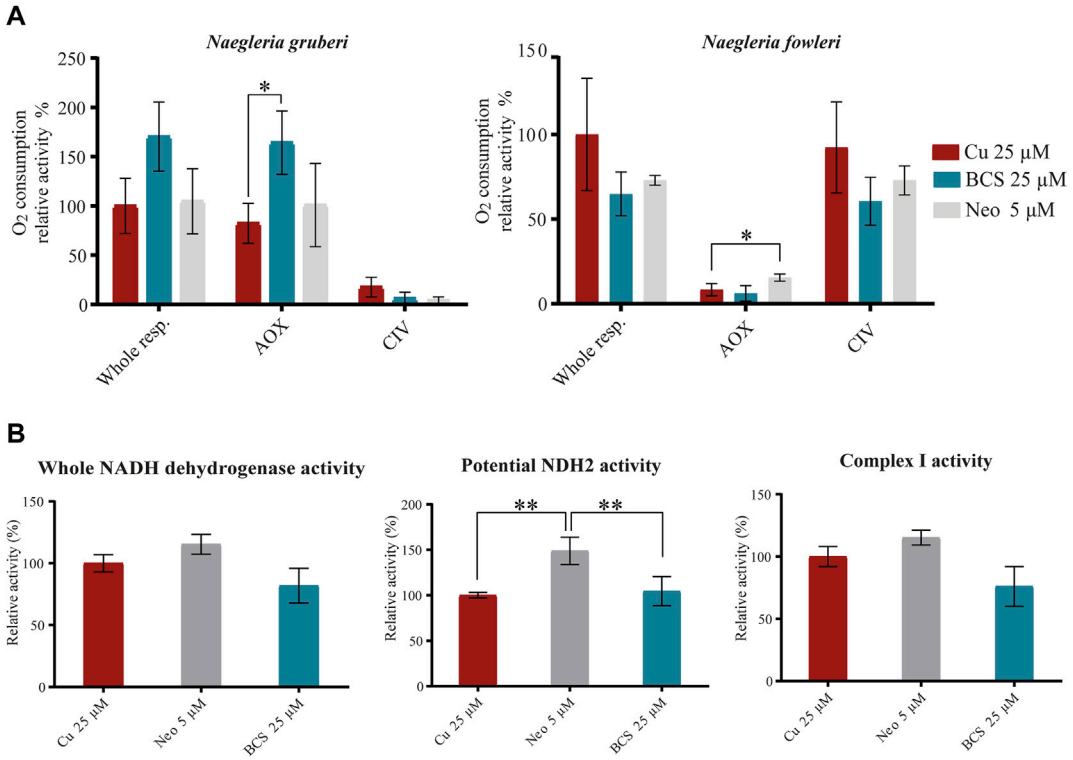

FIGURE 3 | The activity of NgAOX and NfNDH2 reflects the proteomic analysis results. **(A)** Oxygen consumption of NgAOX is increased due to copper deprivation. Oxygen consumption was measured in *N. gruberi* and *N. fowleri* cells incubated for 72 h with 25 M BCS or 5 µM neocuproine, and control cells were supplemented with 25 µM Cu_2SO_4. Specific inhibitors of alternative oxidase (SHAM) and complex IV (KCN) were used to distinguish the activities of these enzymes. For easier interpretation, oxygen consumption activity was calculated as the relative activity, where the whole respiration of control samples (Cu 25 µM) corresponds to 100%. The graphs show the mean of three biological replicates with the standard deviation. To evaluate the statistical confidence, Student's t test was used (* indicates a *p* value ≤0.05). **(B)** The enzyme activity of NfNDH2 is increased under low copper conditions. Spectrophotometric measurement of NADH dehydrogenase activity was measured using nonnatural Q2, the analog of Q10, at 340 nm on *N. fowleri* cells incubated in low or normal copper conditions. The potential NDH2 activity was measured after preincubation of the cells with rotenone. The activity of complex I was calculated by subtracting the potential NDH2 activity from overall NADH dehydrogenase activity. For easier interpretation, the activities are shown as the relative activity (%), and the activities of control cells (Cu 25 µM) correspond to 100%. To evaluate the statistical confidence, Student's t test was used (**indicates a *p* value ≤0.01).

N. gruberi cells exposed for 24 h to two ROS-inducing agents, rotenone and PEITC, by western blot using an NgDJ-1 antibody. Unexpectedly, we observed that treatment with both agents resulted in a decrease in NgDJ-1 expression (**Figure 4B**).

To determine NgDJ-1 cellular localization, we used two different methods: fluorescence microscopy and western blot analysis of crude cell fractions. Both methods revealed mitochondrial localization of NgDJ-1, which is rather unusual for this protein (**Figure 4C**). Predictably, observed molecular weight of DJ-1 on western blots is lower than anticipated (~26 kDa instead of 30 kDa), probably due to cleavage of mitochondrial targeting sequence. More pictures are shown in (**Supplementary Figure S6**).

N. gruberi Iron Uptake is Copper-Regulated

Iron uptake mechanisms in various organisms are frequently interconnected with copper. To determine this connection in both amoebas, we employed blue native electrophoresis analysis allowing visualization of the incorporation of iron radionuclide into cellular protein complexes. In our previous work, we showed that *N. fowleri* prefers to take up the reduced form of iron (Fe^{II}) and that iron acquisition is not induced by iron starvation (Arbon et al., 2020). Here, we show that similarly, the nonpathogenic relative *N. gruberi* preferably acquired a reduced form of iron, indicating a reductive uptake mechanism. Importantly, our results demonstrate that iron uptake is significantly affected by copper availability (**Figure 5A**), suggesting the requirement of copper in some of the iron acquisition system components (e.g., multicopper oxidase). In contrast, iron uptake efficiency in *N. fowleri* remained unaffected by copper deprivation (**Figure 5B**).

DISCUSSION

Copper and host:pathogen Interface

An important host defense process called nutritional immunity occurs at the host-pathogen interface: the host restricts access to essential metals for the pathogen (Hood and Skaar, 2012). Iron sequestration during bacterial infection is well described, and bacterial pathogens have developed a variety of strategies to

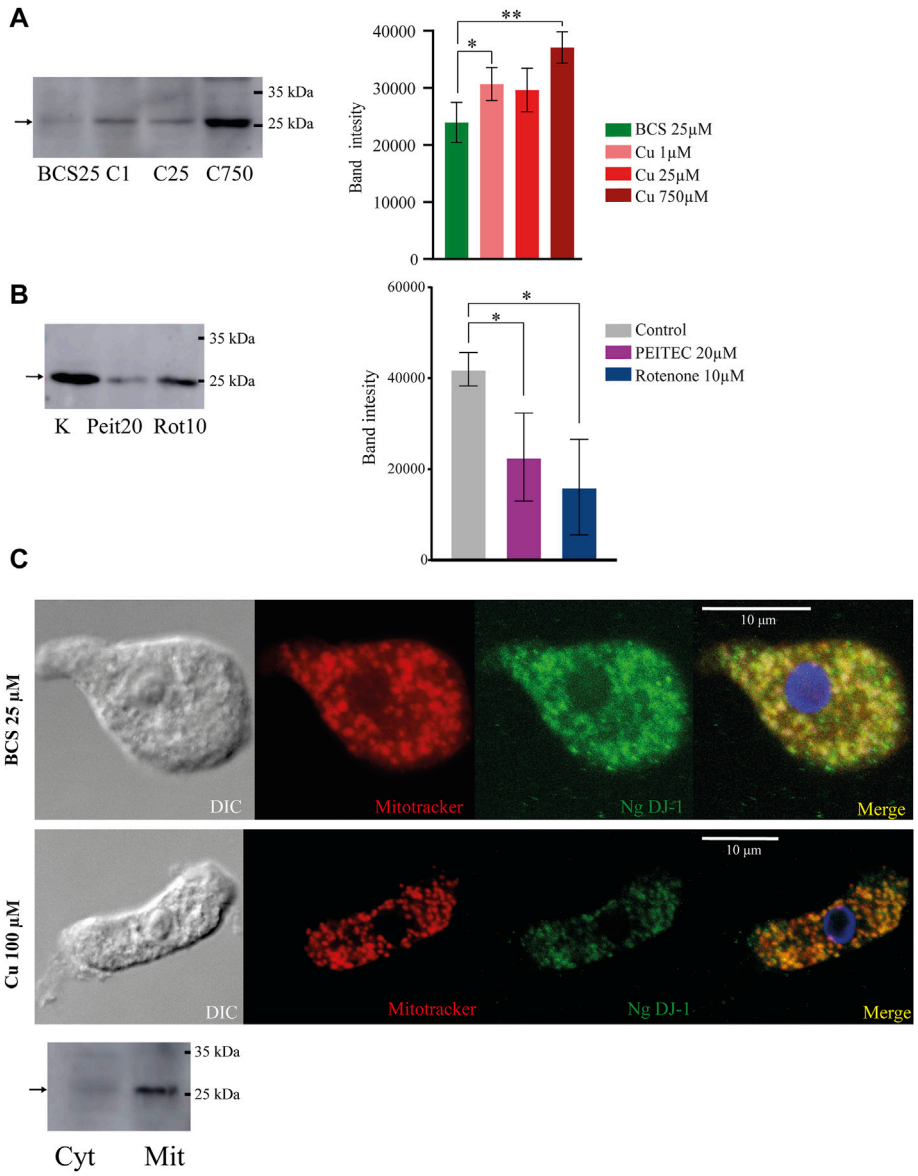

FIGURE 4 | The expression of mitochondrially localized NgDJ-1 is copper-dependent and is not induced by ROS accumulation. **(A)** NgDJ-1 protein expression is copper-dependent. Western blot analysis of whole-cell lysates of cells incubated for 72 h in low or high copper conditions (BCS 25 μM and Cu_2SO_4 1/25/750 μM) using an anti-NgDJ-1 antibody. To compare signal strength in each condition, densitometry of four independent replicates was performed using ImageJ. Changes in signals are demonstrated on the graph showing the mean of the signal with standard deviation error bars (*indicates a *p* value ≤0.05; **indicates a *p* value ≤0.01. **(B)** ROS accumulation does not induce NgDJ-1 expression. Western blot analysis of DJ-1 expression in cells preincubated with the ROS-inducing agents 20 μM PEITC and 10 μM rotenone for 24 h. The control sample (K) was *N. gruberi* without any additions. The graph demonstrates the difference in signal strength in each condition. **(C)** Localization of NgDJ-1 is mitochondrial regardless of copper availability. NgDJ-1 was visualized by immunofluorescence microscopy using a polyclonal antibody (anti-NgDJ-1) on *N. gruberi* cells precultivated with 25 μM BCS and 100 μM Cu_2SO_4 for 72 h. MitoTracker CMXRos (Thermo Fisher) was used for visualization of mitochondria. DIC–differential interference contrast. Mitochondrial localization of NgDJ-1 was also demonstrated by immunoblot detection of cytosolic (Cyt) and mitochondria-enriched (Mit) fractions of *N. gruberi*.

circumvent host-mediated iron limitation (Weinberg, 1975; Posey and Gherardini, 2000; Cassat and Skaar, 2013). In contrast to iron, copper is usually utilized in the opposite manner by host immune cells, which use the toxic properties of this metal to kill pathogens (Festa and Thiele, 2012; Hodgkinson and Petris, 2012; Stafford et al., 2013; Chaturvedi and Henderson, 2014). However, in fungal infections caused by *C. neoformans* and *C. albicans*, the pathogens experience limited copper availability in the host in specific situations. Although host immunity employs the toxic properties of copper in the lungs, which are the main locations of *C. neoformans* infection (Ding et al., 2013), *C. neoformans* tends to disseminate to the brain in immunodeficient hosts, where copper may be restricted. *C. neoformans* adapts to these copper-limited conditions by

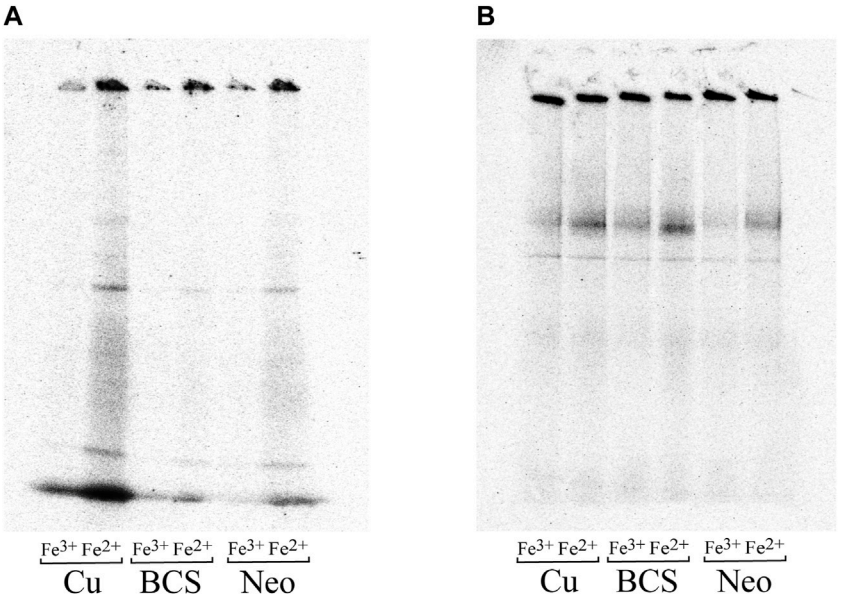

FIGURE 5 | Iron uptake is regulated by copper in *N. gruberi* but not in *N. fowleri*. Ferrous and ferric iron uptake by *N. gruberi* **(A)** and *N. fowleri* **(B)** under copper-rich and copper-deficient conditions. Autoradiography of blue native electrophoresis gels of whole-cell lysates of *N. gruberi* and *N. fowleri* cells incubated with 25 μM BCS (BCS), 5 μM neocuproine (Neo), and 25 μM Cu_2SO_4 (Cu) for 72 h and further incubated with ^{55}Fe(II) (ferrous ascorbate) or ^{55}Fe(III) (ferric citrate) for 1 h.

inducing specific copper uptake transporters (Waterman et al., 2007; Sun et al., 2014). *C. albicans* occupies diverse niches inside the host, but it may disseminate through the bloodstream, and the major location of infection in the murine model is the kidney. In the early stage of kidney infection, copper levels increase briefly, but as the infection progresses, the level of copper drops. *C. albicans* responds to decreasing copper conditions by switching from copper-dependent Cu/Zn SOD to Mn SOD3 and, interestingly, by upregulating alternative oxidase (AOX) to minimize mitochondrial damage and simultaneously maximize COX respiration (Li CX. et al., 2015; Besold et al., 2016; Broxton and Culotta, 2016).

In a recent study, we described how *N. fowleri* handles the toxic properties of copper and identified the key protein of the copper detoxification pathway, a copper-translocating ATPase (Grechnikova et al., 2020). In the present study, we focused on other aspects of copper metabolism and aimed to elucidate the metabolic adaptations of the free-living unicellular organism *N. gruberi* and its pathogenic relative *N. fowleri* to low copper availability.

Copper Acquisition

Our study began with a search for proteins involved in copper acquisition by both amoebas. In eukaryotic cells, the import of copper to the cytoplasm is widely mediated by high-affinity copper transporter (Ctr) localized to the plasma membrane. Ctr is an integral membrane protein conserved from yeast to humans with high specificity for Cu(I) (Zhou and Gitschier, 1997; Kozlowski et al., 2009). In *Saccharomyces cerevisiae*, copper is transported into cells by two high-affinity transporters, CTR1 (Dancis et al., 1994b) and CTR3 (Knight et al., 1996), and a low-affinity copper transporter, CTR2, is responsible for the mobilization of vacuolar copper ions (Rees et al., 2004; Liu et al., 2012). All CTRs of *S. cerevisiae* are regulated by intracellular copper status (Jungmann et al., 1993; Winge et al., 1998). We identified genes encoding potential Ctrs in the genomes of both amoebas, including three genes in *N. gruberi*, and two in *N. fowleri*. Since effective genetic manipulation of these organisms has not been established, we decided to verify copper transport function by expression in yeasts and by functional complementation assay using the ctr1Δ/ctr3Δ mutant yeast strain. One of the proposed CTRs from each amoeba was able to restore copper import function and showed typical localization to the plasma membrane. In contrast to *S. cerevisiae*, neither CTR appears to be regulated by copper starvation at the transcriptional level in *Naegleria*, indicating that the amoebas do not respond to copper starvation at the copper acquisition level or that the regulation is posttranslational.

Branched Mitochondrial ETC

Our proteomic approach to understanding the metabolic adaptations to copper limitation yielded particularly interesting findings: some of the proteins comprising the electron-transporting chain (ETC), the key part of the energy metabolism of a cell, are among the most affected by low copper availability in both amoebas. The ETC of both Naeglerias is branched and, in addition to the classical arrangement of complexes (CI-IV), possesses two nonenergy-conserving components: cyanide insensitive alternative oxidase (AOX) and alternative NADH dehydrogenase (NDH-2), both of which are significantly upregulated in copper-deprived conditions. Branched mitochondrial ETC is also known from plants, fungi, and other

protists, some of which are human pathogens (e.g., *C. albicans*, *C. neoformans*, *Acanthamoeba castellanii*). AOX bypasses complex III and complex IV, but its activity is not coupled to proton translocation; hence, it does not contribute to ATP synthesis. Studies focusing on plants show that two respiration pathways with different energy yields provide the ability to maintain the redox, carbon, and/or energy balance in response to changing demands (Sluse and Jarmuszkiewicz, 1998; Ribas-Carbo et al., 2005; Sieger et al., 2005; Smith et al., 2009; Cvetkovska and Vanlerberghe, 2012; Dahal and Vanlerberghe, 2017). In addition to this function, AOX also decreases the rate of mitochondrial ROS formation (Maxwell et al., 1999; Vishwakarma et al., 2015). In fungi, low copper availability was shown to be connected to impaired respiration (cytochrome c oxidase pathway) (Joseph-Horne et al., 2001), which generally leads to ROS accumulation in the mitochondria; thus, positive regulation of alternative oxidase may compensate for this loss and minimize ROS formation, which was recently demonstrated in *Paracoccidioides brasiliensis* (Petito et al., 2020) and in *C. albicans*, where copper starvation led to mitochondrial SOD1 repression and AOX induction enhanced cytochrome c oxidase activity (Broxton and Culotta, 2016). NDH-2 is a rotenone-insensitive nonproton pumping oxidoreductase that catalyzes a reaction similar to that of complex I, but in contrast to complex I, NDH-2 is not involved in the generation of membrane potential. NDH-2 was identified in plants, fungi, and bacteria as well as in some important parasitic protists, such as *Plasmodium falciparum* and *Toxoplasma gondii* (Marres et al., 1991; Yagi, 1991; Kerscher, 2000; Roberts et al., 2004; Lin et al., 2011). These two members belonging to the phylum Apicomplexa lack genes encoding canonical complex I and possess only homologs of NDH-2 instead (Fry and Beesley, 1991; Gardner et al., 2002; Uyemura et al., 2004). Altogether, NDH-2 is widely distributed in several human pathogens but not in humans themselves; thus, inhibitors of this enzyme could have clinical importance. Several studies have shown that NDH-2 provides a mechanism to remove excessive reducing power to balance the redox state of the cell (Luttik et al., 1998; Overkamp et al., 2000; Melo et al., 2004; Rasmusson et al., 2004). As mentioned above, branched mitochondrial ETC is activated in both studied amoebas upon copper limitation. In addition to AOX, whose activity is increased in both amoebas, NDH-2 is the most upregulated protein in copper-starved *N. fowleri*. Although we cannot conclude the direct consequences of NDH-2 induction for copper starvation in *N. fowleri*, we believe that further studying the exact mechanisms underlying the fascinating maintenance of the delicate balance between ATP production, ROS generation, and redox status in these microorganisms would be exciting.

DJ-1

One of the proteins most affected by copper limitation in *N. gruberi* shows homology to proteins belonging to the DJ-1/ThiJ/PfpI superfamily. Members of this superfamily are present in many organisms from bacteria to humans, and the most studied is the human homolog due to its role in several diseases, such as autosomal recessive early-onset Parkinson's disease (Bonifati et al., 2003). DJ-1 is also suggested to be one of the potential tumor markers and is strongly implicated in the pathogenesis of cancer (Nagakubo et al., 1997; Fan et al., 2015; Yu et al., 2017) and ischemia-reperfusion injury (Wang et al., 2017). Hundreds of publications explore the human homolog of DJ-1 and suggest many diverse functions, with roles as molecular chaperones (Cookson, 2003; Meulener et al., 2005), glyoxalases (Lee et al., 2003), proteases (Chen et al., 2010), and transcriptional regulators (Trempe and Fon, 2013), but the one function connecting these studies is the stress sensor reacting to oxidative stress and protecting cells from ROS (Taira et al., 2004; Inden et al., 2006). Some studies show that cells with a high level of DJ-1 are resistant to oxidative stress and neurotoxins, while lower levels of DJ-1 increase cells' vulnerability to oxidative stress (Inden et al., 2011). Therefore, we assessed the abundance of NgDJ-1 in cells treated with the ROS-inducing agents rotenone and PEITC. However, the expected induction of NgDJ-1 by ROS was not observed; in fact, the protein was downregulated in cells with higher ROS levels.

Human DJ-1 is predominantly localized to the cytoplasm, but it has been reported to be translocated to the mitochondria and nucleus under oxidative stress and to protect cells from oxidative stress-induced cell death (Irrcher et al., 2010; Kim et al., 2012). On the other hand, some studies also show that DJ-1 may be localized to mitochondria even in the absence of oxidative stress, where it directly binds to a subunit of complex I and somehow maintains its activity, since knockdown of DJ-1 in cells decreased complex I activity (Hayashi et al., 2009; Mullett and Hinkle, 2011). A recent study also showed its connection to ATP synthase, where DJ-1 is required for the normal stoichiometry of ATP synthase and to facilitate positioning of the β subunit of ATP synthase to fully close the mitochondrial inner membrane leak (Chen et al., 2019). Interestingly, our results show exclusively mitochondrial localization of NgDJ-1 regardless of copper availability. Only a few studies claim a certain link between copper metabolism and the DJ-1 protein. In 2014, Stefania Girroto and others suggested a putative role of DJ-1 as a copper chaperone for superoxide dismutase (Girotto et al., 2014). Two novel copper-binding sites, one Cu(I) binding site per monomer involving the highly conserved Cys-106 and the second Cu(I) binding site shared between two monomers, were identified, and the kinetics and binding affinity of DJ-1 to copper ions were determined (Girotto et al., 2014). Since the conserved Cys-106 analog is also present in the sequence of NgDJ-1 and the levels of the protein are regulated by copper availability in the amoeba, we may speculate about its role in the copper homeostasis of *N. gruberi*. Because NgDJ-1 is localized only to mitochondria, it may act as a storage site for copper that can be later allocated to complex IV when copper availability is limited, which is somewhat analogous to the case of plastocyanin in *Chlamydomonas* (Kropat et al., 2015). We may also consider the role of this protein as a protein with chelating properties to prevent free copper accumulation, which can cause increased ROS production and lead to impaired respiration. Since the levels of NgDJ-1 are affected by both copper limitation and copper excess, NgDJ-1 may play multiple roles in the amoeba.

Iron Uptake in *N. gruberi*

In our recent work, we showed that *N. fowleri* utilizes a reductive system of iron uptake, as described in the model *S. cerevisiae* (Arbon et al., 2020). This mechanism relies on the extracellular

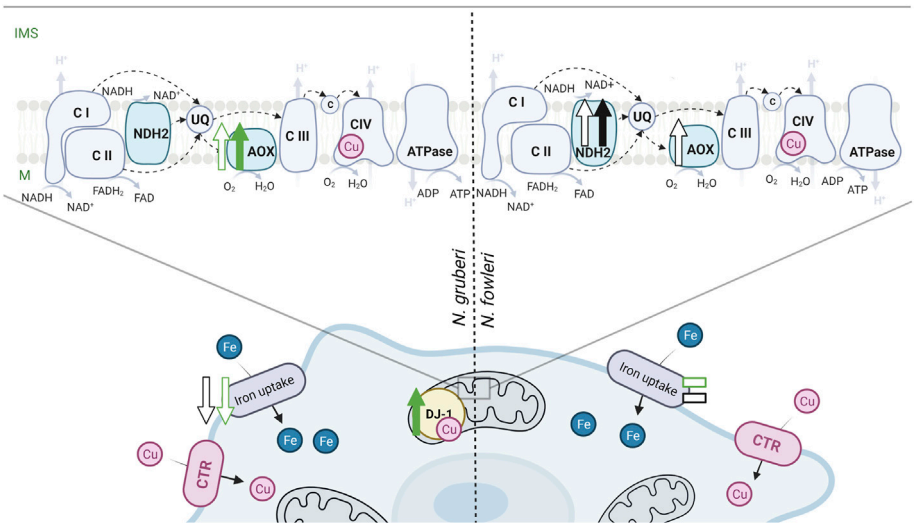

FIGURE 6 | The main effect of copper deprivation on the cellular processes of *N. gruberi* and *N. fowleri*. The green color corresponds to the effect of the copper chelator BCS, and changes caused by neocuproine are depicted in black. Upward pointing arrows represent an increase in copper-deprived conditions, downward pointing arrows denote a decrease in copper-deprived conditions, and dashes indicate no copper-induced changes. Full arrows represent the results from the proteomic analysis, and empty arrows represent the measured activity. Respiration chain complexes are marked by appropriate numbers, UQ–ubichinol/ubichinone, c–cytochrome c. Created with BioRender.com.

reduction of ferric ions from proteins, chelates, or other sources before their import into the cell. In yeast, the high-affinity ferrous-specific iron transport system is composed of multicopper oxidase FET3 and FTR1 permease; thus, copper availability is crucial for maintaining iron homeostasis (Askwith et al., 1994; Kaplan and O'Halloran, 1996; Stearman et al., 1996). Herein, we showed the same preference for the reduced form of iron in *N. gruberi*, but the main and surprising difference is that in contrast to *N. fowleri*, iron uptake efficiency in the nonpathogenic amoeba is decreased in copper-limited conditions, which corresponds to studies on *S. cerevisiae* (Dancis et al., 1994a) and on the model green algae *Chlamydomonas reinhardtii* (Herbik et al., 2002). An interesting question remains whether the pathogenic amoeba employs a copper-independent iron uptake mechanism or prioritizes extremely efficient copper delivery to this system in times of copper deprivation. The second hypothesis is rather unlikely since the *N. fowleri* iron uptake system has been previously shown to not be inducible even by iron starvation (Arbon et al., 2020).

N. gruberi and N. fowleri: So Similar yet so Different. Similarities and Differences

Altogether, our study reveals how *N. gruberi* and *N. fowleri* deal with copper deprivation and highlights the differences between the two amoebas (**Figure 6**). We showed that while both amoebas use Ctr homologs to acquire copper and increase the activity of the branched mitochondrial ETC when copper is limited, their responses to copper limitation differ significantly. Although copper bioavailability limitation in the growth medium results in a more pronounced decrease in the cellular concentration of the metal in *N. fowleri* in comparison to *N. gruberi*, the growth of the pathogen is not affected, and the intracellular copper chelator neocuproine is required to observe a copper-related phenotype. Moreover, even when neocuproine was used to starve the cells for copper, iron uptake efficiency was not affected in *N. fowleri*, unlike *N. gruberi*. To hypothesize whether the particularities in *N. fowleri* copper homeostasis can contribute to its virulence would be an exaggeration, however, one must take into account the fact that copper is an important player in the host-pathogen relationship.

DATA AVAILABILITY STATEMENT

The original contributions presented in the study are included in the article/**Supplementary Material**. The mass spectrometry proteomics data have been deposited to the ProteomeXchange Consortium via the PRIDE (Perez-Riverol et al., 2022) partner repository with the dataset identifier PXD032745, further inquiries can be directed to the corresponding author.

AUTHOR CONTRIBUTIONS

RS, KZ and MG conceived and designed the experiments. KZ, MG performed the experiments. KZ and MG analyzed and interpreted the data. KZ, MG and RS wrote the manuscript. All authors contributed to the article and approved the submitted version.

FUNDING

The project was supported by the Czech Science Foundation (20-28072S), Charles University Grant Agency (343621), CePaViP provided by The European Regional Development Fund and Ministry of Education, Youth and Sports of the Czech Republic (CZ.02.1.01/0.0/0.0/16_019/0000759), the MiCoBion project funded by EU Horizon 2020 (810224), Czech-BioImaging large RI projects (LM2018129 and CZ.02.1.01/0.0/0.0/18_046/0016045, funded by MEYS CR and ERDF), Moore-Simons Project on the Origin of the Eukaryotic Cell (https://doi.org/10.37807/GBMF9738).

ACKNOWLEDGMENTS

Karel Harant and Pavel Talacko from the Laboratory of Mass Spectrometry, Biocev, Charles University, Faculty of Science, where the proteomics and mass spectrometric analyses were performed. Special thanks to Dennis J. Thiele, Ivan Hrdý, Zdeněk Verner and Jan Mach for support and helpful scientific discussions.

SUPPLEMENTARY MATERIAL

The Supplementary Material for this article can be found online at: https://www.frontiersin.org/articles/10.3389/fcell.2022.853463/full#supplementary-material

Supplementary Table 1 | List of whole-cell proteomes of both amoebas under copper-rich and copper-deprived conditions. The list is organized into thirteen sheets containing separately raw data of comparative proteomics results of *N. gruberi* (NG) or *N. fowleri (NF)* cells incubated in 25 μM BCS (BCS) or 5 μM neocuproine (NEO) compared to cells cultured in the presence of 25 μM Cu2SO4 (cu), sheets containing all upregulated (UP) or downregulated (DOWN) proteins under the indicated copper-depleted conditions and the list containing summarized table of significantly changed proteins of both amoebas in both copper-deprived conditions. Upregulated and downregulated proteins were selected and filtered based on the criteria listed in the Methods section.

REFERENCES

Almagro Armenteros, J. J., Tsirigos, K. D., Sønderby, C. K., Petersen, T. N., Winther, O., Brunak, S., et al. (2019). SignalP 5.0 Improves Signal Peptide Predictions Using Deep Neural Networks. *Nat. Biotechnol.* 37, 420–423. doi:10.1038/s41587-019-0036-z

Altschul, S. F., Gish, W., Miller, W., Myers, E. W., and Lipman, D. J. (1990). Basic Local Alignment Search Tool. *J. Mol. Biol.* 215, 403–410. doi:10.1016/s0022-2836(05)80360-2

Amos, B., Aurrecoechea, C., Barba, M., Barreto, A., Basenko, E. Y., Ba˙ Zant, W., et al. (2021). VEuPathDB: The Eukaryotic Pathogen, Vector and Host Bioinformatics Resource center. *Nucleic Acids Res.* 50, D898–D911. doi:10.1093/nar/gkab929

Andreini, C., Bertini, I., Cavallaro, G., Holliday, G. L., and Thornton, J. M. (2008). Metal Ions in Biological Catalysis: From Enzyme Databases to General Principles. *J. Biol. Inorg. Chem.* 13, 1205–1218. doi:10.1007/s00775-008-0404-5

Arbon, D., Ženíšková, K., Mach, J., Grechnikova, M., Malych, R., Talacko, P., et al. (2020). Adaptive Iron Utilization Compensates for the Lack of an Inducible Uptake System in *Naegleria Fowleri* and Represents a Potential Target for Therapeutic Intervention. *Plos Negl. Trop. Dis.* 14, e0007759. doi:10.1371/journal.pntd.0007759

Askwith, C., Eide, D., Van Ho, A., Bernard, P. S., Li, L., Davis-Kaplan, S., et al. (1994). The FET3 Gene of *S. Cerevisiae* Encodes a Multicopper Oxidase Required for Ferrous Iron Uptake. *Cell* 76, 403–410. doi:10.1016/0092-8674(94)90346-8

Bandyopadhyay, S., and Cookson, M. R. (2004). Evolutionary and Functional Relationships within the DJ-1 Superfamily. *BMC Evol. Biol.* 4, 6. doi:10.1186/1471-2148-4-6

Besold, A. N., Culbertson, E. M., and Culotta, V. C. (2016). The Yin and Yang of Copper during Infection. *J. Biol. Inorg. Chem.* 21, 137–144. doi:10.1007/s00775-016-1335-1

Bonifati, V., Rizzu, P., van Baren, M. J., Schaap, O., Breedveld, G. J., Krieger, E., et al. (2003). Mutations in the DJ-1 Gene Associated with Autosomal Recessive Early-Onset Parkinsonism. *Science* 299, 256–259. doi:10.1126/science.1077209

Broxton, C. N., and Culotta, V. C. (2016). An Adaptation to Low Copper in *Candida Albicans* Involving SOD Enzymes and the Alternative Oxidase. *PLoS One* 11, e0168400. doi:10.1371/journal.pone.0168400

Cantoni, D., Osborne, A., Taib, N., Thompson, G., Kazana, E., Edrich, E., et al. (2020). Localization and Functional Characterization of the Alternative Oxidase in *Naegleria*. *bioRxiv*. doi:10.1101/2020.09.26.314807

Cassat, J. E., and Skaar, E. P. (2013). Iron in Infection and Immunity. *Cell Host Microbe* 13, 509–519. doi:10.1016/j.chom.2013.04.010

Chaturvedi, K. S., and Henderson, J. P. (2014). Pathogenic Adaptations to Host-Derived Antibacterial Copper. *Front. Cel. Infect. Microbiol.* 4, 3. doi:10.3389/fcimb.2014.00003

Chen, J., Li, L., and Chin, L.-S. (2010). Parkinson Disease Protein DJ-1 Converts from a Zymogen to a Protease by Carboxyl-Terminal Cleavage. *Hum. Mol. Genet.* 19, 2395–2408. doi:10.1093/hmg/ddq113

Chen, R., Park, H. A., Mnatsakanyan, N., Niu, Y., Licznerski, P., Wu, J., et al. (2019). Parkinson's Disease Protein DJ-1 Regulates ATP Synthase Protein Components to Increase Neuronal Process Outgrowth. *Cell Death Dis* 10 (6), 469. doi:10.1038/s41419-019-1679-x

Choveaux, D. L., Przyborski, J. M., and Goldring, J. P. (2012). A *Plasmodium Falciparum* Copper-Binding Membrane Protein with Copper Transport Motifs. *Malar. J.* 11, 397. doi:10.1186/1475-2875-11-397

Cookson, M. R. (2003). Pathways to Parkinsonism. *Neuron* 37, 7–10. doi:10.1016/s0896-6273(02)01166-2

Cox, J., Hein, M. Y., Luber, C. A., Paron, I., Nagaraj, N., and Mann, M. (2014). Accurate Proteome-Wide Label-Free Quantification by Delayed Normalization and Maximal Peptide Ratio Extraction, Termed MaxLFQ. *Mol. Cel. Proteomics* 13, 2513–2526. doi:10.1074/mcp.m113.031591

Cvetkovska, M., and Vanlerberghe, G. C. (2012). Coordination of a Mitochondrial Superoxide Burst during the Hypersensitive Response to Bacterial Pathogen in *Nicotiana Tabacum*. *Plant Cel Environ.* 35, 1121–1136. doi:10.1111/j.1365-3040.2011.02477.x

Dahal, K., and Vanlerberghe, G. C. (2017). Alternative Oxidase Respiration Maintains Both Mitochondrial and Chloroplast Function during Drought. *New Phytol.* 213, 560–571. doi:10.1111/nph.14169

Dancis, A., Haile, D., Yuan, D. S., and Klausner, R. D. (1994b). The *Saccharomyces Cerevisiae* Copper Transport Protein (Ctr1p). Biochemical Characterization, Regulation by Copper, and Physiologic Role in Copper Uptake. *J. Biol. Chem.* 269, 25660–25667. doi:10.1016/s0021-9258(18)47300-0

Dancis, A., Yuan, D. S., Haile, D., Askwith, C., Eide, D., Moehle, C., et al. (1994a). Molecular Characterization of a Copper Transport Protein in *S. Cerevisiae*: An Unexpected Role for Copper in Iron Transport. *Cell* 76, 393–402. doi:10.1016/0092-8674(94)90345-x

De Jonckheere, J. F. (2004). Molecular Definition and the Ubiquity of Species in the Genus. *Protist* 155, 89–103. doi:10.1078/1434461000167

Ding, C., Festa, R. A., Chen, Y.-L., Espart, A., Palacios, Ò., Espín, J., et al. (2013). *Cryptococcus Neoformans* Copper Detoxification Machinery Is Critical for Fungal Virulence. *Cell Host Microbe* 13, 265–276. doi:10.1016/j.chom.2013.02.002

Fan, J., Yu, H., Lv, Y., and Yin, L. (2015). Diagnostic and Prognostic Value of Serum Thioredoxin and DJ-1 in Non-Small Cell Lung Carcinoma Patients. *Tumor Biol.* 37 (2), 1949–1958. doi:10.1007/s13277-015-3994-x

Festa, R. A., and Thiele, D. J. (2012). Copper at the Front Line of the Host-Pathogen Battle. *Plos Pathog.* 8, e1002887. doi:10.1371/journal.ppat.1002887

Fritz-Laylin, L. K., Ginger, M. L., Walsh, C., Dawson, S. C., and Fulton, C. (2011). The *Naegleria* Genome: A Free-Living Microbial Eukaryote Lends Unique Insights into Core Eukaryotic Cell Biology. *Res. Microbiol.* 162, 607–618. doi:10.1016/j.resmic.2011.03.003

Fritz-Laylin, L. K., Prochnik, S. E., Ginger, M. L., Dacks, J. B., Carpenter, M. L., Field, M. C., et al. (2010). The Genome of *Naegleria Gruberi* Illuminates Early Eukaryotic Versatility. *Cell* 140, 631–642. doi:10.1016/j.cell.2010.01.032

Fry, M., and Beesley, J. E. (1991). Mitochondria of Mammalian *Plasmodium Spp*. *Parasitology* 102 (Pt 1), 17–26. doi:10.1017/s0031182000060297

Fulton, C. (1974). Axenic Cultivation of *Naegleria Gruberi*: Requirement for Methionine. *Exp. Cel Res.* 88, 365–370. doi:10.1016/0014-4827(74)90253-5

García-Santamarina, S., and Thiele, D. J. (2015). Copper at the Fungal Pathogen-Host Axis. *J. Biol. Chem.* 290, 18945–18953. doi:10.1074/jbc.R115.649129

Gardner, M. J., Hall, N., Fung, E., White, O., Berriman, M., Hyman, R. W., et al. (2002). Genome Sequence of the Human Malaria Parasite *Plasmodium Falciparum*. *Nature* 419, 498–511. doi:10.1038/nature01097

Garí, E., Piedrafita, L., Aldea, M., and Herrero, E. (1997). A Set of Vectors with a Tetracycline-Regulatable Promoter System for Modulated Gene Expression in *Saccharomyces Cerevisiae*. *Yeast* 13, 837–848. doi:10.1002/(SICI)1097-0061(199707)13:9<837::AID-YEA145>3.0.CO;2-T

Gietz, R. D., and Schiestl, R. H. (2007). Large-Scale High-Efficiency Yeast Transformation Using the LiAc/SS Carrier DNA/PEG Method. *Nat. Protoc.* 2, 38–41. doi:10.1038/nprot.2007.15

Girotto, S., Cendron, L., Bisaglia, M., Tessari, I., Mammi, S., Zanotti, G., et al. (2014). DJ-1 Is a Copper Chaperone Acting on SOD1 Activation. *J. Biol. Chem.* 289, 10887–10899. doi:10.1074/jbc.m113.535112

Grechnikova, M., Ženíšková, K., Malych, R., Mach, J., and Sutak, R. (2020). Copper Detoxification Machinery of the Brain-Eating Amoeba *Naegleria Fowleri* Involves Copper-Translocating ATPase and the Antioxidant System. *Int. J. Parasitol. Drugs Drug Resist.* 14, 126–135. doi:10.1016/j.ijpddr.2020.10.001

Grigoriev, I. V., Hayes, R. D., Calhoun, S., Kamel, B., Wang, A., Ahrendt, S., et al. (2021). PhycoCosm, a Comparative Algal Genomics Resource. *Nucleic Acids Res.* 49, D1004–D1011. doi:10.1093/nar/gkaa898

Hayashi, T., Ishimori, C., Takahashi-Niki, K., Taira, T., Kim, Y.-C., Maita, H., et al. (2009). DJ-1 Binds to Mitochondrial Complex I and Maintains its Activity. *Biochem. Biophysical Res. Commun.* 390, 667–672. doi:10.1016/j.bbrc.2009.10.025

Herbik, A., Bölling, C., and Buckhout, T. J. (2002). The Involvement of a Multicopper Oxidase in Iron Uptake by the Green Algae *Chlamydomonas Reinhardtii*. *Plant Physiol.* 130, 2039–2048. doi:10.1104/pp.013060

Herman, E. K., Greninger, A., van der Giezen, M., Ginger, M. L., Ramirez-Macias, I., Miller, H. C., et al. (2021). Genomics and Transcriptomics Yields a System-Level View of the Biology of the Pathogen *Naegleria Fowleri*. *BMC Biol.* 19 (1), 142. doi:10.1186/s12915-021-01078-1

Hodgkinson, V., and Petris, M. J. (2012). Copper Homeostasis at the Host-Pathogen Interface. *J. Biol. Chem.* 287, 13549–13555. doi:10.1074/jbc.r111.316406

Hood, M. I., and Skaar, E. P. (2012). Nutritional Immunity: Transition Metals at the Pathogen-Host Interface. *Nat. Rev. Microbiol.* 10, 525–537. doi:10.1038/nrmicro2836

Inden, M., Kitamura, Y., Takahashi, K., Takata, K., Ito, N., Niwa, R., et al. (2011). Protection against Dopaminergic Neurodegeneration in Parkinson's Disease-Model Animals by a Modulator of the Oxidized Form of DJ-1, a Wild-type of Familial Parkinson's Disease-Linked PARK7. *J. Pharmacol. Sci.* 117, 189–203. doi:10.1254/jphs.11151fp

Inden, M., Taira, T., Kitamura, Y., Yanagida, T., Tsuchiya, D., Takata, K., et al. (2006). PARK7 DJ-1 Protects against Degeneration of Nigral Dopaminergic Neurons in Parkinson's Disease Rat Model. *Neurobiol. Dis.* 24, 144–158. doi:10.1016/j.nbd.2006.06.004

Irrcher, I., Aleyasin, H., Seifert, E. L., Hewitt, S. J., Chhabra, S., Phillips, M., et al. (2010). Loss of the Parkinson's Disease-Linked Gene DJ-1 Perturbs Mitochondrial Dynamics. *Hum. Mol. Genet.* 19, 3734–3746. doi:10.1093/hmg/ddq288

Isah, M. B., Goldring, J. P. D., and Coetzer, T. H. T. (2020). Expression and Copper Binding Properties of the N-Terminal Domain of Copper P-type ATPases of African Trypanosomes. *Mol. Biochem. Parasitol.* 235, 111245. doi:10.1016/j.molbiopara.2019.111245

Joseph-Horne, T., Hollomon, D. W., and Wood, P. M. (2001). Fungal Respiration: A Fusion of Standard and Alternative Components. *Biochim. Biophys. Acta - Bioenerg.* 1504, 179–195. doi:10.1016/s0005-2728(00)00251-6

Jungmann, J., Reins, H. A., Lee, J., Romeo, A., Hassett, R., Kosman, D., et al. (1993). MAC1, a Nuclear Regulatory Protein Related to Cu-Dependent Transcription Factors Is Involved in Cu/Fe Utilization and Stress Resistance in Yeast. *EMBO J.* 12, 5051–5056. doi:10.1002/j.1460-2075.1993.tb06198.x

Käll, L., Krogh, A., and Sonnhammer, E. L. L. (2004). A Combined Transmembrane Topology and Signal Peptide Prediction Method. *J. Mol. Biol.* 338, 1027–1036. doi:10.1016/j.jmb.2004.03.016

Kaplan, J., and O'Halloran, T. V. (1996). Iron Metabolism in Eukaryotes-Mars and Venus at it Again. *Science* 271, 1510–1512. doi:10.1126/science.271.5255.1510

Kerscher, S. J. (2000). Diversity and Origin of Alternative NADH:ubiquinone Oxidoreductases. *Biochim. Biophys. Acta - Bioenerg.* 1459, 274–283. doi:10.1016/s0005-2728(00)00162-6

Kim, S.-J., Park, Y.-J., Hwang, I.-Y., Youdim, M. B. H., Park, K.-S., and Oh, Y. J. (2012). Nuclear Translocation of DJ-1 during Oxidative Stress-Induced Neuronal Cell Death. *Free Radic. Biol. Med.* 53, 936–950. doi:10.1016/j.freeradbiomed.2012.05.035

Knight, S. A., Labbé, S., Kwon, L. F., Kosman, D. J., and Thiele, D. J. (1996). A Widespread Transposable Element Masks Expression of a Yeast Copper Transport Gene. *Genes Dev.* 10, 1917–1929. doi:10.1101/gad.10.15.1917

Kozlowski, H., Janicka-Klos, A., Brasun, J., Gaggelli, E., Valensin, D., and Valensin, G. (2009). Copper, Iron, and Zinc Ions Homeostasis and Their Role in Neurodegenerative Disorders (Metal Uptake, Transport, Distribution and Regulation). *Coord. Chem. Rev.* 253, 2665–2685. doi:10.1016/j.ccr.2009.05.011

Kropat, J., Gallaher, S. D., Urzica, E. I., Nakamoto, S. S., Strenkert, D., Tottey, S., et al. (2015). Copper Economy in *Chlamydomonas*: Prioritized Allocation and Reallocation of Copper to Respiration vs. Photosynthesis. *Proc. Natl. Acad. Sci. U.S.A.* 112, 2644–2651. doi:10.1073/pnas.1422492112

Lee, S.-J., Kim, S. J., Kim, I.-K., Ko, J., Jeong, C.-S., Kim, G.-H., et al. (2003). Crystal Structures of Human DJ-1 and *Escherichia coli* Hsp31, Which Share an Evolutionarily Conserved Domain. *J. Biol. Chem.* 278, 44552–44559. doi:10.1074/jbc.m304517200

Li, C. X., Gleason, J. E., Zhang, S. X., Bruno, V. M., Cormack, B. P., and Culotta, V. C. (2015a). *Candida Albicans* Adapts to Host Copper during Infection by Swapping Metal Cofactors for Superoxide Dismutase. *Proc. Natl. Acad. Sci. U. S. A.* 112, E5336–E5342. doi:10.1073/pnas.1513447112

Li, X., Li, J., Hu, X., Huang, L., Xiao, J., Chan, J., et al. (2015b). Differential Roles of the Hemerythrin-Like Proteins of *Mycobacterium Smegmatis* in Hydrogen Peroxide and Erythromycin Susceptibility. *Sci. Rep.* 5, 16130. doi:10.1038/srep16130

Liechti, N., Schürch, N., Bruggmann, R., and Wittwer, M. (2019). Nanopore Sequencing Improves the Draft Genome of the Human Pathogenic Amoeba *Naegleria Fowleri*. *Sci. Rep.* 9, 16040. doi:10.1038/s41598-019-52572-0

Lin, S. S., Gross, U., and Bohne, W. (2011). Two Internal Type II NADH Dehydrogenases of *Toxoplasma Gondii* Are Both Required for Optimal Tachyzoite Growth. *Mol. Microbiol.* 82, 209–221. doi:10.1111/j.1365-2958.2011.07807.x

Liu, L., Qi, J., Yang, Z., Peng, L., and Li, C. (2012). Low-Affinity Copper Transporter CTR2 Is Regulated by Copper-Sensing Transcription Factor Mac1p in *Saccharomyces Cerevisiae*. *Biochem. Biophys. Res. Commun.* 420, 600–604. doi:10.1016/j.bbrc.2012.03.040

Luttik, M. A. H., Overkamp, K. M., Kötter, P., de Vries, S., van Dijken, J. P., and Pronk, J. T. (1998). The *Saccharomyces Cerevisiae* NDE1 and NDE2 Genes Encode Separate Mitochondrial NADH Dehydrogenases Catalyzing the Oxidation of Cytosolic NADH. *J. Biol. Chem.* 273, 24529–24534. doi:10.1074/jbc.273.38.24529

Ma, Z., Strickland, K. T., Cherne, M. D., Sehanobish, E., Rohde, K. H., Self, W. T., et al. (2018). The Rv2633c Protein of *Mycobacterium Tuberculosis* Is a Non-heme Di-iron Catalase with a Possible Role in Defenses against Oxidative Stress. *J. Biol. Chem.* 293, 1590–1595. doi:10.1074/jbc.ra117.000421

Mach, J., Bíla, J., Ženíšková, K., Arbon, D., Malych, R., Glavanakovová, M., et al. (2018). Iron Economy in *Naegleria Gruberi* Reflects its Metabolic Flexibility. *Int. J. Parasitol.* 48 (9-10), 719–727. doi:10.1016/j.ijpara.2018.03.005

Macomber, L., and Imlay, J. A. (2009). The Iron-Sulfur Clusters of Dehydratases Are Primary Intracellular Targets of Copper Toxicity. *Proc. Natl. Acad. Sci. U.S.A.* 106, 8344–8349. doi:10.1073/pnas.0812808106

Marres, C. A. M., Vries, S., and Grivell, L. A. (1991). Isolation and Inactivation of the Nuclear Gene Encoding the Rotenone-Insensitive Internal NADH: Ubiquinone Oxidoreductase of Mitochondria from *Saccharomyces Cerevisiae*. *Eur. J. Biochem.* 195, 857–862. doi:10.1111/j.1432-1033.1991.tb15775.x

Marvin, M. E., Williams, P. H., and Cashmore, A. M. (2003). Tha *Candida Albicans* CTR1 Gene Encodes a Functional Copper Transporter. *Microbiology* 149, 1461–1474. doi:10.1099/mic.0.26172-0

Maryon, E. B., Molloy, S. A., Zimnicka, A. M., and Kaplan, J. H. (2007). Copper Entry into Human Cells: Progress and Unanswered Questions. *Biometals* 20, 355–364. doi:10.1007/s10534-006-9066-3

Maxwell, D. P., Wang, Y., and McIntosh, L. (1999). The Alternative Oxidase Lowers Mitochondrial Reactive Oxygen Production in Plant Cells. *Proc. Natl. Acad. Sci. U.S.A.* 96, 8271–8276. doi:10.1073/pnas.96.14.8271

Melo, A. M. P., Bandeiras, T. M., and Teixeira, M. (2004). New Insights into Type II NAD(P)H:quinone Oxidoreductases. *Microbiol. Mol. Biol. Rev.* 68, 603–616. doi:10.1128/mmbr.68.4.603-616.2004

Meulener, M. C., Graves, C. L., Sampathu, D. M., Armstrong-Gold, C. E., Bonini, N. M., and Giasson, B. I. (2005). DJ-1 Is Present in a Large Molecular Complex in Human Brain Tissue and Interacts with α-synuclein. *J. Neurochem.* 93, 1524–1532. doi:10.1111/j.1471-4159.2005.03145.x

Mistry, J., Chuguransky, S., Williams, L., Qureshi, M., Salazar, G. A., Sonnhammer, E. L. L., et al. (2021). Pfam: The Protein Families Database in 2021. *Nucleic Acids Res.* 49, D412–D419. doi:10.1093/nar/gkaa913

Mull, B. J., Narayanan, J., and Hill, V. R. (2013). Improved Method for the Detection and Quantification of *Naegleria Fowleri* in Water and Sediment Using Immunomagnetic Separation and Real-Time PCR. *J. Parasitol. Res.* 2013, 608367. doi:10.1155/2013/608367

Mullett, S. J., and Hinkle, D. A. (2011). DJ-1 Deficiency in Astrocytes Selectively Enhances Mitochondrial Complex I Inhibitor-Induced Neurotoxicity. *J. Neurochem.* 117, 375–387. doi:10.1111/j.1471-4159.2011.07175.x

Mungroo, M. R., Khan, N. A., Maciver, S., and Siddiqui, R. (2021). Opportunistic Free-Living Amoebal Pathogens. *Pathog. Glob. Health* 49, 1–15. doi:10.1080/21548331.2020.1828888

Nagakubo, D., Taira, T., Kitaura, H., Ikeda, M., Tamai, K., Iguchi-Ariga, S. M. M., et al. (1997). DJ-1, a Novel Oncogene Which Transforms Mouse NIH3T3 Cells in Cooperation Withras. *Biochem. Biophys. Res. Commun.* 231, 509–513. doi:10.1006/bbrc.1997.6132

Nose, Y., Rees, E. M., and Thiele, D. J. (2006). Structure of the Ctr1 Copper trans'PORE'ter Reveals Novel Architecture. *Trends Biochem. Sci.* 31, 604–607. doi:10.1016/j.tibs.2006.09.003

Overkamp, K. M., Bakker, B. M., Kötter, P., van Tuijl, A., de Vries, S., van Dijken, J. P., et al. (2000). *In Vivo* analysis of the Mechanisms for Oxidation of Cytosolic NADH by *Saccharomyces Cerevisiae* Mitochondria. *J. Bacteriol.* 182, 2823–2830. doi:10.1128/jb.182.10.2823-2830.2000

Paul, R., Banerjee, S., Sen, S., Dubey, P., Maji, S., Bachhawat, A. K., et al. (2021). The Novel Leishmanial Copper P-type ATPase Plays a Vital Role in Intracellular Parasite Survival. *J. Biol. Chem.* 298 (2), 101539. doi:10.1016/j.jbc.2021.101539

Perez-Riverol, Y., Bai, J., Bandla, C., García-Seisdedos, D., Hewapathirana, S., Kamatchinathan, S., et al. (2022). The PRIDE Database Resources in 2022: a Hub for Mass Spectrometry-Based Proteomics Evidences. *Nucleic Acids Res.* 50, D543.

Petito, G., de Curcio, J. S., Pereira, M., Bailão, A. M., Paccez, J. D., Tristão, G. B., et al. (2020). Metabolic Adaptation of *Paracoccidioides Brasiliensis* in Response to *In Vitro* Copper Deprivation. *Front. Microbiol.* 11, 1834. doi:10.3389/fmicb.2020.01834

Posey, J. E., and Gherardini, F. C. (2000). Lack of a Role for Iron in the Lyme Disease Pathogen. *Science* 288, 1651–1653. doi:10.1126/science.288.5471.1651

Rasmusson, A. G., Soole, K. L., and Elthon, T. E. (2004). Alternative NAD(P)H Dehydrogenases of Plant Mitochondria. *Annu. Rev. Plant Biol.* 55, 23–39. doi:10.1146/annurev.arplant.55.031903.141720

Rasoloson, D., Shi, L., Chong, C. R., Kafsack, B. F., and Sullivan, D. J. (2004). Copper Pathways in *Plasmodium Falciparum* Infected Erythrocytes Indicate an Efflux Role for the Copper P-ATPase. *Biochem. J.* 381, 803–811. doi:10.1042/bj20040335

Rees, E. M., Lee, J., and Thiele, D. J. (2004). Mobilization of Intracellular Copper Stores by the Ctr2 Vacuolar Copper Transporter. *J. Biol. Chem.* 279, 54221–54229. doi:10.1074/jbc.m411669200

Ribas-Carbo, M., Taylor, N. L., Giles, L., Busquets, S., Finnegan, P. M., Day, D. A., et al. (2005). Effects of Water Stress on Respiration in Soybean Leaves. *Plant Physiol.* 139, 466–473. doi:10.1104/pp.105.065565

Roberts, C. W., Roberts, F., Henriquez, F. L., Akiyoshi, D., Samuel, B. U., Richards, T. A., et al. (2004). Evidence for Mitochondrial-Derived Alternative Oxidase in the Apicomplexan Parasite *Cryptosporidium Parvum*: A Potential Anti-Microbial Agent Target. *Int. J. Parasitol.* 34, 297–308. doi:10.1016/j.ijpara.2003.11.002

Schneider, C. A., Rasband, W. S., and Eliceiri, K. W. (2012). NIH Image to ImageJ: 25 Years of Image Analysis. *Nat. Methods* 9 (7), 671–675. doi:10.1038/nmeth.2089

Sieger, S. M., Kristensen, B. K., Robson, C. A., Amirsadeghi, S., Eng, E. W. Y., Abdel-Mesih, A., et al. (2005). The Role of Alternative Oxidase in Modulating Carbon Use Efficiency and Growth during Macronutrient Stress in Tobacco Cells. *J. Exp. Bot.* 56, 1499–1515. doi:10.1093/jxb/eri146

Sluse, F. E., and Jarmuszkiewicz, W. (1998). Alternative Oxidase in the Branched Mitochondrial Respiratory Network: an Overview on Structure, Function, Regulation, and Role. *Braz. J. Med. Biol. Res.* 31, 733–747. doi:10.1590/s0100-879x1998000600003

Smith, C. A., Melino, V. J., Sweetman, C., and Soole, K. L. (2009). Manipulation of Alternative Oxidase Can Influence Salt Tolerance in *Arabidopsis Thaliana*. *Physiol. Plant* 137, 459–472. doi:10.1111/j.1399-3054.2009.01305.x

Solomon, E. I., Heppner, D. E., Johnston, E. M., Ginsbach, J. W., Cirera, J., Qayyum, M., et al. (2014). Copper Active Sites in Biology. *Chem. Rev.* 114, 3659–3853. doi:10.1021/cr400327t

Stafford, S. L., Bokil, N. J., Achard, M. E., Kapetanovic, R., Schembri, M. A., Mcewan, A. G., et al. (2013). Metal Ions in Macrophage Antimicrobial Pathways: Emerging Roles for Zinc and Copper. *Biosci. Rep.* 33, 541–554. doi:10.1042/BSR20130014

Stearman, R., Yuan, D. S., Yamaguchi-Iwai, Y., Klausner, R. D., and Dancis, A. (1996). A Permease-Oxidase Complex Involved in High-Affinity Iron Uptake in Yeast. *Science* 271, 1552–1557. doi:10.1126/science.271.5255.1552

Sun, T. S., Ju, X., Gao, H. L., Wang, T., Thiele, D. J., Li, J. Y., et al. (2014). Reciprocal Functions of *Cryptococcus Neoformans* Copper Homeostasis Machinery during Pulmonary Infection and Meningoencephalitis. *Nat. Commun.* 5, 5550. doi:10.1038/ncomms6550

Taira, T., Saito, Y., Niki, T., Iguchi-Ariga, S. M. M., Takahashi, K., and Ariga, H. (2004). DJ-1 Has a Role in Antioxidative Stress to Prevent Cell Death. *EMBO Rep.* 5, 213–218. doi:10.1038/sj.embor.7400074

Thomas, P. D., Campbell, M. J., Kejariwal, A., Mi, H., Karlak, B., Daverman, R., et al. (2003). PANTHER: A Library of Protein Families and Subfamilies Indexed by Function. *Genome Res.* 13, 2129–2141. doi:10.1101/gr.772403

Trempe, J.-F., and Fon, E. A. (2013). Structure and Function of Parkin, PINK1, and DJ-1, the Three Musketeers of Neuroprotection. *Front. Neurol.* 4, 38. doi:10.3389/fneur.2013.00038

Tsaousis, A. D., Nývltová, E., Šuták, R., Hrdý, I., and Tachezy, J. (2014). A Nonmitochondrial Hydrogen Production in *Naegleria Gruberi*. *Genome Biol. Evol.* 6, 792–799. doi:10.1093/gbe/evu065

Tyanova, S., Temu, T., Sinitcyn, P., Carlson, A., Hein, M. Y., Geiger, T., et al. (2016). The Perseus Computational Platform for Comprehensive Analysis of (Prote)omics Data. *Nat. Methods* 13, 731–740. doi:10.1038/nmeth.3901

Uyemura, S. A., Luo, S., Vieira, M., Moreno, S. N. J., and Docampo, R. (2004). Oxidative Phosphorylation and Rotenone-Insensitive Malate- and NADH-Quinone Oxidoreductases in *Plasmodium Yoelii* Yoelii Mitochondria *In Situ*. *J. Biol. Chem.* 279, 385–393. doi:10.1074/jbc.m307264200

Vishwakarma, A., Tetali, S. D., Selinski, J., Scheibe, R., and Padmasree, K. (2015). Importance of the Alternative Oxidase (AOX) Pathway in Regulating Cellular Redox and ROS Homeostasis to Optimize Photosynthesis during Restriction of the Cytochrome Oxidase Pathway in *Arabidopsis Thaliana*. *Ann. Bot.* 116, 555–569. doi:10.1093/aob/mcv122

Wang, H., Li, Y.-Y., Qiu, L.-Y., Yan, Y.-F., Liao, Z.-P., and Chen, H.-P. (2017). Involvement of DJ-1 in Ischemic Preconditioning-Induced Delayed Cardioprotection *In Vivo*. *Mol. Med. Rep.* 15, 995–1001. doi:10.3892/mmr.2016.6091

Waterman, S. R., Hacham, M., Hu, G., Zhu, X., Park, Y.-D., Shin, S., et al. (2007). Role of a CUF1/CTR4 Copper Regulatory axis in the Virulence of *Cryptococcus Neoformans*. *J. Clin. Invest.* 117, 794–802. doi:10.1172/jci30006

Wei, Y., Ringe, D., Wilson, M. A., and Ondrechen, M. J. (2007). Identification of Functional Subclasses in the DJ-1 Superfamily Proteins. *PLOS Comput. Biol.* 3, e15. doi:10.1371/journal.pcbi.0030010

Weinberg, E. D. (1975). Nutritional Immunity. Host's Attempt to Withold Iron from Microbial Invaders. *JAMA J. Am. Med. Assoc.* 231, 39–41. doi:10.1001/jama.231.1.39

Winge, D. R., Jensen, L. T., and Srinivasan, C. (1998). Metal-Ion Regulation of Gene Expression in Yeast. *Curr. Opin. Chem. Biol.* 2, 216–221. doi:10.1016/s1367-5931(98)80063-x

Yagi, T. (1991). Bacterial NADH-Quinone Oxidoreductases. *J. Bioenerg. Biomembr.* 23, 211–225. doi:10.1007/bf00762218

Yu, D., Pan, H., Zhang, R., Li, Y., and Nie, X. (2017). Nucleus DJ-1/Park7 Acts as a Favorable Prognostic Factor and Involves Mucin Secretion in Invasive Breast Carcinoma in Chinese Population. *Int. J. Clin. Exp. Med.* 10 (4), 6558–6567.

Zhang, L., Wang, J., Wang, J., Yang, B., He, Q., and Weng, Q. (2020). Role of DJ-1 in Immune and Inflammatory Diseases. *Front. Immunol.* 11, 994. doi:10.3389/fimmu.2020.00994

Zhou, B., and Gitschier, J. (1997). hCTR1: A Human Gene for Copper Uptake Identified by Complementation in Yeast. *Proc. Natl. Acad. Sci. U. S. A.* 94, 7481–7486. doi:10.1073/pnas.94.14.7481

Zimmermann, L., Stephens, A., Nam, S.-Z., Rau, D., Kübler, J., Lozajic, M., et al. (2018). A Completely Reimplemented MPI Bioinformatics Toolkit with a New HHpred Server at its Core. *J. Mol. Biol.* 430, 2237–2243. doi:10.1016/j.jmb.2017.12.007

Conflict of Interest: The authors declare that the research was conducted in the absence of any commercial or financial relationships that could be construed as a potential conflict of interest.

Publisher's Note: All claims expressed in this article are solely those of the authors and do not necessarily represent those of their affiliated organizations, or those of the publisher, the editors and the reviewers. Any product that may be evaluated in this article, or claim that may be made by its manufacturer, is not guaranteed or endorsed by the publisher.

International Journal for Parasitology: Drugs and Drug Resistance 14 (2020) 126–135

Contents lists available at ScienceDirect

International Journal for Parasitology: Drugs and Drug Resistance

journal homepage: www.elsevier.com/locate/ijpddr

Copper detoxification machinery of the brain-eating amoeba *Naegleria fowleri* involves copper-translocating ATPase and the antioxidant system

Maria Grechnikova, Kateřina Ženíšková, Ronald Malych, Jan Mach, Robert Sutak *

Department of Parasitology, Faculty of Science, Charles University, BIOCEV, Vestec, Czech Republic

ARTICLE INFO

Keywords:
Copper
Oxidative stress
Copper-translocating ATPase
Naegleria fowleri
Ionophores
Hemerythrin

ABSTRACT

Copper is a trace metal that is necessary for all organisms but toxic when present in excess. Different mechanisms to avoid copper toxicity have been reported to date in pathogenic organisms such as *Cryptococcus neoformans* and *Candida albicans*. However, little if anything is known about pathogenic protozoans despite their importance in human and veterinary medicine. *Naegleria fowleri* is a free-living amoeba that occurs naturally in warm fresh water and can cause a rapid and deadly brain infection called primary amoebic meningoencephalitis (PAM). Here, we describe the mechanisms employed by *N. fowleri* to tolerate high copper concentrations, which include various strategies such as copper efflux mediated by a copper-translocating ATPase and upregulation of the expression of antioxidant enzymes and obscure hemerythrin-like and protoglobin-like proteins. The combination of different mechanisms efficiently protects the cell and ensures its high copper tolerance, which can be advantageous both in the natural environment and in the host. Nevertheless, we demonstrate that copper ionophores are potent antiamoebic agents; thus, copper metabolism may be considered a therapeutic target.

1. Introduction

Copper is a trace element that is vital for all organisms from bacteria to higher eukaryotes. Based on its ability to cycle between reduced (Cu^{+}) and oxidized (Cu^{2+}) states, copper serves as a cofactor for different enzymes such as cytochrome c oxidase, Cu/Zn-SOD, tyrosinase, and hexose oxidase. High copper concentrations, however, are toxic. The main mechanism underlying copper toxicity is not well understood; it has generally been assumed that copper acts in a manner similar to iron, causing reactive oxygen species production via the Fenton and Haber-Weiss reactions with subsequent damage to macromolecules including nucleic acids, proteins and lipids (Rainsford et al., 1998). Indeed, cells that are exposed to high copper conditions demonstrate signs of oxidative stress (Gaetke and Chow, 2003). Recently, however, it was shown that enzymes containing iron-sulfur (Fe–S) clusters might be the primary targets of copper toxicity. Copper degrades Fe–S clusters by replacing iron, impairing the function of enzymes; additionally, the free iron concentration in the cell is increased, promoting iron toxicity via iron-based Fenton chemistry. Thus, excessive copper promotes iron toxicity and the subsequent oxidative stress (Macomber and Imlay, 2009). Moreover, copper might impair Fe–S clusters biogenesis (Brancaccio et al., 2017; Garcia-Santamarina et al., 2017).

Free copper is virtually nonexistent in living organisms, and there are different mechanisms to regulate cell copper concentrations. One is the downregulation of high-affinity copper transporters during copper excess, which has been shown, for example, in *Candida albicans* (Mackie et al., 2016) and *Aspergillus fumigatus* (Wiemann et al., 2017). Another mechanism is copper sequestration by metallothioneins or glutathione. Metallothioneins are small highly heterogeneous cysteine-rich proteins that bind copper with high stoichiometry; they are found in different organisms, including bacteria, fungi, plants and animals (Capdevila and Atrian, 2011). One of the most extensively characterized metallothioneins, Cup1 from *Saccharomyces cerevisiae*, binds 8 copper ions, while metallothioneins Cmt1 and Cmt2 from a well-studied human pathogen *Cryptococcus neoformans* bind up to 16 and 24 copper ions, respectively (Smith et al., 2017). Glutathione is another intracellular compound that is quite effective in buffering copper and effectively reducing its toxicity (Macomber and Imlay, 2009). Free amino acids such as methionine and histidine probably also participate in copper buffering (Fung et al., 2013; Pearce and Sherman, 1999). A third well-known mechanism of copper detoxification is its export by copper-translocating P-type ATPases. This mechanism is employed by *C. albicans* (Weissman et al., 2000). Although *C. albicans* possesses metallothionein CaCup1, it plays only a minor role in copper

* Corresponding author.
E-mail address: sutak@natur.cuni.cz (R. Sutak).

https://doi.org/10.1016/j.ijpddr.2020.10.001
Received 5 June 2020; Received in revised form 29 September 2020; Accepted 2 October 2020
Available online 7 October 2020

detoxification.

Less is known about copper detoxification in parasitic protists. *In silico* approaches have shown that at least some protists possess homologs of copper-transporting P-type ATPases and copper chaperones (Rasoloson et al., 2004). Most of the experimental evidence is available for *Plasmodium* as one of the most important human protozoan parasites. *Plasmodium falciparum* copper-transporting P-type ATPase (PfCu-P-ATPase), localizing to the plasma membrane of both the parasite and erythrocyte, is probably responsible for decreasing the copper content in the infected erythrocyte, suggesting that *P. falciparum* avoids copper toxicity by copper efflux (Rasoloson et al., 2004). P-type ATPase expression has also been demonstrated in *Trypanosoma brucei brucei,* where it is localized to subcellular vesicles and probably the cell membrane, although its detoxification function has not been confirmed (Isah et al., 2020). In *Trypanosoma cruzi,* a probable copper-transporting ATPase is upregulated in the intracellular stage in host cells compared with the extracellular stage in the insect vector (Meade, 2019). The intracellular stage has to survive in the phagosomal compartment with excessive copper levels, and the upregulation of copper translocating ATPase may indicate its role in detoxification.

Naegleria fowleri is a pathogenic free-living amoeba that is found in warm fresh water and sediments worldwide (Maciver et al., 2020; Mull et al., 2013; Sykora et al., 1983). It is often called a "brain-eating amoeba" because of its ability to infect humans, causing a rapid and deadly brain infection designated as primary amoebic meningoencephalitis (PAM). Infection occurs when water contaminated with *N. fowleri* enters the nose, for example, during swimming. The amoebae migrate via the olfactory nerve to the brain, where they multiply and destroy nerve cells, causing tissue damage and hemorrhagic necrosis. The disease has an abrupt onset, and most patients die within days after symptoms begin (Siddiqui et al., 2016). Treatment options are very limited: antibiotics and antifungals such as amphotericin B, fluconazole, rifampicin and miltefosine are usually used, but death rate is over 95%. Due to the rapid progression of the disease, the diagnosis is usually made after the patient's death (Bellini et al., 2018).

Although the genomes of *N. fowleri* as well as its nonpathogenic relative model amoeba *Naegleria gruberi* have been annotated, little is known about the physiology and biochemistry of this pathogen. Likewise, our understanding of the cellular processes that allow this free-living amoeba to survive and destroy the human host is very limited (Herman et al., 2020). We have recently described how *N. fowleri* respond to limited iron availability and how iron metabolism could potentially be exploited in antiamoebic interventions (Arbon et al., 2020). In the current study, we aimed to characterize the mechanisms employed by *N. fowleri* to deal with toxic copper levels. We show that a combination of antioxidant proteins with copper efflux mediated by copper-translocating ATPase is used to protect the cell and ensure high copper tolerance of *N. fowleri*. We also consider copper metabolism as a possible therapeutic target, since we demonstrated that copper ionophores are potent antiamoebic agents.

2. Materials and methods

2.1. Cell cultures

N. fowleri, strain HB-1, kindly provided by Dr. Hana Pecková (Institute of Parasitology, Biology Center CAS), was maintained in 2% Bactocasitone (Difco, USA), supplemented with 10% heat-inactivated fetal bovine serum (Thermo Fisher Scientific, USA), penicillin (100 U/ml) and streptomycin (100 μg/ml) in 25-cm^2 aerobic cultivation flasks at 37 °C. When required, the culture was cultivated for 72 h with the addition of 25 μM, 100 μM or 1 mM $CuSO_4$ (Sigma-Aldrich, USA). *N. gruberi* strain NEG-M (kindly provided by Lillian Fritz-Laylin, University of Massachusetts Amherst, USA) was cultivated in M7 medium (Fulton, 1974) supplemented with streptomycin (100 μg/ml) in 25-cm^2 aerobic cultivation flasks at 27 °C.

2.2. Copper and ionophore toxicity

To determine the IC_{50} values for copper, *N. fowleri* or *N. gruberi* cells were cultivated for 72 h in quadruplicate in black 96-well plates in 100 μl of medium per well with concentrations of copper up to 20 mM. To determine the IC_{50} values for ionophores, *N. fowleri* cells were grown for 72 h in triplicate in black 96-well plates in 100 μl of medium per well with 1 μM–10 μM concentrations of 8-hydroxyquinoline, pyrithione or disulfiram with or without the addition of 100 μM copper. Dimethyl sulfoxide (DMSO) was added to control cells in the case of DSF and 8-HQ testing as they were diluted in DMSO. The maximum DMSO concentration did not exceed 1%. The cell viability was determined using the CellTiter-Glo® Luminescent Cell Viability Assay (Promega, USA) according to the manufacturer's protocol. Statistical analysis was performed using GraphPad Prism 8.3.1 (www.graphpad.com).

2.3. Copper content determination

N. fowleri cells supplemented with 25 μM, 100 μM or 1 mM copper or with 1 μM 8-HQ in the presence or absence of 100 μM copper were grown in triplicate, washed three times (1000 g, 15 min, 4 °C) in 10 mM Hepes buffer, pH 7.2, containing 140 mM NaCl and pelleted. The pellets were dried at 100 °C, digested in 65% HNO_3 overnight and then for 2 h at 130 °C in Savillex vials and diluted in deionized water (Millipore, USA) to final volume 10 ml. The copper concentration was determined by inductively coupled plasma mass-spectrometry (ICP-MS) using iCAP Q ICP-MS (Thermo Fisher Scientific, USA).

2.4. Whole-cell proteomic analysis

N. fowleri cells supplemented with 25 μM $CuSO_4$ were used as a control, and cells supplemented with 100 μM or 1 mM copper were used for the copper overload investigation. The cells (grown in triplicate) were washed three times with PBS and pelleted. Whole-cell proteomic analysis of the samples was carried out using the method described by Mach et al. (2018) employing nanoflow liquid chromatography coupled with mass spectrometry (MS). The resulting MS data were searched with MaxQuant software (Cox et al., 2014) against the AmoebaDB (Aurrecoechea et al., 2011) *N. fowleri* database downloaded on Aug 6, 2018. The carbamidomethylation of cysteine (Unimod #: 4) was set as a fixed modification, and methionine oxidation (Unimod #: 35) was allowed as a variable modification. Further processing of the data was performed with Perseus software (Tyanova et al., 2016). Normalized label-free quantitation values of intensities were used. We filtered out reverse hits, potential contaminants and proteins identified only by site. Then, we took the log of the intensities (binary logarithms) and filtered out proteins with insufficient numbers of valid quantification values (leaving only those with at least 2 values in at least one group). The Student's t-test with Benjamini-Hochberg correction was used to evaluate significantly changed proteins at the 5% false discovery rate level. Only the proteins that changed more than 1.5-fold or those found in just one condition and having a normalized intensity greater than 23 were considered. The selected proteins were manually annotated using HHpred (Söding et al., 2005) or by sequence alignment with homologous proteins from other organisms using BLAST (Altschul et al., 1990). The mass spectrometry proteomics data have been deposited to the ProteomeXchange Consortium via the PRIDE (Perez-Riverol et al., 2019) partner repository with the dataset identifier PXD018807. The additional information about proteomic experimental procedures is summarized in Table S2. Bioinformatics analysis was performed using Geneious Prime® 2019.2.3 (www.geneious.com).

2.5. Western blotting

N. gruberi cells were grown with the addition of 25 or 750 μM copper. The primary polyclonal antibody against *N. fowleri* protoglobin was

generated as described by Mach et al. (2018). The produced antibodies were used for protoglobin detection in the Western blot analyses of *N. gruberi* whole-cell lysates. For Western blot development, anti-rat IgG peroxidase secondary antibodies (Merck, Germany) and Luminata Forte Western horseradish peroxidase substrate (Merck, Germany) were used.

2.6. Real-time PCR

Total RNA was isolated from *N. fowleri* cultures supplemented with 25 μM or 1 mM copper (grown in quadruplicate) using the High Pure RNA Isolation Kit (Roche, Switzerland). RT-PCR was conducted using the KAPA SYBR® FAST One-Step universal kit (Sigma-Aldrich, USA) according to the manufacturer's protocol in the RotorGene 3000 PCR cycler (Corbett Research, Australia) with the following thermocycle conditions: 42 °C for 30 min (reverse transcription), 95 °C for 5 min, 40 cycles of 95 °C for 10 s, 56 °C for 20 s, and 72 °C for 20 s; and melt-curve analysis from 55 °C to 95 °C with 1 °C step for 5 s per step. The transcript abundance was calculated after normalization to the endogenous reference gene β-actin. The primers are listed in Table 3.

2.7. RACE and cloning

The full 5′ sequence of Nf-CuATPase gene was determined by rapid amplification of 5′ cDNA ends using the FirstChoice™ RLM-RACE kit (Thermo Fischer Scientific, USA) according to the manufacturer's protocol. cDNA was synthesized with SuperScript™ III Reverse transcriptase (Thermo Fisher Scientific, USA). The Nf-CuATPase gene was amplified from cDNA using SapphireAmp® Fast PCR Master Mix (TakaraBio, Japan) and cloned into pCM189 plasmid with the tetracycline-regulatable promotor using FastDigest™ restriction enzymes and T4 DNA ligase (Thermo Fisher Scientific, USA).

2.8. Yeast procedures

Strains BY4741 (MATa; his3D1; leu2D0; met15D0; ura3D0), cup2Δ (BY4741; MATa; ura3Δ0; leu2Δ0; his3Δ1; met15Δ0; YGL166w::kanMX4) and ccc2Δ (BY4741; MATa; ura3Δ0; leu2Δ0; his3Δ1; met15Δ0; YDR270w::kanMX4) were obtained from Euroscarf (euroscarf.de). Yeast transformations were performed according to Gietz and Schiestl (2007). For phenotypic assays, yeast cultures were grown overnight in liquid synthetic complete medium without uracil (SC-ura); 5 μl of six serial ten-fold dilutions starting from OD_{600} 0.2 were plated on agar SC-ura plates. For assays with the cup2Δ strain, plates were supplemented with 1 mM $CuSO_4$ with or without 1 μg/ml doxycycline. For assays with the ccc2Δ strain, plates were supplemented with 50 μM bathophenanthroline disulfonate (BPS) with or without doxycycline, or with 50 μM BPS and 50 μM $(NH_4)_2Fe(SO_4)_2 \cdot (H_2O)_6$ (Sigma-Aldrich, USA). For copper content analysis, we used ICP-AES. Yeast cells were grown overnight in triplicate in liquid SC-ura medium supplemented with 0, 0.05, 0.1 or 0.5 mM copper, washed three times (3000 g, 5 min, 4 °C) in ultrapure water and pelleted. All further manipulations were performed as described above for *N. fowleri*.

Table 1
Selected *N. fowleri* proteins that were significantly changed in 1 mM $CuSO_4$ compared with 25 μM $CuSO_4$. Arrows indicate upregulation (no downregulated proteins were selected).

Fold change	Gene number in AmoebaDB database	Annotation
↑ 11.2	NF0109980	Predicted protein
↑ 4.9	NF0013290	Probable methanethiol oxidase
↑ 4.3	NF0127030	Hemerythrin
↑ 3.6	NF0021200	Copper-transporting ATPase
↑ 3.5	NF0028890	Glutathione S-transferase
↑ 3.5	NF0117840	Protoglobin
↑ 2.1	NF0071710	Deferrochelatase/peroxidase
↑ 2.1	NF0042620	Glutathione S-transferase
↑ 1.9	NF0036980	Thioredoxin reductase
↑ 1.9	NF0112140	Sulfiredoxin
↑ 1.8	NF0061690	Protoglobin domain-containing protein
↑ 1.8	NF0108900	Glutathione S-transferase

Table 2
The changes in transcript abundancy of selected genes in 1 mM $CuSO_4$ compared with 25 μM $CuSO_4$ determined by real-time PCR. Arrows indicate down-regulation or upregulation. Significantly changed genes (p-value < 0.05) are marked with a star. Cells were grown in quadruplicate.

	Fold change	p-value
Nf-CTR (1)	↓ 1.17	4.3914
Nf-CTR (2)	↓ 2.27	0.2666
Nf-CuATPase	↑ 4.21*	0.0491
Nf-Hemerythrin	↑ 4.71*	0.0057
Nf-Protoglobin	↑ 7.10*	0.0002

3. Results

3.1. Copper and copper ionophores are toxic to N. fowleri

Excess copper is toxic for *N. fowleri*, although it survives at relatively high copper concentrations: the half maximal inhibitory concentration (IC_{50}) of copper for *N. fowleri* is 1.62 mM (95% confidence interval from 1.48 to 1.70, Fig. 1). Copper is dramatically more toxic for *N. fowleri* when provided in the presence of lipid-soluble ionophores – substances that transport ions across the plasma membrane, such as pyrithione (PyS), disulfiram (DSF) or 8-hydroxyquinoline (8-HQ). We tested the toxicity of these compounds in the absence of copper and with the addition of 100 μM copper – a relatively low concentration that is well below the IC_{50} and does not inhibit *N. fowleri* growth. Dimethyl sulfoxide (DMSO) was added to the control cells for the testing of DSF and 8-HQ, as they were diluted in DMSO. The maximum concentration of DMSO did not exceed 1%, and we did not observe any significant effect of DMSO on the growth of amoebae even at the highest concentration used. All three tested ionophores showed copper-dependent amoebicidal activity (Fig. 1). The IC_{50} of DSF in the presence of copper was 2.09 μM, and the IC_{50} of PyS was 1.05 μM and of 8-HQ was 2.09 μM. We believe that these results show a promising potential of ionophores as future potent antiamoebic agents.

3.2. Copper accumulation in N. fowleri

To determine how copper concentrations in the growth medium influence the amount of copper accumulated in cells, we used inductively coupled plasma mass spectrometry (ICP-MS). As a control, we used amoebae grown in 25 μM $CuSO_4$. The copper concentration in the growth medium before adding $CuSO_4$ was less than 1 μM. Copper accumulation in the amoebae was dependent on the concentration of free copper in the medium (Fig. 2): copper content in control cells was 84.10 ± 17.85 ng/mg dry mass, while the addition of 100 μM copper to the medium increased the copper content in the amoebae ~3.5-fold. The amount of copper in cells supplemented with 1 mM $CuSO_4$ was 369.21 ± 20.03 ng/mg dry mass which was slightly higher than in medium with 100 μM $CuSO_4$, however, the difference was not statistically significant.

Additionally, we determined the amount of copper in cells treated with the ionophore 8-HQ in the absence or presence of 100 μM $CuSO_4$ (Fig. 2). In the cells which were not supplemented with $CuSO_4$ the copper content was 8.64 ± 1.09 ng/mg, while supplementation with copper increased it to 259.08 ± 48.62 ng/mg. This number was close to the copper content in the cells grown with 100 μM $CuSO_4$ without the ionophore. Thus, the treatment of *N. fowleri* with the copper ionophore 8-HQ did not increase the amount of copper in the cells.

Table 3
Primers used for real-time PCR and product sizes.

	Forward primer	Reverse primer	Product size
Nf β-actin	TTGGTATGGAAGCTGCTGGT	AACCTCCAATCCAGACCGAG	231
Nf-CTR (1)	TGGTGAAGAGAAAGGTGACCA	ATCCGACAGTGTTACCAGCA	225
Nf-CTR (2)	GTGAAACTACAGAGCATGAGGA	CTCCTGACTGAAGAGCTCGT	220
Nf-CuATPase	ATTGGTGGAACCGTCAATGT	GCAAGATGACAGCAGGAACA	178
Nf-Hemerythrin	CCAACAGATCCAGTGCTTCA	TGTGATTCACCAACCATTGC	210
Nf-Protoglobin	CGAGGAACAACGTGTCAAGA	TTGTTGAGCAAAGCAGCATC	175

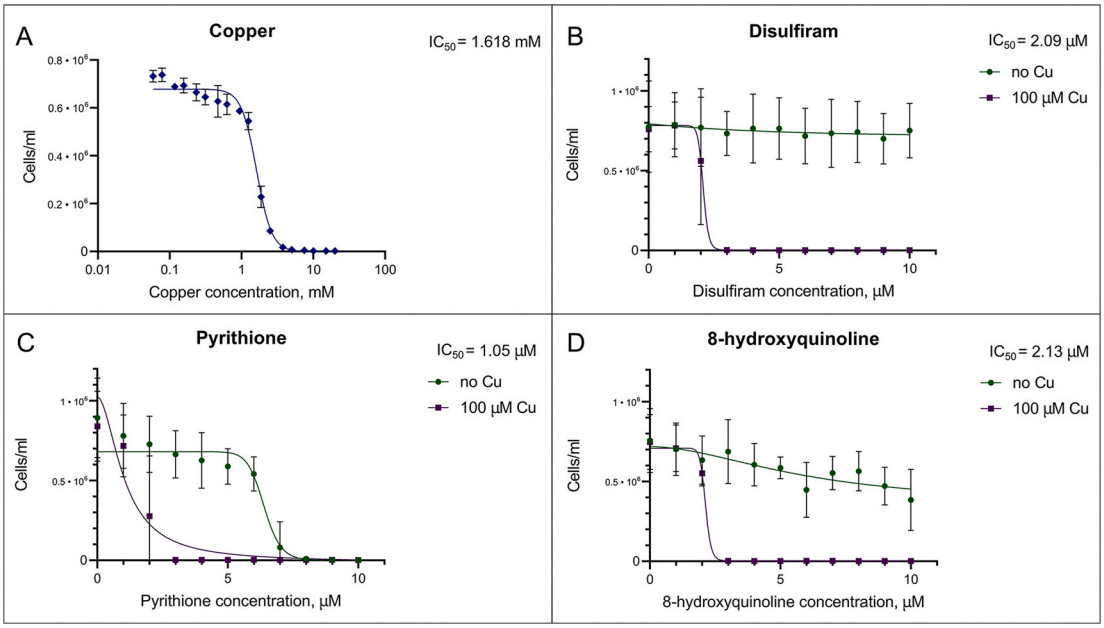

Fig. 1. Copper and copper ionophore toxicity to *N. fowleri*. **A**. Copper toxicity to *N. fowleri* cells after 72 h in the presence of different concentrations of $CuSO_4$. Cells were grown in quadruplicate. **B-D**. Determination of the IC_{50} of ionophores on *N. fowleri* in the presence or absence of 100 µM $CuSO_4$. Cells were grown in triplicate.

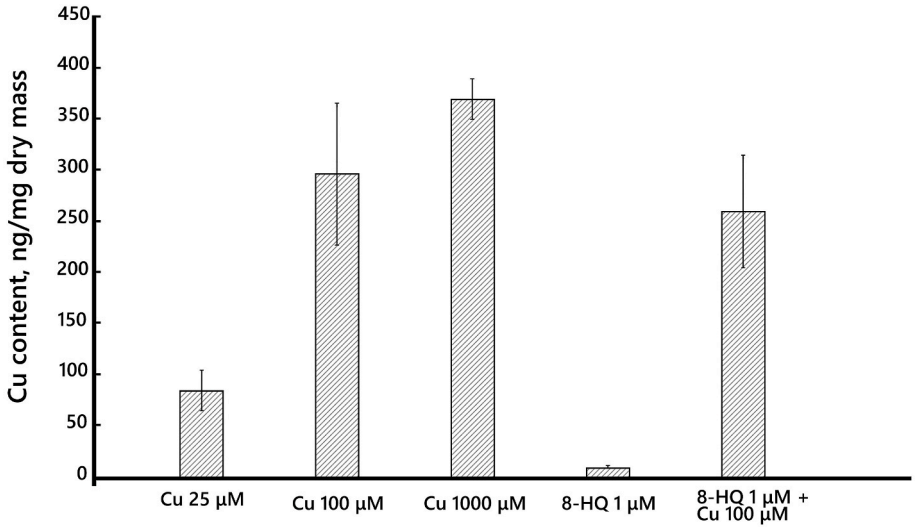

Fig. 2. Copper content in *N. fowleri* cells grown in media supplemented with 25 µM, 100 µM or 1 mM $CuSO_4$, or with 1 µM 8-HQ in absence or presence of 100 µM $CuSO_4$. Data represent the mean with 95% confidence intervals of three replicates.

3.3. Proteomic analysis of the N. fowleri response to high copper concentrations identified a set of detoxification proteins

To identify the proteins responsible for copper detoxification in *N. fowleri*, we analyzed the whole-cell proteomes (including soluble and membrane proteins) of amoebae grown in medium supplemented with 25 µM $CuSO_4$ as a control and either 100 µM or 1 mM $CuSO_4$, with the latter being considered a toxic copper concentration. We identified 57 proteins that were significantly changed when the cells were grown in 1 mM copper: 36 upregulated and 21 downregulated (Supplementary

Table 1). When 100 μM copper was added to the medium, there were no statistically significant changes in protein expression levels compared with the control conditions. The proteins most relevant for this study are summarized in Table 1.

The most upregulated protein (NF0109980 in AmoebaDB Database (Aurrecoechea et al., 2011)) did not show any significant homology to known proteins. It contained 133 amino acid residues, including 4 cysteine-proline motifs and 6 histidines, which might indicate copper- or iron-binding properties (Kung et al., 2006; Wu et al., 2010; Zhang and Guarente, 1995). The second most upregulated protein (NF0013290) showed homology to methanethiol oxygenases and to a family of selenium-binding proteins.

Importantly, we observed a 3.6-fold upregulation of a protein homologous to copper-translocating P-type ATPase (which we named Nf-CuATPase). Copper transporting ATPases have been shown to mediate copper tolerance and detoxification in *C. albicans* (Weissman et al., 2000) and *P. falciparum* (Rasoloson et al., 2004), suggesting a similar role in *N. fowleri*.

Moreover, among the 36 upregulated proteins, at least 9 are known or proposed to be oxidative stress related, namely, three glutathione S-transferases (GSTs), thioredoxin reductase, sulfiredoxin, deferrochelatase/peroxidase (dye-decolorizing peroxidase), a hemerythrin-like and two protoglobin-like proteins. Since a homolog of protoglobin is also present in the genome of the nonpathogenic amoeba *N. gruberi*, we were curious to determine whether its expression was affected by copper toxicity similarly to in *N. fowleri*. Western blot analysis using a specific antibody against *N. gruberi* protoglobin confirmed the induction of protein expression under conditions of copper toxicity (Supplementary Fig. 1), suggesting a common detoxification mechanism in *Naegleria*.

3.4. Bioinformatics analysis of Nf-CuATPase confirms its structural similarity to copper-translocating ATPases

Since the annotation of Nf-CuATPase in the AmoebaDB database (Aurrecoechea et al., 2011) is incomplete at the N-terminal end of the protein, we performed a rapid amplification of cDNA ends (RACE) to obtain the full mRNA sequence. The correct Nf-CuATPase gene had 1330 amino acids with no introns. Topology prediction programs, including CCTop (Dobson et al., 2015), Phobius (Käll et al., 2004), Scampi (Bernsel et al., 2008) and others, proposed 8 transmembrane domains and 3 cytosolic segments, including a long N-terminal part (Fig. 3) containing 5 CXXC motifs, which are considered to be involved in binding heavy metals such as copper and cadmium (Solioz and Vulpe, 1996). The overall topology with the first small and second big cytosolic loop was characteristic of P-type ATPases. The number of transmembrane domains indicated a heavy metal ATPase: it had four transmembrane domains between the N-terminus and small cytosolic loop (while nonheavy metal ATPases only have two) and, in contrast, only two transmembrane domains preceding the C-terminus instead of four or six characteristic of nonheavy metal ATPases (Solioz and Vulpe, 1996). The second cytoplasmic loop of Nf-CuATPase encompassed the highly conserved D^{1013}-K-T-G-T^{1017} phosphorylation motif containing the aspartate residue, which is phosphorylated by ATP, and the G^{1217}-D-G-I-N-D-A-P^{1224} site presumably involved in ATP binding (Møller et al., 1996). The first cytoplasmic domain contained the invariant T^{851}-G-E^{853} motif, which is probably necessary for stabilization of phosphorylated aspartate (Kühlbrandt, 2004). There was a proline residue 43 amino acids upstream of the phosphorylation site in the predicted transmembrane domain, which is conserved in all P-type ATPases and considered to be involved in ion transduction. Together with two surrounding cysteines, it forms the C^{969}–P–C^{971} motif, which is believed to be necessary for the translocation of heavy metals. Downstream from the phosphorylation site, a histidine-proline dipeptide was present. This is a peculiar feature for heavy metal ATPases, and although its function is unknown, it is not found in other ATPases (Solioz and Vulpe, 1996). Alignments with other copper-transporting ATPases with confirmed function are presented on Fig. S3.

3.5. RT-PCR of selected copper-regulated genes

The genome of *N. fowleri* contains two homologs of yeast and human high-affinity copper transporters (CTRs) that presumably mediate copper influx. It would be rational to expect copper influx to be downregulated at high copper concentrations, as shown in *C. albicans* (Mackie et al., 2016) and *C. neoformans* (Ding et al., 2013). We did not identify any CTRs in our proteomic data, which was not unexpected considering that membrane transporters might be lost during sample preparation for proteomic analyses (Harwood et al., 2014). Thus, to investigate the regulation of putative *N. fowleri* copper transporters at high copper concentrations, we conducted RT-PCR using cells grown with 25 μM or 1 mM $CuSO_4$. Additionally, we investigated relevant genes encoding proteins that were upregulated by toxic copper levels based on the proteomic analysis (Nf-CuATPase, hemerythrin and protoglobin) to determine whether they were regulated at the transcriptional or translational level.

Our results showed that, while there was no statistically significant

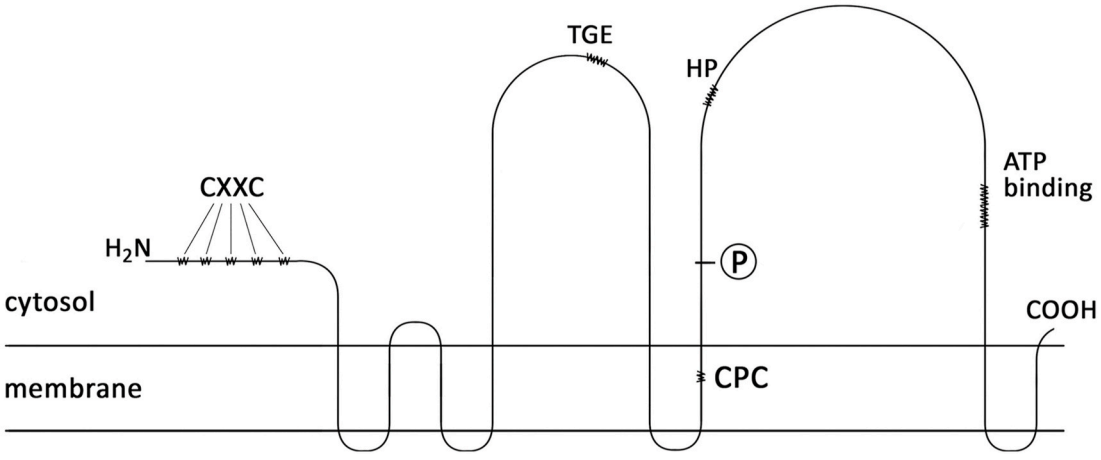

Fig. 3. Schematic representation of the Nf-CuATPase membrane topology and of its key features: 5 CXXC motifs near the N-terminus are supposed to be involved in copper binding; the TGE motif is needed for stabilization of phosphorylated aspartate; the CPC motif in the transmembrane domain is necessary for copper translocation; P indicates conserved aspartate, which is phosphorylated and dephosphorylated in the enzymatic cycle; the HP motif with unknown function is typical for heavy metal ATPases; the ATP binding site participates in ATP binding.

change in the CTR1 and CTR2 transcription levels between control and copper-loaded cells, Nf-ATPase was indeed upregulated at the transcriptional level and increased 4.21 ± 1.57 times under copper overload (Table 2). Nf-protoglobin and Nf-hemerythrin were also increased 7.10 ± 2.28 and 4.71 ± 1.07 times, respectively. Thus, the response of amoebae to copper stress appeared to occur at the transcriptional level, in contrast to the iron-starvation-induced changes that were almost exclusively post-transcriptional in *N. fowleri* (Arbon et al., 2020).

3.6. *N. fowleri Cu-ATPase complements the S. cerevisiae cup2Δ mutant*

To validate a role for Nf-CuATPase in copper detoxification, we cloned the gene into a yeast expression plasmid pCM189 with the tetracycline-regulatable promotor and transformed two *S. cerevisiae* strains impaired in copper metabolism: the cup2Δ strain lacks a copper metallothionein transcription activator and fails to grow at high copper concentrations; the ccc2Δ strain is deficient in trans-Golgi copper-translocating ATPase and is unable to grow on media containing iron chelators due to inefficient copper incorporation into the multicopper iron oxidase involved in iron acquisition. In agreement with the proposed role in copper detoxification, Nf-CuATPase enables the cup2Δ strain to grow at high copper concentrations, and the effect is lost in the presence of doxycycline, which blocks transcription from the plasmid (Fig. 4). Similar to the copper transporting ATPase of *C. albicans* CaCrp1 (Weissman et al., 2000), Nf-CuATPase was unable to functionally complement the ccc2Δ mutant and restore its defective growth on medium containing the iron chelator bathophenanthroline disulfonate (BPS) (Fig. 4), indicating that it does not translocate copper into trans-Golgi vesicles. To localize Nf-CuATPase, we overexpressed the Nf-CuATPase-GFP fusion as well as Nf-CuATPase fused to the hemagglutinin (HA) epitope tag in the cup2Δ mutant; however, neither of the fusion proteins complemented the mutant copper sensitivity (data not shown). Thus, we decided to establish the localization of the protein indirectly to determine whether Nf-CuATPase exports copper from the cell or compartmentalizes it within the cell.

3.7. *Analysis of copper content in transformed yeast*

To determine whether copper was transported outside or accumulated within the cell, we carried out ICP-AES analysis of copper content in wild type yeast cells (BY4741) containing empty pCM189, cup2Δ mutant cells with empty plasmid and cup2Δ cells expressing Nf-CuATPase (Fig. 5). From the obtained data, it was evident that copper content in wild type and cup2Δ yeasts was significantly higher than in Nf-CuATPase-expressing cup2Δ cells. The amount of copper in wild type grown in 0.05 and 0.1 mM copper was approximately twice as high compared with the Nf-CuATPase-expressing mutant, which strongly suggested that Nf-CuATPase exports copper.

4. Discussion

Copper is an essential element for life. There are at least thirty enzymes containing copper cofactors catalyzing redox reactions or transporting dioxygen (Flemming and Trevors, 1989). However, copper is toxic when present in excess as it displaces iron in Fe–S clusters and promotes oxidative stress, possibly via the Fenton reaction caused by released iron (Macomber and Imlay, 2009). Copper toxicity is employed by innate immune cells in host-parasite interactions: macrophages actively accumulate copper and use it against pathogens (Sheldon and Skaar, 2019; White et al., 2009). High copper resistance is crucial for the

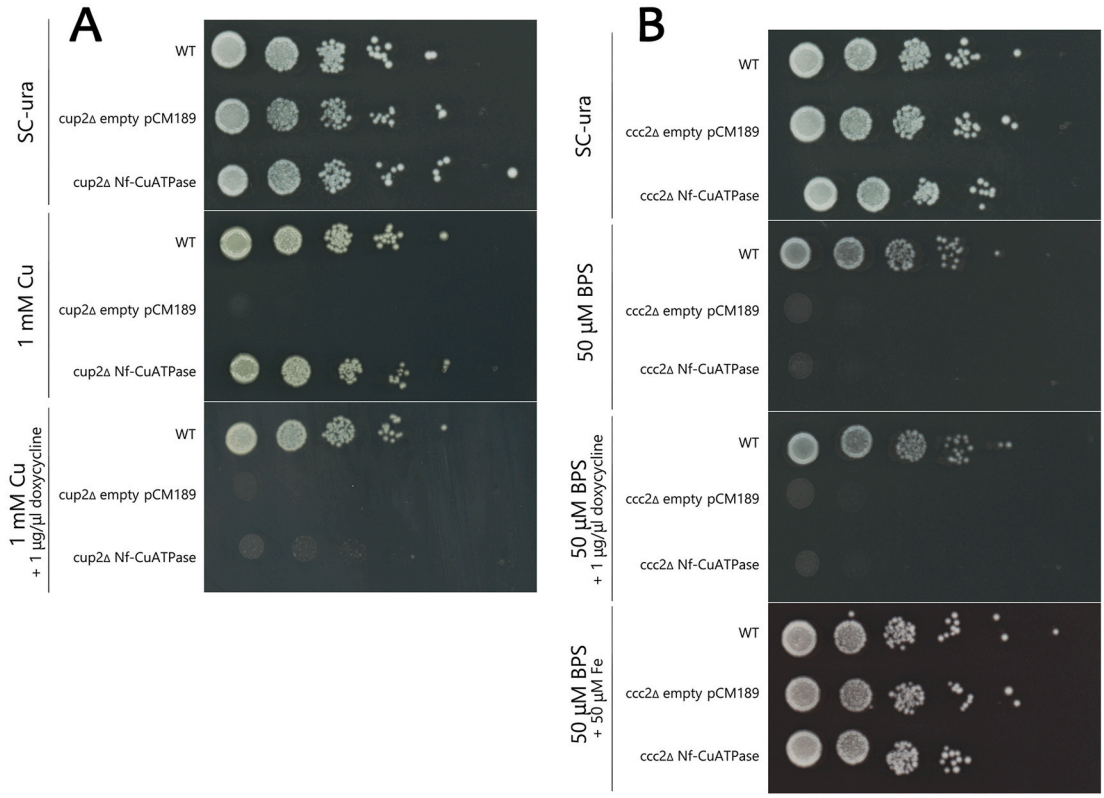

Fig. 4. Nf-CuATPase functional complementation of the *S. cerevisiae* cup2Δ copper sensitivity and inability to complement ccc2Δ defective growth on medium containing the iron chelator. Wild type strain BY4741 (WT) transformed with empty tetracycline-regulatable plasmid, cup2Δ and ccc2Δ mutant strains transformed with empty plasmid or plasmid carrying Nf-CuATPase were spotted on synthetic complete medium without uracil (SC-ura) and grown for 3 days at 30 °C. **A.** The cup2Δ mutant with empty vector failed to grow on SC-ura supplemented with 1 mM $CuSO_4$, while cup2Δ-expressing Nf-CuATPase grew normally. This effect was eliminated by doxycycline, which blocks transcription from the vector. **B.** Nf-CuATPase was unable to restore ccc2Δ mutant defective growth on medium containing the 50 µM iron chelator bathophenanthroline disulfonate (BPS). Iron supplementation restored the growth of the mutant.

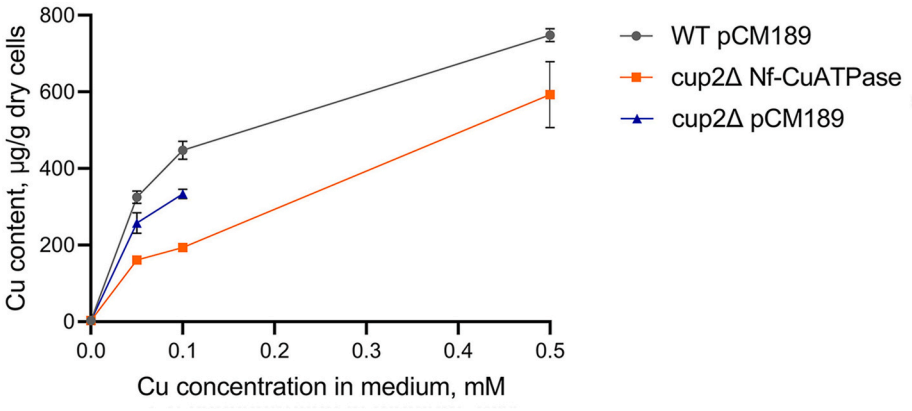

Figure 5. Copper content in *S. cerevisiae* cells grown under different copper concentrations. Wild type strain BY4741 (WT) transformed with empty plasmid (pCM189) and cup2Δ mutant strain transformed with the empty plasmid or the plasmid carrying Nf-CuATPase were grown overnight in liquid SC-ura medium supplemented with 0, 0.05, 0.1 or 0.5 mM $CuSO_4$ and analyzed for copper content. The amount of copper in wild type and mutant cells with empty plasmid was higher than in Nf-CuATPase-expressing mutant cells, suggesting that Nf-CuATPase exports copper. Cup2Δ with empty plasmid failed to grow at copper concentrations higher than 0.1 mM. Cells were grown in triplicate; data represent the mean with 95% confidence intervals.

virulence of many pathogenic species, and deletions of copper resistance-related genes result in severe virulence reduction (Hodgkinson and Petris, 2012). Resistance to copper is higher in pathogenic yeasts *C. albicans* and *C. neoformans* compared with nonpathogenic *S. cerevisiae*, suggesting that efficient copper detoxification is essential for occupation of niches within a host (Ding et al., 2013; Weissman et al., 2000).

In this study, we explored copper resistance of the human pathogenic protist *N. fowleri*. The half maximal inhibitory concentration (IC_{50}) of copper on *N. fowleri* was 1.62 mM (Fig. 1), which was lower than that obtained for *C. neoformans* but higher than that estimated for *S. cerevisiae* (although comparisons are difficult because the chemistry of metals may differ in different media even for the same species). The IC_{50} of copper on *C. neoformans* was shown to be 2.3 mM (Ding et al., 2013), on *C. albicans* approximately 10 mM (Weissman et al., 2000), on *S. cerevisiae* approximately 1.1 mM and on *N. gruberi* (a close nonpathogenic relative of *N. fowleri*) approximately 1.05 mM (this work, Supplementary Fig. 2). Unlike *C. neoformans*, *N. fowleri* infection progresses from the primary site directly to the brain, a niche that is rather depleted of copper bioavailable to pathogens: experimental evidence showing the upregulation of high-affinity copper importers in *C. neoformans* during brain infection is in agreement with the reduced copper availability in the brain (Smith et al., 2017). Thus, it is questionable whether such a high copper tolerance plays a role in the pathogenicity of *N. fowleri*. Conversely, we cannot exclude the possibility that the parasite faces high copper concentrations during immune response in later stages of the disease.

Nevertheless, high copper tolerance may be beneficial for *N. fowleri* in its natural habitats. The levels of biologically available copper in the environment are rising as a result of anthropogenic activities (Flemming and Trevors, 1989). Elevated copper levels have been widely documented in surface waters and especially sediments which are the natural habitat of *N. fowleri* (Mull et al., 2013; Sykora et al., 1983). The addition of copper changes sediment microbial communities structure and modifies the levels of biological processes (Ahmed et al., 2018). Organisms that are highly tolerant to elevated copper, including *N. fowleri*, may thrive in such environments and become more prevalent.

Copper toxicity is exploited not only by the immune system but also in chemotherapeutic interventions. The lipophilic substances that reversibly bind ions and transfer them across the cell membrane, called ionophores, show anticancer and antimicrobial activity (Ding and Lind, 2009; Helsel et al., 2017). Several ionophores, such as 8-hydroxyquinoline (8-HQ), pyrithione (PyS), thiosemicarbazones and others, are known to increase the copper content in cells (Helsel et al., 2017; Reeder et al., 2011). The mechanism of ionophore action is not completely understood.

Ionophores 8-HQ, PyS, disulfiram (DSF) and thiomaltol have been shown to have strong fungicidal activity against *C. neoformans* in the presence of copper (Helsel et al., 2017). Also, derivatives of 8-HQ have been tested as potential drugs for Alzheimer disease: *in vitro* assays, experiments with transgenic mice and pilot phase clinical trials demonstrated their neuroprotective effects and high blood brain barrier permeability (Adlard et al., 2008; Song et al., 2015; Yang et al., 2018). Since *N. fowleri* is a parasite occupying brain, we proposed that some of the copper ionophores may be repurposed as potential agents against primary amoebic meningoencephalitis if they show strong antiamoebic properties, although investigation of mechanism of action and cellular targets is needed.

In our study, we tested the effect of 8-HQ, PyS and DSF on *N. fowleri* in the absence and presence of copper (Fig. 1). All three compounds demonstrated copper-dependent amoebicidal activity with the lowest IC_{50} for PyS (1.05 µM) and slightly higher IC_{50} for 8-HQ and DSF (~2.1 µM), representing ionophore antimicrobial efficiency similar to that observed against *C. neoformans* (Helsel et al., 2017). We believe that these results are promising, especially considering the possibility of employing more effective ionophore derivatives. A remarkable approach is the use of inactive prochelator which is converted to 8-HQ via reactive oxygen species produced by the immune system, a strategy shown to be effective *in vivo* against *C. neoformans* (Festa et al., 2014). Nevertheless, it is important to understand the mechanism of action and cellular targets of ionophores in *N. fowleri*. Since the antiamoebic properties of these ionophores are copper-mediated, we studied the mechanisms generally exploited by *N. fowleri* for copper detoxification.

First, we studied the copper content in *N. fowleri* cells grown in different copper concentrations. The amount of copper in the amoebae under normal conditions was 84.10 ± 17.85 ng per mg dry mass. The addition of copper to growth medium up to 1 mM concentrations did not affect the growth of amoebae, although the amount of copper inside the cells significantly increased: 100 µM and 1 mM copper in the medium increased the copper content in the amoebae to 295.90 ± 61.09 and 369.21 ± 17.70 ng/mg, respectively (Fig. 2). Further, we determined the copper content in the cells grown with the addition of the ionophore 8-HQ in the absence or presence of 100 µM $CuSO_4$ (Fig. 2). The amount of copper in the cells grown in 100 µM $CuSO_4$ with 8-HQ was the same as in the cells grown in the same copper concentration without the ionophore. Thus, the addition of 8-HQ did not increase the amount of copper in the amoebae. Presumably, this ionophore rather promoted copper toxicity against the amoebae than mediated killing of the cells by increasing intracellular copper concentration.

To inspect the proteins involved in copper detoxification, we analyzed the whole-cell proteomes of amoebae grown in media containing different concentrations of $CuSO_4$. The most upregulated protein NF0109980 (11.2-fold change in 1 mM CuSO4) showed homology to an unknown protein from another species of the same genus, *N. gruberi,* but not to any other known proteins. The protein is rather short: it contains

101 amino acid residues, containing 6 histidines, including H-(X)7-H and H-(X)12-H motifs, and 4 cysteine-proline motifs, which might indicate that it binds copper (Kung et al., 2006; Wu et al., 2010) or interacts with heme (Ogawa et al., 2001; Shimizu, 2012; Zhang and Guarente, 1995).

The second most upregulated protein (NF0013290) was a probable methanethiol oxidase: this enzyme oxidizes methanethiol to formaldehyde and hydrogen sulfide. Its bacterial homolog was recently shown to be copper-dependent, and the enzyme is widely distributed among bacteria from different environmental samples and participates in global marine carbon and sulfur cycling (Eyice et al., 2018). However, the role of methanethiol oxidase in *N. fowleri* metabolism is obscure. Upregulation of this enzyme may demonstrate an increased turnover of cellular sulfur-containing compounds and mobilization of available sulfur sources for the synthesis of protective compounds such as glutathione. Glutathione balance is highly important for copper homeostasis. It effectively buffers copper and reduces its toxicity.

The importance of glutathione and thiol groups for *N. fowleri* subjected to high copper concentrations is emphasized by upregulation of three probable GSTs, thioredoxin reductase and sulfiredoxin. *i*/GSTs are known to participate in detoxification processes conjugating glutathione to different compounds (Vuilleumier and Pagni, 2002). The data regarding the influence of copper on GSTs are controversial; however, there is evidence that GSTs may be inhibited by increased copper concentrations (Cunha et al., 2007; Letelier et al., 2006; Salazar-Medina et al., 2010). Additionally, certain GSTs are upregulated at the transcriptional level under copper toxicity (Rhee et al., 2007). Thus, upregulation of GST expression may compensate for its reduced enzymatic activity. *ii*/Thioredoxin reductase and thioredoxin comprise the major cellular disulfide reducing system. Thioredoxins are multifunctional dithiol-containing proteins: they are used as a substrate for reductive enzymes, or function as protein disulfide oxidoreductases, or regulate the enzymes or receptors (Holmgren, 1985). Thioredoxin reductase is an enzyme that specifically reduces the disulfide bond in the active site of oxidized thioredoxin (Arnér and Holmgren, 2000). The thioredoxin reductase/thioredoxin system regenerates the proteins inactivated by oxidative stress (Fernando et al., 1992; Holmgren and Lu, 2010). *iii*/-Sulfiredoxin is an antioxidant protein that reduces sulfinic acid to cysteine residues (Biteau et al., 2003). Sulfiredoxin and subsequent thioredoxin action regenerate thiol groups in various proteins. Another function of sulfiredoxin is to deglutathionylate proteins. Glutathionylation occurs under oxidative stress conditions when a glutathione thiol radical reacts with a thiol group of protein forming a disulfide bond, and sulfiredoxin reverses this process (Findlay et al., 2006).

The upregulation of these proteins indicates that the thiol-reducing system is of particular importance under copper overload and assumes that copper causes oxidative stress, either directly or indirectly.

Interestingly, a hemerythrin-like protein was highly upregulated (4.3-fold) under copper overload. Hemerythrins are ancient iron-containing oxygen-binding respiratory proteins of some marine invertebrates (Bailly et al., 2008). Hemerythrin-like proteins are also found in bacteria, archaea and some eukaryotic groups including humans; however, their functions are not clear. They are proposed to be oxygen or iron sensors, oxygen carriers, or to act as protectors under oxidative stress conditions (Alvarez-Carreño et al., 2018). Also, among the proteins that were considerably upregulated under excessive copper we found two homologs of a heme-containing protein, protoglobin. Protoglobins are ancient archaeal and bacterial proteins that can bind O_2, CO and NO. Their functions remain unknown, although they have been proposed to participate in CO metabolism for methanogenesis or in scavenging reactive nitrogen and oxygen species, or to act as oxygen sensors (Pesce et al., 2013). The upregulation of hemerythrin and protoglobin in copper-overloaded *N. fowleri* cells is intriguing and may indicate their protective role against oxidative stress. Macomber and Imlay (2009) proposed that free iron is released from Fe–S clusters due to the action of copper. We believe that hemerythrin may participate in iron buffering to prevent the Fenton reaction. This hypothesis is supported by the finding that hemerythrin is dramatically regulated by iron availability in both *N. fowleri* and *N. gruberi* (Arbon et al., 2020; Mach et al., 2018). However, both hemerythrin and protoglobin of *N. fowleri* failed to functionally complement the cup2Δ yeast mutant (data not shown), probably due to the lack of some redox partner or other interacting protein in the yeast cell. Thus, the exact function of hemerythrin and protoglobin in *Naegleria* metal homeostasis and/or oxidative stress response remains to be elucidated.

Importantly, the proteomic analysis revealed the upregulation of a P-type copper translocating ATPase (Nf-CuATPase), a protein homologous to CaCrp1 of *C. albicans* as well as human ATP7A and ATP7B and *S. cerevisiae* CCC2. CaCrp1 is localized to the plasma membrane and extrudes copper into the environment, thus functioning as the main copper detoxification system in *C. albicans* (Weissman et al., 2000). Detoxification of copper by the efflux pump was also demonstrated for *A. fumigatus* (Wiemann et al., 2017) and *P. falciparum* (Rasoloson et al., 2004). However, *S. cerevisiae* CCC2 is localized to the Golgi apparatus and is not employed for copper detoxification (Yuan et al., 1997). Human ATP7A and ATP7B are normally localized to the Golgi network and participate in copper trafficking but not detoxification (Lutsenko et al., 2007). Additionally, a copper translocating ATPase was recently demonstrated to be expressed in *T. brucei brucei*, although its detoxification or trafficking function has not been confirmed (Isah et al., 2020).

Bioinformatics analysis of the Nf-CuATPase sequence predicted a topology typical of copper-translocating ATPases and indicated the presence of all the sites required for functional ATP-dependent copper transport, including a cysteine-containing binding site, conserved phosphorylation and ATP-binding sites, among others (Fig. 3, Fig. S3). Due to the lack of established protocols for *N. fowleri* transfection or knockout, we employed a yeast model to investigate the mechanism of Nf-CuATPase copper detoxification. To test whether Nf-CuATPase extrudes copper from the cytosol to the environment or actions in the trans-Golgi compartment, we cloned Nf-CuATPase into a yeast expression vector and tested its functional complementation in two *S. cerevisiae* mutants, cup2Δ and ccc2Δ. The first one failed to express metallothioneins for copper detoxification, and the second one lacked Golgi-localized ATPase CCC2. Nf-CuATPase allowed the cup2Δ strain to grow in high copper concentrations, but it was unable to functionally complement ccc2Δ (similarly to copper-transporting ATPase of *C. albicans* CaCrp1 (Weissman et al., 2000),), indicating that it did not translocate copper into trans-Golgi vesicles but rather functioned in a copper toxicity resistance mechanism. Thus, it might be localized to the plasma membrane, as observed for *C. albicans* CaCrp1, or to some subcellular compartment such as the vacuole, shown to play a role in maintaining copper homeostasis in *S. cerevisiae* (Szczypka et al., 1997). We were not able to establish the localization of Nf-CuATPase using the GFP fluorescent tag or hemagglutinin epitope tag since the fusion proteins did not complement the cup2Δ mutant copper sensitivity, possibly due to mislocalization or loss of function caused by the fusions. However, we found that Nf-CuATPase-expressing cup2Δ yeasts grown in media with copper overload accumulated less copper than wild type cells and cup2Δ cells with an empty plasmid. These results indicated that Nf-CuATPase transported copper outside the cell rather than compartmentalizing it within the cell. Thus, it is more probable that Nf-CuATPase localizes to the plasma membrane and mediates copper efflux, akin to *C. albicans* CaCrp1, although more studies will be needed to verify the localization of this protein once appropriate antibodies or effective transfection system for *N. fowleri* are available.

We observed no significant increase of the copper content in the cells grown with 1 mM extracellular copper compared to the cells grown with 100 μM copper, which could be the effect of either upregulation of copper export or the restriction of copper import. It is known that *C. albicans*, *C. neoformans* and *A. fumigatus* downregulate copper importers under copper overload (Ding et al., 2011; Mackie et al., 2016;

Wiemann et al., 2017). Although the *N. fowleri* genome contains two CTR homologs that might function in copper influx, RT-qPCR data demonstrated that their expression was not significantly changed at the transcriptional level. Apparently, *N. fowleri* relies more on the removal of excessive copper by Nf-CuATPase than on copper influx restriction.

In conclusion, our data demonstrate that *N. fowleri* employs a range of different strategies to ensure its high copper tolerance, including copper efflux and production of antioxidant enzymes and obscure hemerythrin-like and protoglobin-like proteins. This capability can be advantageous for amoebae both in the natural environment and in the host. Nevertheless, copper metabolism may be considered a therapeutic target since copper ionophores have been demonstrated to be potent antiamoebic agents.

Declaration of competing interest

The authors declare that they have no conflicts of interests.

Acknowledgements

This work was supported by Research and Development for Innovations Operational Programme "The equipment for metabolomic and cell analyses" [grant number CZ.1.05/2.1.00/19.0400]; Ministry of Education, Youth and Sports of the Czech Republic [grant numbers NPU II LQ1604, CePaViP CZ.02.1.01/0.0/0.0/16_019/0000759]; Czech Science Foundation [grant number 20-28072S]; MiCoBion project funded from EU Horizon 2020 [grant number 810224]; Charles University Grant Agency [grant number 1218120].Special thanks to Prof. Dennis J. Thiele for helpful scientific discussion.

Appendix A. Supplementary data

Supplementary data to this article can be found online at https://doi.org/10.1016/j.ijpddr.2020.10.001.

References

Adlard, P.A., Cherny, R.A., Finkelstein, D.I., Gautier, E., Robb, E., Cortes, M., Volitakis, I., Liu, X., Smith, J.P., Perez, K., Laughton, K., Li, Q., Charman, S.A., Nicolazzo, J.A., Wilkins, S., Deleva, K., Lynch, T., Kok, G., Ritchie, C.W., Tanzi, R.E., Cappai, R., Masters, C.L., Barnham, K.J., Bush, A.I., 2008. Rapid restoration of cognition in Alzheimer's transgenic mice with 8-hydroxy quinoline analogs is associated with decreased interstitial Aß. Neuron 59, 43–55.

Ahmed, A.M., Lyautey, E., Bonnineau, C., Dabrin, A., Pesce, S., 2018. Environmental concentrations of copper, alone or in mixture with arsenic, can impact river sediment microbial community structure and functions. Front. Microbiol. 9, 1–13.

Altschul, S.F., Gish, W., Miller, W., Myers, E.W., Lipman, D.J., 1990. Basic local alignment search tool. J. Mol. Biol. 215, 403–410.

Alvarez-Carreño, C., Alva, V., Becerra, A., Lazcano, A., 2018. Structure, function and evolution of the hemerythrin-like domain superfamily. Protein Sci. 27, 848–860.

Arbon, D., Ženíšková, K., Mach, J., Grechnikova, M., Malych, R., Talacko, P., Sutak, R., 2020. Adaptive iron utilization compensates for the lack of an inducible uptake system in *Naegleria fowleri* and represents a potential target for therapeutic intervention. PLoS Negl. Trop. Dis. 14, 1–25.

Arnér, E.S.J., Holmgren, A., 2000. Physiological functions of thioredoxin and thioredoxin reductase. Eur. J. Biochem. 267, 6102–6109.

Aurrecoechea, C., Barreto, A., Brestelli, J., Brunk, B.P., Caler, E.V., Fischer, S., Gajria, B., Gao, X., Gingle, A., Grant, G., Harb, O.S., Heiges, M., Iodice, J., Kissinger, J.C., Kraemer, E.T., Li, W., Nayak, V., Pennington, C., Pinney, D.F., Pitts, B., Roos, D.S., Srinivasamoorthy, G., Stoeckert, C.J., Treatman, C., Wang, H., 2011. AmoebaDB and MicrosporidiaDB: functional genomic resources for Amoebozoa and microsporidia species. Nucleic Acids Res. 39, 612–619.

Bailly, X., Vanin, S., Chabasse, C., Mizuguchi, K., Vinogradov, S.N., 2008. A phylogenomic profile of hemerythrins, the nonheme diiron binding respiratory proteins. BMC Evol. Biol. 8, 1–11.

Bellini, N.K., Santos, T.M., da Silva, M.T.A., Thiemann, O.H., 2018. The therapeutic strategies against *Naegleria fowleri*. Exp. Parasitol. 187, 1–11.

Bernsel, A., Viklund, H., Falk, J., Lindahl, E., Von Heijne, G., Elofsson, A., 2008. Prediction of membrane-protein topology from first principles. Proc. Natl. Acad. Sci. U. S. A. 105, 7177–7181.

Biteau, B., Labarre, J., Toledano, M.B., 2003. ATP-dependent reduction of cysteine-sulphinic acid by *S. cerevisiae* sulphiredoxin. Nature 425, 980–984.

Brancaccio, D., Gallo, A., Piccioli, M., Novellino, E., Ciofi-Baffoni, S., Banci, L., 2017. [4Fe-4S] cluster assembly in mitochondria and its impairment by copper. J. Am. Chem. Soc. 139, 719–730.

Capdevila, M., Atrian, S., 2011. Metallothionein protein evolution: a miniassay. J. Biol. Inorg. Chem. 16, 977–989.

Cox, J., Hein, M.Y., Luber, C.A., Paron, I., Nagaraj, N., Mann, M., 2014. Accurate proteome-wide label-free quantification by delayed normalization and maximal peptide ratio extraction, termed MaxLFQ. Mol. Cell. Proteomics 13, 2513–2526.

Cunha, I., Mangas-Ramirez, E., Guilhermino, L., 2007. Effects of copper and cadmium on cholinesterase and glutathione S-transferase activities of two marine gastropods (*Monodonta lineata* and *Nucella lapillus*). Comp. Biochem. Physiol. C Toxicol. Pharmacol. 145, 648–657.

Ding, C., Festa, R.A., Chen, Y.L., Espart, A., Palacios, Ò., Espín, J., Capdevila, M., Atrian, S., Heitman, J., Thiele, D.J., 2013. *Cryptococcus neoformans* copper detoxification machinery is critical for fungal virulence. Cell Host Microbe 13, 265–276.

Ding, C., Yin, J., Tovar, E.M.M., Fitzpatrick, D.A., Higgins, D.G., Thiele, D.J., 2011. The copper regulon of the human fungal pathogen *Cryptococcus neoformans* H99. Mol. Microbiol. 81, 1560–1576.

Ding, W.Q., Lind, S.E., 2009. Metal ionophores - an emerging class of anticancer drugs. IUBMB Life 61, 1013–1018.

Dobson, L., Reményi, I., Tusnády, G.E., 2015. CCTOP: a Consensus Constrained TOPology prediction web server. Nucleic Acids Res. 43, W408–W412.

Eyice, Ö., Myronova, N., Pol, A., Carrión, O., Todd, J.D., Smith, T.J., Gurman, S.J., Cuthbertson, A., Mazard, S., Mennink-Kersten, M.A.S.H., Bugg, T.D.H., Andersson, K. K., Johnston, A.W.B., Op Den Camp, H.J.M., Schäfer, H., 2018. Bacterial SBP56 identified as a Cu-dependent methanethiol oxidase widely distributed in the biosphere. ISME J. 12, 145–160.

Fernando, M.R., Nanri, H., Yoshitake, S., Nagata-Kuno, K., Minakami, S., 1992. Thioredoxin regenerates proteins inactivated by oxidative stress in endothelial cells. Eur. J. Biochem. 209, 917–922.

Festa, R.A., Helsel, M.E., Franz, K.J., Thiele, D.J., 2014. Exploiting innate immune cell activation of a copper-dependent antimicrobial agent during infection. Chem. Biol. 21, 977–987.

Findlay, V.J., Townsend, D.M., Morris, T.E., Fraser, J.P., He, L., Tew, K.D., 2006. A novel role for human sulfiredoxin in the reversal of glutathionylation. Canc. Res. 66, 6800–6806.

Flemming, C.A., Trevors, J.T., 1989. Copper toxicity and chemistry in the environment: a review. Water. Air. Soil Pollut. 44, 143–158.

Fulton, C., 1974. Axenic cultivation of *Naegleria gruberi*. Requirement for methionine. Exp. Cell Res. 88, 365–370.

Fung, D.K.C., Lau, W.Y., Chan, W.T., Yan, A., 2013. Copper efflux is induced during anaerobic amino acid limitation in escherichia coli to protect iron-sulfur cluster enzymes and biogenesis. J. Bacteriol. 195, 4556–4568.

Gaetke, L.M., Chow, C.K., 2003. Copper toxicity, oxidative stress, and antioxidant nutrients. Toxicology 189, 147–163.

Garcia-Santamarina, S., Uzarska, M.A., Festa, R.A., Lill, R., Thiele, D.J., 2017. *Cryptococcus neoformans* iron-sulfur protein biogenesis machinery is a novel layer of protection against Cu stress. mBio 8, 1–18.

Gietz, R.D., Schiestl, R.H., 2007. High-efficiency yeast transformation using the LiAc/SS carrier DNA/PEG method. Nat. Protoc. 2, 38–41.

Harwood, M.D., Russell, M.R., Neuhoff, S., Warhurst, G., Rostami-Hodjegan, A., 2014. Lost in centrifugation: accounting for transporter protein losses in quantitative targeted absolute proteomics. Drug Metab. Dispos. 42, 1766–1772.

Helsel, M.E., White, E.J., Razvi, S.Z.A., Alies, B., Franz, K.J., 2017. Chemical and functional properties of metal chelators that mobilize copper to elicit fungal killing of *Cryptococcus neoformans*. Metallomics 9, 69–81.

Herman, E.K., Greninger, A., van der Giezen, M., Ginger, M.L., Ramirez-Macias, I., Miller, H.C., Morgan, M.J., Tsaousis, A.D., Velle, K., Vargová, R., Rodrigo Najle, S., MacIntyre, G., Muller, N., Wittwer, M., Zysset-Burri, D.C., Elias, M., Slamovits, C., Weirauch, M., Fritz-Laylin, L., Marciano-Cabral, F., Puzon, G.J., Walsh, T., Chiu, C., Dacks, J.B., 2020. A comparative 'omics approach to candidate pathogenicity factor discovery in the brain-eating amoeba *Naegleria fowleri*. bioRxiv, 2020.01.16.908186.

Hodgkinson, V., Petris, M.J., 2012. Copper homeostasis at the host-pathogen interface. J. Biol. Chem. 287, 13549–13555.

Holmgren, A., 1985. Thioredoxin. Annu. Rev. Biochem. 54, 237–271.

Holmgren, A., Lu, J., 2010. Thioredoxin and thioredoxin reductase: current research with special reference to human disease. Biochem. Biophys. Res. Commun. 396, 120–124.

Isah, M.B., Goldring, J.P.D., Coetzer, T.H.T., 2020. Expression and copper binding properties of the N-terminal domain of copper P-type ATPases of African trypanosomes. Mol. Biochem. Parasitol. 235, 111245.

Käll, L., Krogh, A., Sonnhammer, E.L.L., 2004. A combined transmembrane topology and signal peptide prediction method. J. Mol. Biol. 338, 1027–1036.

Kühlbrandt, W., 2004. Biology, structure and mechanism of P-type ATPases. Nat. Rev. Mol. Cell Biol. 5, 282–295.

Kung, C.C.S., Huang, W.N., Huang, Y.C., Yeh, K.C., 2006. Proteomic survey of copper-binding proteins in *Arabidopsis* roots by immobilized metal affinity chromatography and mass spectrometry. Proteomics 6, 2746–2758.

Letelier, M.E., Martínez, M., González-Lira, V., Faúndez, M., Aracena-Parks, P., 2006. Inhibition of cytosolic glutathione S-transferase activity from rat liver by copper. Chem. Biol. Interact. 164, 39–48.

Lutsenko, S., LeShane, E.S., Shinde, U., 2007. Biochemical basis of regulation of human copper-transporting ATPases. Arch. Biochem. Biophys. 463, 134–148.

Mach, J., Bíla, J., Ženíšková, K., Arbon, D., Malych, R., Glavanakovová, M., Nývltová, E., Sutak, R., 2018. Iron economy in *Naegleria gruberi* reflects its metabolic flexibility. Int. J. Parasitol. 48, 719–727.

Maciver, S.K., Piñero, J.E., Lorenzo-Morales, J., 2020. Is *Naegleria fowleri* an emerging parasite? Trends Parasitol. 36, 19–28.

Mackie, J., Szabo, E.K., Urgast, D.S., Ballou, E.R., Childers, D.S., MacCallum, D.M., Feldmann, J., Brown, A.J.P., 2016. Host-imposed copper poisoning impacts fungal micronutrient acquisition during systemic *Candida albicans* infections. PLoS One 11, 1–18.

Macomber, L., Imlay, J.A., 2009. The iron-sulfur clusters of dehydratases are primary intracellular targets of copper toxicity. Proc. Natl. Acad. Sci. U. S. A. 106, 8344–8349.

Meade, J.C., 2019. P-type transport ATPases in *Leishmania* and *Trypanosoma*. Parasite 26, 69.

Moller, J.A., Juul, B., Maire, M. le, 1996. Structural organization, ion transport, and energy transduction of P-type ATPases. Biochim. Biophys. Acta 1286, 1–51.

Mull, B.J., Narayanan, J., Hill, V.R., 2013. Improved method for the detection and quantification of *Naegleria fowleri* in water and sediment using immunomagnetic separation and real-time PCR. J. Parasitol. Res. 2013, 608367.

Ogawa, K., Sun, J., Taketani, S., Nakajima, O., Nishitani, C., Sassa, S., Hayashi, N., Yamamoto, M., Shibahara, S., Fujita, H., Igarashi, K., 2001. Heme mediates derepression of Maf recognition element through direct binding to transcription repressor Bach1. EMBO J. 20, 2835–2843.

Pearce, D.A., Sherman, F., 1999. Toxicity of copper, cobalt, and nickel salts is dependent on histidine metabolism in the yeast *Saccharomyces cerevisiae*. J. Bacteriol. 181, 4774–4779.

Perez-Riverol, Y., Csordas, A., Bai, J., Bernal-Llinares, M., Hewapathirana, S., Kundu, D. J., Inuganti, A., Griss, J., Mayer, G., Eisenacher, M., Pérez, E., Uszkoreit, J., Pfeuffer, J., Sachsenberg, T., Yilmaz, Ş., Tiwary, S., Cox, J., Audain, E., Walzer, M., Jarnuczak, A.F., Ternent, T., Brazma, A., Vizcaíno, J.A., 2019. The PRIDE database and related tools and resources in 2019: improving support for quantification data. Nucleic Acids Res. 47, D442–D450.

Pesce, A., Bolognesi, M., Nardini, M., 2013. Protoglobin: Structure and Ligand-Binding Properties, vol. 63, pp. 79–96.

Rainsford, K.D., Milanino, R., Sorenson, J.R.J., Velo, G.P. (Eds.), 1998. Copper and Zinc in Inflammatory and Degenerative Diseases. Springer Science+Business Media, Dordrecht.

Rasoloson, D., Shi, L., Chong, C.R., Kafsack, B.F., Sullivan, D.J., 2004. Copper pathways in *Plasmodium falciparum* infected erythrocytes indicate an efflux role for the copper P-ATPase. Biochem. J. 381, 803–811.

Reeder, N.L., Xu, J., Youngquist, R.S., Schwartz, J.R., Rust, R.C., Saunders, C.W., 2011. The antifungal mechanism of action of zinc pyrithione. Br. J. Dermatol. 165, 9–12.

Rhee, J.S., Lee, Y.M., Hwang, D.S., Lee, K.W., Kim, I.C., Shin, K.H., Raisuddin, S., Lee, J. S., 2007. Molecular cloning and characterization of omega class glutathione S-transferase (GST-O) from the polychaete *Neanthes succinea*: biochemical comparison with theta class glutathione S-transferase (GST-T). Comp. Biochem. Physiol. C Toxicol. Pharmacol. 146, 471–477.

Salazar-Medina, A.J., García-Rico, L., García-Orozco, K.D., Valenzuela-Soto, E., Contreras-Vergara, C.A., Arreola, R., Arvizu-Flores, A., Sotelo-Mundo, R.R., 2010. Inhibition by Cu^{2+} and Cd^{2+} of a Mu-class glutathione S-transferase from shrimp *Litopenaeus vannamei*. J. Biochem. Mol. Toxicol. 24, 218–222.

Sheldon, J.R., Skaar, E.P., 2019. Metals as phagocyte antimicrobial effectors. Curr. Opin. Immunol. 60, 1–9.

Shimizu, T., 2012. Binding of cysteine thiolate to the Fe(III) heme complex is critical for the function of heme sensor proteins. J. Inorg. Biochem. 108, 171–177.

Siddiqui, R., Ali, I.K.M., Cope, J.R., Khan, N.A., 2016. Biology and pathogenesis of *Naegleria fowleri*. Acta Trop. 164, 375–394.

Smith, A.D., Logeman, B.L., Thiele, D.J., 2017. Copper acquisition and utilization in fungi. Annu. Rev. Microbiol. 597–623.

Söding, J., Biegert, A., Lupas, A.N., 2005. The HHpred interactive server for protein homology detection and structure prediction. Nucleic Acids Res. 33, 244–248.

Solioz, M., Vulpe, C., 1996. CPx-type ATPases: a class of P-type ATPases that pump heavy metals. Trends Biochem. Sci. 21, 237–241.

Song, Y., Xu, H., Chen, W., Zhan, P., Liu, X., 2015. 8-Hydroxyquinoline: a privileged structure with broad-ranging pharmacological potentials. Med. Chem. Commun. 6, 61–74.

Sykora, J.L., Keleti, G., Martinez, A.J., 1983. Occurrence and pathogenicity of *Naegleria fowleri* in artificially heated waters. Appl. Environ. Microbiol. 45, 974–979.

Szczypka, M.S., Zhu, Z., Silar, P., Thiele, D.J., 1997. *Saccharomyces cerevisiae* mutants altered in vacuole function are defective in copper detoxification and iron-responsive gene transcription. Yeast 13, 1423–1435.

Tyanova, S., Temu, T., Sinitcyn, P., Carlson, A., Hein, M.Y., Geiger, T., Mann, M., Cox, J., 2016. The Perseus computational platform for comprehensive analysis of (prote) omics data. Nat. Methods 13, 731–740.

Vuilleumier, S., Pagni, M., 2002. The elusive roles of bacterial glutathione S-transferases: new lessons from genomes. Appl. Microbiol. Biotechnol. 58, 138–146.

Weissman, Z., Berdicevsky, I., Cavari, B.Z., Kornitzer, D., 2000. The high copper tolerance of *Candida albicans* is mediated by a P-type ATPase. Proc. Natl. Acad. Sci. U. S. A. 97, 3520–3525.

White, C., Lee, J., Kambe, T., Fritsche, K., Petris, M.J., 2009. A role for the ATP7A copper-transporting ATPase in macrophage bactericidal activity. J. Biol. Chem. 284, 33949–33956.

Wiemann, P., Perevitsky, A., Lim, F.Y., Shadkchan, Y., Knox, B.P., Landero Figueora, J. A., Choera, T., Niu, M., Steinberger, A.J., Wüthrich, M., Idol, R.A., Klein, B.S., Dinauer, M.C., Huttenlocher, A., Osherov, N., Keller, N.P., 2017. *Aspergillus fumigatus* copper export machinery and reactive oxygen intermediate defense counter host copper-mediated oxidative antimicrobial offense. Cell Rep. 19, 1008–1021.

Wu, Z., Fernandez-Lima, F.A., Russell, D.H., 2010. Amino acid influence on copper binding to peptides: cysteine versus arginine. J. Am. Soc. Mass Spectrom. 21, 522–533.

Yang, X., Cai, P., Liu, Q., Wu, J., Yin, Y., Wang, X., Kong, L., 2018. Novel 8-hydroxy-quinoline derivatives targeting β-amyloid aggregation, metal chelation and oxidative stress against Alzheimer's disease. Bioorganic Med. Chem. 26, 3191–3201.

Yuan, D.S., Dancis, A., Klausner, R.D., 1997. Restriction of copper export in *Saccharomyces cerevisiae* to a late Golgi or post-Golgi compartment in the secretory pathway. J. Biol. Chem. 272, 25787–25793.

Zhang, L., Guarente, L., 1995. Heme binds to a short sequence that serves a regulatory function in diverse proteins. EMBO J. 14, 313–340.